



University of
Salford
MANCHESTER

**IMPLEMENTATION OF MECHANISTIC-EMPIRICAL
APPROACH FOR STRUCTURAL DESIGN OF
HYDRATED LIME MODIFIED FLEXIBLE
PAVEMENT**

AHMED FARHAN MUWAYEZ AL-TAMEEMI

School of Computing, Science and Engineering
The University of Salford
Greater Manchester
United Kingdom

Submitted in Partial Fulfillment of the Requirements for the
Degree of Doctor of Philosophy in Civil Engineering
March 2017

ABSTRACT

The need for improved mechanistic procedures for design, maintenance, and rehabilitation of highway and airport pavements has been recognized for many years. Mechanistic methods are based on the principles of mechanics in contrast to the particular purpose and empirical procedures that are often used.

The objective of this study is the development of Mechanistic-Empirical design method by the implementation of hydrated lime effect in the proposed pavement section. Enhancing the paving material performance-related properties during design is an important step to minimize the efforts, pavement layers' thicknesses and cost as well as develop the serviceability and design life. This can be done by modifiers, and one of the effective modification materials is the hydrated lime. Accordingly, the advantages of hydrated lime in the resistance to fatigue cracking and permanent deformation are utilized as main factors in the adopted Mechanistic-Empirical approach of this study.

To achieve the objective of this study, three types of asphalt concrete mixtures that represent the pavement asphaltic courses (Wearing, Leveling and Base) of the asphalt concrete layer were produced and evaluated. As mineral filler materials, ordinary limestone dust and hydrated lime were used in this study. Five different hydrated lime percentages were selected, namely 1, 1.5, 2, 2.5 and 3 percent as partial replacement of limestone dust filler by total weight of aggregate besides a control mixture without hydrated lime. For the hydrated lime modified mix design, the introducing of lime into the mixtures was done by adding dry hydrated lime by total aggregate weight following the normal procedure for adding mineral filler.

The experimental programme conducted in this study comprises of four main steps. Firstly, evaluate the effect of hydrated lime (HL) on asphalt cement physical properties. Penetration and the softening point (ring and ball) tests were conducted to study the influence of hydrated lime on asphalt cement consistency and stiffness. Secondly, the design of asphalt concrete mixtures following Marshall design procedure. The use of Marshall apparatus is to obtain the optimum asphalt content in specific values of stability, air void and density for control and hydrated lime modified mixes. This method also covers the evaluation of mixtures' resistance to plastic flow

(Marshall stability and flow). Thirdly, determine and evaluate the control and hydrated lime modified Hot Mix Asphalt (HMA) pavement mechanical responses to the two major distresses (fatigue cracking and rutting) that generally occurred in the pavement. In particular, these distresses could give an indication of failure criteria in the mechanistic-empirical design process. Finally, evaluation of pavement mixtures resistance to moisture damage regarding the effect of hydrated lime. The determined optimum asphalt contents by Marshall design procedure as related to the effect of hydrated lime were used in preparing further mixes specimens with different geometry and size for fatigue and rutting tests. The testing temperatures for permanent deformation and resilient modulus were 20°C, 40°C and 60°C, for fatigue it was 20°C and for the moisture susceptibility the temperature was 25°C. The fatigue and permanent deformation tests were done under the repeated loading using the pneumatic repeated load system (PRLS).

The addition of 2.5% of hydrate lime results in a reduction in the penetration of about 28.1% of penetration at 0% of hydrated lime addition percentage to the asphalt cement. The softening point at 3% of HL is greater than softening point temperature degree at 0% by about 27%. Accordingly, the higher the addition percent of hydrated lime as a partial replacement with the mineral filler, the higher consistency and stiffness of the lime modified asphalt cement. The general trend of the tests data showed that the addition of hydrated lime up to 2.5% as a partial replacement of ordinary limestone mineral filler produced a considerable improvement in Marshall and volumetric properties, increased mixtures modulus of elasticity, enhanced the pavement resistance to rutting and fatigue cracking as well as remarkably decreased the mixtures susceptibility to moisture damage.

Statistical analysis was made for prediction of fatigue life and permanent deformation of pavement as related to physical properties and hydrated lime effect; one equation is to predict the number of repetition to fatigue cracking, and the other one was about the prediction of the permanent strain in the asphaltic pavement layers. Using the permanent strain model, permanent deflection in a pavement can be calculated by multiplying the strain by the depth of the asphalt concrete layer. The models could be used as failure criteria and to give an impression of the future behavior of asphalt concrete mixtures.

Mechanistic-Empirical design process was conducted for a typical three-dimensional pavement model of five layers employing Finite Element Analysis (FEA) using the general

purpose software (ANSYS). The analyses were compared with another approach (Multi-layered Elastic Theory) by using the KENPAVE software after considering the influence of hydrated lime on the asphalt pavement properties and the effect of temperature on pavement layers resilient modulus values as related to the depth of flexible pavement. The performance analyses and results illustrated that the asphalt concrete layer in the pavement section reached the optimum thickness of 210 mm of asphaltic layer modified with optimum value of hydrated lime (2.5%) after iterations began with 180mm with an increment of 10mm. The profit in thickness was 30mm since the total thickness of asphalt concrete layer without hydrated lime (control mixtures) that gave approximately the same damage ratio (lower than unity) was 240 mm.

PUBLICATIONS

Al-Tameemi, A.F., Wang, Y. and Albayati, A., (2015). Experimental study of the performance related properties of asphalt concrete modified with hydrated lime. *Journal of Materials in Civil Engineering*, ASCE, 28(5), p.04015185.

Al-Tameemi, A.F., Wang, Y. and Albayati, A., (2015). Influence of hydrated lime on the properties and permanent deformation of the asphalt concrete layers in pavement. *Romanian Journal of Transport Infrastructure*, 4(1), pp.1-19.

A paper outside the current Ph.D. research work:

Albayati, A., Wang, Y., & Al-Tameemi, A. (2015). The Use of Bonded Asphalt Surfaces for Bridge Decks. *Proceedings of the LJMU 14th Annual International Conference on Asphalt, Pavement Engineering and Infrastructure. 11th – 12th February 2015, Liverpool, UK. Volume 14, ISBN 978-0-9571804-6-8.*

ACKNOWLEDGEMENTS

First and above all, I would like to thank God, for all his giving.

I would like to express my appreciation to my advisor Dr. Yu Wang, thank you for encouraging my research and for allowing me to grow as a research scientist. Without your supervision and constant help, the considerable achievements would not have been possible.

I would especially like to thank Dr. Amjad Albayati, my external co-supervisor, for his valuable guidance and facilitating my laboratory work. Thanks also extended to the staff of the Highway Materials, Soil and Construction Materials Laboratories in Civil Engineering Department and the Consulting Engineering Bureau, University of Baghdad in Iraq for their help in using the various facilities in preparing and testing specimens, especially Mr. Ahmed Mahir.

Words cannot express how grateful I am to all my family and in-laws for all their support before and during my study, especially my beloved mother for her constant, unconditional love, prayer and being my source of strength. While he is no longer with me, I owe a debt of gratitude to my father. He intensely supported me to the last moment of his life until passing away untimely just few months after starting my PhD study journey with no last goodbye. I would like to thank my dear wife (Shaymaa) and sons (Yousif and Ibrahim) for their love, great support, consideration and encouragement, tolerance and being constant sources of inspiration.

Finally, special thanks go to the Iraqi Ministry of Higher Education and Scientific Research and the University of Al-Nahrain for funding this work.

TABLE OF CONTENT

ABSTRACT	i
PUBLICATION AND CONFERENCES ATTENDANCE.....	iv
ACKNOWLEDGEMENTS	v
TABLE OF CONTENT	vi
LIST OF TABLES	xii
LIST OF FIGURES	xv
ABBREVIATIONS	xxi
Chapter One.....	1
Introduction.....	1
1.1 General.....	1
1.2 Problem Statement.....	2
1.3 Aim and Objectives	4
1.4 Research Methodology.....	5
1.5 Structure of the Thesis.....	7
Chapter Two	9
Literature Review	9
2.1 General.....	9
2.2 The Bond in Asphalt Concrete	10
2.2.1 The Role of Asphalt Binder in the Mixture	10
2.2.2 The Influence of Aggregate Characteristics on Adhesion	10
2.2.3 Mineral Filler Influence on the Mixture	11
2.3 Hydrated Lime.....	13
2.4 The Influence of Hydrated Lime	15
2.4.1 Volumetric and Performance-Related Properties of Hot Mix Asphalt.....	15
2.4.2 Moisture Susceptibility	18
2.4.3 Fatigue Cracking.....	20
2.4.4 Permanent Deformation (Rutting)	30
2.4.4.1 Rutting Caused by Weak Subgrade.....	32
2.4.4.2 Rutting Caused by Weak Asphalt Layer	33

2.4.4.3 Evaluation of Asphalt Mixture Resistance to Rutting.....	34
2.4.4.4 Lime Influence on Permanent deformation.....	35
2.5 Methods of Adding Hydrated Lime into the Asphalt Concrete Mixture.....	39
2.5.1 Addition of Dry Hydrated Lime to Dry Aggregate	39
2.5.2 Addition of Dry Hydrated Lime to Wet Aggregate.....	39
2.5.3 Addition of Hydrated Lime in the Form of Slurry.....	40
2.6 Mechanical-Empirical Method for Pavement Design	40
2.6.1 Background	40
2.6.2 Mechanistic-Empirical Design Related Flexible Pavement Distresses	43
2.6.3 Failure Criteria of Mechanistic Empirical Method.....	43
2.6.4 Fatigue and Rutting Prediction Models	44
2.6.4.1 Fatigue Cracking Prediction Models.....	44
2.6.4.2 Permanent Deformation Prediction Models.....	49
2.7 Flexible Pavement Analysis	52
2.7.1 Elastic Layered Analysis Approach for Flexible Pavement	53
2.7.1.1 One Layer Method	53
2.7.1.2 Multi-Layer Theory.....	53
2.7.2 Linear Elastic Layered Programmes for Multilayered Systems	55
2.7.3 Finite Element Analysis Programmes for Pavements.....	57
2.7.3.1 Axisymmetric and Two-dimensional Finite Element Analysis	57
2.7.3.2 Three-Dimensional Finite Element Analysis	58
2.7.3.3 Finite Element Pavement Analysis Programmes Characteristics	59
2.7.3.4 General Purpose Finite Element Programmes	59
2.8 Summary.....	61
Chapter Three	64
Materials and Testing Programme	64
3.1 Introduction	64
3.2 Materials.....	64
3.2.1 Asphalt Cement.....	65
3.2.2 Mineral Filler	65
3.2.3 Aggregate.....	67

3.3 Hydrated Lime Effect Investigation by Experimental Work	71
3.3.1 Asphalt Cement Tests	71
3.3.1.1 Penetration Test.....	71
3.3.1.2 Softening Point Test.....	72
3.3.2 Mixture Preparation	73
3.3.3 Marshall Mix Design	74
3.3.4. Permanent Deformation.....	78
3.3.4.1 Preparation of Permanent Deformation Specimens	78
3.3.4.2 Testing of Permanent Deformation Specimens.....	80
3.3.5 Flexural Fatigue Cracking	84
3.3.5.1 Flexural Beam Specimen	84
3.3.5.2 Repeated Flexural Beam Fatigue Test	86
3.3.6 Moisture Susceptibility	89
3.4 Summery of Mixture Design and Testing Procedure	91
3.5 Specimens Designation	94
3.6 Summary	95
Chapter Four.....	96
Tests Results	96
4.1 Introduction	96
4.2 Influence of Hydrated Lime on Asphalt Cement.....	96
4.3 Influence of Hydrated Lime on Marshall Properties of Asphalt Concrete Mixtures	99
4.3.1 Optimum Asphalt Content.....	99
4.3.2 Density of Asphalt Concrete Mixtures	104
4.3.3 Marshall Stability.....	106
4.3.4 Marshall Flow	108
4.4 Influence of Hydrated Lime on Volumetric Properties of Asphalt Mixtures.....	110
4.4.1 Air Voids.....	110
4.4.2 Voids in Mineral Aggregate (VMA)	113
4.4.3 Voids Filled with Asphalt (VFA)	114
4.5 Influence of Hydrated Lime on Performance Related Properties of Asphalt Mixtures	116
4.5.1 Hydrated Lime Influence on Resilient Modulus (Mr).....	116

4.5.2 Hydrated Lime Influence on Resilient Strain	118
4.5.3 Hydrated Lime Influence on permanent deformation.....	120
4.5.4 Hydrated Lime Influence on Fatigue Cracking	129
4.5.4.1 Initial Tensile Strain-Fatigue failure Life Relationship	130
4.5.4.2 Hydrated Lime Influence on The Parameters of Fatigue Equations	136
4.5.4.3 Hydrated Lime Influence on the Stress level and Number of Load repetitions	138
4.5.4.4 Hydrated Lime Influence on the Stress level and Initial Tensile Strain.....	140
4.5.4.5 Hydrated Lime Influence on the Average of Fatigue Life	142
4.5.4.6 Hydrated Lime Influence on the Average of Initial Tensile Strain.....	145
4.5.4.7 Hydrated Lime Influence on the Average of Initial Flexural Stiffness.....	146
4.5.5 Hydrated Lime Influence on Moisture Susceptibility.....	147
4.5.5.1 Conditioned and Unconditioned Tensile Strength of mixtures.....	149
4.5.5.2 Effect of Hydrated Lime Addition on Tensile Strength Ratio (TSR).....	151
4.6 Summary and Further Discussion	153
Chapter Five	156
Statistical Modelling of Fatigue Life and Permanent Deformation	156
5.1 Introduction	156
5.2 Models Development Process	158
5.2.1 Identifying the Dependent Variables	158
5.2.2 Listing Potential Predictors.....	158
5.2.3 Gathering the Required Observations for the Potential Models	158
5.2.4 Identifying Several Possible Models	158
5.2.5 Using Statistical Software to Estimate the Models.....	158
5.2.6 Determining whether the Required Conditions are satisfied	158
5.2.7 Using the Engineering Judgment and the Statistical Output to Select the Best Model ..	159
5.3 Predictor and Dependent Variables Identification.....	160
5.4 Selecting Sample Size	161
5.5 Regression Modelling.....	163
5.6 Checking for Outliers	164
5.7 Checking for Normality.....	166

5.8 Multicollinearity	167
5.9 Goodness of Fit.....	170
5.10 Validation of the Developed Models.....	180
5.10.1 Introduction.....	180
5.10.2 Validation Methods.....	180
5.10.2.1 Examination of Model Predictions and Coefficients	180
5.10.2.2 Collection of New Data	180
5.10.2.3 Comparison with Previously Developed Models	181
5.10.2.4 Data Splitting	181
5.10.2.5 Prediction Sum of Squares (PRESS)	181
5.10.3 Selection of Validation Methods	181
5.10.4 Analysis of Error.....	182
5.10.4.1 Distribution of Error.....	187
5.10.4.2 Mean of Error Distribution.....	187
5.11 Examination of R-Critical Value.....	188
5.12 Analysis of Results	188
5.13 Models' Parameters Limitation	190
5.14 Summary.....	191
Chapter Six	193
Development of Mechanistic-Empirical Design Approach Using Numerical Modelling.....	193
6.1 Introduction	193
6.2 Parameters Required For Flexible Pavement Analysis and Design	195
6.2.1 Traffic Loading	195
6.2.1.1 Loading Configuration and Dimensions	195
6.2.1.2 Contact Area between the Tire and Pavement	198
6.2.2 Temperature Consideration.....	199
6.2.2.1 Asphalt Concrete Pavement Temperature as Related to Air Temperature	199
6.2.2.2 Prediction of Resilient Modulus as Related to Temperature and Depth.....	202
6.2.3 Material Response Properties	206
6.2.4 Miner's Hypothesis.....	210

6.3 Finite Element Analysis.....	210
6.3.1 Finite Element Modelling of Pavement Structure.....	211
6.3.2 FEA Results Comparison with Multi-Layer Elastic Theory.....	220
6.4 Mechanistic-Empirical Analysis Procedure Summary.....	233
6.5 The Results of Mechanistic-Empirical Analysis.....	235
6.5.1 Critical Pavement Responses as Related to HMA Thickness and Lime Influence.....	237
6.5.1.1 Asphalt Concrete Courses Thicknesses Related to Pavement Critical Responses...242	
6.5.1.2 Asphalt Concrete Courses Thicknesses Related to Total HMA Thickness.....	245
6.5.2 Fatigue Life and Permanent Deformation Developed in This Study.....	246
6.6 Summary and Further Discussion.....	251
Chapter Seven.....	253
Conclusions and Recommendations.....	253
7.1 Conclusions.....	253
7.2 Recommendations for Future Research.....	256
References.....	258
Appendix (A).....	272

LIST OF TABLES

Table (2-1) Laboratory Fatigue Tests (Tangella et al., 1990)	24
Table (2-2) Factors Affecting Controlled Stress and Strain Tests (Tangella et al., 1990)	26
Table (2-3) Results of Static Creep Test (Savitha et. al., 2012)	29
Table (2-4) Results of fatigue and stiffness modulus of the mix (Savitha et. al., 2012)	29
Table (2-5) Deformation in (mm) After 20,000 Passes for many Anti-Stripping Treatments in Colorado (Aschebrener and Far, 1994).....	37
Table (2-6) Number of load repetitions corresponding to 7.5 mm and 5.0 mm rutting failure criteria in specimens (Collins et al., 1997)	37
Table (2-7) Evaluation of results of Creep test procedure found by Little et al. (1994)	38
Table (2-8) Several Coefficients of Permanent Deformation Models for Various Agencies...	50
Table (3-1) Physical Properties of AC 40/50.....	65
Table (3-2) Physical properties of Hydrated Lime and Limestone.....	66
Table (3-3) Chemical Composition of Hydrated Lime and Limestone.....	66
Table (3-4) Physical Properties of Aggregate.....	67
Table (3-5): Asphalt Concrete Mixtures Gradings (SCR/R9, 2003)	68
Table (3-6) Selected Gradations for Studied Asphalt Concrete Courses	69
Table (3-7) Filler Content Replacement with Hydrated Lime in the Mixtures for Different Pavement Courses	74
Table (3-8) Permanent Deformation Test selected parameters	84
Table (3-9) Summery of Specimens Dimensions and Purpose of Testing	93
Table (3-10) Summery of Specimens Number Made for Mixes Adopted in the Study	94
Table (4-1) Effect of mineral filler (Hydrated lime) on Asphalt Cement Penetration and Softening Point results.....	97

Table (4-2) Marshall Design properties for Wearing course.....	103
Table (4-3) Marshall Design properties for Leveling course.....	104
Table (4-4) Marshall Design properties for Base course.....	104
Table (4-5) The Results of Fitting Parameters using the Eq. (3-7) at 20°C	128
Table (4-6) The Results of Fitting Parameters using the Eq. (3-7) at 40°C	128
Table (4-7) The Results of Fitting Parameters using the Eq. (3-7) at 60°C	129
Table (4-8) Fatigue life parameters using Eq. (3-11) for Wearing mixture	135
Table (4-9) Fatigue life parameters using Eq. (3-11) for Leveling mixture	135
Table (4-10) Fatigue life parameters using Eq. (3-11) for Base mixture	136
Table (4-11) Influence of hydrated lime addition on TSR of Wearing mixture	148
Table (4-12) Influence of hydrated lime addition on TSR of Leveling mixture	148
Table (4-13) Influence of hydrated lime addition on TSR of Base mixture	149
Table (5-1) Error of proposed models according to sample size	162
Table (5-2) Explanation of Outlier Evaluation Method for Fatigue Live Model	165
Table (5-3) Explanation of Outlier Evaluation Method for Permanent Deformation Model ...	166
Table (5-4) Correlation Coefficient Matrix for Fatigue ($\ln N_f$) model	169
Table (5-5) Correlation Coefficient Matrix for Permanent Deformation ($\log(\epsilon_p)$) model	169
Table (5-6) Summary of Fatigue life Model ($\ln N_f$)	172
Table (5-7) The Results of ANOVA of Fatigue life Model ($\ln N_f$)	173
Table (5-8) Stepwise Regression Details of Coefficients of the Fatigue Life ($\ln N_f$) Model ...	174
Table (5-9) Summary of Permanent Deformation Model ($\log \epsilon_p$)	176
Table (5-10) The Results of ANOVA of Permanent Deformation Model ($\log \epsilon_p$)	177

Table (5-11) Stepwise Regression Details of Coefficients of the Permanent Deformation Model ($\log \epsilon_p$)	178
Table (5-12) The Residuals Statistics Summary of the Fatigue Life Model ($\ln N_f$)	188
Table (5-13) The Residuals Statistics Summary of the Permanent Deformation Model ($\log \epsilon_p$)	188
Table (5-14) Summary Results of Developed Models	189
Table (5-15) Limitation of Fatigue Life Model variables	190
Table (5-16) Limitation of Permanent Deformation ($\log \epsilon_p$) Model variables	191
Table (6-1) Worksheet Proposal for Estimating the 80-kN ESAL Applications.....	193
Table (6-2) Resilient Modulus of Asphalt Concrete Mixtures at Various Depths	207
Table (6-3) Poisson Ratios for Different Paving Materials (Southgate et. al., 1977)	210
Table (6-4) The Adequate Element Size for each Layer in the Pavement Model	213
Table (6-5) Material properties of proposed pavement structure layers	235
Table (6-6): Mechanistic-Empirical Critical Outputs of the Analysis of Pavement Model.....	236
Table (6-7) Rut Depth Criteria According to AASHTO (1993)	249
Table (6-8) Rut Depth Prediction in Asphaltic Layer of Pavement Model ($N = N_{ESAL} = 2318000$)	250
Table A-1 Marshall Test Results for the Wearing coarse	268
Table A-2 Marshall Test Results for the Leveling coarse	270
Table A-3 Marshall Test Results for the Base coarse	272

LIST OF FIGURES

Figure (1-1) Mechanistic-Empirical Approach Flow Chart... Mechanistic-Empirical Approach Flow Chart (NCHRP 1-37, 2004)	6
Figure (2-1) Components of Asphalt Mastics (Harris et al., 1995).....	13
Figure (2-2) Static creep test results (Satyakumar et al., 2013).....	16
Figure (2-3) Dynamic creep test results (Satyakumar et al., 2013).....	16
Figure (2-4) Stiffness modulus test results (Satyakumar et al., 2013).....	17
Figure (2-5) Schematic of fatigue cracking starting directions (NCHRP Report 673, 2011)	21
Figure (2-6). Illustration of stress and strain within pavement layers (NCHRP, 2002)	22
Figure (2-7) Fatigue cracking in flexible pavement	22
Figure (2-8) Constant Stress and Constant Strain Phenomena (NCHRP, 2004)	25
Figure (2-9) The Influence of Additives on Fatigue (Kim et al., 1995).....	27
Figure (2-10) Influence of Additives (Dry) on Permanent deformation (Kim et al., 1995).....	28
Figure (2-11) Influence of Additives (Moisturized) on Permanent Deformation (Kim et al., 1995)...	28
Figure (2-12) Permanent Deformation (Rutting) in Flexible Pavement	30
Figure (2-13) Description of Rutting Types (NCHRP, 2002).....	31
Figure (2-14) Rutting from Weak Subgrade (McGennis et al., 1995).....	33
Figure (2-15) Rutting from weak asphalt mixture (McGennis et al., 1995).....	34
Figure (2-16) Hydrated Lime Influence on Resilient Modulus Before and After Lottman Conditioning (Epps et al., 1992).....	36
Figure (2-17) Hydrated Lime Influence on Resilient Modulus Before and Following Lottman Conditioning (Epps et al., 1992).....	36
Figure (2-18) MEPDG Design Process (NCHRP 1-37A, 2004)	42
Figure (2-19) Tensile and Compressive Strains in Flexible Pavements (Huang, 2004)	43
Figure (2-20) Multilayered Elastic System in Axisymmetric Condition (Kim, 2007)	55
Figure (2-21) Three Typical FE Analysis Models for Pavements (Kim et al., 2010)	57
Figure (3-1): Selected Wearing Gradation of Combined Aggregate and Mineral Filler	69
Figure (3-2): Selected Leveling Gradation of Combined Aggregate and Mineral Filler	70
Figure (3-3): Selected Base Gradation of Combined Aggregate and Mineral Filler	70
Figure (3-4) Penetration Test of bitumen material (McGennis et al., 1995)	71
Figure (3-5) Softening Point Test of bitumen (Millard, 1993).....	72
Figure (3-6). Marshall Stability (McGennis et al., 1995).....	76

Figure (3-7) Marshall apparatus to determine stability and Flow.....	76
Figure (3-8) Maximum specific gravity calculation for asphalt concrete specimen	78
Figure (3-9) Compaction Efforts versus Density.....	80
Figure (3-10) PRLS Connected to LVDT and Data Acquisition System.....	81
Figure (3-11) Permanent Deformation Test in Pneumatic Repeated Load System (PRLS).....	81
Figure (3-12) Typical relationship between the permanent strain and number of load repetitions (Walubita et al, 2013)	83
Figure (3-13) Preparation of specimens for fatigue cracking test.....	85
Figure (3-14) Schematic Loading Configuration of the Beam.....	88
Figure (3-15) Setting and testing of flexural beam specimen.....	88
Figure (3-16) Indirect Tensile Strength Test of a Specimen Before and After Failure	91
Figure (3-17) Mixture Design and Testing Procedure	92
Figure (3-18) Example of samples nomenclature adopted in this study.....	94
Figure (4-1) Influence of Hydrated Lime on Mortar penetration	98
Figure (4-2) Influence of Hydrated Lime on Mortar Softening Point	98
Figure (4-3) Marshall Mix Design Properties for Control Wearing mixture (CW)	100
Figure (4-4) Marshall Mix Design Properties for Control Leveling (CL) mixture	101
Figure (4-5) Marshall Mix Design Properties for Control Base (CB) mixture	102
Figure (4-6) Hydrated lime influence on density with respect to AC% for Wearing course	105
Figure (4-7) Hydrated lime influence on density with respect to AC% for Leveling course	105
Figure (4-8) Hydrated lime influence on density with respect to AC% for Base course	106
Figure (4-9) Hydrated lime influence on stability with respect to AC% for Wearing course	107
Figure (4-10) Hydrated lime influence on stability with respect to AC% for Leveling course.....	107
Figure (4-11) Hydrated lime influence on stability with respect to AC% for Base course.....	108
Figure (4-12) Hydrated lime influence on Flow with respect to AC% for Wearing course.....	109
Figure (4-13) Hydrated lime influence on Flow with respect to AC% for Leveling course	109
Figure (4-14) Hydrated lime influence on Flow with respect to AC% for Base course	110
Figure (4-15) Hydrated lime influence on AV% with respect to AC% for Wearing course	111
Figure (4-16) Hydrated lime influence on AV% with respect to AC% for Leveling course	111
Figure (4-17) Hydrated lime influence on AV% with respect to AC% for Base course.....	112
Figure (4-18) Hydrated lime porosity as compared to other mineral fillers (EuLA, 2011)	112
Figure (4-19) Hydrated lime influence on VMA % with respect to AC% for W course.....	113
Figure (4-20) Hydrated lime influence on VMA % with respect to AC% for L course.....	114
Figure (4-21) Hydrated lime influence on VMA % with respect to AC% for B course	114

Figure (4-22) Hydrated lime influence on VFA % with respect to AC% for Wearing course	115
Figure (4-23) Hydrated lime influence on VFA % with respect to AC% for Leveling course	115
Figure (4-24) Hydrated lime influence on VFA % with respect to AC% for Base course.....	116
Figure (4-25) Hydrated lime influence on resilient modulus for W, L and B at 20°C.....	117
Figure (4-26) Hydrated lime influence on resilient modulus for W, L and B at 40°C.....	117
Figure (4-27) Hydrated lime influence on resilient modulus for W, L and B at 60°C.....	118
Figure (4-28) Hydrated lime influence on resilient strain for W, L and B at 20°C.....	119
Figure (4-29) Hydrated lime influence on resilient strain for W, L and B at 40°C.....	119
Figure (4-30) Hydrated lime influence on resilient strain for W, L and B at 60°C.....	120
Figure (4-31) Influence of Hydrated Lime on Permanent Deformation at 20°C.....	122
Figure (4-32) Influence of Hydrated Lime on Permanent Deformation at 40°C.....	123
Figure (4-33) Influence of Hydrated Lime on Permanent Deformation at 60°C.....	124
Figure (4-34) Fitting results of permanent deformation for the secondary portion at 20°C.....	125
Figure (4-35) Fitting results of permanent deformation for the secondary portion at 40°C	126
Figure (4-36) Fitting results of permanent deformation for the secondary portion at 60°C	127
Figure (4-37) Hydrated lime Influence on fatigue cracking relationship for Wearing course	131
Figure (4-38) Hydrated lime Influence on fatigue cracking relationship for Leveling course	132
Figure (4-39) Hydrated lime Influence on fatigue cracking relationship for Base course	133
Figure (4-40) Effect of Hydrated Lime on K1 fatigue parameter of asphalt mixtures	137
Figure (4-41) Effect of Hydrated Lime on K2 fatigue parameter of asphalt mixtures	137
Figure (4-42) Applied stress versus fatigue cycles to failure of Wearing course mixture	138
Figure (4-43) Applied stress versus fatigue cycles to failure of Leveling course mixture	139
Figure (4-44) Applied stress versus fatigue cycles to failure of Base course mixture	139
Figure (4-45) Applied stress versus Tensile Strain of Wearing course mixture	141
Figure (4-46) Applied stress versus Tensile Strain of Wearing course mixture	141
Figure (4-47) Applied stress versus Tensile Strain of Wearing course mixture	142
Figure (4-48) Hydrated lime Influence on the average fatigue life of asphalt mixtures	143
Fig (4-49) Schematic drawing of crack-pinning mechanism (Phillips and Harris, 1977)	144
Figure (4-50) Hydrated lime Influence on the average Initial Tensile Strain of asphalt mixtures	146
Figure (4-51) Hydrated lime Influence on the average Initial Flexural Stiffness of asphalt mixtures	147
Figure (4-52) Effect of hydrated lime on Controlled and after Freeze-Thaw cycle Tensile Strength of Wearing mixture	150
Figure (4-53) Effect of hydrated lime on Controlled and after Freeze-Thaw cycle Tensile Strength of Leveling mixture	150

Figure (4-54) Effect of hydrated lime on Controlled and after Freeze-Thaw cycle Tensile Strength of Base mixture	151
Figure (4-55) Hydrated lime Influence on Tensile Strength Ratio of Asphalt Concrete Mixes	152
Figure (4-56) TSR Gain of Asphalt Concrete Mixes Due to Hydrated Lime Addition	153
Figure (4-57) Optimum Hydrated Lime Percentage Regarding Pavement Performance as a Replacement of Mineral Filler	155
Figure (5-1) Typical Strategy for Regression Analysis (Kutner et al., 2005)	159
Figure (5-2) Fatigue life model new estimated versus observed values.....	183
Figure (5-3) Histogram of Regression Standardized Residual of Fatigue Life Model ($\ln N_f$)	184
Figure (5-4) Normal Probability Plot of Regression Standardized Residual of Fatigue Life Model ($\ln N_f$)	184
Figure (5-5) Scatter Plot of Regression Standardized Residual of Fatigue Life Model ($\ln N_f$)	185
Figure (5-6) Permanent deformation (ϵ_p) model new estimated versus observed values	185
Figure (5-7) Histogram of Regression Standardized Residual of Permanent Deformation Model ($\log \epsilon_p$)	186
Figure (5-8) Normal Probability Plot of Regression Standardized Residual of Permanent Deformation Model ($\log \epsilon_p$)	186
Figure (5-9) Scatter Plot of Regression Standardized Residual of Permanent Deformation Model ($\log \epsilon_p$)	187
Figure (6-1) Mechanistic-Empirical Design Approach Flow Chart	194
Figure (6-2) 80 kN (18-kip) ESAL Configuration.....	195
Figure (6-3) Dimensions of the Contact Area between Tire and Pavement (Huang, 2004)	199
Figure (6-4) Contour Atlas for Mean Annual Air Temperature of Iraq (IMOS website)	201
Figure (6-5) Temperature Effect on the Resilient Modulus of Wearing Course Mixtures	202
Figure (6-6) Temperature Effect on the Resilient Modulus of Levelling Course Mixtures	203
Figure (6-7) Temperature Effect on the Resilient Modulus of Base Course Mixtures	203
Figure (6-8) Influence of Temperature on the Resilient Modulus of Control Mixtures	204
Figure (6-9) Influence of Temperature on the Resilient Modulus of Modified Mixtures (2.5% of Hydrated Lime).....	205
Figure (6-10) Pavement Structure and Loading Configuration for FE Analysis	212
Figure (6-11) Mesh Density of FE Model in ANSYS	214
Figure (6-12) FEM of the Pavement Structure with Loading Configuration	215
Figure (6-13) Boundary Conditions of the pavement Model	216
Figure (6-14) SOLID45 Element Geometry (ANSYS 12, 2009)	217

Figure (6-15) CONTA174 Element geometry (ANSYS 12, 2009)	218
Figure (6-16) Targe170 Element geometry (ANSYS 12, 2009)	219
Figure (6-17) Newton-Raphson Iterative Solution (2 Load Increments) (ANSYS 1998)	220
Figure (6-18) The n-layer system in cylindrical coordinates (Huang, 2004)	222
Figure (6-19) Graphical Information of KENPAVE Inputs and Results (Case: 0% of HL, 230mm HMA Thickness)	223
Figure (6-20) Vertical Stress Distribution for Control and Hydrated Lime Modified Mixtures at Different AC Thicknesses	224
Figure (6-21) Vertical Strain Distribution for Control and Hydrated Lime Modified Mixtures at Different AC Thicknesses	226
Figure (6-22) Horizontal Strain Distribution for Control and Hydrated Lime Modified Mixtures at Different AC Thicknesses	228
Figure (6-23) Vertical Displacement Distribution for Control and Hydrated Lime Modified Mixtures at Different AC Thicknesses	230
Figure (6-24) Vertical Stress Contour Distribution	231
Figure (6-25) Vertical Displacement Contour Distribution	231
Figure (6-26) Vertical Strain Contour Distribution	232
Figure (6-27) Horizontal Strain Contour Distribution	232
Figure (6-28) HMA layer thickness versus tensile horizontal strain regarding HL Percent Effect	237
Figure (6-29) HMA layer thickness versus fatigue load repetitions regarding HL Percent effect	238
Figure (6-30) HMA layer thickness versus compressive vertical strain regarding HL Percent Effect	240
Figure (6-31) HMA layer thickness versus rutting load repetitions regarding HL Percent Effect	240
Figure (6-32) HMA layer thickness versus maximum damage ratio regarding HL Percent Effect	241
Figure (6-33) Effect of Thickness of Each Course on Tensile Strain	243
Figure (6-34) Effect of Thickness of Each Course on Fatigue Life	243
Figure (6-35) Effect of Thickness of Each Course on Compressive Strain	244
Figure (6-36) Effect of Thickness of Each Course on Repetitions to Rutting	244
Figure (6-37) Effect of Thickness of Each Course on Damage Ratio	245
Figure (6-38) The Ratio of Each Course Thickness to The Total Layer Thickness	246
Figure (A-1) Marshall Mix Design Properties for H1W mixture	274
Figure (A-2) Marshall Mix Design Properties for H1.5W mixture	275
Figure (A-3) Marshall Mix Design Properties for H2W mixture	276
Figure (A-4) Marshall Mix Design Properties for H2.5W mixture	277

Figure (A-5) Marshall Mix Design Properties for H3W mixture	278
Figure (A-6) Marshall Mix Design Properties for H1L mixture	279
Figure (A-7) Marshall Mix Design Properties for H1.5L mixture	280
Figure (A-8) Marshall Mix Design Properties for H2L mixture	281
Figure (A-9) Marshall Mix Design Properties for H2.5L mixture	282
Figure (A-10) Marshall Mix Design Properties for H3L mixture	283
Figure (A-11) Marshall Mix Design Properties for H1B mixture	284
Figure (A-12) Marshall Mix Design Properties for H1.5B mixture	285
Figure (A-13) Marshall Mix Design Properties for H2B mixture	286
Figure (A-14) Marshall Mix Design Properties for H2.5B mixture	287
Figure (A-15) Marshall Mix Design Properties for H3B mixture	288

ABBREVIATIONS

AADT	Annual Average Daily Traffic
AASHTO	American Association of State Highway and Transportation Officials
AC	Asphalt Cement
ANOVA	Analysis of Variance
ASTM	American Society for Testing and Materials
AV	Air Voids (%)
B	Base Course
CB	Control Base
CL	Control Leveling
CW	Control Wearing
D	Damage Ratio
D_d	Directional Distribution Factor
ESAL	Equivalent Single Axle Loads
EULA	European Lime Association
FEA	Finite Element Analysis
FHWA	Federal Highway Administration.
G_{mb}	Bulk Gravity of Mixture (g/cm ³)
G_{mm}	Theoretical Maximum Density of mixture (g/cm ³)
H1.5B	Base with 1.5% of Hydrated Lime
H1.5L	Leveling with 1.5% of Hydrated Lime
H1.5W	Wearing with 1.5% of Hydrated Lime
H1B	Base with 1% of Hydrated Lime
H1L	Leveling with 1% of Hydrated Lime
H1W	Wearing with 1% of Hydrated Lime
H2.5B	Base with 2.5% of Hydrated Lime

H2.5L	Leveling with 2.5% of Hydrated Lime
H2.5W	Wearing with 2.5% of Hydrated Lime
H2B	Base with 2% of Hydrated Lime
H2L	Leveling with 2% of Hydrated Lime
H2W	Wearing with 2% of Hydrated Lime
H3B	Base with 3% of Hydrated Lime
H3L	Leveling with 3% of Hydrated Lime
H3W	Wearing with 3% of Hydrated Lime
HL	Hydrated Lime
HMA	Hot Mix Asphalt
IMOS	Iraqi Meteorological Organization and Seismology
IQR	Inter Quartile Range
KENPAVE	<u>K</u> entucky Multilayer <u>p</u> avement program
L	Leveling coarse
MF	Marshall Flow (mm)
M-E PDG	Mechanistic-Empirical Pavement Design Guide
MLET	Multi Linear Elastic Theory
MR	Resilient Modulus
MS	Marshall Stability (kN)
N	Number of repetition to failure in permanent deformation
NCHRP	National Cooperative Highway Research Program
N_f	Fatigue life at failure repetition (cycle)
NLA	National Lime Association

OAC	Optimum asphalt content (%)
P200	Percent passing sieve number 200 of size equal 0.075 μm (%)
P4	Percent passing sieve number 4 of size equal to 4.75 mm (%)
P_A	Percent of aggregate by weight of total mix (%)
PCU	Passenger Car Unit
PRLS	Pneumatic Repeated Load System
P_s	Percent of added asphalt content by weight of total mix (%)
Q1	the first quartile, in which 25% of observed data values are lower than
Q3	third quartile, which is the value that 75% of observed data values are less than
R²	The coefficient of determination
SCRB	State Commission of Roads and Bridges
SHRP	Strategic Highway Research Program
SPSS	Statistical Package for the Social Sciences
SSD	Saturated Surface Dry
T	Temperature adopted in the laboratory tests (°C)
TSR	Tensile Strength Ratio
VFA	Voids Filled with Asphalt = $\frac{VMA-AV}{VMA} \times 100$
VMA	Voids in Mineral Aggregate = $100 - \frac{P_A \times G_{mb}}{G_{A\ bulk}}$
W	wearing course
ε_p	Permanent micro strain at load repetition (N)
ε_t	Initial tensile micro strain

Chapter One

Introduction

1.1 General

The flexible pavement is the most widely paving system adopted in many countries all over the world. The reasons for using this form of paving are; the availability of raw materials (aggregate, mineral filler and asphalt cement), economy and comparatively ease of construction and maintenance. Besides, the flexible pavement is capable of withstanding traffic loading through the resistance of the applied stresses on its surface and transfer them with a gradual decrease into lower layers. In details, the asphalt concrete layer is prepared of a flexible mixture of higher stiffness to provide a stable, durable and safe traffic use quality surface with a suitable skid resistance, while the granular layers are designed to transfer and distribute the loads safely to the subgrade layer. The subgrade layer is also compacted and designed to withstand traffic loading. In general and based on many construction design standards and requirements, such as the Iraqi standards, the flexible pavement consists of about three major layers constructed on the subgrade layer. The forms of layers could be; subbase, granular base, and asphaltic layer (leveling (binder) and wearing course) or granular subbase with the asphaltic layer (base, leveling (binder) and wearing).

The need for improved mechanistic procedures for design, maintenance, and rehabilitation of highway and airport pavements has been recognised for many years. Mechanistic methods are based on the principles of mechanics in contrast to the particular purpose and empirical procedures that are often used (NCHRP, 2004).

The Mechanistic-Empirical Pavement Design Guide (M-E PDG) is an important and improved guide for pavement design, which considered as the chain between mechanical characteristics and models and empirical concepts and equations. The method developed by the researchers in a project under the National Cooperative Highway Research Programme (NCHRP 1-37, 2004). The NCHRP is administered by the Transportation Research Board (TRB) and sponsored by the member departments of the American Association of State Highway and

Transportation Officials (AASHTO), in cooperation with the Federal Highway Administration (FHWA) (trb.org, 2017).

The project represents a major advancement in pavement design and analysis. It uses site specific traffic and climatic conditions and materials properties to predict cracking and rutting performance of flexible pavement structures. The inclusion of basic material properties into distress prediction models through fundamentally based test methods has facilitated the design of pavements based on site and material characteristics (NCHRP, 2004).

In the application of total or gradual increasing axle load, the stress and strain mostly determined and adopted in empirical equations in order to find permanent deformation and fatigue cracking damage in a condition of repetitive mechanical and thermal loading to failure. Generally, pavement mechanical responses are used to determine many distresses with the empirical formulas. These responses are the tensile strain at the bottom of asphalt concrete layer, the compressive strain that occurred vertically at the top of the subgrade layer, vertical stress on the pavement surface under tire pressure and tensile stress at the bottom of the asphaltic layer (Huang 2004).

The hot mix asphalt (HMA) mechanical properties are mainly affected by paving materials characteristics and mix design, and these influencers are binder type, aggregate blend and properties, asphalt concrete mixture volumetric properties and the modifications of asphalt cement or aggregate. Positive influence on the mechanical properties of hot mix asphalt has been found through hydrated lime treatment (Sebaaly, 2006). The hydrated lime particles structure is of various-sized portions. The larger particles act as a filler and enhance the stiffness of the asphaltic mixture while the smaller particles increase the asphalt viscosity and improve its cohesion (Mohammad et al., 2000). The hydrated lime has been successfully used in asphaltic paving mixtures for a long time, and it is still an active research area as explained by the high number of recent publications. As seen in chapter two, literature approved the efficiency of hydrated lime in improving the asphaltic concrete mixtures resistance to the main distresses that may happen in the flexible pavement, i.e., rutting, fatigue cracking and moisture damage.

1.2 Problem Statement

Heavy and repeated traffic loads and the variation of environmental conditions are two of the main factors causing the development of distresses, such as moisture damage, fatigue cracking,

and the accumulation of permanent deformation (rutting) in flexible pavements. Accordingly, there is a crucial need for enhancing the ability of asphalt concrete mixture to resist distresses happened in the pavement. Asphalt mixes may need to be modified to satisfy the desired specification requirements. Modification by additives is one of the techniques adopted to improve pavement properties. One of the effective additives is the hydrated lime (i.e., calcium hydrate [Ca(OH)₂]) that is relatively available and cheap material as compared to other additives and modifiers like polymers. Recently, the use of hydrated lime as mineral filler and antistripping material, fatigue and permanent deformation resistant material has raised more attention.

Employment of hydrated lime as a filler material in the construction of asphalt concrete pavement (wearing, leveling and base asphaltic mixes layers) could be a significant step of the possible steps for enhancing the asphalt paving mixtures physical characteristics as well as improve material performance related properties to fit the required standards.

Research and development in the structural design of hot mix asphalt (HMA) pavements over the past fifty years has focused on the shift from empirical design equations to a more powerful and adaptive design scheme (Angela et al., 2006).

The Mechanistic-Empirical design process that presented by the NCHRP 1-37 (2004), which is based on the methods in (AASHTO, 1993), could be one of the important steps for the contribution of development of the flexible pavement design. The Mechanistic-Empirical design of flexible pavements involves an iterative process by the designer. The designer must perform a trial pavement design and then analyse the design to decide if it fits the performance criteria set by the designer. Adjustment is needed when the design does not meet the performance criteria and repeat analysing until reaching the required performance criteria (NCHRP 1-37A, 2004). The process of iteration is performed on pavement layer thickness after considering the design input parameters to reach the optimum asphalt concrete layer thickness in which the trial design section meets the performance criteria.

The new M-E PDG represents a challenging addition in the way that pavement design and analysis is conducted. However, the M-E design method still under validation-implementation by researchers and design agencies.

Implementation of a new aspect or idea into this important pavement design method could be a step of contribution to developing it with other researchers proposals. Additional work could

be introduced to the M-E design process through modification of pavement asphaltic mixture by hydrated lime and try to use the modified mixture in the iteration process instead of increase asphalt concrete layer thickness directly. In other words, during the iteration process of M-E pavement design and after calculating the damage ratio of a trial case of a control asphalt concrete thickness, in case of the layer thickness is not adequate, there will be another try for the same thickness but with modified mixtures with optimum hydrated lime percent instead of going for increasing the layer thickness directly. This could be a useful step in the process to reach an optimum thickness of asphalt concrete layer that meets the performance criteria (fatigue cracking and permanent deformation failure criteria models) with less thickness as compared with control mixtures.

In conclusion, the enhancement of the paving material performance-related properties during design is an important step to reduce the efforts, pavement layers and cost of paving construction with the increment in serviceability and design life. The advantages of adding hydrated lime into the asphalt mixture can be used to improve resistance to fatigue cracking and permanent deformation and introduce a step in thickness optimisation process of M-E design using a modification of mixtures by hydrated lime. The fatigue cracking and permanent deformation are utilised as main factors in the Mechanistic-Empirical approach adopted in this study.

1.3 Aim and Objectives

The aim of this research is to provide a framework for the Mechanistic-Empirical design approach of flexible pavement with the implementation of hydrated lime effect on the asphalt concrete mixture during the optimisation of pavement thickness in the design process. The method could be used by local agencies and design engineers in Iraq instead of the currently used methods that based on the empirical approach. Mechanistic procedures are based on the principles of material mechanics and pavement structural responses in contrast to empirical procedures that are often used.

To achieve the aim of the study, the objectives can be summarised as follows:

1. Investigate the influence of adding hydrated lime as partial replacement of the mineral filler of the mix on the performance-related properties of the asphalt concrete mixtures. The use of hydrated lime is not a new concept; hence the Iraqi standard specification (SCR/R9, 2003) has

identified the importance of introducing 1.5% of hydrated lime by total weight of aggregates since 2003. However, there is a need for further research efforts to achieve the following goals:

- To evaluate and compare the laboratory performance-based properties (Marshall stability and resistance to plastic flow, volumetric properties, resistance to fatigue cracking, resistance to permanent deformation at different temperatures and the moisture susceptibility) between the hydrated lime modified asphalt concrete mixtures and the control (non-modified) ones.
- To determine the optimum content of hydrated lime that gives the best results for improving the performance of asphalt mixtures regarding the major distresses that usually happen in the flexible pavement such as fatigue cracking, rutting (permanent deformation) and moisture damage. In this study, a thorough investigation was performed on different types of asphalt concrete courses, i.e., wearing, leveling (binding), and base which represent the sublayers of asphalt concrete layer in the flexible pavement system.

2. After determination of the optimum percent of hydrated lime in the mixtures, a study is needed for employment of hydrated lime influence on asphalt concrete mixtures in the Mechanistic-Empirical design approach for calculating the desired optimum Hot Mix Asphalt (HMA) layer thickness. The design is based on estimating the pavement critical responses (stresses and strains) at specific (critical) locations in the pavement structure utilising numerical modelling. The design also relies on the long-term performance analysis and failure criteria (allowable number of load repetitions related to fatigue cracking and rutting). According to critical pavement responses and the failure criteria output, iteration process may be applied to reach the optimum value of asphalt concrete thickness considering modification with hydrated lime.

1.4 Research Methodology

Three aggregate gradations were implemented in this research, which belong to wearing, binder and base course. One source of aggregate included in the test factorial was the crushed stone aggregate from Alnibaie Quarry north of Baghdad. One type of asphalt cement of 40-50 penetration grade were brought from Aldurah refinery located in the south of Baghdad. For the preparation of mix design, Marshall Procedure was followed after finishing the test of all the raw materials and confirming that these materials satisfied the requirement of Iraqi specifications (SCR/R9).

Ordinary limestone dust and hydrated lime were used as mineral fillers in this study. The total percent of mineral filler in the mixes were 7%, 6% and 5% by total weight of aggregate for Wearing, Leveling and Base courses respectively. Five different percentages (1.0%, 1.5%, 2.0%, 2.5% and 3.0%) of hydrated lime were added as partial replacement of limestone dust. The application of hydrated lime into the mixtures was made by adding dry hydrated lime following the usual procedure of adding mineral filler.

The experimental programme conducted in this study contains two main steps. Firstly, the design of asphalt concrete mixture following Marshall design procedure. The use of Marshall apparatus is to obtain the optimum asphalt content in specific values of stability, air void and density for control and hydrated lime modified mixes. Furthermore, this method covers the evaluation of mixtures' resistance to plastic flow (Marshall stability and flow). Secondly, the determined optimum asphalt contents were used in preparing further mixes specimens with different geometry and size for fatigue cracking and permanent deformation tests. The prepared mixes were evaluated for permanent deformation and resilient modulus at 20°C, 40°C and 60°C, and fatigue at 20°C under the repeated loading using the Pneumatic Repeated Load System (PRLS) as well as moisture susceptibility.

The next step of the study is designing of flexible pavement considering the influence of hydrated lime on the mixtures performance by adopting the Mechanistic-Empirical design method to reach an optimum thickness of the asphaltic concrete layer. The mechanistic part of M-E design was made by numerical three-dimensional finite element modelling of a flexible pavement of five layers by adopting the general-purpose programme, ANSYS, to calculate the pavement responses (maximum stresses and strains) at specific (critical) locations in the pavement structure. The results were validated with the pavement axisymmetric multi-layered elastic analytical software, KENPAVE, and the outputs were close and acceptable with average differences of around 12%. The M-E method adopted failure criteria models, fatigue life and rutting, and damage ratio (Miner's hypothesis) to estimate the allowable load repetitions to failure based on the values of critical tensile and compressive strains at the bottom of the asphalt concrete layer and the top of subgrade layer respectively. Accumulative deformation at the surface of wearing course was studied as well. An iterative process was done to calculate the critical damage rate for each trial case mixture (thickness of the layer and hydrated lime percentage) to determine the minimum asphalt concrete layer thickness required to withstand loading conditions. The effect of climate

(air temperature) was adopted in the design method by finding relationships between the temperature and resilient modulus for each type of asphalt concrete mixture based on the laboratory work achieved in this study. Later, a study was conducted to find the temperature at the centre of each asphalt concrete layer as related to the ambient temperature and finally estimating the variation of pavement layers stiffnesses with respect to pavement depth due to the change in temperature. The flow chart in the Figure (1-1) explains the general steps of the Mechanistic-Empirical pavement design method presented by AASHTO through the NCHRP 1-37, 2004.

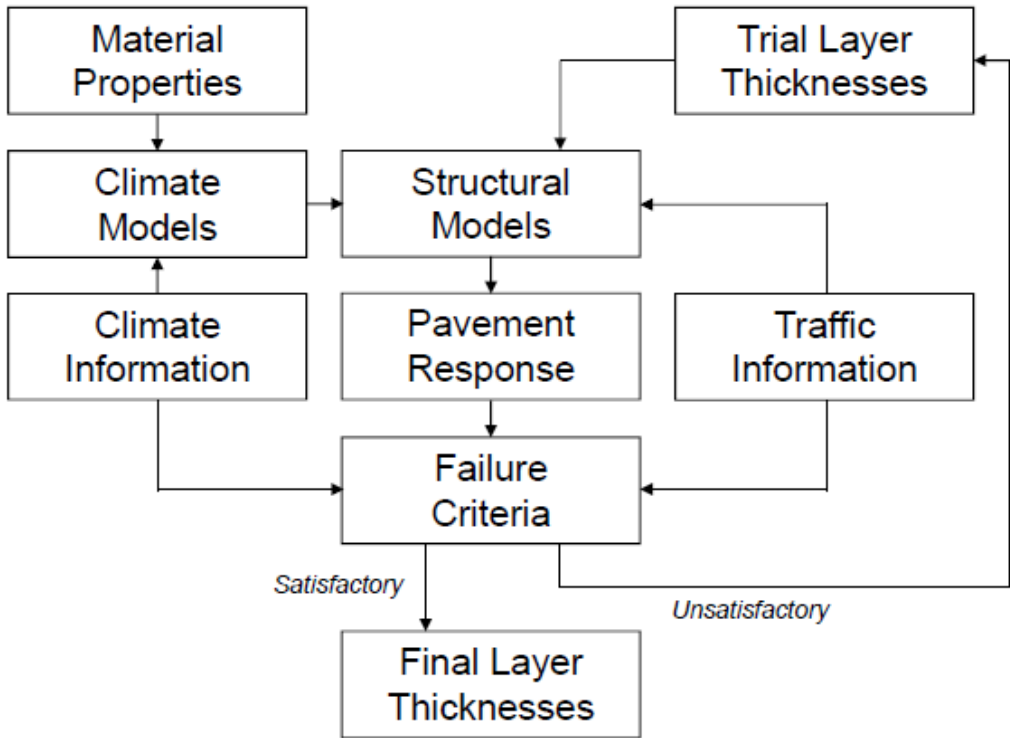


Figure (1-1) Mechanistic-Empirical Approach Flow Chart (NCHRP 1-37, 2004)

1.5 Structure of the Thesis

This thesis is made up of seven main chapters as described below:

- 1. Chapter One** begins with the general background, provides problem statement, describes the study aim and objectives, gives a brief description of the research methodology and lists the thesis outline.

2. **Chapter Two** shows the review of the literature regarding the influence of hydrated lime on the asphalt concrete mixtures, the permanent deformation (rutting), fatigue cracking and mechanistic and empirical design with the presentation of several models of rutting and fatigue cracking. In addition, a review of the techniques adopted for pavement analysis and design were presented in this chapter. Several pavement mechanistic methods were presented such as multilayered elastic theory and finite element analysis by using computer software of variable techniques like axisymmetric, two or three-dimensional analysis.
3. **Chapter Three** explores the materials used in the study and methodology in details. This chapter includes the material properties and data calculation approaches and tests used to achieve the goals. The approaches were offered in several sections corresponding to the defined goals listed in chapter one.
4. **Chapter Four** introduces the laboratory work results and discussion. Findings are presented and discussed in details.
5. **Chapter Five** presents a statistical analysis of laboratory work outputs and performance related parameters. Multi-linear regression models of fatigue life and permanent deformation were developed as related to hydrated lime influence and the other properties of asphalt concrete mixtures.
6. **Chapter Six** involves an application of a Mechanistic-Empirical (M-E) approach that based on the review and background mentioned in chapter one and chapter two with a modification in the way of iterations of asphaltic layer thickness estimation. The modified M-E approach was adopted to decide the optimum thickness of asphalt concrete layer in the flexible pavement regarding the effect of the optimum percent of partially added hydrated lime as filler into the asphaltic mixtures.
7. **Chapter Seven** provides the conclusions and recommendations.

The thesis also involves an appendix of Marshall design properties in details with graphical presentation of Marshall and volumetric characteristics of the studied asphalt concrete mixtures.

Chapter Two

Literature Review

2.1 General

This chapter is divided into two main sections. The first part, a literature survey of the influence of lime modification on the performance-related properties of flexible pavement is presented. The second section is a review of the development of mechanistic-empirical design method and its failure criteria and local models and forms submitted by other researchers and agencies as well as presentation of numerical methods of modelling and analysis of flexible pavement.

There are four main patterns of distresses happen in flexible pavement; rutting, fatigue cracking, thermal cracking and moisture damage. The rutting is caused by high temperature and heavy traffic loading while the fatigue cracking is caused by high application of load repetitions in moderate temperatures. The moisture and ageing damage are considered as significant distresses that affect the asphalt concrete pavements. Thermal cracking happens at low temperatures when thermal stresses exceed the fracture limit of the pavement mixtures strength (Asam, 2011).

There has an important development in many aspects of life with the construction growth that started a long time ago. Mostly, every change or development in any field has advantages and disadvantages and accordingly, this has resulted in increased traffic volume higher than the design load volume. The heavy traffic loads, as well as high ambient air temperatures, are the main factors that contribute to the development of distresses in both newly constructed and mature, flexible pavements. The distresses; permanent deformation (rutting) and fatigue (alligator) cracking as well as moisture damage are the most significant failure forms observed in the flexible pavement.

Highways and roads are crucial in all of the world's cities including Baghdad, and it is vital to assess materials performance and design criteria before and after construction to reach the optimum design set regarding local conditions. Moreover, the evaluation of pavement material and design process will lead to an efficient maintenance process on the pavement in short and long term of pavement design life. Jony (2010) reflected evidence about a deterioration of asphalt mixture properties after construction, regarding the distresses appearing in the pavement, through

an observation of laboratory tests on asphalt mixtures and the repetition of divergence failures in the field. He made a comparison of deviations between results of laboratory tests for flexible pavement in Baghdad roads and sites actual performance of mature pavement after a given period indicating a marked divergence. He adopted his study through evaluation of aggregate gradation of the asphalt mixture, bitumen percentage, Marshall stability, the degree of compaction and asphalt layer thickness.

2.2 The Bond in Asphalt Concrete

2.2.1 The Role of Asphalt Binder in the Mixture

A review of asphalt cement components is necessary to understand the bonding between asphalt and aggregate in the flexible pavement structure. In a Strategic Highway Research Program (SHRP) report made by Robertson (1991), he reviewed the chemical characteristics and asphalt components. Asphalt binder is involved different hydrocarbon molecular groups, such as aliphatic, aromatic carbon, and a combination of both of aliphatic and aromatic carbon segments. These functional groups play a significant role in the interaction between asphalt cement and aggregate surfaces. The interfacial bonding strength relies on the relative tendency of the functional groups to be adsorbed onto the aggregate particles surfaces and replaced by water.

Studies made by Plancher and Petersen (1976), Plancher et al. (1977), Crutis et al. (1992), and Petersen et al. (1987) classified the tendency of bitumen functional groups to adsorb onto and debonding from the aggregate surfaces. The most actively adsorbed polar composites, like carboxylic acids and anhydrides, shows that they are sensitive to water effect and can be replaced by water easily. Other components like ketones nitrogen-based pyridines and phenolics seem to be more resistant against water influence.

2.2.2 The Influence of Aggregate characteristics on adhesion

The Aggregates typically produce a complex surface onto that particular bitumen chemical functionalities preferentially adsorb by associating with aggregate adsorption positions (Roberts et al., 1996). The interfacial bonding forces depend on the kind of aggregate surface and its activities, which themselves rely on the characteristics of minerals and the present metallic ions. Typical minerals in aggregates comprise silica, feldspars, ferromagnesian, limestone and clay minerals (Roberts et al., 1996).

Petersen et al. (1987) demonstrated that silica mineral (SiO_2), rich in quartz, composes the majority of quartzites and granites. Silica is essential due to its natural plenty of siliceous surfaces in about the most of the aggregates used in constructions. Active places on these surfaces range from surface hydroxyl groups of variable acidities to hydrogen bonding places of high acidity. Furthermore, Little and Jones (2003) remarked that feldspar minerals have mobile species within their crystal structures. Limestone is composed essentially of CaCO_3 which, after crushing, shows calcium ions with electropositive properties. The calcium ions are then available for competition between water and bitumen. Cheng et al. (2002) measured the bonding energy using a sorption device, and they found that the limestone has a higher bonding energies per unit mass than the granite. Little and Petersen (2005) studied the stripping in the asphalt pavement mix, and they found that the aggregate surfaces with metallic elements, like calcium, showed enhancement in the resistance to stripping. The improvement is because of that such metallic elements adequately connect with acids in bitumen, and create hydrophobic salts that are not soluble in water. Jamieson et al. (1995) found that interfacial bonding is increased by relatively high concentrations of iron, calcium, magnesium and aluminium at the aggregate surface. Yoon and Tarrer (1988) stated that some of the aggregate physical characteristics that affect moisture susceptibility are the surface roughness, porosity, shape, and friability. The more the rough aggregate particles surface, the more bonding between them.

2.2.3 Mineral Filler Influence on the Mixture

American Association of State Highways and Transportation Officials (AASHTO, 2007) defined mineral fillers as finely divided mineral material such as limestone dust, slag and rock dust, fly ash, cement, hydrated lime or other fine mineral material. In general, mineral fillers have two benefits for asphalt concrete mixtures. The first one is their importance as a portion of the aggregate that fills the air voids between the other coarser aggregate particles in the hot mix asphalt (HMA) and thereby strengthen the mixtures. Secondly, through the mixing process, the asphalt and filler form the mastic (a binder with a higher consistency), which bonds coarser aggregate particles together. The majority of the filler stays suspended in the binder while the minority is a part of the bearing framework (Harris and Stuart, 1995). Mastic, which is a material that higher in consistency than the asphalt cement, can make the asphalt concrete stiffer and enhance the

adhesive ability. Besides, it produces thicker asphalt binder that reduces the time of ageing process in the pavement.

Kavussi and Hicks (1997) found that fillers can enhance the workability and affect the compaction process and air void in the asphalt mixture. They reported that using different mineral fillers with variable properties leads to the change in physical and/or chemical properties of the resulted asphalt cement. The change depends on the following factors:

1. Type and source of mineral filler (limestone dust, fly ash, hydrated lime, etc.)
2. Physical and chemical effectiveness of the filler, and
3. The concentricity of the filler used in the mixture.

The mineral fillers have to be supplied to the asphalt concrete mixture constantly with the exact proportions, or else, the properties of asphalt mix will be harmfully influenced. The excessive amount of mineral filler minimises the Voids in Mineral Aggregate (VMA) to a limit where an adequate content of asphalt cement cannot be added to a durable mixture. Furthermore, high amount of filler increases the surface area of aggregate and that will significantly decrease the thickness of asphalt cement film that coats the aggregate surface (Lee, 2007).

Mineral filler characteristics vary with the particle size of the filler. If the mineral filler particles size is smaller than 10 microns, the filler acts as an extender (increase the asphalt cement effectively by increasing the asphalt cement volume in the mix) of the asphalt cement since the thickness of most asphalt films in dense-graded HMA is less than 10 microns. While, when the mineral filler size is higher than 10 microns, it functions more similar to aggregate. If an excessive quantity of the larger sized particles of mineral filler is present, the asphalt content may increase because of increased VMA. Thus, it is necessary to take into consideration the mineral filler particles size accompanied with its amount in the mixture for evaluation of designed mix to examine the presence of an excessive mass of fine materials (Roberts et al., 1996).

When the asphalt cement and filler are mixed with a lack of amount to achieve the minimum air void, this will lead to a stiff mortar in a dry condition while the extra quantity of the asphalt cement reduces the stiffness of the asphalt concrete mixture (Harris and Stuart, 1995).

Figure (2-1) shows the volumetric conception of asphalt and filler in the asphalt concrete mix. The Figure explains the volume of asphalt and mineral filler before and after mixing. The amount of the volume occupied by the fixed asphalt (asphalt infiltrated into the fillers voids) depends on the type of mineral filler.

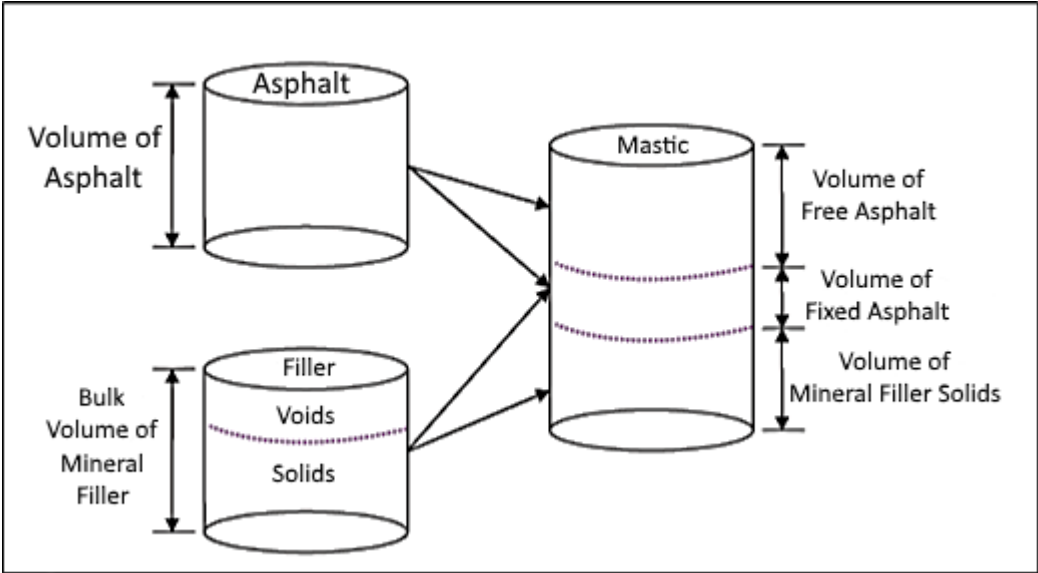
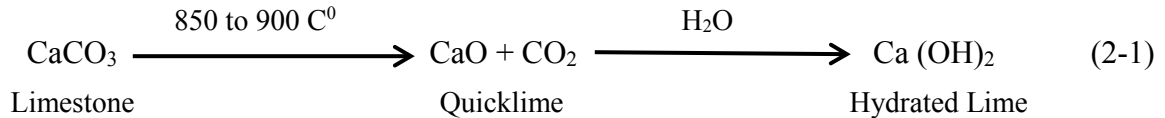


Figure (2-1) Components of Asphalt Mastics (Harris and Stuart, 1995)

However, the increase of the mastic stiffness may result in brittle mixtures, which may crack under low-temperature conditions. Based on the research of Chen and Peng (1998), the direct tensile test results on mastic (asphalt cement and mineral filler mix) show that there is an increase of tensile stress and strain as a result of adding more mineral filler.

2.3 Hydrated Lime

The Hydrated lime (Ca(OH)_2) is a dry dust. The main part of its components is the calcium hydroxide Ca(OH)_2 . The hydrated lime is made by applying hydrating process (by a specific system called hydrators) of quicklime, which is basically calcium oxide (CaO). Quicklime is produced by applying high temperature (around 900°C) on highly pure limestone that manufactured of calcium carbonate (CaCO_3) in dedicated ovens (Boynton 1980). The formula presented below shows the production of hydrated lime from limestone (Crossley, 1998).



The main physical characteristics of lime for soil stabilisation, as addressed by Boynton (1980), are specific gravity, bulk density, particle size, the heat of hydration and solubility of hydrated lime. The molecular weight of CaO and Ca(OH)₂ are 56.08 and 74.10, respectively, due to the additional H₂O molecule connected. The molecular weight ratio provides the equal amounts of lime available to react with the soil. High calcium lime provides more available calcium for stabilisation than Mg(OH)₂ because Ca(OH)₂ is about 100 times more soluble. Moreover, MgO in dolomitic quicklime may delay the reaction rate of lime that results in the expansion after compaction due to its hydration being slow, although it does not influence the Ca(OH)₂ solubility.

In the application of hydrated lime, the National Lime Association (NLA, 2006) reported that the ordinary grade of the hydrated lime, which is adequate for the majority of chemical purposes, must have to pass 85 percent or more the sieve No.200 (mesh size of 75 µm). For particular usage, the passing percentage must be 99.5 at least the sieve No. 325 (mesh size of 45 µm).

Hydrated lime has considered as a useful additive to enhance the performance properties of hot mix asphalt pavement. The addition of the hydrated lime to low-grade aggregate will make the aggregate in the mixture more suitable for pavement construction usage. Occasionally, the coating of the aggregate surface with the asphalt cement is not easy due to their acidic nature. Although, the adding of hydrated lime increases the percentage of coated surfaces area and improves the bonding between aggregate and asphalt cement (Boynton, 1980).

The European Lime Association (EuLA) in 2010 justified that the reason behind the effect of hydrated lime in asphalt mixtures is the proper bonding between the main components of the asphalt concrete mixture; bitumen and aggregate. The influence of hydrated lime could be on both of the aggregate particles and the asphalt cement. The hydrated lime has been noticed to be able to modify of the roughness (precipitates) and composition (ions of calcium) of the surface of aggregate, making it more adhesive to bitumen material (asphalt). Furthermore, the hydrated lime could treat the adhering between the small clayey particles and the aggregate surface, minimising

their negative influence on the asphalt concrete mixture (by forming a weak film between the aggregate and the asphalt cement, which can be displaced by water). EuLA (2010) mentioned that the high porosity of hydrated lime could demonstrate its stiffening influence on bitumen at moderate and high temperatures due to the increase of the mastic viscosity because of the high volume of solids. The temperature reliance and the kinetics of the stiffening influence might show that the hydrated lime is not always stiffened asphalt concrete mixtures and its efficiency could be more noticeable in the regions with high temperatures in which the permanent deformation (rutting) is considered as the main distress.

The employing of hydrated lime has a strong influence on the durability of asphalt mixtures. The agencies in the North American States and relying on their field experience, found that the addition hydrated lime enhances some performance properties of asphalt concrete mixtures. An addition of about 1% to 1.5% of hydrated lime (by the weight of aggregate) increased the durability of asphalt concrete pavements by about by 20% to 50% of the service life, and that means 2 to 10 years (EuLA, 2010).

2.4 The Influence of Hydrated Lime

2.4.1 Volumetric and Performance-Related Properties of Hot Mix Asphalt

Many studies have been carried on to investigate the influence of hydrated lime on asphalt concrete mixtures; Albayati (2012), Little and Epps (2001), Sebaaly et. al. (2001) and Albayati and Ahmed (2013). They found that asphalt pavement mixtures that modified by hydrated lime gained a reduction in asphalt hardening age, the increase of flexural stiffness and resilient modulus under moderate and high temperatures. Furthermore, they observed improvement in the pavement durability, enhancement of the ability to resist permanent deformation, significant efforts in the resistance to fatigue (alligator) cracking, improvement in asphalt pavement resistance to thermal cracking, and moisture damage.

The addition of hydrated lime as a replacement of the mineral filler has a significant effect on mixture volumetric properties. The mixes with higher hydrated lime content possess higher optimum asphalt content due to the high surface area of hydrated lime particles. The maximum value of optimum asphalt content (5.34%) was achieved at 3% of hydrated lime addition, as compared to the lowest value of asphalt cement content (4.73%) that obtained at 0 % of hydrated lime (Albayati, 2012).

Satyakumar et al. (2013) adopted a study on the influence of three types of mineral fillers; fly ash, phosphogypsum and hydrated lime. They found that adding 1.5% of hydrated lime by the total weight of specimens increased stiffness modulus up to 54.99% as compared to the original mix. The addition of the same percentage of the other two mineral fillers showed a slight increase in stiffness in comparison with hydrated lime (8.06% for fly ash and 8.43% for phosphogypsum). They concluded that the most beneficial mineral filler among the studied types is the hydrated lime, and its optimum percentage that gave the best results is 1.5% by the total weight of the mix. The effect of hydrated lime is presented in Figures (2-2) to (2-4) that show the output of tests related to the study representing static creep, dynamic creep and the indirect tensile tests results respectively.

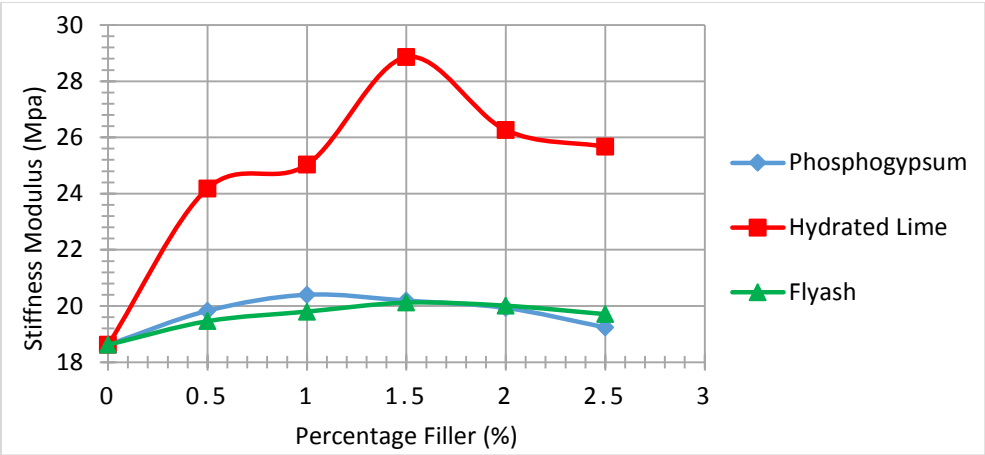


Figure (2-2) Static creep test results (Satyakumar et al., 2013)

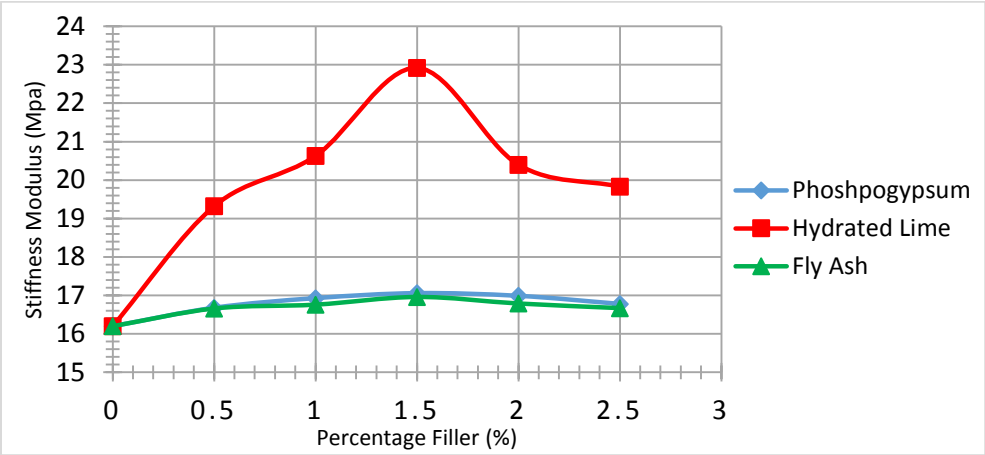


Figure (2-3) Dynamic creep test results (Satyakumar et al., 2013)

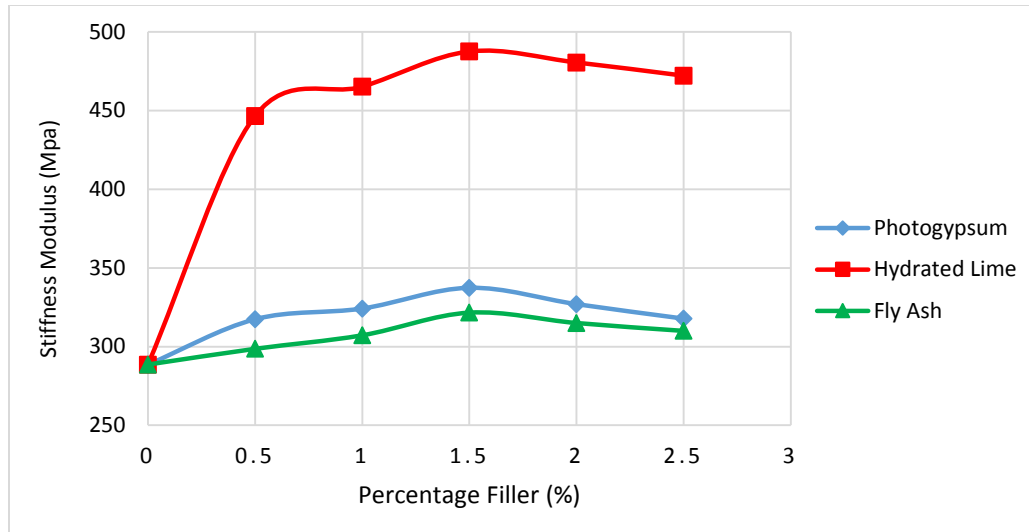


Figure (2-4) Stiffness modulus test results (Satyakumar et al., 2013)

Albaiti (2012) studied the influence of Polystyrene and hydrated lime as additives to asphalt cement on the indirect tensile strength and predicted a statistical model of indirect tensile strength in asphalt concrete paving materials under the local prevailing conditions. The author pointed out that an optimum value of 5% of hydrated lime and 6 % of polystyrene improved the tensile strength and temperature susceptibility of the asphalt mixture. The model indicated that the value of indirect tensile strength increased with the increase of hydrate lime amount, Polystyrene resins, aggregate max size, the asphalt content and the number of blows (compaction effort). In addition, the tensile strength value decreased with the rise of temperature. The test was conducted according to the (ASTM D 4123) standards. The indirect tensile strength was calculated as follows:

$$ITS = \frac{2000P}{\pi dt} \quad (2.1)$$

Where:

P = the ultimate applied load to failure (N),

d = the diameter of the specimen (mm), and

t = the thickness of the specimen (mm).

2.4.2 Moisture Susceptibility

The moisture damage happens due to the debonding between the aggregate particles surfaces and the binder (asphalt cement) as a result of water presence on the interfacial area between the binder and aggregate particles. This failure leads to deterioration of strength, stiffness and durability in the asphalt mixture. Moisture damage in asphalt pavement is considered as a premature failure and frequently happens within a few years after construction (Lee, 2007).

The hydrated lime has been confirmed as an important and powerful mineral filler or additive for asphalt concrete mixtures. The reason for its importance is its ability to enhance the properties related to fatigue performance and moisture resistance. The reactions between hydrated lime and asphalt mixture components are in both physical and chemical ways. As an inert mineral filler, hydrated lime physically decreases the volumetric asphalt content through the filling of air voids. Besides, it can increase the fatigue resistance and the stability due to the dispersion of small mineral particles in the asphalt mix in which will prevent cracks from development and growth (Sangyum et al., 2011).

Sangyum et al. (2011) conducted a laboratory work to evaluate the impact of hydrated lime on asphalt concrete mixtures performance and volumetric properties. They assessed the behaviour of mixes for both conditioned (moisturised) and unconditioned (dry) specimens and compared the results. They found that with the addition of hydrated lime, the mixtures became more resistant to moisture damage, rutting and fatigue cracking.

Kandhal (1992) declared the importance of the type of mineral filler in the asphalt concrete mix. He found that excessive amount of dust and presence of clay particles that coat the aggregate surfaces lead to pavement failure due to moisture effect. This issue can frustrate the required contact between the bitumen and aggregate particles by providing a path for water to penetrate in between them. He reported that there are other factors like unequal aggregate drying which produced a moisture content residual in aggregate also leads uncoating of aggregate surfaces and eventually makes the mixture more susceptible to moisture.

Hydrated lime addition to the asphalt mix, and due to its reaction with the aggregate surface, leads to reinforcing the bonding between asphalt and aggregate. In the same time of treating aggregate, the hydrated lime reacts with bitumen as well. In the asphalt concrete mix, the high polar molecules of asphalt react to create water soluble solvents that advocate moisture

damage such as stripping. The hydrated lime reaction with these polar molecules produced unsolvable salts in which water is not attracted anymore (Petersen et al., 1987). Moreover, the scattering of the small hydrated lime particles in the mix produces a stiffer and tougher mix, through diminishing the chance that the bonding between the aggregate surfaces and asphalt cement will be mechanically broken, even with the absence of water.

According to Huang et al. (2010), lime is very chemically active in nature; this makes it very effective to reduce moisture damage to asphalt pavements. Huang cites three major mechanisms that contribute to the effectiveness of lime. Firstly, the reaction between lime and the aggregate surface leads to the chemical product that strongly bonds with asphalt cement regardless moisture existence. Secondly, lime reacts with silica and calcium in aggregate to produce calcium-rich bonding surface for the acidic polar elements of asphalt cement. Thirdly, hydrated lime reacts with the carboxylic acids and 2-quinolones in the asphalt cement reducing the amount of polar components of water to react and bond with the active surface of the aggregate.

Huang et al. (2005) investigated the impact of hydrated lime addition on the moisture resistance of HMA through the indirect tensile strength test. They added the hydrated lime directly to the binder before mixture preparation. Based on the results, they found that the resistance to moisture damage was significantly improved.

Esarwi et al., (2008) tested two types of asphalt binders, each with and without hydrated lime. They used both Marshall and Superpave mix design procedures by adding 2% hydrated lime of the total weight of the aggregate. They found that the majority of the hydrated lime modified specimens were able to meet acceptable Tensile Strength Ratio (TSR). Also, a few mix designs that originally failed to meet TSR requirements without hydrated lime were able to meet those requirements with hydrated lime.

Gorkem and Sengoz (2009) conducted a similar study using hydrated lime at 1, 1.5 and 2.0% concentrations, and two types of aggregates; basalt and limestone. They observed that by adding lime to both aggregate types, the Tensile Strength Ratio (TSR) increased. However, a much more significant increase was shown for the basalt aggregate as compared to limestone. The authors suggested that this significant increase could be due to that hydrated lime forms indissoluble salty components on the aggregate surfaces leading to improved bonding.

Haung et al. (2010) studied how the lime particle fineness affected its performance as an asphalt anti-stripping additive. To accomplish this, they placed commercially available lime in a Los Angeles abrasion machine for a set of rotation times; 0, 500, and 2500. This device pulverised the particles into smaller particles with increasing revolutions. Afterwards, a 1% concentration of the lime was added to an asphalt mix from which specimens were made and tested for moisture damage. Results showed that increasing the fineness of lime particles increased the TSR.

Boyes (2011) studied the performance of several asphalt additives against moisture damage: Cement Dust, fly ash, limestone and a chemical anti-stripping additive on modified Lottman indirect tensile test (AASHTO T 283) and the immersion-compression test (AASHTO T 165). Hydrated lime was added by 1%, 1.5%, and 2% as a slurry, wet and directly mixed with asphalt. The tests result indicated that Tensile Strength Ratio (TSR) values were higher than those for the control mixes. The hydrated lime produced enhanced resistance to moisture damage among the other additives. Regarding the index of retained compressive strength, he found that the fly ash specimens had the highest value followed by hydrated lime, then anti-stripping agent and finally cement dust treated specimens.

2.4.3 Fatigue Cracking

Fatigue cracking is the accumulation of damage happens due to the effect of enormous load repetitions applied on the asphalt pavement (Pell, 1962). The fatigue cracking usually happens in moderate temperatures while rutting often occurs at high temperatures. The reason for this is that the hot mix asphalt is more brittle and stiffer in moderate temperatures. Brittle materials have a tendency of cracking instead of deformation under the load repetitions (NCHRP 673, 2011).

In the last four decades, several studies have demonstrated that fatigue (alligator) cracking of asphalt concrete pavement usually starts at the bottom of the hot mix asphalt layer. Then, it propagates to the surface of the layer (bottom-up cracking) as a result of the bending of pavement layer. Fatigue cracking happens because of the development of flexural stresses at the bottom of the asphalt concrete layer (NCHRP, 2004). The tensile stress is generated at the bottom of the asphalt concrete layer in the pavement structure. When the tensile stress exceeds the strength of the material, a flaw is formed initially, and due to repeated traffic loading, a crack starts to propagate gradually to the surface of the pavement. However, in another case in thick pavements

(Uhlmeier et al., 2000), the effective tensile stress tends to be on the surface of the pavement. Cracks start to generate and propagate from the top to bottom of the pavement layer. The two kind of cracking behaviour are shown in Figure (2-5).

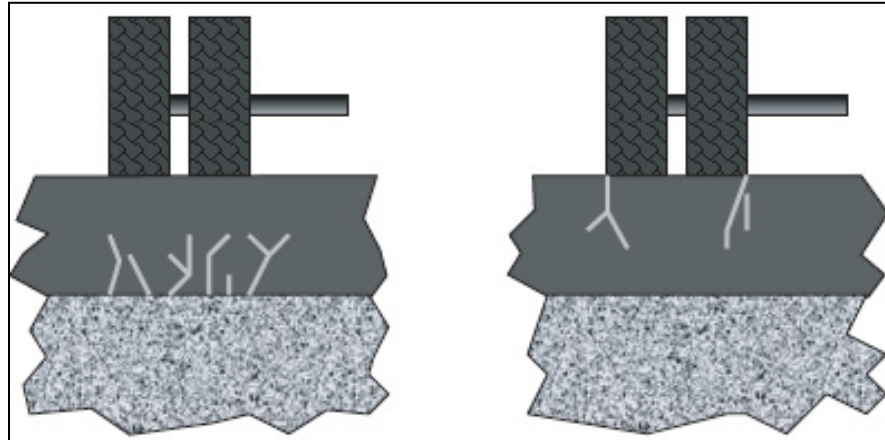


Figure (2-5) Schematic of fatigue cracking starting directions (NCHRP Report 673, 2011)

The fatigue cracking in its severe condition is named as alligator cracking due to the similarity between the shape of cracks and the texture of alligator body. The cracks will remarkably influence the performance of the pavement. They make the surface of pavement rough and uncomfortable to ride and damage the structure of pavement through giving air and moisture a chance to infiltrate inside it. Finally, this kind of distress could lead to full-scale cracked areas, potholes and then overall pavement failure (NCHRP 673, 2011). For good design, flexible pavements should have an adequate structure of a strength greater than the tensile stresses that may occur in the asphalt layer. Moreover, compressive stresses in the subgrade should be not higher than the strength of that layer as well. Figure (2-6) shows the tensile stress and strain (ϵ_t) that occurred in the bottom of the asphaltic layer in the pavement and the vertical compressive stress and strain (ϵ_v) on the top of the subgrade.

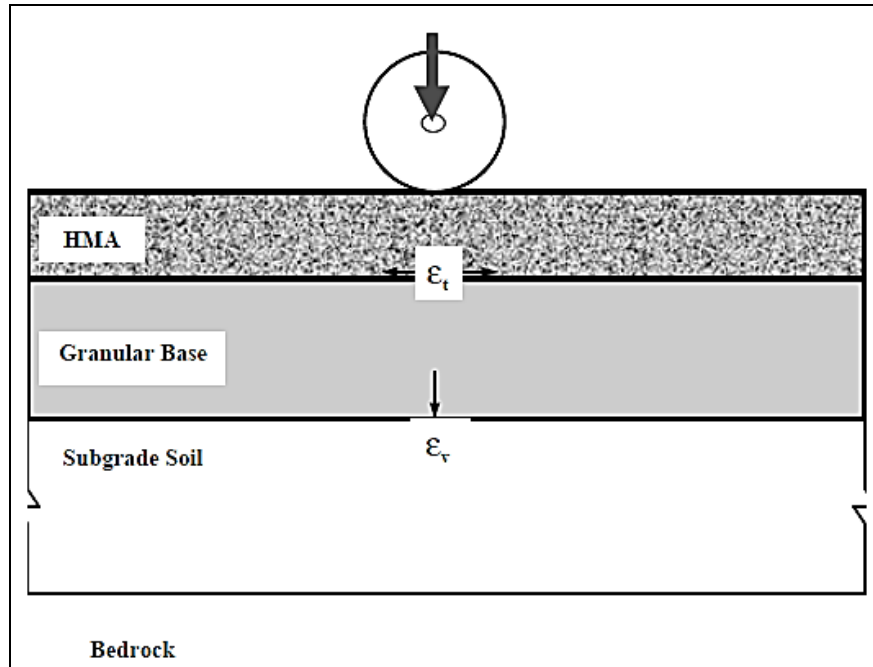


Figure (2-6). Illustration of stress and strain within pavement layers (NCHRP, 2002)



a) Fatigue (Alligator) cracks

b) Cracks with Potholes

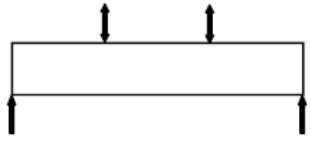
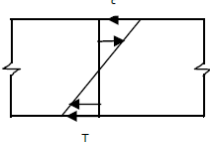
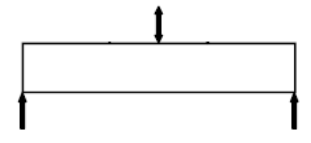
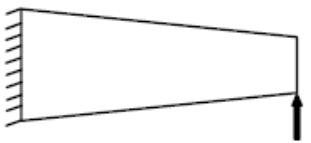
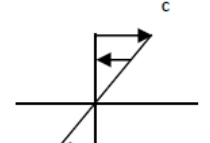
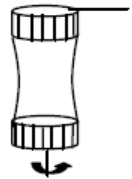
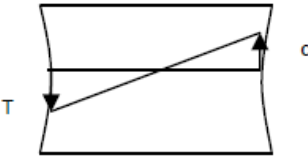
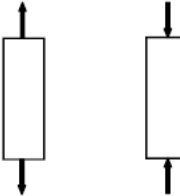
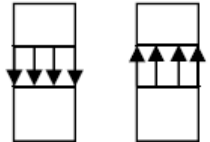
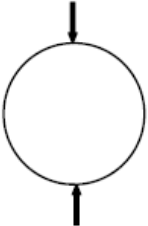
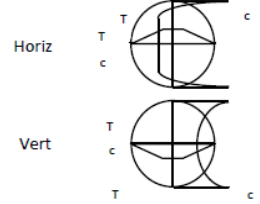
Figure (2-7) Fatigue Cracking in Flexible Pavement

Tangella et al. (1990) presented a summary of fatigue test methods. There are several cases of tests; third-point flexural, center-point flexural, cantilever flexural, rotating cantilever, uniaxial, and diametral. They mentioned the fundamental characteristics of tests and their state of stress and the presence of a zone of uniform stress. As stated in the Table (2-1), it can be seen that the repeated load flexural, rotating cantilever, and axial tests have a uniaxial state of stress while the diametral test has a biaxial stress state.

The third-point fatigue test could be more accurate to simulate the defect that may occur in situ in the asphalt concrete pavement. Since the stress applied to the specimen is covering a bigger part of it as compared with others like cantilever test (Tayebali et al., 1994).

In the laboratory, there are two forms of controlled loading that utilised for fatigue characterization: constant stress and constant strain. In the constant stress (load) testing, the applied stress throughout the fatigue testing maintains constant. Since the repeated loading induces damage in the test specimen, the stiffness of the mixture is decreased due to the microcracking observed. This, in turn, causes an increment in tensile strain with load repetitions. For the constant strain testing mode, the strain stays fixed with the number of load repetitions. As a result of specimen damage due to the loading repetitions; the stress has to be decreased to achieve the same strain. This leads to a reduction in stiffness as a function of load repetitions (NCHRP, 2004). The constant stress and constant strain phenomena are shown in Figure (2-8).

Table (2-1) Laboratory Fatigue Tests (Tangella et al., 1990)

Test	Loading Configuration	Stress Distribution	State of Stress	Does Failure occur in a uniform bending moment or tensile stress zone?
Third Point Flexure			Uniaxial	Yes
Center Point Flexure		Same as above	Uniaxial	No
Cantilever			Uniaxial	No
Rotating Cantilever			Uniaxial	Yes
Axial			Uniaxial	Yes
Diametral			Biaxial	No

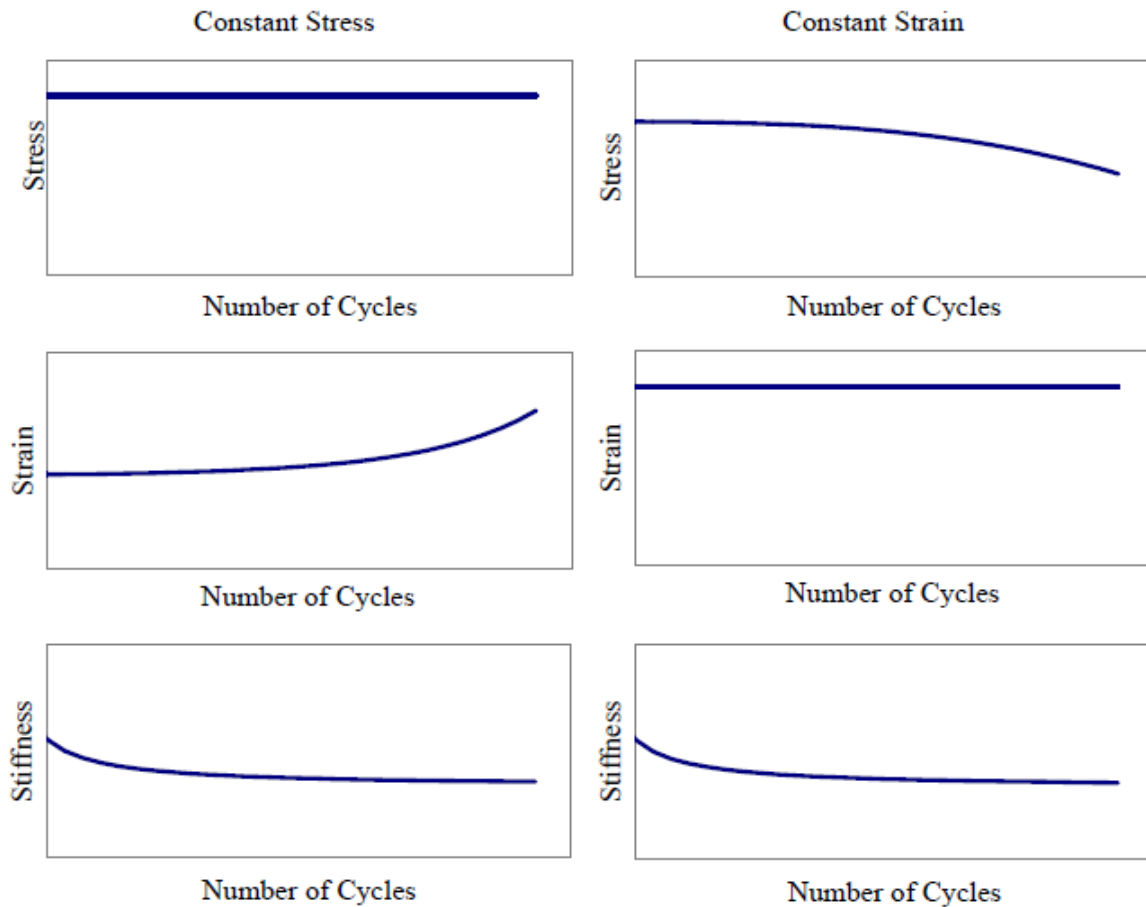


Figure (2-8) Constant Stress and Constant Strain Phenomena (NCHRP, 2004)

The constant stress sort of loading is considered applicable to thick asphalt pavement layers, usually 8 inches and more. For this kind of structure, the main load-carrying component is the thick asphalt layer, and the strain rises as the material becomes weaker under repeated loading. However, with the reduction in the stiffness, because of the thickness, changes in the stress are not significant, and this fact leads to a constant stress situation. The constant strain loading type is regarded more applicable to thin asphalt pavement layers, usually less than 2 inches and the pavement layer is not the main load-carrying component. The strain in the asphalt layer is ruled by the underlying layers and is not considerably affected by the variation in the asphalt layer stiffness (NCHRP, 2004). Controlled stress tests are more severe than controlled strain tests, and the energy is absorbed more rapidly. The initially dissipated energy per cycle is high, and the rate

of energy dissipation is faster in the controlled stress mode of loading (Ghuzlan and Carpenter 2000). A summary of some of the factors affecting controlled stress and controlled strain tests are listed in Table (2-2) (Tangella et al. 1990).

Table (2-2) Factors Affecting Controlled Stress and Strain Tests (Tangella et al. 1990)

VARIABLES	CONTROLLED-STRESS (LOAD)	CONTROLLED-STRAIN (DEFLECTIONS)
Thickness of asphalt concrete layer	Comparatively thick asphalt bound layers	Thin asphalt-bound layer, < 3 Inches
Definition of failure; number of cycles	Well-defined since specimen fractures	Test is discontinued when the load level has been reduced to a proportion of its initial value
Scatter in fatigue test data	Less scatter	More scatter
Required number of specimens	Smaller	Larger
Simulation of long- term influences	Long-term influences such as aging lead to increased stiffness and increased fatigue life	Long-term influences leading to stiffness increase will lead to reduced fatigue life
Fatigue life (N)	Generally shorter life	Generally longer life
Effect of mixture variables	More sensitive	Less sensitive
Rate of energy dissipation	Faster	Slower
Rate of crack propagation	Faster than occurs in situ	More representative of in situ conditions
Beneficial effects of rest periods	Greater beneficial effect	Lesser beneficial effect

Kim et al. (1995) conducted a study on the effect of lime on HMA characteristics related to the main distresses that may occur in asphalt pavement. They demonstrated that the resistance to fatigue cracking and permanent deformation could be enhanced with lime. Figure (2-9) shows that addition of the hydrated lime enhances the fatigue related life of the flexible pavement according to the calculation made by adopting laboratory tests on fatigue properties and life prediction. As shown in Figures (2-10) and (2-11), the permanent deformation (rutting) in asphalt concrete pavements have been decreased due to the addition of hydrated lime. The figures also show that hydrated lime has better performance than the liquid anti-strip materials.

The small particles of hydrated lime resist and minimise tiny cracks since the particles tend to fill in the small air pockets between bitumen and aggregate and prevent the cracks from coalescing into large cracks that can find their way through the asphalt pavement layers. The chemical components of lime make it attracting acid composition of bitumen material to its surface. The increase of hydrated lime particles effective volume produces more influence as compared with other types of fillers at restricting the micro cracks development (Lesueur and Little, 1999).

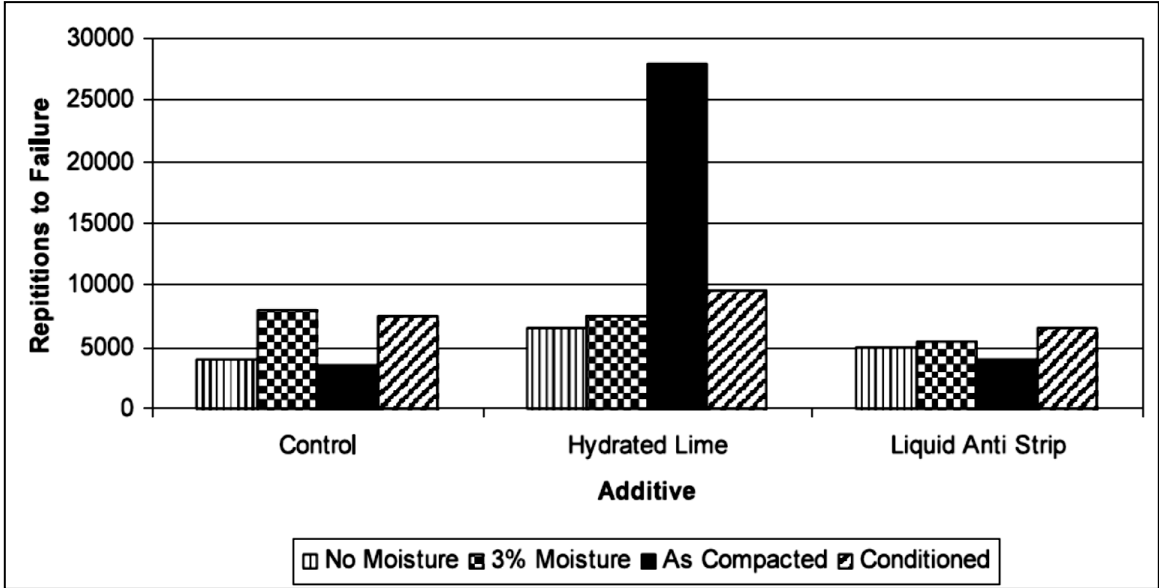


Figure (2-9) The Influence of Additives on Fatigue (Kim et al., 1995)

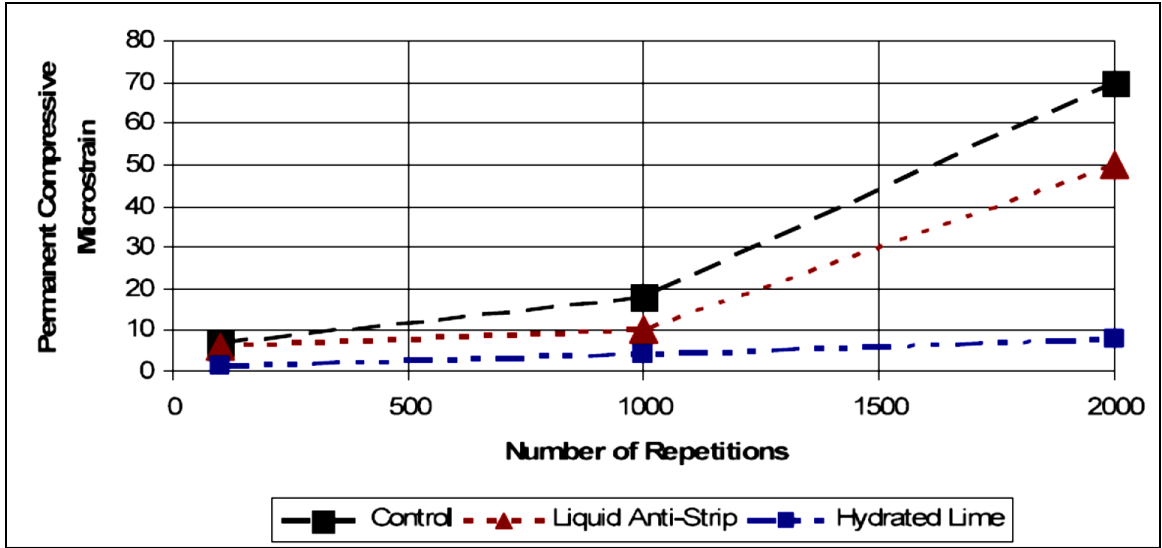


Figure (2-10) Influence of Additives (Dry) on Permanent deformation (Kim et al., 1995)

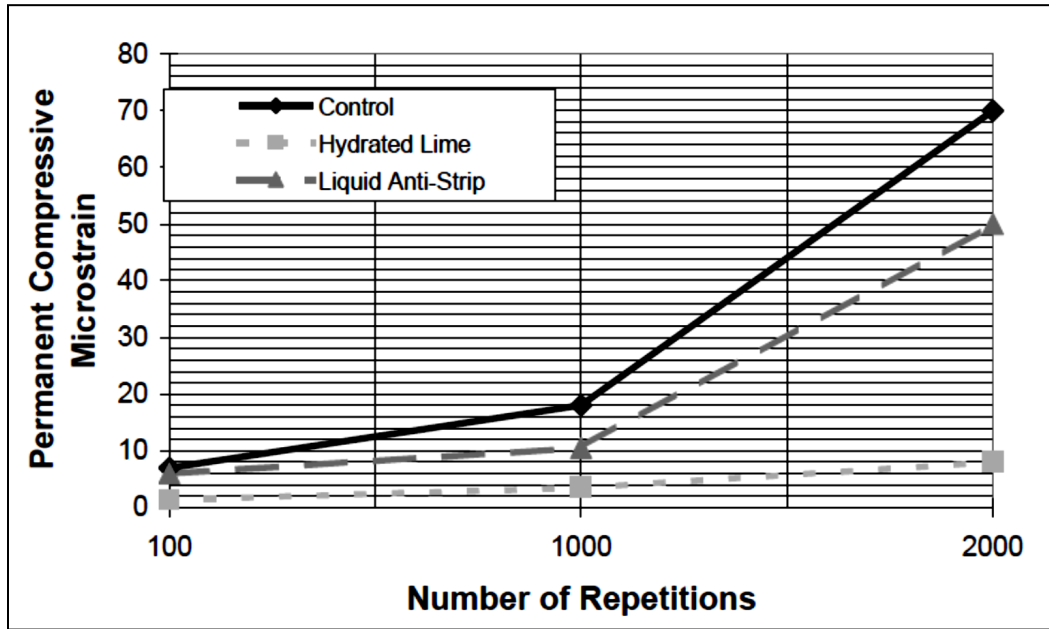


Figure (2-11) Influence of Additives (Moisturized) on Permanent Deformation (Kim et al., 1995)

Savitha et al. (2012) investigated the influence of hydrated lime and another type of mineral filler (phosphogypsum) on the asphalt mixtures properties. They concluded that the stiffness modulus could be increased by 27% with an addition of 3% of hydrated lime to the paving mixture in terms of the total weight of the aggregate. This enhancement is greater than the percentage of stiffness modulus (11%) that gained by adding the same amount of phosphogypsum (3%). Tables (2-3) and (2-4) illustrate a comparison of results between the effect of hydrated lime and phosphogypsum on permanent deformation and fatigue characteristics respectively.

Table (2-3) Results of static creep Test (Savitha et al., 2012)

Properties	Sample without Lime	Sample with Lime	Sample with phosphogypsum
Initial micro Strain	0.401573	0.347074	0.375650
Maximum micro Strain	1.035889	0.814815	0.932032
Permanent micro Strain	0.888680	0.682832	0.745896
Stiffness Creep Mpa	9.65	12.27	10.73

Table (2-4) Results of fatigue and stiffness modulus of the mix (Savitha et al., 2012)

Properties	Control mix	Sample with lime	Sample phosohogypsum
Stability(KN)	9.87	13.20	11.75
Load repetition	750	985	828
Deformation	8.00	9.75	12.58
Stiffness modulus (MPa)	985.0	1175	1061.6

Aljumaily (2008) conducted several tests on the performance and properties of the asphalt concrete mixture. These tests were Marshall mix design, the indirect tensile strength for evaluating the retained strength, permanent deformation, and fatigue characteristics. He used three types of mineral filler (hydrated lime, Portland cement, and soft sandstone). The results showed that hydrated lime could have an effect on the rutting susceptibility and fatigue life of flexible pavements by improving the resistance to rutting and fatigue cracking distresses. It is also effective in increasing the resistance to moisture damage due to the improvement in the Tensile Strength Ratio (TSR) in the lime modified mixtures as compared to the other mixtures.

2.4.4 Permanent Deformation (Rutting)

The permanent deformation is usually the load-associated distress that considered as a dominant factor in the performance of HMA concrete pavements. The typical way of development and the form of rutting is a depression under the location of wheels (longitudinal path) with noticeable upheavals on path's sides. The main agents that highly affect the permanent deformation (rutting) shape and depth are pavement structure (layer thicknesses and material properties), traffic volume and distribution, and site environment conditions.



Figure (2-12) Permanent Deformation (Rutting) in Flexible Pavement

In 2002, National Cooperative Highway Research Program (NCHRP, 2002) classified rutting into the following categories and as shown in Figure (2-13):

1. Wear rutting, which is due to the advanced lack of coated aggregate particles in the pavement surface layer, and it occurs because of the combination of environmental and traffic influences.
2. Structural rutting, which happens because of the vertical permanent deformation in the pavement structure under traffic load repetitions and it is a reflection of the permanent deformation of the subgrade.
3. Instability rutting, which is due to the condensation (pavement volume reducing, and thus, density increment) and lateral displacement (shear deformation) of material within the pavement asphaltic concrete layers. Dawley et al. (1990) stated that the majority of HMA rutting is due to primarily to the instability rutting.

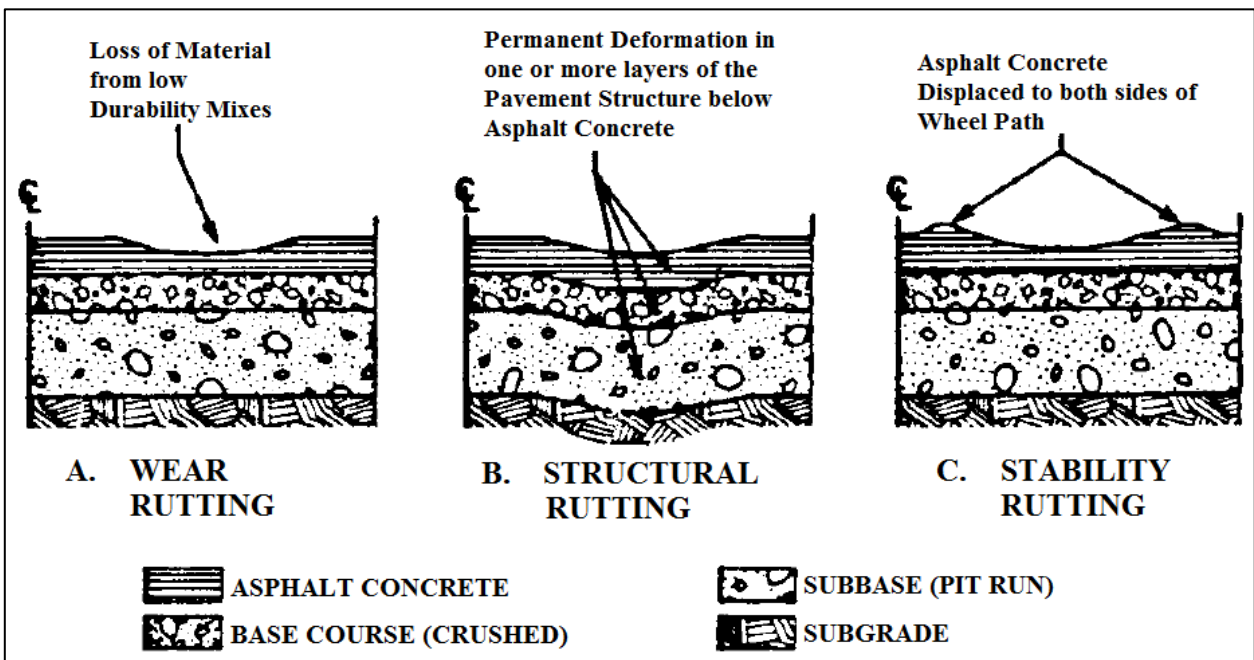


Figure (2-13) Description of Rutting Types (NCHRP, 2002)

Rutting develops gradually over the life of the service of the pavement when the incremental, volumetric, and shear permanent strains accumulate. The incremental permanent strains will be functions of the traffic loading repetitions, the stiffness, permanent deformation, and induced stresses in the asphalt concrete layer. In a poorly designed pavement or mixture,

excessive rutting may develop very quickly as a consequence of the shear failure within the asphalt.

Permanent deformation (or rutting) in asphalt pavements is a load associated type of distress, and hence the conditions of loading have a significant influence on the magnitude and rate of accumulation of permanent deformation. In the field, asphalt pavements are subjected to complex loading with varying magnitude and frequency. In the laboratory, the test has to be undertaken with loading conditions that simulate the field loading conditions as closely as possible. There is a necessity of testing specimens at an appropriate level of those type of stresses that the asphalt pavement will be subjected to in the field (Iqbal, 2004).

Eisemann et al. (1989) studied deformation phenomenon in asphalt concrete pavement using wheel trucking apparatus. He calculated the permanent deformation (rutting) depth as well as the volume of displaced materials underneath the surface of the tire and in the rise areas adjacent to the deformed path. The researchers found that:

- In the first stages of traffic loading, the growth of unrecoverable deformation in the wheel path is clearly larger than the development in the adjacent rise zones. The consolidation or compaction due to traffic loading is the major mechanism of permanent deformation in the first stage.
- The next phase is when the amount of decrease of permanent deformation under the path of tires is approximately the same value of the increase in the volume of adjacent rise zone. These findings suggest that the greatest percentage of the densification under traffic loading is finished in the first stage of pavement service life, and additional permanent deformation is because of shear stresses (that is deformation without size change). Therefore, the primary mechanism of rutting for the rest of pavement service life is the shear deformation.

2.4.4.1 Rutting Caused by Weak Subgrade

Rutting is caused by an excessively repeated load applied to subgrade, subbase or base below the asphalt concrete layer. As a result of the insufficient thickness of the asphalt concrete and base layers on the subgrade, the stresses developed due to load applications on the surface asphalt concrete layer will not be reduced to a tolerable level that the subgrade can withstand. Thus, this type of rutting is considered to be more of a structural problem than a material problem

and is often referred to as structural rutting. The intrusion of moisture can also be a cause for the weakening of the subgrade (McGennis et al., 1995). In this type of rutting, the accumulated permanent deformation occurs in the subgrade. Figure (2-14) illustrates rutting from weak subgrade.

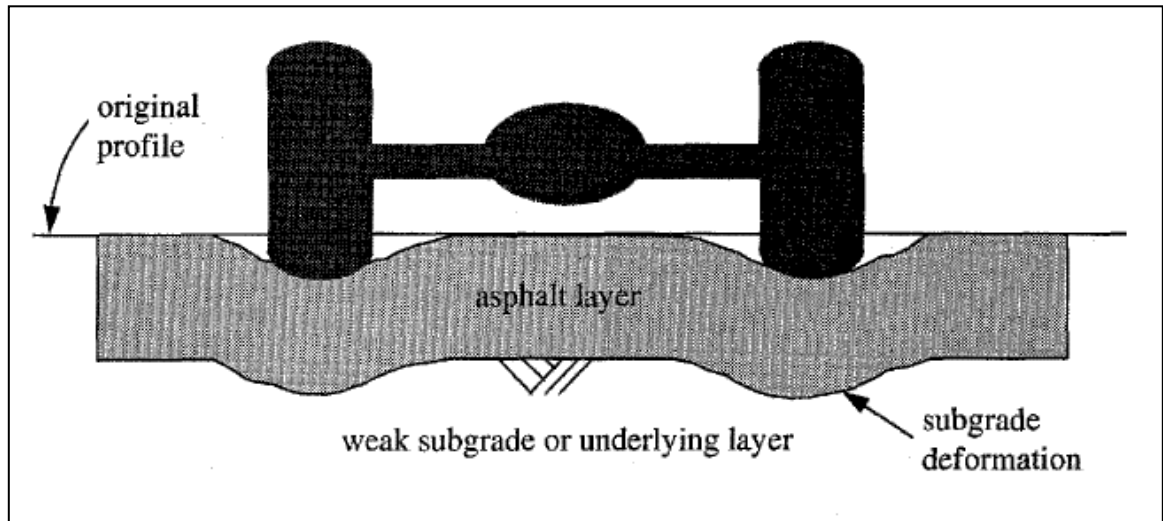


Figure (2-14) Rutting from Weak Subgrade (McGennis et al., 1995)

2.4.4.2 Rutting Caused by Weak Asphalt layer

Permanent deformation (rutting) occurs in the asphaltic concrete layer of the flexible pavement has recently been noted as one of the major distresses affecting pavement in its asphalt layers. Rutting happens due to the increase of vehicle tire pressure and axle load repetitions (McGennis et al., 1995). Thus, the asphalt mixtures nearest the pavement surface are under the highest pressures. Brown and Cross (1992) presented a study on rutting in asphalt concrete pavement in the United States. They implemented a comprehensive data and sample survey to evaluate material properties, layers thicknesses and rut depth in the layers. Their study is adopted for the majority of United States areas regarding the differences in climate, the aggregate gradation, origin, density and surface angularity as well as type and amount of asphalt cement. The study considered different agencies limitations and construction instructions. Based on rutting position, they concluded that the most of the rutting could be found in the 3 to 4 inches near the

surface of asphalt concrete layers. Also, the rutting in the subgrade is mostly small as compared with rutting in the surface layer. Figure (2-15) present the rutting resulting from weak asphalt mixture.

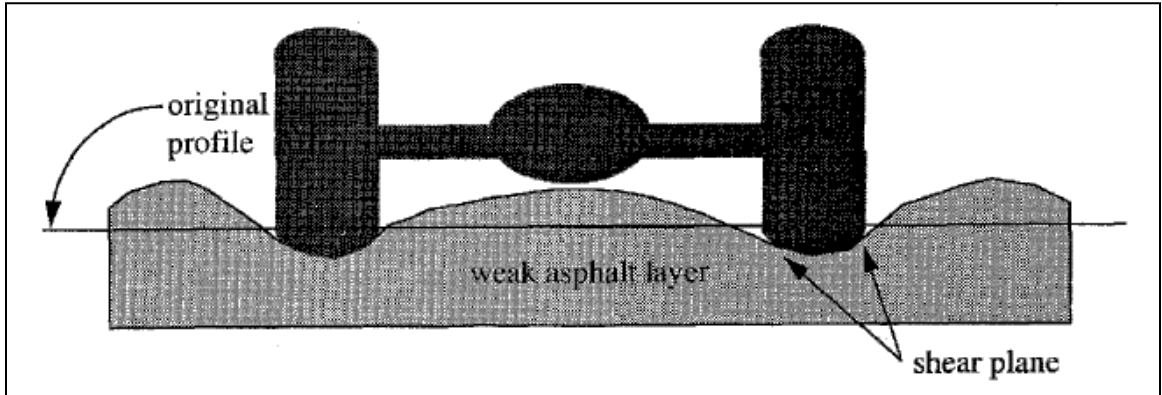


Figure (2-15) Rutting from weak asphalt mixture (McGennis et al., 1995)

2.4.4.3 Evaluation of Asphalt Mixture Resistance to Rutting

The employment of tests results in the design process and building of functional equations based on these outputs is considered as one of the commonly used methods for prediction of rutting in the flexible pavement. The prediction of distress effect on asphalt concrete mixture properties needs relevant techniques to determine the response and representative parameters of the model as well as simulate the response behaviour in the field. The purpose of testing materials is to achieve as much as possible the same practical conditions of the pavement in situ. Several tests have been designed to study the rutting response of pavements. Researchers and agencies have widely used some of these tests for calculating of permanent deformation. The tests are categorised as follows (Witczak et al., 2002):

- The uniaxial stress test: it is done by applying dynamic, repeated or creep loading on unconfined cylindrical specimens.
- The triaxial stress test: testing of cylindrical samples in a confined condition under repeated, dynamic or creep loading.
- The diametral test: it can be done for mould specimens under repeated or creep loading.
- Wheel track test: it can be done by applying a repetitive passing of a wheel with a specific load on slab samples or an actual pavement section.

2.4.4.4 Lime Influence on Permanent deformation

Al-Suhaibani (1992) investigated the properties of mineral filler of hydrated lime and other types of locally available fillers in Saudi Arabia. He studied the mixtures mechanical properties through laboratory work, which consists of Marshall test, indirect tensile strength test, resilient modulus test and Hveem stability. He concluded that the properties and percentage of mineral filler affect the rutting susceptibility of the mixes, and the hydrated lime enhances the resistance to permanent deformation (rutting).

The influence of hydrated lime as a filler in the asphalt concrete reduces the chance of HMA to deform at high temperatures, especially at the beginning of service life in which the asphalt is on its highest susceptibility to rutting. The hydrated lime stiffens the asphalt film coating the aggregate surface and enhances its bonding. Moreover, the effect of hydrated lime on improving the bonding between aggregate and asphalt leads to reducing susceptibility to moisture. In sum, hydrated lime increased rutting resistance (Satyakumar et. al., 2013).

Important researches have been undertaken in the United States to investigate the multifunctional benefits of hydrated lime. As illustrated in Figures (2-16) and (2-17), Epps et al. (1992) found that using the hydrated lime as additive led to the increase of the resilient modulus of asphalt concrete mixtures. Based on their conclusions, the enhancement of stiffness made the mixes stronger to withstand the stresses caused by traffic loading and distribute them in the pavement sections, and that reduces the strains as well. Thus, the prospect of permanent deformation (rutting) occurrence in the pavement reduces. Aschenbrener and Far (1994), as well as Collins et al. (1997), carried out wheel track laboratory test as presented in the Tables (2-5) and (2-6) respectively. The mixes illustrated in the Table (2-5) were prepared with and without additives. The additives are hydrated lime, and liquid anti-stripping materials produced by two companies, A and B, and each manufacturer made two different kinds of the liquid additives, 1 and 2. The results illustrated that hydrated lime increases the ability of mixtures to resist rutting. Creep tests have been adopted in Texas (Table 2-7) also demonstrate that hydrated lime support stability of mixtures at high temperature, through increasing of resistance to rutting (Little, 1994).

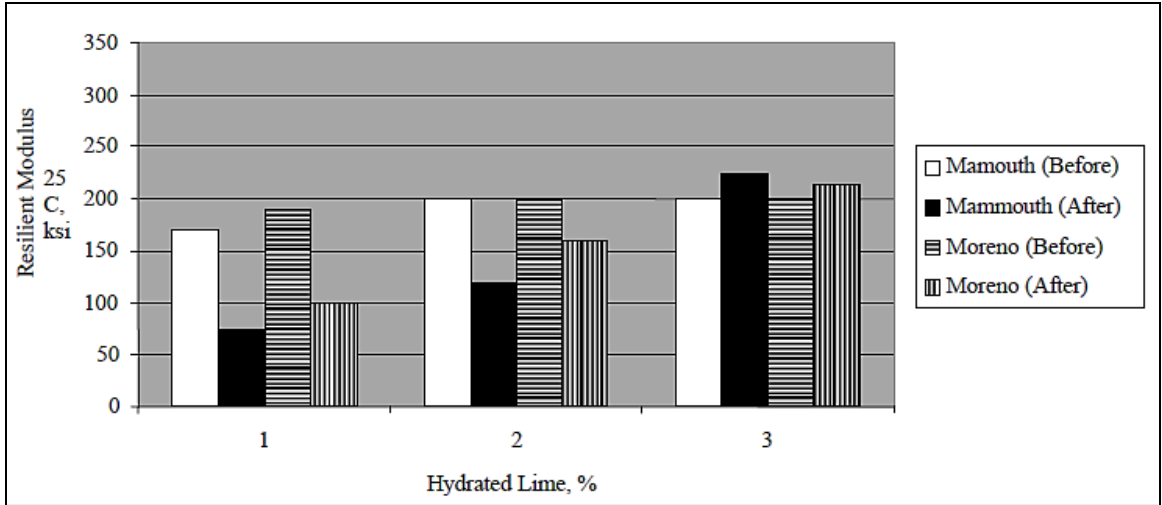


Figure (2-16) Hydrated Lime Influence on Resilient Modulus Before and After Lottman Conditioning (Epps et al., 1992)

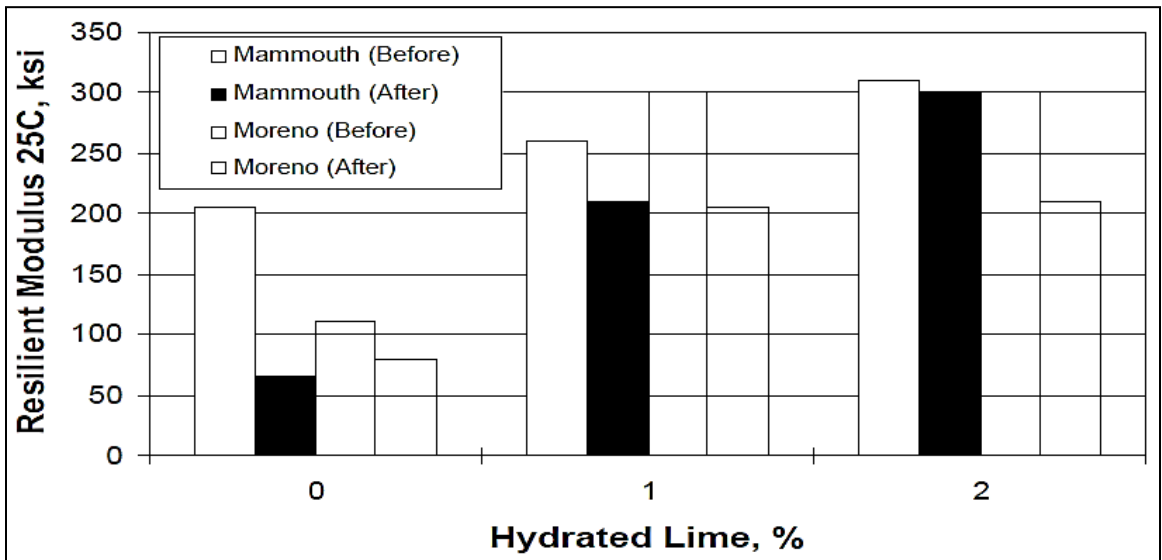


Figure (2-17) Hydrated Lime Influence on Resilient Modulus Before and Following Lottman Conditioning (Epps et al., 1992)

Table (2-5) Deformation in (mm) After 20,000 Passes for many Anti-Stripping Treatments in Colorado (Aschebrener and Far, 1994)

	No Treatment	1 % Hydrated Lime	Additive "A"		Additive "B"	
			Type 1	Type 2	Type 1	Type 2
Mix 1	(17.0) ¹	1.4	2.2	3.1	6.3	7.4
Mix 2	(>20)	2.3	8.1	8.4	5.3	(14.6)
Mix 3	(>20)	2.5	(13.7)	8.5	(>20)	(12.4)
Mix 4	8.7	2.3	6.2	4.7	5.0	4.3

¹ Values in parentheses mean that the failure is due to excessive deformation.

Table (2-6) Number of load repetitions corresponding to 7.5 mm and 5.0 mm rutting failure criteria in specimens (Collins et al., 1997)

Aggregate	Specimens with Lime		Specimens without Lime	
	Vacuum Saturation	Freeze-Thaw	Vacuum Saturation	Freeze-Thaw
Source 1	7803 ^c (2240) ^d	5000 (1467)	1748 (5000)	5609 (2166)
Source 2	3685 (1303)	5242 (1796)	3310 (1177)	3507 (931)
Source 3	2974 (1065)	2332 (680)	1805 (736)	452 (302)
Source 4	2496 (734)	4240 (1242)	1983 (732)	2045 (579)

^c Number of Repetitions corresponding to 7.5 mm

^d Number of Repetitions corresponding to 5.0 mm

Table (2-7) Evaluation of results of Creep test procedure found by Little et al. (1994)

	1-Hour Strain, in./in., ϵ_p		1-Hour Creep Modulus, E_c , psi		Properties of Steady State Region of Creep Curve		
	From Test	Criterion	From Test	Criterion	From Test	Criterion	Tertiary Creep
C1 ¹	0.020	Failure	--	Failure	--	--	Yes
C2	0.009	HRS ³	2,200	HRS	0.40	HRS	Yes
C3	Failure	--	--	--	--	--	--
L1 ²	0.0018	HRR ⁴	10,500	HRR	0.20	HRR	No
L2	0.052	MRR ⁵	3,750	MRR	0.25	MRR	No
L3	0.0032	HRR	6,110	HRR	0.20	HRR	No

¹ C1=Control specimen (without lime), ² L1=Lime-treated, ³ HRS= High Rut Susceptibility, ⁴ HRR=High Rut Resistance, ⁵ MRR=Moderate Rut Resistance.

Kandhal and Parker (1998) mentioned that there are several factors affecting the permanent deformation (rutting) in flexible pavements. Some of these factors related to the filler portion of the mix such as properties of mineral filler, fine aggregate angularity and plastic fines in the fine aggregate. Other factors that they mentioned could be governed by the effect of type and amount of mineral filler such as asphalt cement content and air voids.

The permanent deformation parameters, slope, and intercept were significantly influenced by the addition of deferent percentages of hydrated lime. The modified mixes show higher resistance to permanent deformation when the percentage of hydrated lime is increased as a filler substitute (Albayati 2012).

Mohammed and Altinsoy (2002) evaluated the properties of asphalt concrete mixture containing hydrated lime with two aggregate types and two different asphalt cement types (AC-30 and polymer modified) by adding 1.5% of hydrated lime. Hamburg Wheel Tracking Device (HWTD) and indirect tensile resilient modulus tests were adopted. The study reveals that hydrated lime provides stronger adhesion between aggregate and binder. This improvement was especially evident in tests performed at high temperatures. The polymer modified mixtures showed the most improvement due to the stiffness attributed by the hydrated lime addition. These work showed that

hydrated lime could enhance the elasticity properties of the mixtures to reduce accumulated permanent deformation.

2.5 Methods of Adding Hydrated Lime into the Asphalt Concrete Mixture

It has frequently been recognised that using of hydrated lime in the asphalt concrete mixes is advantageous, although, the best way for introducing of hydrated lime to the mix still controversial. Transportation agencies and contractors have used one or more of three common ways to add lime to asphalt concrete mixtures. The three procedures, accompanying with a brief summary of each with its main positive and negative characteristics, are as following (Button et al. 1983):

2.5.1 Addition of dry hydrated lime to dry aggregate

This method is the simplest way of adding hydrated lime to the asphalt concrete mixtures. In the early 1980s, the state of Georgia in the United States first approved this process. In this addition method, the hydrated lime introduced to the drum mixer with the aggregate and contact directly to the aggregate particles surfaces and that leads to improving the bonding between asphalt cement and aggregate particles. The particles of hydrated lime that does not contact with aggregate will mix with the asphalt cement. The reaction between hydrated lime and the highly polar molecules in the asphalt produces unresolved salts that do not attract water, hence, decreasing the potential of asphalt concrete mix to stripping due to moisture effect and oxidation.

2.5.2 Addition of dry hydrated lime to wet aggregate

Adding dry hydrated lime to wet aggregate is the most general method of adding hydrated lime to asphalt mixes. In this method, hydrated lime is metered into the aggregate that already has a moisture content of 2% to 3% over its saturated-surface-dry (SSD) condition.

In this technique, the aggregate of the mixture has to be moisturised with a water content of about 2 to 3 percent beyond the saturated surface-dry (SSD) condition, and then the dry hydrated lime is added to it. The mix (aggregate and hydrated lime) has to be thoroughly mixed. Many transportation departments and agencies decide that the aggregate-lime mix stays for about 48 hours before drying for adequate reaction.

The benefits of adding dry hydrated lime to wet aggregate are that the asphalt mixture affords sufficient coverage and permits for a relatively better application as compared to the dry hydrated lime to dry aggregate technique. These benefits are reasonable since moisture ionises

hydrated lime and maintains a distribution of it on the aggregate surface. The part of hydrated lime that fails to bond with the aggregate finally gets blended with the asphalt cement, hence offering the same enhancements that are found in the dry method. The major drawback of this process is the additional effort and fuel needed to dry the aggregate earlier to asphalt concrete mix production.

2.5.3 Addition of hydrated lime in the form of slurry

In this addition process, the hydrated lime is mixed with water to form a slurry and then introduced it to the aggregate to provide a higher coverage of the aggregate surfaces. The slurry is mainly made from hydrated lime, although occasionally made from quicklime. In this method, the treated aggregate can be marinated or directly used. The advantages of adopting this procedure are stripping resistance, least lime loss due to dusting and carrying out by the wind and providing the best coverage of hydrated lime on the aggregate particles surfaces. The main disadvantages of applying this method are the extra amount of fuel to be consumed throughout the aggregate drying and the necessity to buy and manage specific, expensive devices.

2.6 Mechanical-Empirical Method for Pavement Design

2.6.1 Background

At the beginning of the twentieth century, the pavement design was based on purely empirical processes. Since 1920, efforts have been made to implement loading and responses in the pavement design formulas. However, these attempts were not well known enough until the Second World War when the rapid increase in traffics and air travelling contributed the generation of new design procedure called mechanistic design (Huang, 1993).

The rapid growth of the aircraft load and the need for travel during the Second World War encouraged the USA Engineers Corps to improve the thickness design charts of military airfields. The newly developed method made by them was also employed in highway applications and design, where the loads are more repetitive, but the impact is less (Yoder and Witczak, 1975).

Huang (2004) has presented an important review on the development of pavement design methodology development around 1940's (World War II period) and found that:

1. There was a significant change in the design methods for flexible pavements, from the early empirical methods to the modern mechanistic–empirical methods. With the availability of high-

speed microcomputers and sophisticated testing methods, the trend toward mechanistic methods appears.

2. The most practical and widely used mechanistic–empirical method for flexible pavement design is based on Burmeister's elastic layered theory, which limits the horizontal tensile strain at the bottom of asphalt layer and the vertical compression strain on the top of subgrade layer. With modification, the method can be applied to multilayered systems consisting of elastic, viscoelastic and nonlinear elastic materials.

A new Mechanistic-Empirical Pavement Design Guide (MEPDG) has recently been developed (NCHRP 1-37A, 2004) and is currently under validation-implementation by many states. The design guide represents a challenging addition in the way that pavement design and analysis is conducted. Design inputs comprise traffic configurations, material characterization, climatic factors, performance models, and other factors. Performance prediction and pavement life are estimated based on the multi-layered elastic theory and the empirically-developed failure criteria (Kim et al., 2010).

The MEPDG is an analysis mechanism that facilitates prediction of pavement performances over time for a given pavement structure subjected to variable circumstances, such as traffic and climate. The mechanistic-empirical design of new and reconstructed flexible pavements needs an iterative procedure by the designer. The designer must choose a trial pavement design and then analyse the design to decide if it meets the performance criteria set by the designer. If the trial design does not meet the performance criteria, the design is adjusted and reanalysed until the design serves the performance criteria (NCHRP 1-37A, 2004).

The MEPDG plays a significant change in performing the design methods of pavement (Li et al., 2011). The MEPDG modifies not only the way of the design procedure and inputs, but it helps to improve the way that engineers and researchers study, develop and carry out efficient and functional design of pavement. The employment of the MEPDG design method requires the designers and researchers to have more knowledge about pavement design input parameters and the performance of the pavement. Furthermore, the cooperation is vital among highway agency engineering staff who work in pavement structure, materials, traffic, and geotechnical field to classify the right inputs for the pavement design (Li et al., 2011). The benefits of mechanistic methods are the enhancement of the reliability of design, the capability to predict the types of

distresses, and the feasibility to extrapolate from the limited field and laboratory data (Huang, 2004).

The MEPDG technique relies primarily on the characterization of paving materials properties. It needs some of the input data in four main sections: traffic loading, paving material properties, the effect of environment, and pavement structure responses and failure criteria models. As seen in Figure (2-18), the design strategy accounts for the environmental influence that may affect the pavement responses. Mechanistic techniques are used to find pavement responses. The mechanistic method estimates the pavement structural response, the stress and strain, in the pavement layers. The transfer function (empirical distress model) is employed to determine the main distresses happen in the pavement; fatigue cracking and rutting directly.

The MEPDG approach employs JULEA, a multilayer elastic analysis software, to calculate the stresses, strains, and displacements happen in the flexible pavement structure that resulting from traffic loading and climate influence. The calculated responses are then introduced into the pavement performance prediction models that present the accumulated damage over the entire design period. The accumulated damage at the design period is associated to the main distresses expected to happen in the pavement such as fatigue cracking, and rutting, as well as thermal cracking and roughness of pavement surface and these, distresses are predicted using models calibrated with field measurements. These models are the primary empirical part of the mechanistic-empirical design method (NCHRP 1-37A, 2004).

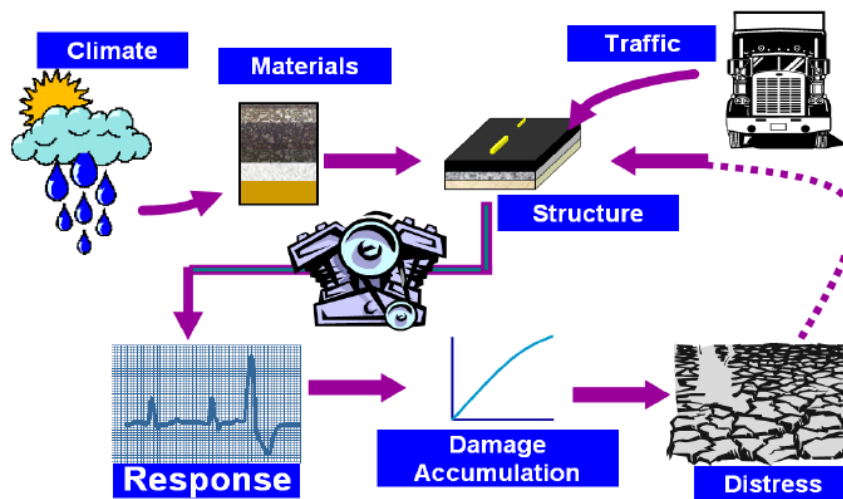


Figure (2-18) MEPDG Design Process (NCHRP 1-37A, 2004)

2.6.2 Mechanistic-Empirical Design Related Flexible Pavement Distresses

The most well-known formats of load-associated distresses that cause a reduction in service life and performance of asphalt concrete pavement are fatigue (alligator) cracking and permanent deformation (rutting). The achievement of adequate pavement structure is the target in designing asphalt concrete pavement to minimise the tensile stresses in the bottom of asphalt layers and make them less than their strength. In addition, its purpose is to lessen the compressive stresses on the top of subgrade layer below the strength and bearing capacity of that layer.

2.6.3 Failure criteria of Mechanistic Empirical method

The employment of vertical compressive strain to manage the permanent deformation depends on the fact that there is a proportional relationship between plastic and elastic strains in the pavement materials. Therefore, by controlling the elastic strains that happen on the subgrade layer, the elastic strain in the other layers located above the subgrade will be limited as well. Hence, the value of permanent deformation on the surface of the pavement will be controlled in sequence (Huang, 2004).

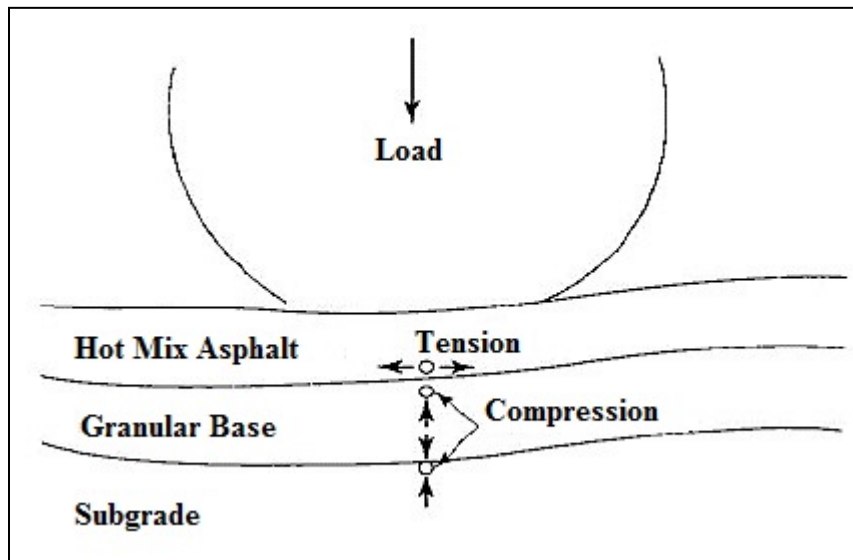


Figure (2-19) Tensile and compressive strains in flexible pavements (Huang, 2004)

2.6.4 Fatigue and Rutting Prediction Models

Fatigue cracking and rutting (permanent deformation) are the major distresses that related to the structure of hot mix asphalt pavement. The prediction of fatigue cracking and permanent deformation relies on studying the response of pavement regarding stress and strain as important inputs. The prediction will be helpful for essential management and maintenance of pavement. Furthermore, The durable and properly predicted models can be adopted to evaluate the loading set for different vehicles to assign cost management for these vehicles. In addition, the models are used in the design process of the pavement, and they can be implemented in studying and evaluating many methodologies of design (Adrian and Samer, 2000).

2.6.4.1 Fatigue Cracking Prediction Models

In general, the fatigue cracking related models of asphalt concrete mixtures are expressed as relationships between the number of repetition of the applied load to failure and the initial tensile strain or stress. Numerous models have been presented regarding fatigue of asphalt pavement cracking. Some of the models were developed according to the characteristics of particular institutes, and others were the output of extensive laboratory work based on the basic fatigue formula.

The calculation process can be done by adopting one of many fatigue tests available at various levels of stress and strain (Tayebali et al., 1994). Monismith et al. (1966), Pell (1967) and Pell and Cooper (1975) found that the number of load repetitions to failure (fatigue life) showed better correlations with tensile strains than with tensile stresses. Accordingly, the basic fatigue failure relationship could be expressed by the following equation:

$$N_f = K_1 \left(\frac{1}{\varepsilon_0} \right)^{K_2} \quad (2-2)$$

Where:

N_f = the number of load applications to failure,

ε_0 = initial maximum tensile strain, and

k_1 and k_2 = experimentally determined material coefficients.

Later, other researchers considered the effects of stiffness and mixture variables, (Bonnaure et al. 1982) and revised equation (2-2) to be:

$$N_{fat} = (0.3PI - 0.015PI \times V_b - 0.198) \times S_{mix}^{-0.28} \times \varepsilon^{-0.2} \quad (2-3)$$

Where:

N_{fat} = number of load applications,

PI = penetration Index,

V_b = binder volume,

S_{mix} = mixture stiffness (KPa), and

ε = initial strain.

In order to consider and evaluate the effects of the variations in loading and frequency on fatigue life, Monismith et al. (1985) added an asphalt concrete mixture stiffness term into the equation (2-2) as follows:

$$N_f = f_1 \left(\frac{1}{\varepsilon_0} \right)^{f_2} \left(\frac{1}{S_0} \right)^{f_3} \quad (2-4)$$

Where:

S_0 = Initial flexural stiffness, and

f_1, f_2, f_3 = Experimentally determined coefficients.

Pell and Cooper (1975) studied the influence of volumetric asphalt content (V_b) and the air void (V_a) percentage on the fatigue performance of hot mix asphalt (HMA) and introduced these properties as follows:

$$N_f = K_1 \left(\frac{1}{\varepsilon_0} \right)^{K_2} \left(\frac{1}{S_0} \right)^{K_3} \left(\frac{V_b}{V_b + V_a} \right)^{K_4} \quad (2-5)$$

Where:

V_b = Volumetric asphalt content,
 V_a = Air void content,
 k_1, k_2, k_3 and k_4 = Experimentally determined parameters.

The Asphalt Institute (AI) Fatigue Model

The laboratory fatigue equations developed by the Asphalt Institute (AI, 1982) are based on the constant stress criterion and can be expressed as

$$N_f = 0.0432 \times \varepsilon_o^{-3.291} \times S_o^{-0.854} \quad (2-6)$$

Where:

ε_o = maximum tensile strain at the bottom of asphalt concrete layer,

S_o = stiffness modulus of asphalt concrete layer,

$C = 10M$ = function of volume of voids and volume of asphalt,

$$M = 4.84 \times \left(\frac{V_b}{V_b + V_a} - 0.69 \right),$$

V_a = air void volume, and

V_b = asphalt volume content.

After multiplying by a factor of 18.4 to account for the differences between laboratory and field conditions, the fatigue failure criterion becomes as follows:

$$N_f = 0.0796 \times \varepsilon_o^{-3.291} \times S_o^{-0.854} \quad (2-7)$$

Based on AASHO Road Test data and observed cracking in the field, laboratory-field shift factors of 13.4 and 18.45 for 10 percent and 45 percent cracking (in the wheel path areas) respectively were obtained by Finn et al. (1987). Deacon et al. (1994) in the SHRP A-003 studies

recommended a shift factor ranging from 10 to 14 depending on the amount of surface cracking that can be tolerated.

Shell Model:

For flexible pavement consist of three layers; HMA asphalt concrete surface layer, base layer and subgrade layer with infinite depth, a linear elastic system was adopted. Shell (1978) developed relationships for asphaltic layer strain fatigue and subgrade layer compressive strain for traffic loading. The model below is to find fatigue life at a temperature of 21°C:

$$N_f = 6.85 \times 10^{-2} \times \epsilon_t^{-5.671} \times S^{2.363} \quad (2-8)$$

Walid (2001) developed an empirical model for the prediction of pavement fatigue life based on AASHTO Road test data:

$$N_f = 9.73 \times 10^{-15} \times \epsilon_t^{-5.16} \quad (2-9)$$

Strategic Highway Research Program (SHRP) Model

A comprehensive laboratory work carried out in American Strategic Highway Research Program (SHRP) Project No.A-003 by Deacon et al. (1994) on the evaluation of performance properties of asphalt mixes. They developed the following equation:

$$N_f = 2.738 \times 10^5 \times e^{(0.077 \times \text{VFA})} \times \epsilon_o^{-3.624} \times S_o^{-2.72} \quad (2-10)$$

Where:

N_f = the number of load repetitions to a 50% reduction in stiffness,

VFA= voids filled with asphalt,

ε_o = the initial flexural strain, and

S_o = the initial flexural stiffness modulus in psi,

e = exponential function

Ismael (2006) established the relationship between fatigue life and stiffness, tensile strain in this model:

$$N_f = 7.2 \times 10^6 - 2 \times S + 635000 \times \varepsilon_t \quad (2-11)$$

Where:

N_f = the number of failure Repetitions.

S = asphalt stiffness modulus, @ 20°C, in Pa, and

ε_t = maximum tensile strain at the bottom of asphalt layer, mm/mm, $\times 10^{-5}$.

Al-khashaab (2009) studied effects of tensile strain and elastic modulus by developing the following equation:

$$N_f = 2.1422 \times 10^{-10} \times e^f \times \varepsilon_o^{-4.081} \times S_o^{-0.737} \quad (2-12)$$

$$f = 0.889 \times A_c + 1.351 \times \eta - 0.155 \times A_v$$

$$S_o = e^m$$

$$m = 8.876 - 0.0432 \times A_v - 0.03 \times T - 0.0447 \times A_c + 1.456 \times \eta$$

Where

N_f = number of failure repetition,

e = base of natural logarithm (2.718),

f = factor (function of volumetric properties),

A_c = asphalt content, percent (by weight of total mix),

η = rotational viscosity at 135 °C of asphalt (Pa.s),

A_v = air void content of compacted mixture,

ε_o = initial tensile strain at 5th repetition of bending beam, mm /mm, and

S_o = initial flexural stiffness modulus MPa.

2.6.4.2 Permanent Deformation Prediction Models

Numerous models have been developed for prediction of permanent deformation in the flexible pavement by the representation of either plastic deformation or the amount of rutting. These models were based basically on experimental testing data or field observation of performance-related data. In general, fatigue and permanent deformation models have been made by developing relationships between the load repetition numbers and asphalt concrete stiffness and/or the strains in the pavement. Most rutting models take the following form (Mathew and Krishna, 2009):

$$N_r = f_1 \times \varepsilon_c^{f_2} \quad (2-13)$$

Where:

N_r = the allowable number of load repetition to rutting failure.

ε_c = vertical strain at the top of subgrade.

f_1, f_2 = laboratory regression constants.

Part of the prediction models are reported in the following sections:

Asphalt Institute Model

The Asphalt Institute produces one of the widely used models to predict the number of axle loads that cause a specific amount of rut depth in the flexible pavement to occur (Huang 1993). This failure amount equals to 0.5 inch (12.5 mm). The model is:

$$N_d = 1.365 \times 10^{-9} \times \varepsilon_c^{-4.447} \quad (2-14)$$

Where:

N_d = axle load to rut depth criteria, 0.5 inch

ε_c = vertical compressive strain on the top of the subgrade.

The Asphalt Institute model, as well as other models with the same form but different regression coefficients and boundary conditions, are presented in the Table (2-8).

Table (2-8) Several Coefficients of Permanent Deformation Models for Various Agencies

No.	Organization	f_1	f_2
1	Asphalt Institute	1.365E_09	4.477
2	Shell Research	6.15E_07	4
3	US Army Corps of Engineers	1.81E_15	6.527
4	Belgian Road Research Center	3.05E_09	4.35
5	Transport and Road Research Laboratory	1.13E_06	3.75

Note: The f_1 and f_2 are the laboratory regression constants according to Eq. (2-13)

Other models for prediction of rutting depth as related to asphalt concrete material characteristics are presented as follows:

Morris model

Based on a large amount of data obtained from laboratory testing, Morris (1974) reached to a regression model with a polynomial shape to predict the plastic strain in the flexible pavement. The model elements include the average of tension and compression stresses (σ_1 and σ_3), the degree of temperature (T) and the number of load repetition (N) with an error of estimate (e). The functional form of the expression is:

$$\epsilon_p = f(\sigma_1, \sigma_3, T, V, N) \pm e \quad (2-15)$$

Uzan Model

Uzan (1983) developed a model that correlates the permanent deformation with the effects of traffic distribution and the length of the strain edge. The general form of the model is:

$$R_d = [(P \cdot a) / E] \cdot a_1 \cdot N^{a_2} \quad (2-16)$$

Where:

R_d = rut depth per application

P = contact pressure

a = radius of contact of one wheel of the standard dual wheel

E = subgrade resilience modulus

N = number of load application

a_1 and a_2 = functions of the materials properties and pavement geometry.

AASHTO Road Test Model

As reported by Chen and Huang (2001) the AASHTO models for rut depth prediction are strongly influenced by the traffic volume, deflection of the pavement surface and the stress on the top of the base. Two models have been developed for thin and thick asphalt pavement layers. For less than 6 inch pavement, the model is:

$$\text{Log } R_R = -5.617 + 4.343 \text{Log}(d) - 0.167 \text{Log}(N_{18}) - 1.118 \text{Log}(\sigma_c) \quad (2-17)$$

While for full depth pavement, the model is:

$$\text{Log } R_R = -1.173 + 0.717 \text{Log}(d) - 0.658 \text{Log}(N_{18}) + 0.666 \text{Log}(\sigma_c) \quad (2-18)$$

Where:

R_R = rate of rutting in micro-inch per axle repetition

d = surface deflection in micro-inch under a load of 9000 lb

N_{18} = number of 18-kip single axle repetition/100000

σ_c = vertical compressive stress at the asphalt –based interface (psi).

SHRP Model

The calculation of the rut depth in this method is depending on the summation of the product of plastic strain and the corresponding layer thickness during the analysis period for all seasons (Harold and Van 1994). It could be expressed as:

$$RD_j = \sum_{i=1}^j \Delta(RD_i) = \sum_{i=1}^j \sum_{k=1}^n \varepsilon_{ik}^p \cdot h_k \quad (2.19)$$

Where:

RD_j = rut depth accumulated up to season j

ΔRD_i = rut depth in season i

ε_{ik}^p = permanent strain during season i in layer k

h_k = thickness of layer k .

2.7 Flexible Pavement Analysis

The analysis of flexible pavement is developing from empirical procedures to mechanistic techniques. The limitations in computational abilities make the design of pavement firstly governed by empirical techniques that were restricted to some pavement materials and environmental circumstances. The change in these conditions would make the design process divergent from its expectations, and the errors increase. The accuracy in computation of stresses and strain in the pavement is the main factor that the mechanistic approach depends on, and the finite element analysis is one of most regularly used techniques as a tool for modelling simulation and mechanistic analysis. In this section, there will be a review of mechanistic analysis methods for the flexible pavement structural modelling, the multi-layer elastic method and finite element approach.

2.7.1 Elastic Layered Analysis Approach for Flexible Pavement

The analysis of flexible pavement structure has begun with traditional solutions of Boussinesq (1885) and Burmister (1943). Many other approaches have been developed based on these two methods to evaluate the stresses and strains in the pavement.

2.7.1.1 One Layer Method

The pavement with no surface can be treated as elastic layered systems in the semi- infinite half-space. These are axisymmetric cases to specify the vertical, tangential and radial stress conditions (Kim et. al, 2009).

Boussinesq (1885) answered the condition of the pavement of semi-infinite linear elastic, and homogeneous half-space by using a concentrated loading. He connected constitutive and kinematic equations with the equilibrium equations. Nevertheless, the solution that Boussinesq suggested, was not directly applicable to the structure of flexible pavement as each layer had a different modulus of elasticity and Poisson's ratio.

In 1958, Foster and Ahlvin combined the Boussinesq's study concentrated loading on circular area uniformly distributed loading to be applied for the analysis of flexible pavement structure. They provided charts for finding the vertical and horizontal stresses and the elastic strains in the semi-infinite half-space for an incompressible solid. Then, Ahlvin and Ulery (1962) tabulated the distribution of deflection, stress and strain outputs at a considerable number of points with variable Poisson's ratio values in the homogeneous half-space model.

2.7.1.2 Multi-Layer Theory

The Boussinesq's equations were an elastic solution for one layer pavement system. Burmister (1943) developed the Boussinesq's equations to be applicable for two-layer pavement structure, and later (1945) he extended his theory to cover the pavement system of three layers which considered as advanced flexible pavement analysis. This theory can be adopted to estimate the material mechanical responses for a multi-layered system of a greater number of pavement layers. The Figure (2-20) shows the multi-layered system. The assumptions of Burmister's theory (Huang, 2004) are:

1. Each layer of the pavement is homogeneous, isotropic, and linearly elastic.
2. Weightless and infinite layers are considered.

3. The pavement layers are of finite thickness except for the bottom layer that its thickness is infinite.
4. The applied load on the pavement surface is a circular uniformly distributed pressure.
5. The interface between two layers is continuous.

In a comparison made concerning the critical pavement responses, the theory of the multi-layer system of Burmister was more accurate than the one layer theory of Boussinesq (Kim, 2007).

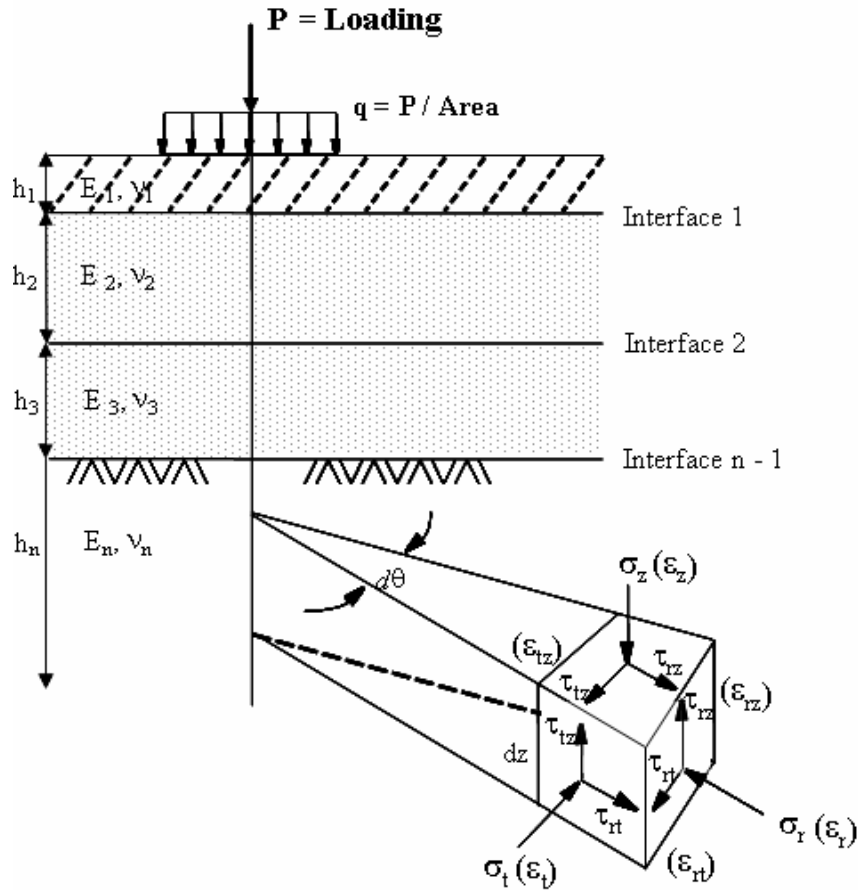


Figure (2-20) Multilayered Elastic System in Axisymmetric Condition (Kim, 2007)

2.7.2 Linear Elastic Layered Programmes for Multilayered Systems

The appearance of powerful computers encouraged the researchers to develop many computer programmes for application of pavement analysis and design based on the multi-layer linear elastic theory. The main objective of these softwares was overcoming the complication in computing the pavement responses like stresses, strains and deformations using multi-layer elastic theory and getting mechanistic solutions.

Warren and Dieckman (1963) developed a programme called CHEVRON (based on Chevron Research Company). That programme sanctioned analyses the application of one circular load on the pavement surface, and output was inquired at particularised intervals from the centre of the loaded area. Later, Hwang and Witczak (1979) made a modification on the programme to

include the nonlinear elastic behaviour of granular base materials and the linear elastic subgrade soil in the DAMA programme used by the Asphalt Institute. Based on the multi-layer elastic theory and with a limitation of the number of pavement layers of up to five, the DAMA software could be applied for analysis of pavement subjected to single or dual wheel load.

Shell Research (De Jong et al., 1973) revealed BISAR (Bitumen Stress Analysis in Roads) programme that adopted the multi-layered elastic theory developed by Burmister. The programme estimated the mechanical responses of multi-layer pavement structures and analysis them with different loading cases. The advantages of the programme were using various values of modulus of elasticity, Poisson's ratios, and layers thicknesses.

Kopperman et al. (1986) developed ELSYM5 programme at the University of California, for calculation of principal stresses, strain and deformations at desired locations by adopting the multi-layered elastic theory of five pavement layers and under different wheel loading.

The KENLAYER programme that developed by Huang (1993) at University of Kentucky implemented the solution of multilayer elastic system with application of circular loading area. The programme manipulated different wheels set and material properties. It adopted the fatigue and permanent strain equations as flexible pavement failure criteria developed by the Asphalt Institute for performing damage analysis by finding the minimum allowable number of load repetitions to failure and compare it to the existing traffic loading.

Federal Aviation Administration (FAA) in 1993 developed LEDFAA programme to design the thickness of airport pavement structures. The programme performed advanced design method using the multi-layered elastic theory. They found that the programme results showed that linear elastic design could give a better prediction of wheel load interactions for the Boeing 777 aeroplane since the landing gear configurations and layered pavement structures can be modelled directly using the layered elastic design procedure.

2.7.3 Finite Element Analysis Programmes for Pavements

The application of finite element modelling has been widely used for pavement structure analysis and design. The reason behind its getting widespread attention from pavement modelling is its remarkably varied implementation of mechanical properties (Kim et al., 2010). In this part of the chapter, some of two and three-dimensional finite element solutions that used for pavement analysis are summarised. As shown in Figure (2-21), three sorts of analysis models, axisymmetric, 2-D plane, and 3-D, are typically adopted by researchers to investigate the performance of multilayered pavement structures.

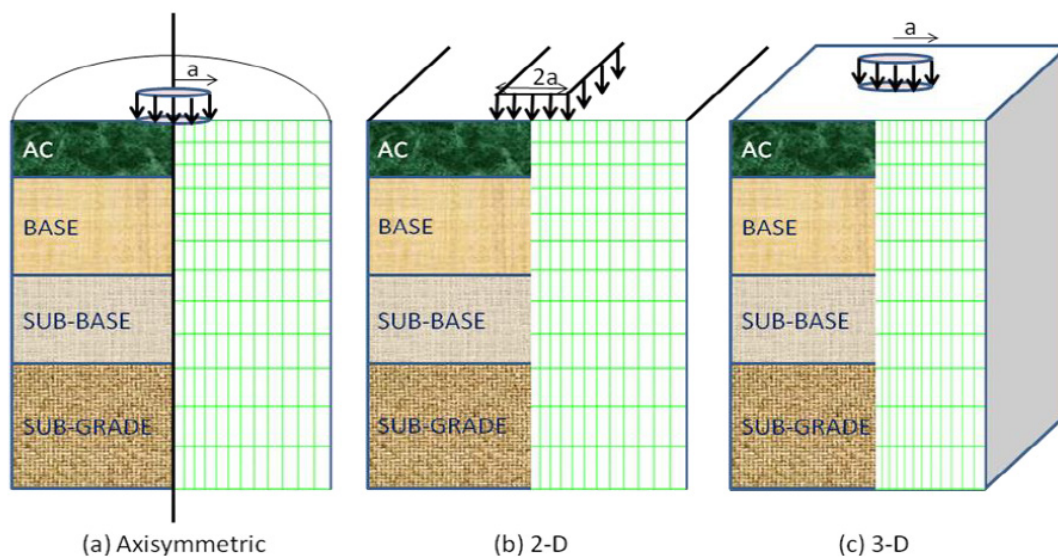


Figure (2-21) Three Typical FE Analysis Models for Pavements (Kim et al., 2010)

2.7.3.1 Axisymmetric and Two-dimensional Finite Element Analysis

Hicks (1970) made a model of three-layer pavement section including an asphalt concrete of a thickness of 102 mm, 305 mm of a granular base and the lower layer is a clay subgrade. A uniformly distributed load was applied on a circular area. He adopted the finite element method and used two types of material resilient modulus modelling according to the way of computing, the first one was by bulk stress and the other one by the confining pressure. The solution involved an application of four equal wheel load increments. He found that fair change in the resilient modulus of pavement layers was observed as a result of considerable variations in the pavement structure responses to the applied load.

Raad and Figueroa (1980) developed the ILLI-PAVE finite element programme at the University of Illinois, and Harichandran et al. (1989) developed the MICH-PAVE that based on finite element method as well at the Michigan State University. Both programmes are widely used for flexible pavement analysis and adopt axisymmetric modelling method using the K- θ model for the granular materials and the bilinear approximation for fine-grained subgrade soils. The principal stresses in the pavement layers (granular and subgrade) were governed by Mohr-Coulomb theory, so they did not exceed materials strength. In MICH-PAVE programme, an adjustable boundary of a limited depth under the subgrade surface, rather than fixed boundary that located deeper in the subgrade layer and that reduced the time and storage consuming as compared to other programmes.

Thompson and Garg (1999) proposed an engineering Procedure for estimation of critical pavement responses adopting the superposition of single wheel pavement responses. They employed two analysis approaches, axisymmetric finite element and multilinear elastic layered system to calculate responses. Their approach used the average value of resilient modulus of the pavement layer that acquired from axisymmetric ILLI-PAVE finite element programme. The results of ILLI-PAVE finite element analysis were used as input data for the multilayered elastic analysis.

2.7.3.2 Three-Dimensional Finite Element Analysis

Chen et al. (1995) investigated the influence of the tire inflation pressure and heavy axle loading on the performance of flexible pavement by making a three-dimensional finite element model. The pavement structure layers were considered to be homogeneous and linear elastic materials. They compared the results of their study to an elastic layered programme, ELSYM5 (Kopperman et al., 1986), for a circular uniformly distributed pressure and they found that there was a good agreement between the two approaches.

Helwany et al. (1998) considered a three-layer flexible pavement system with application of several sorts of axle loading, with different configurations and tire pressures. They used two-dimensional (DAC SAR) and three-dimensional (NIKE3D) finite element programmes. The preliminary analysis of one layer pavement model using both programmes showed an agreement the Boussinesq's solutions. The study suggested that adopting finite element modelling of pavements could be remarkably beneficial to predict accurate pavement structure responses.

Shoukry et al. (1999) employed three-dimensional finite element model for back-calculation of modulus of elasticity of pavement structures and they compared the outcomes with the predictions of back-calculation programmes such as EVERCALC, MODCOMP, and MODULUS. The displacements were calculated from the falling weight deflectometer tests. The pavement layers were modelled as linear elastic layers with 8-noded solid brick elements. They found that the proposed three-dimensional finite element analysis had a decent agreement with the back-calculated layer modulus of elasticity estimated by the other programmes.

Wang (2001) used three-dimensional finite element analysis to study the flexible pavement structures responses including different materials, model dimensions and various loadings. He developed an effective meshing tool for a three-dimensional model consolidating multiple layers, interface bonding, and several loading configurations. He found that spatially different tire and pavement pressures significantly influenced the stresses and strains in the flexible pavement model.

2.7.3.3 Finite Element Pavement Analysis Programmes Characteristics

The finite element analysis technique extends the best way of investigation for the multilayered pavement structures. Three and two-dimensional as well as axisymmetric finite element models have different element creation and consider variable directional mechanisms of stresses and strains. Three-dimensional finite element analysis can analyse all three directional response components and should predict more accurate pavement responses (Kim, 2007).

2.7.3.4 General Purpose Finite Element Programmes

ANSYS, ABAQUS, and ADINA are widely used general-purpose finite element programmes that can afford decent analyses of different engineering problems. Despite the fact that the modelling of pavement structure has dramatically progressed in recent years, the analysis of pavements by general-purpose programmes has not been employed for modelling of flexible pavement frequently. Formerly, a few researchers have studied the pavement responses using the general-purpose finite element programmes.

Hu et al. (2015) used using ANSYS programme for the development of a linear elastic three-dimensional model of flexible pavement with fully bonding between layers to compute the deformation of each asphalt concrete layer regarding some variable like the asphalt concrete layer modulus, the asphaltic layer thickness, wheel loads, and tire inflation pressure. They found that the deformation in pavement significantly influenced by resilient modulus of asphaltic layers, while the variation in the pavement thickness and wheel loading had less influence on pavement displacement.

Ying and Yiling, (2015) made a three-dimensional model by employing ANSYS programme with linear elastic properties of pavement materials and briefly described the calculation of the stress distribution and displacement on the surface under the applied tire pressure.

Ševelová and Florian (2013) used the ANSYS software as an FE modelling tool to develop a two-dimensional model of low volume roads for to determination of stress and deformation in any point of the pavement structure and hence produce data required for the reliability analysis. The low volume roads usually built of compacted stones and granular coarse and fine aggregate layers with no need for asphalt concrete layer of high modulus of elasticity. Their model was of four layers; cover, base, subbase and subgrade. They compared two material characteristics for modelling of unbound non-homogenous materials used in low volume roads. The first one is linear elastic model according to Hook theory (H model), and the second model is nonlinear elastic-plastic Drucker-Prager (D-P model). They found that the Stresses predicted by the Drucker-Prager method are generally lower than the stresses obtained from H model particularly for small values of resilient modulus.

Shi and Guo (2008) performed a linear three-dimensional finite element method to present design parameters for highway tunnel flexible pavement with an application of dual wheel load on a rectangular contact area. The model included three layers, and the layers are surface asphalt concrete, base course and bedrock course. They investigated the horizontal tensile stress at the surface of the asphalt layer, the horizontal tensile stress at the bottom of the asphalt concrete layer and the vertical shear stress at the surface of the asphalt layer. They concluded that the increase in asphalt layer thickness had a slight effect on reducing the damage caused by the vertical shear stress and its optimum value was 14 cm, and base course with higher stiffness modulus should be agreed, and its thickness adjusted base on the bedrock modulus.

Sinha et al. (2014) studied the influence of subbase material type on the flexible pavement life. Three kinds of commonly occurring materials were used; coarse sand, conventional subbase material (CSM) and stone dust with four types of industrial waste materials. They carried out a finite element analysis of the pavement structure using ANSYS software, and they found that using of industrial waste in the subbase layer decreased the life to 60 to 83 percent. They made suggestions for design possibilities to counterbalance the decline in the life of the pavement.

2.8 Summary

The hydrated lime has been successfully used in asphaltic paving mixtures for a long time, and it is still an active research area as explained by the high number of recent publications. As seen in the literature, there are many proofs of the efficiency of hydrated lime in enhancing the asphalt concrete pavement resistance to major distresses happen in it such as rutting, fatigue cracking and moisture damage. All available test methods demonstrate the hydrated lime beneficial impact. It makes the asphalt cement stiffer than the normal mineral filler does, which is an influence that adequately shown in the literature, and it is recognised more above the room temperature. The asphalt cement stiffening by hydrated lime enhanced the mechanical properties of the asphalt paving mixture. The addition of hydrated lime to asphalt concrete mixtures improves the bonding between asphalt cement and aggregate particles due to its reaction with the aggregate surface. In the same time of dealing with the aggregate surface, the hydrated lime reacts with bitumen as well.

The effect of hydrated lime on the moisture susceptibility had studied (Esarwi et al., (2008) and Gorkem and Sengoz (2009)) by adding up to 2% of hydrated lime as a percent of the total weight of the aggregate. They found that the majority of the modified specimens were able to meet acceptable Tensile Strength Ratio (TSR) as compared to the control mixes that some of them failed to meet TSR requirements. They suggested that the enhancement in the bonding between aggregate surface and asphalt cement was because of hydrated lime forming insoluble components on the aggregate surfaces and preventing reaction with water.

It has been recognised that using of hydrated lime in the asphalt concrete mixes is advantageous. Although, the best way for introducing of hydrated lime to the mix still

controversial. Generally, transportation agencies and contractors have used one or more of three common ways to add lime to asphalt concrete mixtures; adding dry hydrated lime to dry aggregate, dry hydrated lime to wet aggregate, and adding hydrated lime in the form of a slurry. The main benefits of second and third methods the coverage and permits for a relatively better coverage of hydrated lime on the aggregate particles surfaces as compared to the dry hydrated lime to dry aggregate technique with less lime loss due to dusting and carrying out by the wind. However, they need further effort, fuel and time to dry the aggregate earlier to asphalt concrete mix production and the necessity to buy and manage specific, expensive devices.

A new Mechanistic-Empirical Pavement Design Guide (MEPDG) has recently been developed (NCHRP 1-37A, 2004) and is currently under validation-implementation by many states. The design guide represents a challenging addition in the way that pavement design and analysis is conducted. Design inputs comprise traffic configurations, material characterization, climatic factors, performance models, and other factors. Performance prediction and pavement life are estimated based on the multi-layered elastic theory and the empirically developed failure criteria (Kim et al., 2010).

The mechanistic-empirical design of flexible pavements requires an iterative procedure by the designer. The designer must make a trial pavement design and then analyse the design to determine if it fits the performance criteria set by the designer. Adjustment is needed when the design does not meet the performance criteria and repeat analysing until reaching the required performance criteria (NCHRP 1-37A, 2004). The process of iteration is performed on pavement layer thickness after considering the design inputs.

Implementation of a new aspect or idea into this important pavement design method could be a step of contribution to developing it with other researchers' proposals. The modification of pavement asphaltic mixture by hydrated lime and try to use the modified mixture in the iteration process instead of increase thickness directly. This could be a useful step in the process to reach an optimum thickness of asphalt concrete layer that meets the performance criteria (fatigue cracking and permanent deformation failure criteria models) with less thickness as compared with control mixtures.

A survey of the way of pavement analysis and design was presented in this chapter. The analysis of flexible pavement is developing from empirical to mechanistic methods. The limitations in computational capabilities cause the pavement design firstly ruled by empirical techniques that were restricted to some pavement materials and environmental circumstances. Many pavement mechanistic approaches were presented by researchers and pavement design agencies such as multilayered elastic theory and finite element analysis by using computer software of variable techniques like axisymmetric, two or three-dimensional analysis.

ANSYS is one of the widely used general-purpose finite element programmes that can provide satisfactory analyses of different engineering problems. Although the modelling of pavement structure has been dramatically progressed in recent years, the analysis of pavements by general-purpose programmes has not been employed for modelling of flexible pavement frequently. Formerly, a few researchers have studied the pavement responses using the ANSYS finite element programme.

Chapter Three

Materials and Testing Programme

3.1 Introduction

The purpose of the testing programme conducted in this study is to determine and evaluate the hydrated lime modified HMA pavement mechanical responses to the major distresses (fatigue cracking, rutting and moisture susceptibility) that generally occurred in the pavement. In particular, fatigue cracking and rutting considered as failure criteria in the mechanistic-empirical design process. Accordingly, the need of laboratory work is important for that purpose. The laboratory work consists of the preparation of asphalt concrete mixtures regarding each percent of hydrated lime partial replacement of mineral filler (limestone dust). Furthermore, penetration and the softening point (ring and ball) tests were adopted to study the influence of hydrated lime on asphalt cement consistency and stiffness. The performance related properties of asphalt concrete mixtures were evaluated by conducting the following tests; Marshall test, for mixture design and to investigate the resistance to plastic flow, density-voids characteristics, and stability. The second test is Moisture Susceptibility test to investigate the influence of moisture damage on the non-modified (control) and hydrated lime modified asphalt concrete mixtures. The other test is flexural beam fatigue for evaluating the fatigue performance and finally uniaxial repeated loading test to determine the resilient and permanent deformation of control and modified asphalt concrete mixtures.

3.2 Materials

The materials that used in the experimental part of this research are locally available in Iraq, and these materials are asphalt cement, aggregate, and fillers. They have been characterized using routine types of tests, as detailed in sections 3.2.1, 3.2.2 and 3.2.3, and the results were compared with Iraqi State Corporation for Roads and Bridges specifications (SCRB, R/9 2003).

3.2.1 Asphalt Cement

Asphalt cement of (40/50) penetration grade is used in this study, which is produced in Aldorah refinery, southwest of Baghdad. A set of ASTM tests was conducted for the identification of the basic physical properties of asphalt cement and their meeting the Iraqi specifications limits. The asphalt cement physical properties are illustrated in Table (3-1).

Table (3-1) Physical Properties of AC 40/50

Tests	units	40/50 AC test results	SCRB Specification
Penetration (25C, 100gm, 5 sec). ASTM D5	1/10mm	42	40-50
Softening point (Ring & Ball). ASTM D36	°C	49	----
Specific gravity (25°C). ASTM D70	----	1.04	----
Flash Point (Cleveland open cup). ASTM D92	°C	293	Min.232
Ductility (25°C, 5 cm/min). ASTM D113	cm	120	Min100
Residue after thin film oven test (ASTM D1754)			
Penetration (25C, 100gm, 5 sec). ASTM D5	1/10mm	25	Min 55% of original
Ductility (25°C, 5 cm/min). ASTM D113	cm	80	Min 25

3.2.2 Mineral Filler

The mineral filler is a nonplastic material and its particles pass sieve No. 200 (0.075 mm in diameter). In this work, the main effective parameter that the research will evaluate is the mineral filler type effect on the properties that related to the performance of asphalt concrete mixtures and the design criteria of mechanistic-empirical method. The control mixtures were prepared using limestone dust as mineral filler at a content of 7, 6 and 5 percents. These percentages are the mid-range set by the SCRB specification for three types of mixes; IIIA, II and I for wearing, leveling and base course respectively. Hydrated lime has been known to be a promising potential material for pavements due to its unique physical/chemical/mechanical characteristics.

The Iraqi State Corporation for Roads and Bridges specifications (SCRB, R/9 2003) has recommended using the hydrated lime in a percentage of 1.5% by the total weight of aggregate as an anti-stripping additive for hot mix asphalt pavement.

In this study, the hydrated lime is used in a dry form (adding dry lime to dry aggregate) prior to asphalt adding and mixing process. The addition of hydrated lime was in six contents; 0%, 1.0%, 1.5%, 2.0%, 2.5% and 3.0% by total weight of aggregate as a limestone dust partially replacement. The limestone dust and hydrated lime were obtained locally from lime factory in Karbala governorate, southeast of Baghdad. The physical properties and chemical composition of hydrated lime and limestone are presented in the tables (3-2) and (3-3) respectively.

Table (3-2) Physical properties of hydrated lime and limestone

Material property	Hydrated lime	Limestone dust(filler)
Specific gravity(gm./cm ³)	2.43	2.71
Specific surface (m ² /Kg) *	394	246
Passing No. 100 Mesh (150 μm), %	100	100
Passing No. 200 Mesh (75 μm), %	99	87

*Tested by Blaine Air Permeability at material laboratory of civil engineering department/University of Baghdad according to ASTM-C204, 2004.

Table (3-3) Chemical composition of hydrated lime and limestone

Chemical composition	Limestone	Hydrated lime
% CaO	68.3	56.1
% SiO ₂	2.23	1.38
% Al ₂ O ₃	N/A	0.72
% Fe ₂ O ₃	N/A	0.12
% MgO	0.32	0.13
% SO ₃	1.2	0.21
% Loss On Ignition (L. O. I.)	27.3	40.65

3.2.3 Aggregate

The aggregate used in this laboratory work was crushed quartz obtained from Amanat Baghdad asphalt concrete mix plant located in Al-Taji, north of Baghdad. Its source is Al-Nibaie quarry. The aggregate used in this study is widely applied in the majority of Baghdad city and other cities for HMA pavement construction. The aggregate (coarse and fine) was sieved and recombined in proper proportions to meet the wearing (surface), leveling (binder) and the base course gradation as required by SCRB specification (SCRB, R/9 2003). Conventional tests were performed on the aggregate to evaluate their physical properties against the specification limits set by the SCRB. The physical properties of the aggregate are presented in Table (3-4) whereas the requirements for the asphalt concrete mixtures gradations and the selected aggregate gradations for the pavement asphalt concrete layers (wearing, leveling and base) are presented in table (3-5) and (3-6) respectively. Figures (3-1), (3-2) and (3-3) present the gradations of aggregate for the studied layers mixtures. However, sieve analysis was conducted to separate the aggregate according to the sieve size. The specifications of hot mix asphalt mixture define the aggregate particles to be in particular size limits and each size of aggregate particles to be in a specific proportion.

Table (3-4) Physical Properties of Aggregate

Properties	Al-Nibaie aggregate		SCRB Properties limitations
	Coarse Aggregate	Fine Aggregate	
Bulk specific gravity (g/cm³) (ASTMC127 and C128)	2.52	2.643	N/A
Apparent specific gravity (g/cm³) (ASTM C127 and C128)	2.55	2.68	N/A
Percent water absorption (ASTM C127 and C128)	0.13	0.520	N/A
Percent wear (Los-Angeles Abrasion) (ASTM C131)	19.0		30 Max
Fractured pieces, %	96		90 Min
Sand equivalent, % (ASTM D 2419)		59	45 Min
Soundness loss by sodium sulfate solution,% (C-88)	4.12		12 Max

Table (3-5): Asphalt Concrete Mixtures Gradings (SCRB/R9, 2003)

Sieve size		Type I	Type II	Type IIIA	Type IIIB
inch	mm	Base Course	Binder or Leveling Course	Surface or Wearing Course	
		% Passing by Weight of Total aggregate + Filler			
1 ½ in	37.5	100			
1	25.0	90 - 100	100		
¾	19.0	76 - 90	90-100	100	
½	12.5	56 - 80	76 - 90	90 - 100	100
⅜	9.5	48 - 74	56 - 80	76 - 90	90 - 100
No. 4	4.75	29 - 59	35 - 65	44 - 74	55 - 85
No. 8	2.36	19 - 45	23 - 49	28 - 58	32 - 67
No. 50	0.3	5 - 17	5 - 19	5 - 21	7 - 23
No. 200	0.075	2 - 8	3 - 9	4 - 10	4 - 10
Asphalt Cement (% weight of total mix)		3 - 5.5	4 - 6	4 - 6	4 - 6

Table (3-6) Selected Gradations for Studied Asphalt Concrete Courses

Sieve size		Type I	Type II	Type IIIA
inch	mm	Base Course	Leveling Course	Wearing Course
		Percent Passing (%)		
1.5	37.0	100		
1	25.0	95	100	
¾	19.0	83	95	100
½	12.5	68	80	95
⅜	9.5	61	69	83
No. 4	4.75	44	50	59
No. 8	2.36	32	35	37
No. 50	0.3	11	13	13
No. 200	0.075	5	6	7

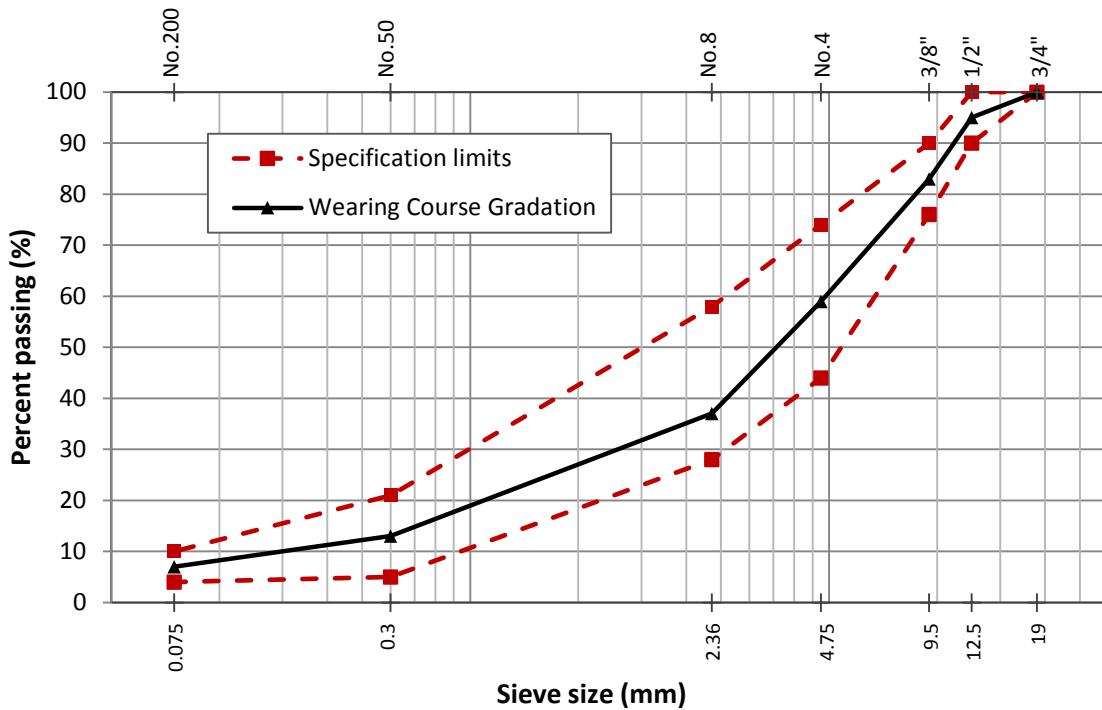


Figure (3-1): Selected Wearing Gradation of Combined Aggregate and Mineral Filler

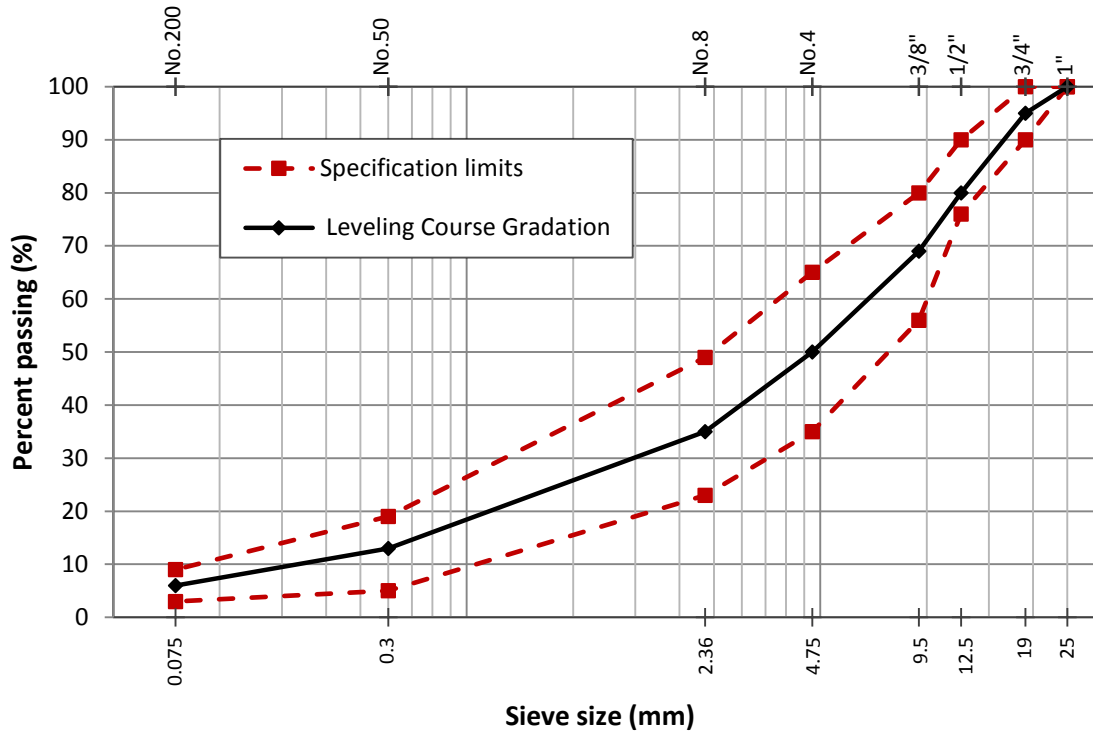


Figure (3-2): Selected Leveling Gradation of Combined Aggregate and Mineral Filler

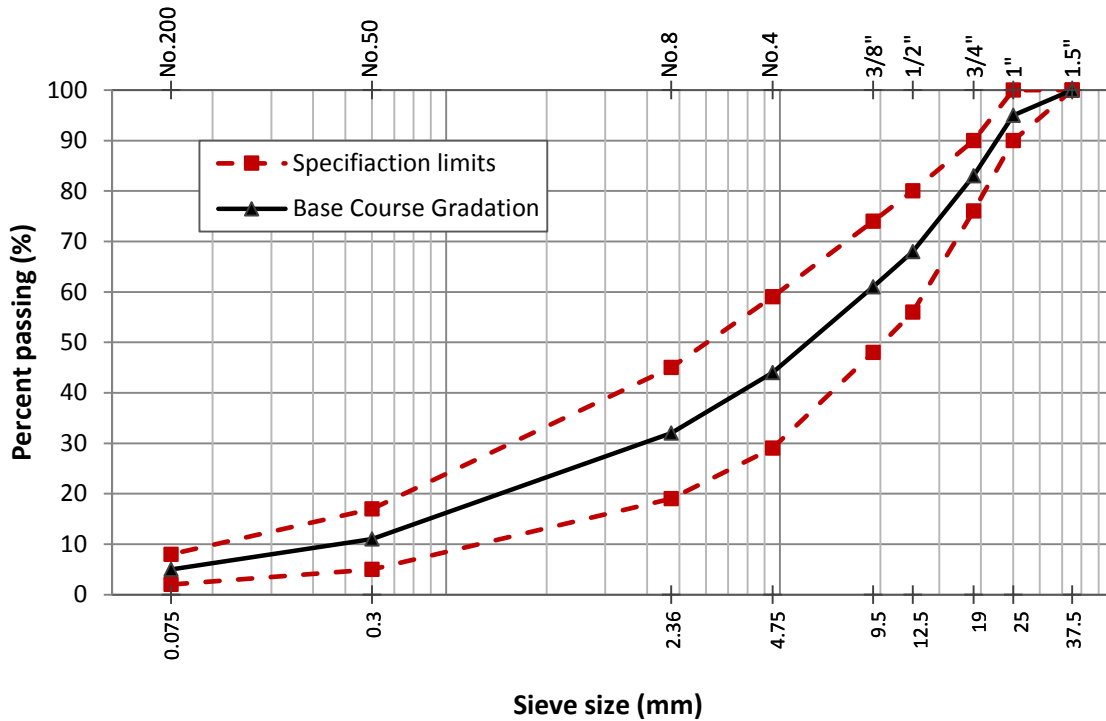


Figure (3-3): Selected Base Gradation of Combined Aggregate and Mineral Filler

3.3 Hydrated lime effect investigation by experimental work

The experimental work started by calculating the optimum asphalt content for all the asphalt concrete mixes through the process of Marshall mix design. Then, the asphalt concrete mixes were made at their optimum asphalt content and tested to evaluate the engineering properties, permanent deformation and fatigue characteristics. The permanent deformation and fatigue properties were assessed using uniaxial repeated loading and repeated flexural beam tests.

3.3.1 Asphalt cement tests

There are many tests designated to determine the consistency and stiffness of bitumen material (asphalt cement) in which the main reason to use it is for the bonding between aggregate particles when making the asphalt concrete mixture. Penetration and softening point are the most important tests that adopted by the majority of agencies and standard specifications in the field of flexible pavement. These tests are briefly described here:

3.3.1.1 Penetration Test

Penetration is the distance in tenths of millimeter that a standard needle penetrates vertically into a sample of asphalt that melted and cooled under controlled, specified conditions of load, time and temperature. The penetration test is used as a measurement of consistency according to ASTM D5 (ASTM Vol. 04.03, 2004). The higher values of penetration mean softer consistency. Figure (3-4) shows the penetration test of asphalt cement.

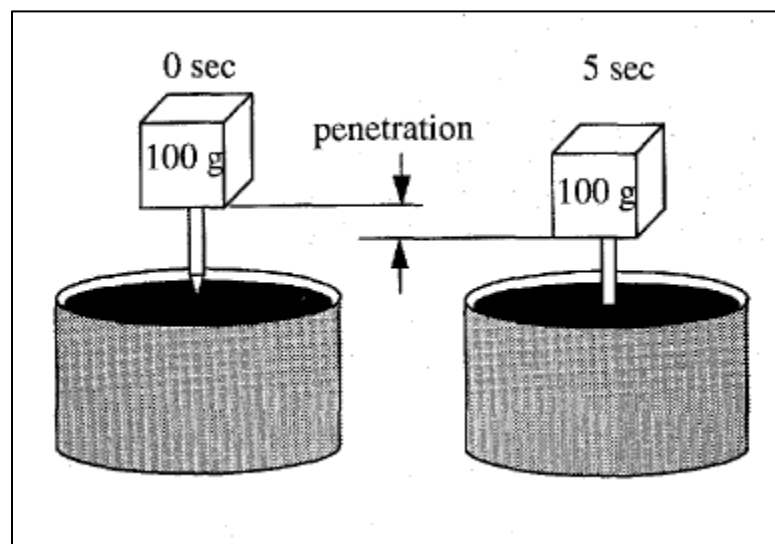


Figure (3-4) Penetration test of bitumen material (McGennis et al., 1995)

3.3.1.2 Softening Point Test

The softening point test (also known as Ring & Ball method) is the temperature at which a steel ball of constant weight laying on the asphalt cement specimen and falls a distance of 25.4 mm (1 inch). Because of temperature increment and due to decreasing of asphalt cement stiffness that affected by temperature, the ball gradually falls through the asphalt cement specimen. It is an indication of the internal tendency to flow at elevated temperature. Figure (3-5) illustrates the apparatus of softening point test for asphalt cement. The test is done according to ASTM D36 in which a full description of this test is there.

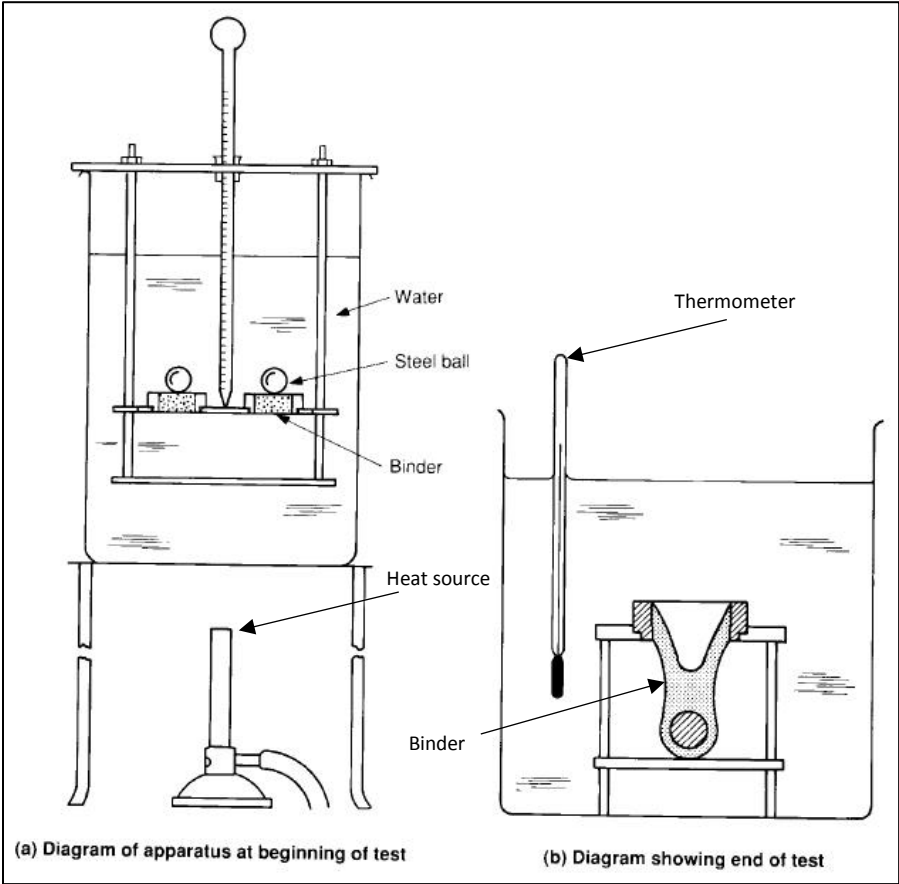


Figure (3-5) Softening Point Test of bitumen (Millard, 1993)

In this study, penetration and softening point tests have been adopted to evaluate the influence of partial replacement of mineral filler (limestone dust) with hydrated lime on the mastic properties. There are three flexible pavement courses evaluated in this study; Wearing, Leveling, and Base and each one of them was assessed by producing mixtures with different hydrated lime content and since this section is for asphalt cement assessment and not related to other components of the asphalt concrete mixture, it is enough to adopt one of the courses for that purpose and no need to repeat that on the other courses due to similarity. The change in the filler components percentage for the wearing course was selected to be evaluated with the optimum asphalt cement content for each mixture that had a different percentage of added hydrated lime as replacement for an initial percentage of lime mineral filler of 7 in terms of total aggregate weight.

3.3.2 Mixture Preparation

The aggregate was first sieved, washed, and dried to constant weight at 110°C to meet the Iraqi specifications (section R9) table R9/3 grading of pavement layers. Five different percent of hydrated lime (1, 1.5, 2.0, 2.5, and 3.0) were added by total weight of aggregate with the same reduction in the amount of limestone dust filler. Each mix was designed with the same aggregates gradation to avoid variability due to physical and mineralogical characteristics of the aggregates. The variable factor which is causing differentiation in mixes is the hydrated lime percentage named as H. Limestone mineral filler was reduced after every hydrated lime amount increased in the mix as shown in Table (3-7) for the mixes of wearing, leveling and base course.

Table (3-7) Filler Content replacement with Hydrated Lime in the Mixtures for Different Pavement Courses

Mixture = Coarse Aggregate + Fine Aggregate + Filler (Limestone + HL) + asphalt						
Hydrated Lime Content (%)	Wearing Course		Leveling Course		Base Course	
	Mixture	Limestone Content (%)	Mixture	Limestone Content (%)	Mixture	Limestone Content (%)
0	CW	7	CL	6	CB	5
1	H1W	6	H1L	5	H1B	4
1.5	H1.5W	5.5	H1.5L	4.5	H1.5B	3.5
2	H2W	5	H2L	4	H2B	3
2.5	H2.5W	4.5	H2.5L	3.5	H2.5B	2.5
3	H3W	4	H3L	3	H3B	2

3.3.3 Marshall Mix Design

The mix design and preparation followed the Marshall method as summarized in the manual series No. 2 of Asphalt Institute (Asphalt Institute, 1984). The Marshall design process includes the determination of plastic flow resistance of cylindrical samples of asphaltic pavement mixture laterally loaded on by Marshall loading device. To prepare the materials for testing, the aggregate (Coarse, Fine, and filler (Limestone and Hydrated Lime)) was heated to the temperature of 160°C. The bitumen material (asphalt cement) was heated to a temperature of about 140°C in which its kinematics viscosity is 170 centistokes with a tolerance of ±20 centistokes. Then, the asphalt cement was added to the heated aggregate to achieve the certain amount, and blended thoroughly, until all aggregate particles are covered with asphalt cement. Thereafter, the specimens were made for Marshall test to decide the optimum asphalt content for each mixture. The prepared mixtures were placed in a preheated and lubricated molds of 101.6 mm (4 in) in diameter by 63.5 mm (2.5

in) in height, and compacted by means of the automatic Marshall compactor with 75 blows per end. The compaction effort was done with a hammer of 4.536 kg (10 lb) weight that slides and a free fall of 457 mm (18 in) on the top and bottom face of each specimen. The specimens were allowed to be cooled to room temperature. To calculate the optimum asphalt content, five asphalt content selected for each mix and the range of asphalt cement percentage by the total weight of the mixture was from 4.3% to 5.5% for Wearing, 4.0% to 5.2% for Leveling and from 3.7% to 4.9% for Base course with a constant increasing of 0.3 percent in asphalt content. Three specimens for each mix were made, and the average results of their properties was took. Accordingly, each mixture in the courses Wearing, Leveling and Base needed 15 samples to find its optimum value of asphalt cement.

The Marshall stability and flow and the other volumetric properties of mixes were obtained according to the description in method in the standards ASTM D6926-10 and ASTM-D-1559 (2004). The cylindrical specimen was conditioned at first by placing in water bath of 60°C for ½ to ¾ hour, and after that compressed by Marshall apparatus on the side surface with a constant loading rate of 50.8 mm/min (2 inch/min) until it failed. Based on this process the optimum asphalt content was determined in terms of the average value of the parameters below:

- Asphalt content at maximum density
- Asphalt content at maximum stability
- Asphalt content at 4% air voids (4.5% for base course as a mid-value of SCRB specifications).

Figures (3-6) shows schematic of Marshall apparatus loading, stability and flow. The test machine is presented in Figure (3-7).

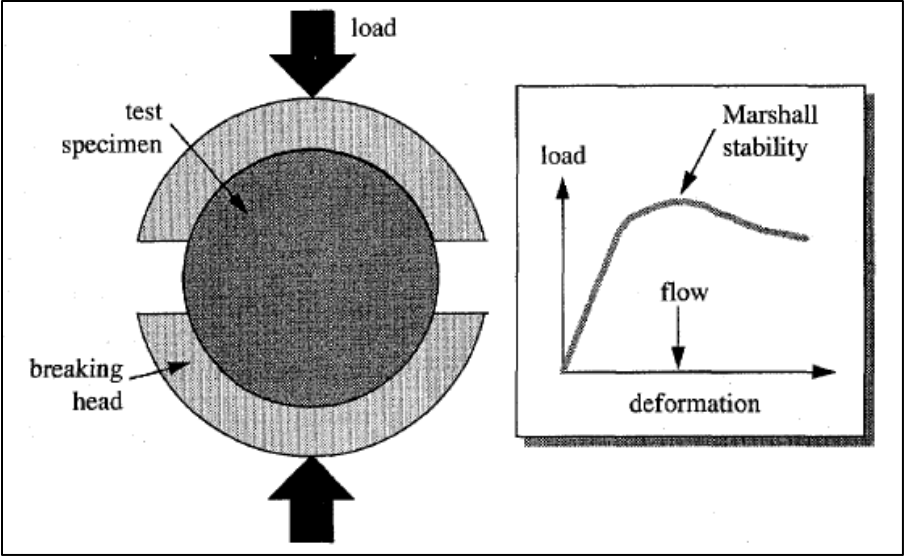


Figure (3-6) Marshall Stability (McGennis et al., 1995)



Figure (3-7) Marshall Apparatus for Determination of Stability and Flow

Air void percentage (ASTM D3203), bulk density and specific gravity (ASTM D2726) and the maximum (theoretical) specific gravity (no voids in mix) (ASTM D2041) were calculated for the tested specimens. Figure (3-8) presents a specimen being processed to calculate its maximum specific gravity.

The calculation of air void (AV), bulk specific gravity (G_{mb}), and maximum theoretical specific gravity (G_{mm}) is briefly described as follows:

- Bulk Specific Gravity (G_{mb}): The weight of the specimen is measured in air and in water at 25°C and in condition of saturated surface dry. The bulk specific gravity can be calculated as follows:

$$G_{mb} = \frac{W_a}{W_{ssd} - W_w} \quad (3-1)$$

Where:

G_{mb} = bulk specific gravity of the compacted specimen,

W_a = weight of specimen in air (gm),

W_{ssd} = weight of saturated surface dry specimen (gm), and

W_w = weight of specimen in water (gm).

- Maximum specific gravity: The maximum specific gravity of loose paving mixture for any asphalt content percent should be obtained in the laboratory as the follows:

$$G_{mm} = \frac{A}{A+B-C} \quad (3-2)$$

Where:

G_{mm} = Maximum specific gravity of loose paving mixture,

A = Weight of dry sample in air, (gm),

B = Weight of flask filled with water at 25°C (gm), and

C = Weight of flask and sample filled with water at 25°C (gm).

- Air voids (AV): It is the total volume of the small pockets of air between the coated aggregate particles throughout the compacted mixtures. It is obtained by first determining the maximum theoretical specific gravity of the specimen and then expressing the

difference between this and the bulk density as a percentage of the theoretical density and according to the following relationship:

$$AV = \frac{G_{mm} - G_{mb}}{G_{mm}} \quad (3-3)$$

Where:

AV = voids in total mix, i.e. in the specimen (%),

G_{mm} = maximum theoretical specific gravity (gm/cm^3), and

G_{mb} = bulk specific gravity of the compacted specimen (gm/cm^3).



Figure (3-8) Maximum Specific Gravity Calculation for Asphalt Concrete Specimen

3.3.4. Permanent Deformation

3.3.4.1 Preparation of Permanent Deformation Specimens

The dimensions of the cylindrical specimens used in this work are 101.6mm (4inch) in diameter and 203.2mm (8 inch) in height. The various fractions of aggregate as were separated into portions, as retained on the following set of sieves; (1", 3/4", 1/2", 3/8", No.4, No.8, No.50, No.200 and pan) using dry sieve analysis. The aggregate that passed sieve No.200 (0.075mm) was discarded since the material passing sieve No.200 that used in this study is the mineral filler (limestone and hydrated lime). According to the gradations requirements shown in Table (3-4) for wearing, leveling and base mixes, the aggregate was combined for each mix into batch of 3800gm

on the mixing bowl and heated to 160°C in a temperature controlled oven. Asphalt cement was also heated in a container to a temperature of 140°C, the required amount of asphalt cement for each mix was then poured to the mixing bowl on the electrical balance. For two minutes, the content of the bowl was thoroughly mixed by hand on a hot plate. To ensure uniform mixing temperature, the bowl with its content was placed into an oven of 140°C for 10 minutes. Meanwhile, the cylindrical mould of a diameter of 101.6 mm (4 in) and a height of 254 mm (10 in) was preheated in the oven with 100°C. A paper disk of a diameter of 101.6 mm (4 in) was inserted to cover the mould base plate, and then the interior wall of the mould was lubricated by oil to facilitate the specimen extraction later. By means of a funnel, approximately half of the mixture pushed to the mold, the mixture then shoveled in the mold with a preheated spatula 15 times on the circumference and 10 times on the inner side. The second half of the batch placed in the mold and the preceding procedure was repeated. The compaction of specimen made by double plunger method with a load of around 22679.6 kg (50000 lb) on each face of the specimen for one minute. The compression made by hydraulic compression machine existed in the Material laboratory of Civil Engineering Department of the University of Baghdad. The load is applied to each end of the specimen for one minute. Finally, the specimen is carefully transferred to a smooth, flat surface and allowed to cool at room temperature and then extracted from the mold using a hydraulic extractor. The specimen was then numbered and stored in a bag to be ready for testing.

The above compaction procedure was developed after several trials utilising compression machine to obtain densities for the cylindrical specimens similar to the densities of specimens prepared according to Marshall mix design. These trails began with fixing the weight of asphalt mixture (approximately 4000 gm) for the specimens and varying the compaction efforts (i.e., 9071.8, 13607.7, 18143.7, 22679.6 and 27215.5 kg) applied to each face of the specimen for one minute. Then, the densities of the compacted specimens were determined and plotted versus the compaction efforts as shown in Figure (3-9). In conclusion, the densities of the permanent deformation cylindrical specimens for each mixture type similar to that required by the Marshall specimens could be achieved by using the load related to it, applied to each end of the specimen for a one minute.

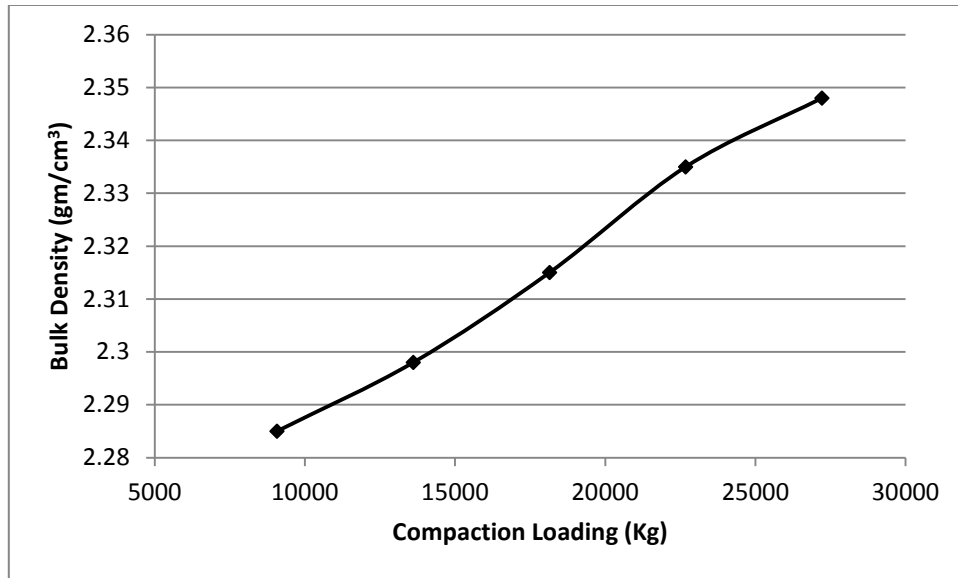


Figure (3-9) Compaction Efforts versus Density

3.3.4.2 Testing of Permanent Deformation Specimens

Uniaxial repeated loading test was conducted on cylindrical specimens, 101.6 mm (4 in) in diameter and 203.2 mm (8 in) in height, using the Pneumatic Repeated Load System (PRLS). In this test, repetitive compressive loading for up to 10,000 repetitions with a stress level of 138 kPa (20 psi) was applied in a rectangular form wave with a constant loading frequency of 1 Hz (0.1 second load duration followed by 0.9 second rest period) and the axial permanent deformation was measured under the different loading repetitions. The axial permanent deformation was recorded by using Linear Variable Differential Transducer (LVDT) on the upper face of the specimen via data acquisition system (Wykeham Farrance Engineering Limited) as illustrated in Figure (3-10). Figure (3-11) presents setting and the initial state of the specimen in the testing machine and failure of the specimen after testing. The output data were recorded using a digital camera and then calibrated to get the final reading.



Figure (3-10) PRLS Connected to LVDT and Data Acquisition System



a. Initial state of specimen



b. Failed specimen

Figure (3-11) Permanent Deformation Test in Pneumatic Repeated Load System (PRLS)

The PRLS was used to characterize the rutting behavior of the various mixtures in the form of the performance model assess rutting in the HMA layer by relating the permanent strain (ϵ_p) to the resilient axial strain (ϵ_r) and the number of loading cycles (N).

During the test, the permanent axial deformation (P_d) were recorded at (1,2,10,100,500,1000,2000,3000,4000,5000,6000,7000,8000,9000,10000 repetitions) or until the specimen fail. The permanent strain (ϵ_p) is calculated according to the following equation:

$$\epsilon_p = \frac{P_d}{h} \quad (3-4)$$

Where

ϵ_p = axial permanent microstrain

P_d = axial permanent deformation

h = specimen height.

In addition, throughout this test the resilient deflection is measured at each load repetition of 50 to 100, and then the resilient strain (ϵ_r) and resilient modulus (M_r), which is the most important variable to mechanistic design approaches for pavement structures, are calculated as follows:

$$\epsilon_r = \frac{\Delta r}{h} \quad (3-5)$$

$$M_r = \frac{\sigma}{\epsilon_r} \quad (3-6)$$

Where, ϵ_r is the axial resilient strain, Δr is the average of axial resilient deflection recorded (the axial resilient deflection took the difference between the high deformation reading and the low deformation reading at the recorded repetition numbers), h is the specimen original height, M_r is the resilient modulus, σ is the repeated axial stress.

The permanent deformation results are normally represented in the form of the relationship between the permanent strain and the number of the load repetition. In general, the relationship presents a character of three distinctive zones, i.e.: primary, secondary, and tertiary (Walubita et al, 2013). Many characteristic models have been proposed so far to describe the permanent deformation of asphalt concrete pavement layers. In this study, the permanent deformation results in the secondary zone were characterized using a power relationship between the cumulative permanent strain and the number of the load repetition. It takes the form of the Equation (3.7), which was originally suggested by Barksdale (1972) and Monismith et al. (1975).

$$\epsilon_p = aN^b \tag{3-7}$$

Where, ϵ_p is the permanent strain, N is the number of stress applied, a is the intercept coefficient of the linear log-log relationship and b is the slope of the relationship line. Eq. (3-7) becomes a linear function in the form of log-log display, i.e.: $\log \epsilon_p = \log a + b \log N$.

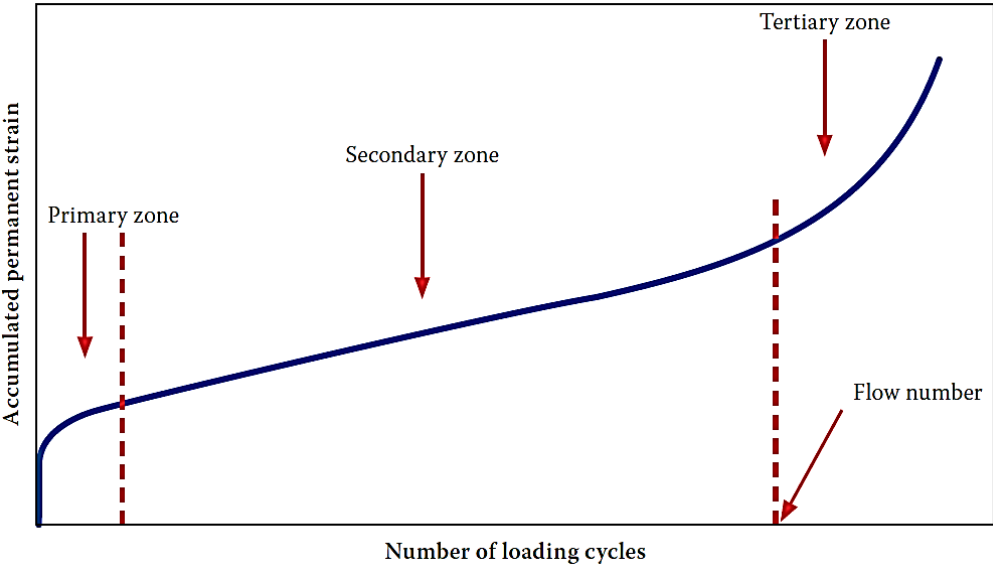


Figure (3-12) Typical relationship between the permanent strain and number of load repetitions (Walubita et al, 2013)

The details of the criteria and boundary conditions adopted in the permanent deformation testing design are summarized in Table (3-8).

Table (3-8) Permanent Deformation Test selected parameters

Parameter	Selected value	
Temperature	20°C	
	40°C	
	60°C	
Applied stress	138 kPa (20 Psi)	
Resilient strain	At 50 to 100 th	
Maximum loading repetitions	10,000	
Conditioning time	2 hours	
Load cycle time	1Hz	0.1 second haversine load
		0.9 second rest period

3.3.5 Flexural Fatigue Cracking

3.3.5.1 Flexural Beam Specimen

A cuboid beam specimen of dimensions 381×76×76 mm (15×3×3 in) with an approximately 5450 gm needed of asphalt concrete mixture to produce one specimen regarding mix design formula. Four specimens were tested for each hydrated lime modification percent (control and modified mixes). Accordingly, 72 specimens were fabricated in this experiment at a range of 4 stress levels per each mixture. Four trial mixes were compacted with different loads (54431, 58967, 635023 and 68039 Kg) using a "double plunger" arrangement by applying static load using compressive machine device located at laboratory of material at civil engineering department to accomplish the desired density required for each specimen; the 65771 Kg, which gave density above Marshall Density of 2.3 gm/cm³, was selected. The mix design method used volumetric properties at optimum asphalt content with each hydrated lime percent. To prepare the beam specimens for this test, loose mixes were poured into preheated steel mold and pressed in a compressive machine under the gradual application of a static load for 2 minutes according to (ASTM-D1074-96). The compaction temperature is typically selected 150°C to promote homogeneity. The mixture was shoveled prior to compaction, and the mold was made "free floating" by using a "double plunger" arrangement. Finally, the specimen was extracted by holding it tight using the compressive machine to remove it from the molds after 24 hour. Figure (3-13)

shows the specimen molds, the compression process, the specimen extraction and specimens ready to test respectively.



a. Flexural beam specimen molds



b. Compaction of beam specimens



c. Extraction of specimen



d. Beam specimens

Figure (3-13) Preparation of specimens for fatigue cracking test

3.3.5.2 Repeated Flexural Beam Fatigue Test

In this study, the third-point loading test with free rotation beam holding fixture at all loading and reaction point was usually used to estimate cracking potential in the flexural beam fatigue test. The purpose of using third-points loading was to get pure bending in the middle third area of the beam. The numbers of cycles (fatigue life) that caused complete failure of the beam were commonly considered as an indicator of fatigue cracking potential (Huang, 2004). Figure (3-17) shows a schematic loading configuration of the beam. The details of the factorial variables in the experimental design of the flexural beam fatigue test are:

- Stress Levels: Four levels of stress, 223, 310, 402, 490 N, were selected as targets, control stress, time loading 0.1 second and rest period 0.4 second (Huang, 2004). A range of stress selected so that the specimens would fail within a range from 100 to 100,000 repetitions.
- Test Temperature: One level of the test temperature $20 \pm 1^\circ\text{C}$ was used.

A number of 72 specimens and tests was made to simulate these variables. Pneumatic repeated load device with control stress was used. In order to use third-point loading for the flexural test, the specimen was left in the chamber for six hours at (20°C) to allow uniform distribution of temperature within the specimen. A digital camera was used for recording the deflection at mid-span of the beam until failure. An aluminum steel rod supporting the LVDT was fixed at the upper point of the beam to sense the difference in deflection. The vertical deflection during the test of the beam at the mid-span was measured with LVDT. It was connected to data acquisition system where the deflection at various time intervals was stored and analyzed for finding strain at any number of cycles desired for every test.

This test was performed in stress controlled mode with flexural stress level applied at the frequency of 1 Hz with 0.1 s loading and 0.4 s unloading times and in a rectangular waveform shape. The test of specimens is undertaken according to specifications of SHRP standards at 20°C (68°F) on beam specimens 76 mm (3 in) x 76 mm (3 in) x 381 mm (15 in). In the fatigue test, the initial tensile strain of each test has been determined at about the 200th repetition by using (Eq.3-10) shown below, and the initial strain was plotted versus the number of repetition to failure on log scales, the failure of the beam was happened when the specimen breakdown. The general equations for analysis of a simply supported beam are as follows (Huang, 2004):

$$\sigma = \frac{3Pa}{bd^2} \quad (3-8)$$

$$E_s = \frac{Pa(3L^2-4a^2)}{4bd^3\Delta} \quad (3-9)$$

$$\varepsilon_t = \frac{\sigma}{E_s} = \frac{12h\Delta}{3L^2-4a^2} \quad (3-10)$$

Where:

ε_t = Tensile strain

σ = Flexural stress

E_s = Stiffness modulus based on center deflection of beam specimen.

h = Height of the beam

Δ = Dynamic deflection at the center of the beam.

L = Length of span between supports.

a = Distance from support to the load point ($L/3$)

In controlled stress fatigue tests, it has already been stated that crack initiation is followed by a very short crack propagation stage culminating imminently in total failure; in contrast to a much longer crack propagation stage in the controlled strain mode, a definition was introduced Hopman et al. (1989). Thus, fatigue life relationship results in a log strain (ε_t) versus log N_f are plotted. This results in a relationship for fatigue tests of the form (Monismith et al., 1971):

$$N_f = k_1(\varepsilon_t)^{-k_2} \quad (3-11)$$

Where:

N_f = Number of repetitions to failure

k_1 = fatigue constant, value of N_f when $\varepsilon_t = 1$

k_2 = inverse slope of the straight line in the logarithmic relationship

Figures (3-14) and (3-15) show the loading configuration of fatigue test, setting and testing flexural beam specimen and the beams after failure respectively.

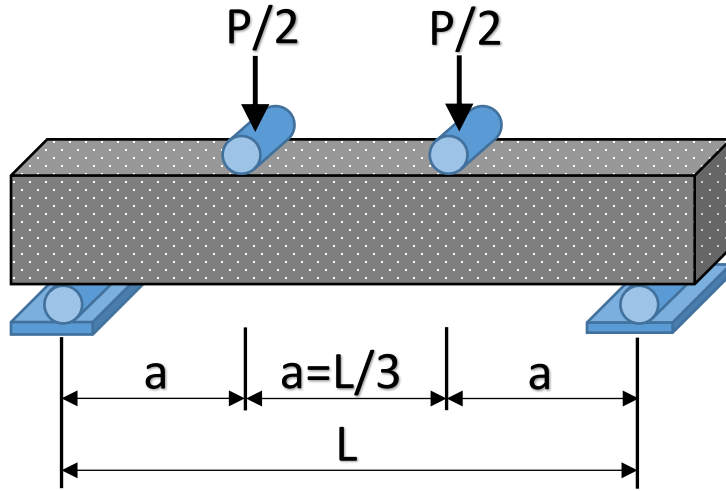
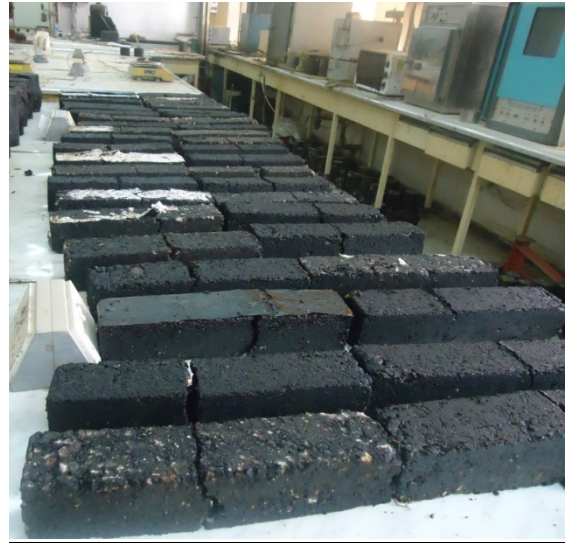


Figure (3-14) Schematic of Loading Configuration of the Beam



a. Specimens setup and testing in PRLS



b. Specimens failed after testing

Figure (3-15) Setting and testing of flexural beam specimen

3.3.6 Moisture Susceptibility

The ASTM-D4867/D4867M-09 designation was performed to examine the influence of hydrated lime on the moisture susceptibility of the asphalt concrete mixtures. For each one of the asphalt mixtures investigated in this research, the test procedure adopted was as follows; six specimens of 63.5 mm (2.5 in) in height and 101.6 mm (4 in) in diameter, prepared using Marshall compactor in the case of optimum asphalt content. All specimens were compacted to achieve 7.0 ± 0.5 % of air voids by adjusting Marshall compactor blows to be in a range between 40 to 45 on each face of the specimen based on trial mixes. The reason behind implemented targeted air voids content was not meant to simulate the actual field conditioning process but to accelerate the moisture damage in a way that can be measured under laboratory conditions. The six specimens of each mix were divided into two sets of three.

The first set of three specimens were then tested in a dry (Unconditioned state), while the second set was tested in a saturated (Conditioned state). For the dry set, the samples were placed in a water bath maintained 25 °C for one hour and then tested to obtain their ultimate indirect tensile strength. This was achieved by Versa Tester under an applied load with a constant deformation rate of 50.8 mm/minute through two diametrically opposed rigid (steel) strips on both the top and bottom of the specimen. The strips dimensions are 12.5 mm (0.5 in.) wide by a 63.5 mm (2.5 in.) long, and they are curved at the interface with the sample that has a 102 mm (4 in.) diameter. The strips were used to induce tensile stress parallel to and along the diametral vertical axis of the cylindrical test specimen. The ultimate value of load at failure was recorded and the indirect tensile strength computed using equation (3-12). Finally, the average value of the indirect tensile strength for the dry set (Std) was computed.

For the conditioned set of specimens, the samples were placed in a flask filled with water at room temperature of about 25 °C. A vacuum of about 70 kPa or 525 mm Hg (20 in. Hg) was applied for 5 minutes to obtain the desired saturation level. The specimens then wrapped with plastic film using tape to hold the wrapping. Each specimen then placed in a leak-proof plastic bag containing approximately 3 mL of distilled water, and the bag sealed with a tape. After that the specimens were placed in a freezer at a temperature of -18 °C for 16 hours, after removal of samples from the freezer they were immersed in a water bath of 60°C for 24 hours. After 3 minutes and when thawing of the specimens surfaces happened the bags and wrapping were removed from the samples.

The cycle of freezing and thawing was performed to simulate the expected damage effect on wetted pavement by traffic stresses. Before beginning of the indirect tensile strength test, the specimens were placed in water bath at 25°C for one hour. The average value of the indirect tensile strength for the conditioned set (S_{tm}) is then computed. Figure (3-16) shows a sample before and after conducting the indirect tensile test, the first plot (a) is of a specimen in the beginning of test and the second plot (b), the specimen after failure with vertical cracks appeared on it.

The indirect tensile strength ratio of each mix was determined according to the equation (3-13) by dividing the tensile strength at the condition state to the tensile strength at the dry (unconditioned) state.

The recorded peak values of compressive load were used to calculate tensile strength of the sample using the following equation:

$$S_t = \frac{2000P}{\pi t D} \quad (3.12)$$

S_t = tensile strength, kPa

P = maximum load, N.

t = specimen height immediately before tensile test, mm

D = specimen diameter, mm.

The tensile strength ratio was calculate as follows:

$$TSR = \frac{S_{tm}}{S_{td}} \times 100 \quad (3-13)$$

Where,

TSR = tensile strength ratio, %

S_{tm} = average tensile strength of the moisture conditioned subset, kPa, and

S_{td} = average tensile strength of the dry subset, kPa.



a. Initial state of specimen



b. Failed specimen

Figure (3-16) Indirect Tensile Strength Test of a Specimen Before and After Failure

3.4 Summary of Mixture Design and Testing Procedure

The following major tasks were conducted in performing the testing programme:

1. Determine the main physical characteristics and properties of raw materials (aggregate, Asphalt cement and mineral filler) as well as chemical components to check their meeting to the required standards of SCRB to prepare for the mix design step.
2. Design asphalt concrete mixtures regarding the replacement percentage of the normal limestone dust by hydrated lime mineral filler and evaluate the pavement mixture properties throughout the following:
 - Resistance to plastic flow by Marshall test,
 - Permanent deformation and stiffness by uniaxial repeated load test,
 - Repeated flexural beam fatigue test, and
 - Effect of moisture on the asphalt concrete paving material by ASTM-D4867/D4867M-09 designation.

The mixtures design and testing process are shown in Figure (3-17). Further information about the specimens details and testing conditions are presented in Tables (3-9) and (3-10).

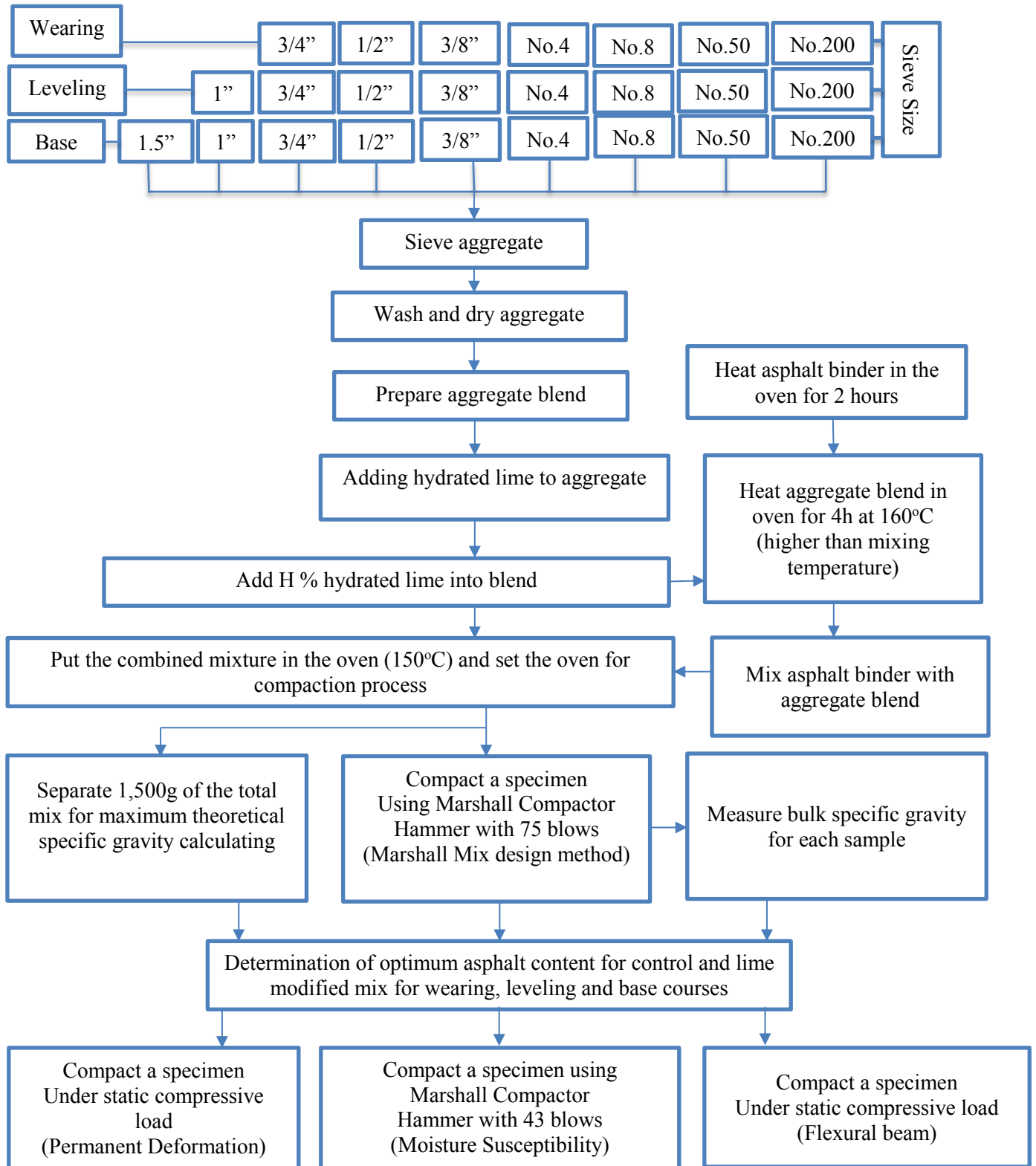


Figure (3-17) Mixture Design and Testing Procedure

Table (3-9) Summary of Specimens Dimensions and Purpose of Testing




Dimensions	Shape of specimens	Testing purpose
Diameter = 101.6 mm Height = 63.5 mm		Marshall mix design and volumetric properties 60°C (30 to 45 min) Loading rate 50.8 mm/min Effect of Moisture on Asphalt concrete mixtures Freeze-Thaw cycle (-18, 60°C) and 25°C Loading rate 50.8 mm/min
Diameter = 101.6 mm Height = 203.2 mm		Permanent Deformation Temperature 20°C Temperature 40°C Temperature 60°C Loading 20 Psi Duration 0.1s load period 0.9 rest period
Length = 381 mm Depth = 76 mm Width = 76 mm		Fatigue Cracking Stress level 223 N Stress level 310 N Stress level 402 N Stress level 490 N Temperature 20°C Duration 0.1s load period 0.4 rest period

Table (3-10) Summary of Specimens Number Made for Mixes Adopted in the Study

Tests	Tests conditions and criteria	Control mix	1.0% HL	1.5% HL	2.0% HL	2.5% HL	3.0% HL
Marshall Mix Design	60°C (30 to 45 min) Loading rate 50.8 mm/min	45	45	45	45	45	45
Effect of Moisture on Asphalt concrete mixtures	Unconditioned set: 25°C. Conditioned set: Freeze-Thaw cycle (-18, 60°C). Loading rate 50.8 mm/min	18	18	18	18	18	18
Permanant Deformation Under 138kPa (20 Psi)	Temperature 20°C	3	3	3	3	3	3
	Temperature 40°C	3	3	3	3	3	3
	Temperature 60°C	3	3	3	3	3	3
Fatigue Cracking at 20°C	Stress level 223 N	3	3	3	3	3	3
	Stress level 310 N	3	3	3	3	3	3
	Stress level 402 N	3	3	3	3	3	3
	Stress level 490 N	3	3	3	3	3	3

Note: Total Number of specimens=504

3.5 Specimens Designation

Designation or nomenclature has been made for the studied mixes regarding the layer name and the amount of hydrated lime that were the substitute to the mineral filler. The nomenclature consists of three characters; the first letter refers to the hydrated lime (H), followed by a number representing the addition amount of hydrated lime. The last letter refers to layer type (wearing (W), leveling (L) or Base (B)) as explained in the example in Figure (3-18).

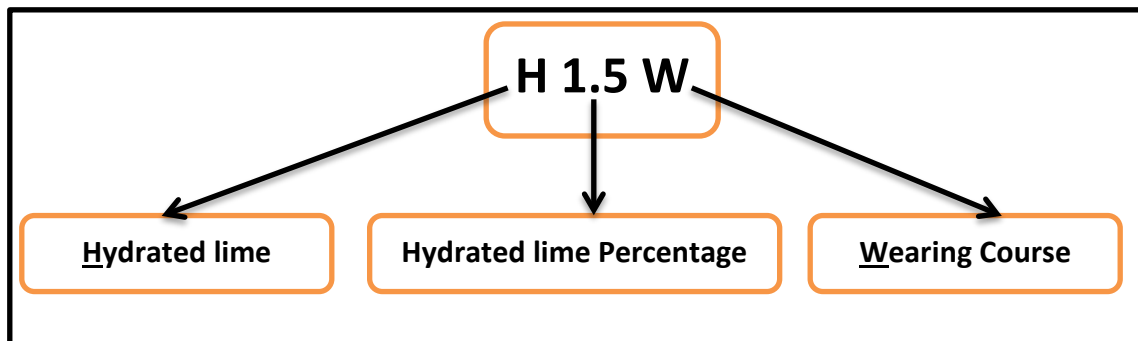


Figure (3-18) Example of samples nomenclature adopted in this study

3.6 Summary

By means of Marshall Mix design method, the optimum asphalt content (OAC) as well as volumetric properties were obtained for each hydrated lime content (as a partial substitute to the limestone dust) for proposed asphalt concrete layers; Wearing, Leveling and Base. The OAC's were adopted for the preparation of further mixtures of various specimens' dimensions and different criteria and testing purposes. The prepared mixes were subjected to further tests to evaluate the permanent deformation, fatigue cracking and moisture susceptibility.

The performance testing of the hot mix asphalt (HMA) mixtures was detailed. The performance related tests have been done under static and dynamic loading systems. Firstly, a constant load rate (50.8mm/minute) of Marshall apparatus of cylindrical specimens with a diameter of 101.6 mm (4 inches) and height of 63.5 mm (2.5 inches). Secondly, repeated load of both cylindrical specimens with a diameter of 101.6 mm (4 inches) and height of 203.2 mm (8 inches) and rectangular beam specimens under the PRLS at different rates of stress and temperatures. Thirdly, with the same specimen dimensions and constant load rate of Marshall test and according to the ASTM-D4867/D4867M-09 designation, the effect of hydrated lime on the moisture susceptibility of the asphalt concrete mixtures was inspected. In addition, the main physical properties and chemical components of the material used were tested according to a set of tests adopted by ASTM Standards (Volume 04.03). These tests are recommended by Iraqi Specifications (SRCB/R9 2003 Revision).

Chapter Four

Tests Results

4.1 Introduction

In this study, the impact of hydrated lime on the asphalt cement consistency has been evaluated by means of Penetration and Softening Point tests. Furthermore, HMA specimens with various compaction modes and geometry were prepared based on their optimum asphalt content (OAC) for all the asphalt concrete mixes using Marshall mix design method. Asphalt concrete mixes that made at respective OAC were tested to evaluate the performance characteristics as related to the effect of moisture on asphalt concrete, temperature variation, permanent deformation and fatigue cracking. These properties were evaluated using Marshall test apparatus, pneumatic repeated loading and repeated flexural beam tests.

4.2 Influence of Hydrated lime on Asphalt Cement

Penetration and softening point tests were adopted to assess the hydrated lime influence on the binder (asphalt cement) properties. These tests conducted on the hydrated lime modified and non-modified binder. As mentioned in chapter three, the wearing course was selected to be evaluated at its optimum binder percentage. The assessment of wearing course was done for each different percent of added hydrated lime as a replacement with an initial percentage of lime mineral filler of 7%. The mastic (asphalt-filler mix) consistency was determined for a series of hydrated lime addition amount. The tests outputs are illustrated in the table (4-1) and presented graphically in Figures (4-1) and (4-2).

It can be found from the illustrated data in table and figures mentioned above, the hydrated lime addition has a significant effect on the consistency of asphalt-filler mix. Regarding the penetration test, the increasing in hydrated lime amount leads to decreasing in the penetration. For instance, adding of 2.5% of hydrate lime resulted in a reduction of 28.1% in penetration as compared with its value at 0% of hydrated lime added to the asphalt-filler mix (7% of limestone dust). An approximated average of reduction rate in the penetration can be concluded as 4.7 unit

(1/10 mm) at hydrated lime increment rate of 1%. In contrast, a gradual rise of the softening point has been recorded with increasing of the hydrated lime percent. The softening point at 3% of hydrated lime is greater than softening point temperature degree when hydrated lime is 0% by about 27%. It can be noticed that the increment rate of the temperature of softening point is about 4°C to 5°C for every 1% of hydrated lime replacement. Based on the above, it could be discussed that the higher the addition percent of hydrated lime as a partial replacement with the mineral filler, the higher consistency and stiffness of the lime modified asphalt cement (mastic). The resulted mastic in asphalt concrete mixture could contribute to the resistance to the deformation that may happen in the flexible pavement mixtures due to traffic loading.

Table (4-1) Effect of Hydrated Lime Addition on Asphalt Cement Penetration and Softening Point Results

Hydrated Lime %	0	1	1.5	2	2.5	3
Limestone dust %	7	6	5.5	5	4.5	4
Optimum Asphalt Cement, %	4.9	4.9	5	5.2	5.2	5.3
Penetration, 1/10 mm (25°C, 100gm, 5 sec). ASTM D5 (Original* value is 42)	32	30	28	27	23	18
Softening point, °C (Ring & Ball). ASTM D36 (Original* value is 49)	52	55	57	60	63	66

*Original value: is the property of pure asphalt cement (without modification)

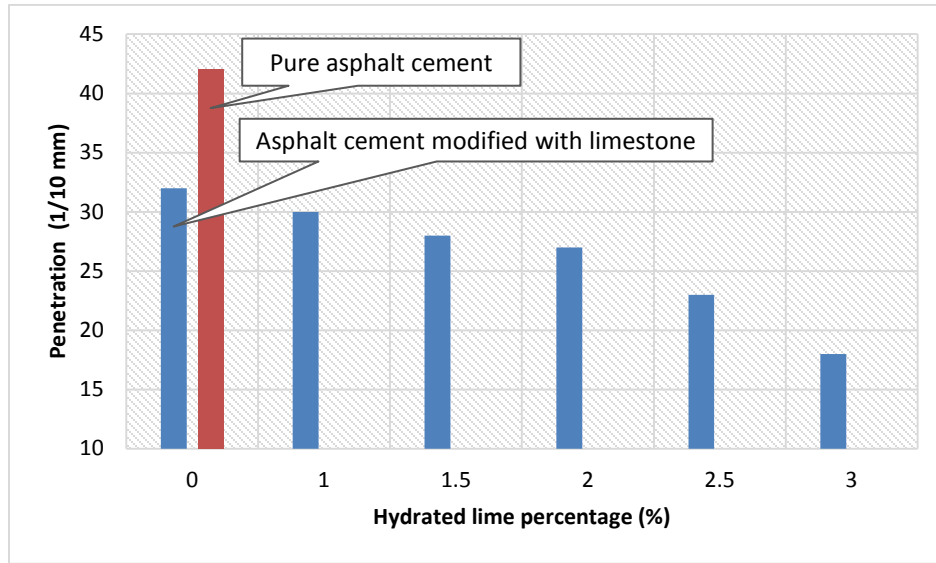


Figure (4-1) Influence of Hydrated Lime on Mortar Penetration

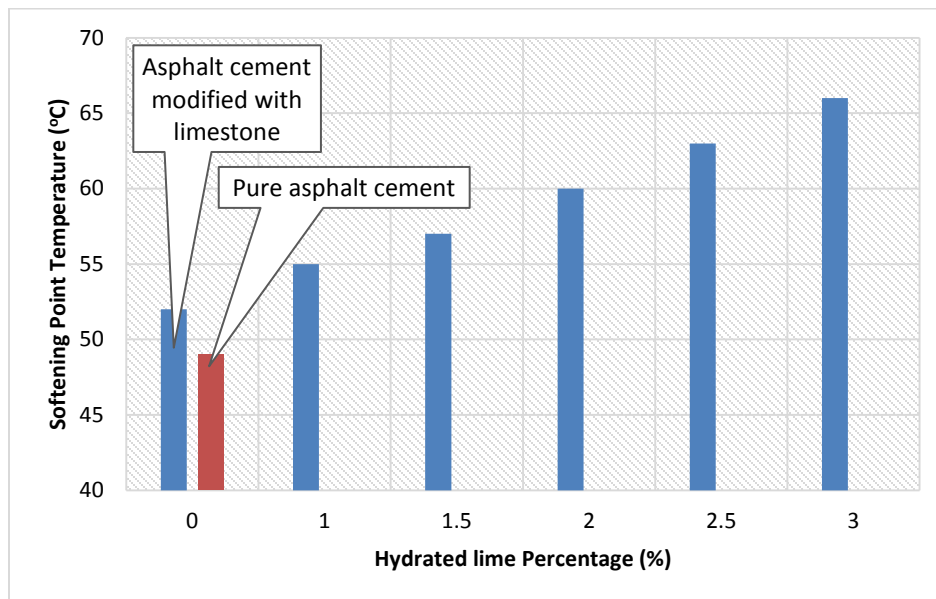


Figure (4-2) Influence of Hydrated Lime on Mortar Softening Point

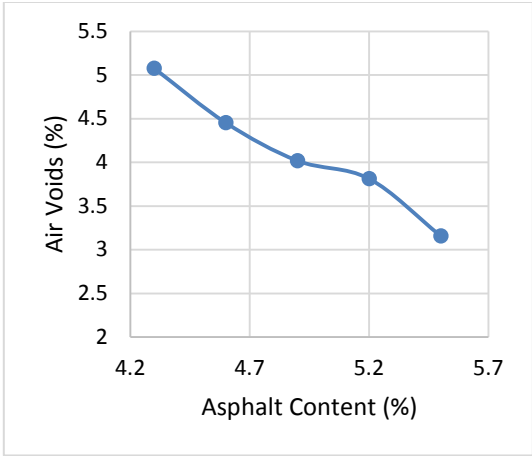
4.3 Influence of Hydrated lime on Marshall properties of asphalt concrete mixtures

4.3.1 Optimum Asphalt Content

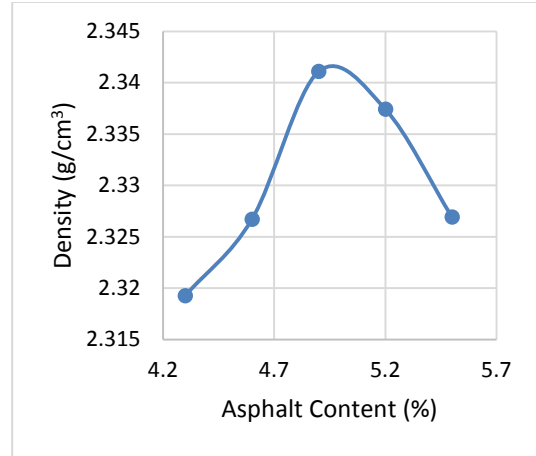
The results of Marshall test obtained from the control and hydrated lime modified asphalt concrete mixtures were presented and tabulated in the appendix A. The results of each mixture were plotted as percent of asphalt (by total weight of the mix) on a normal scale. They are presented in the figures shown hereafter for Wearing, Leveling and Base courses respectively. Points illustrated on the plots are average of triplicate test specimens. The optimum asphalt content (OAC) was found according to the asphalt cement amount at the following values:

- Maximum density
- Maximum Marshall stability
- Four percent of air voids.

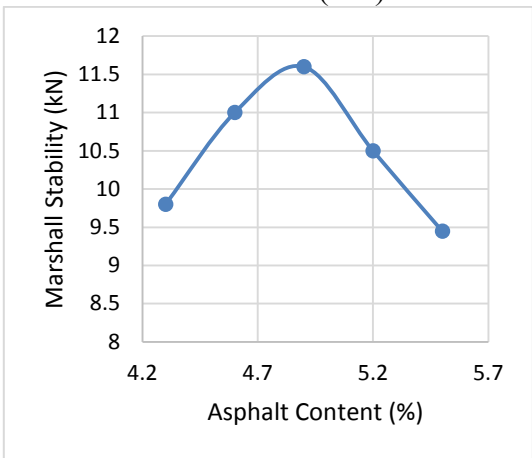
The OAC for each mixture is then calculated as the numerical average of the values of the asphalt contents as noted above. Detailed outputs of Marshall test for the control mixtures (without hydrated lime) regarding the asphalt cement increment are presented in the Figures from (4-3) to (4-5) for wearing, leveling, and base course, and the rest of the outputs are presented in appendix A.



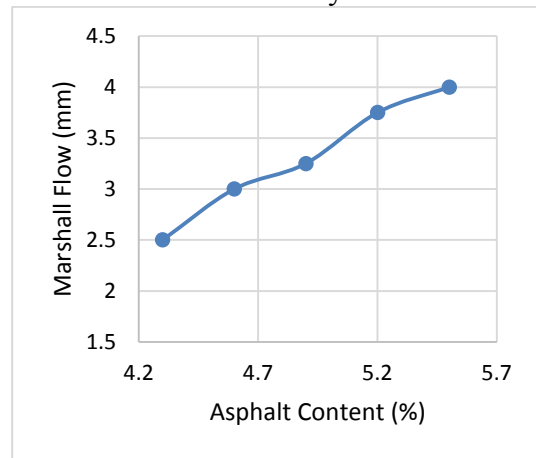
a. Air Voids (AV)



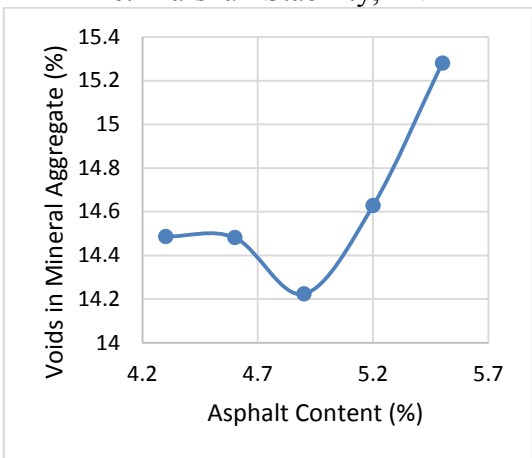
b. Density



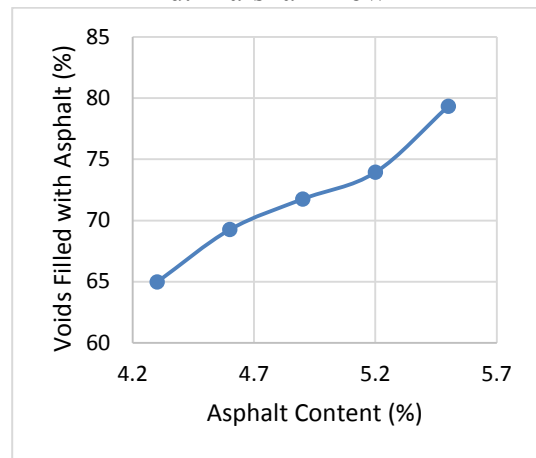
c. Marshall Stability, kN



d. Marshall Flow

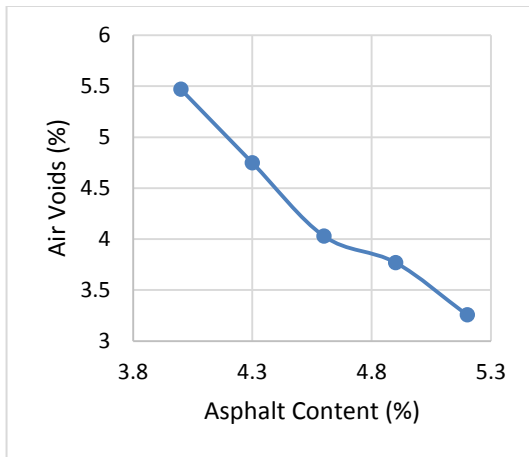


e. Voids in Mineral Aggregate (VMA)

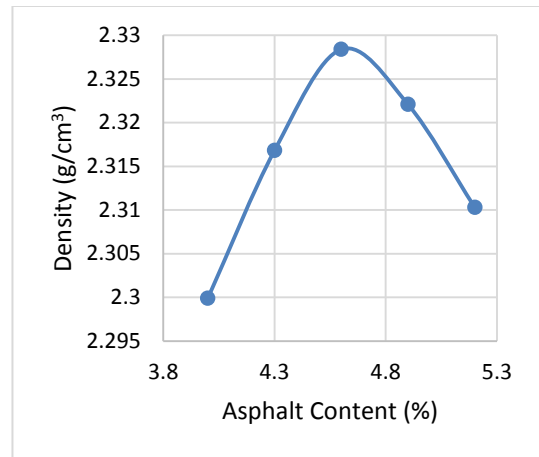


f. Voids Filled with Asphalt (VFA)

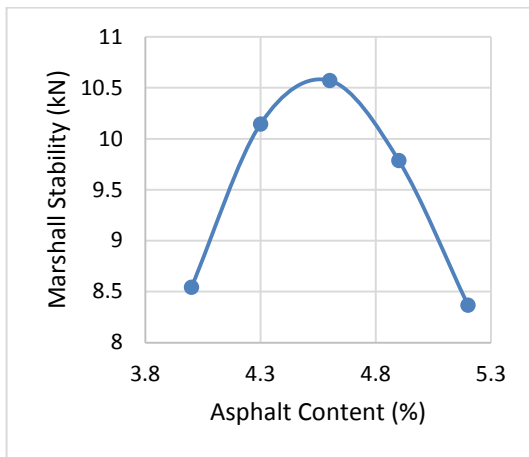
Figure (4-3) Marshall Mix Design Properties for Control Wearing Mixture (CW)



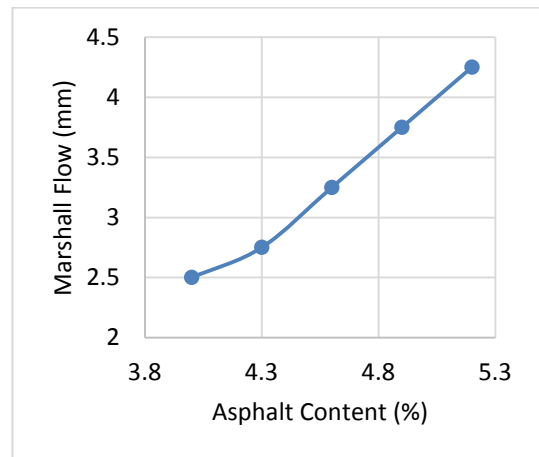
a. Air Voids (AV)



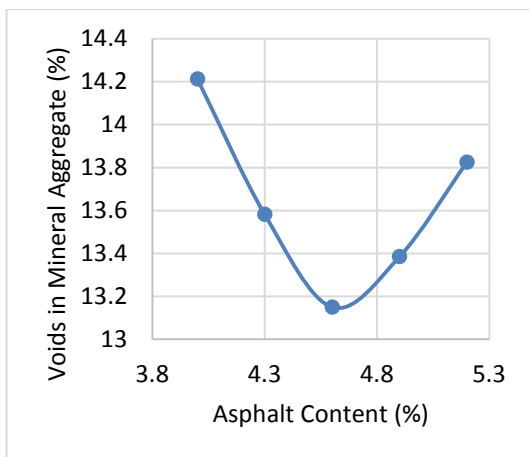
b. Density



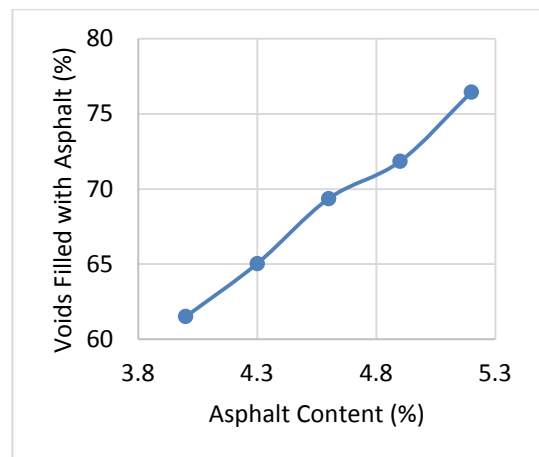
c. Marshall Stability, kN



d. Marshall Flow

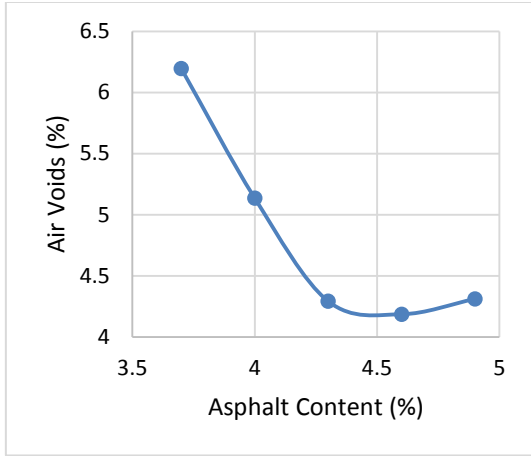


e. Voids in Mineral Aggregate (VMA)

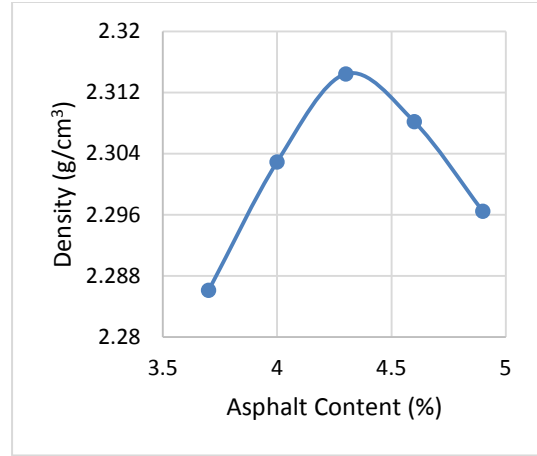


f. Voids Filled with Asphalt (VFA)

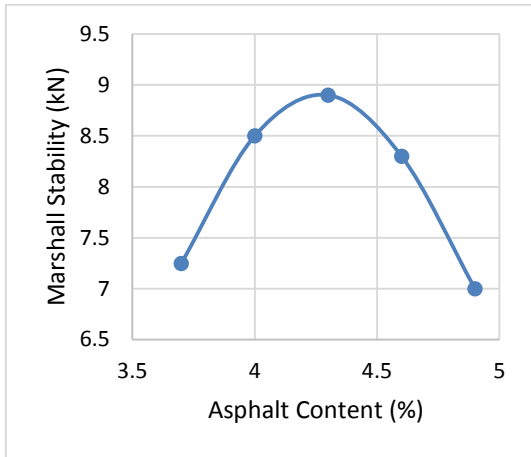
Figure (4-4) Marshall Mix Design Properties for Control Leveling (CL) Mixture



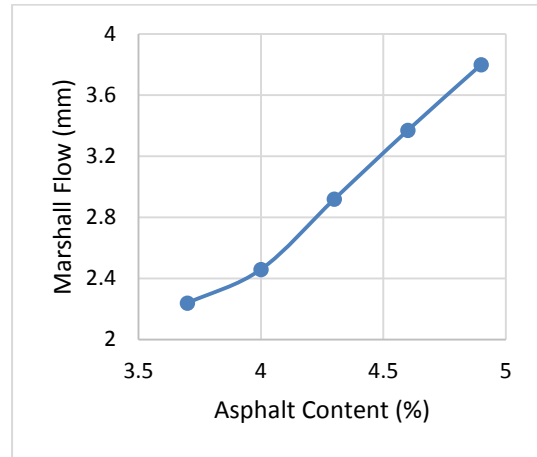
a. Air Voids (AV)



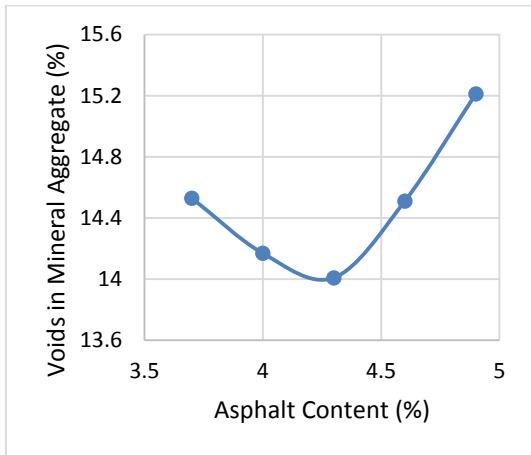
b. Density



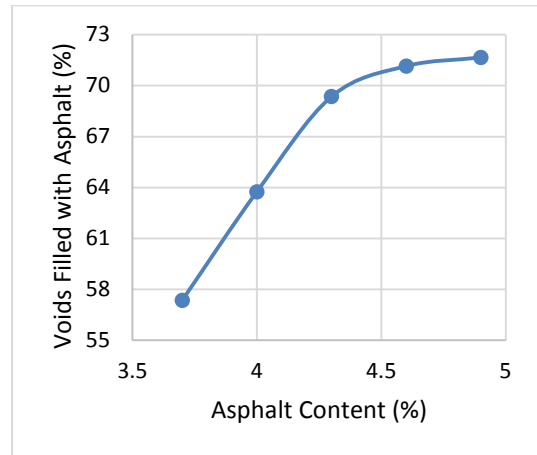
c. Marshall Stability, kN



d. Marshall Flow



e. Voids in Mineral Aggregate (VMA)



f. Voids Filled with Asphalt (VFA)

Figure (4-5) Marshall Mix Design Properties for Control Base (CB) Mixture

After consideration of OAC calculation process, the optimum results of Marshall and volumetric properties for control and hydrated lime modified mixes are presented in Tables (4-2), (4-3) and (4-4) for W, L and B layers respectively. Examinations of the presented data shown in the tables indicated that mixtures appeared to be “riches” (contained slightly more asphalt) than the control mixture. Mixtures prepared with H3W, H3L and H3B have OAC values of 5.3, 5 and 4.7 percent respectively that are higher than those prepared with lower hydrated lime content. The lowest optimum values of asphalt content were related to the control mixtures; 4.9% and 4.6% and 4.3% for W, L and B, respectively. The mineral filler in each of the control mixes was entirely consisting of limestone dust only. The differences in the optimum asphalt content can be attributed to the relatively higher specific surface area of hydrated lime (1.6 times) as compared to the limestone dust. Thus, more asphalt cement is required to wrap onto its surface (Al-Suhaibani et al. 1992, Shahrour and Saloukeh 1992). It can be found that the hydrated lime makes the mix demands more asphalt cement amount to reach the optimum value.

Table (4-2) Marshall Design properties for Wearing course

Mixture	OAC, %	Density, g/cm³	G_{mm}, g/cm³	Stability, kN	Flow, mm	AV, %	VMA, %	VFA, %
SCRB requirement				min. 8	2.0-4.0	3.0-5.0	min. 14	
Control (CW)	4.9	2.34	2.439	11.6	3.25	4.018	14.22	71.74
H1W	4.9	2.339	2.437	12.13	3	4.01	14.18	71.7
H1.5W	5	2.33	2.428	12.4	2.8	4.08	14.4	72.4
H2W	5.2	2.33	2.431	14.4	3	4.14	14.68	72.74
H2.5W	5.3	2.316	2.42	13	2.8	4	15.2	71.47
H3W	5.3	2.309	2.41	12	2.6	4.1	15.4	71.2

Table (4-3) Marshall Design properties for Leveling course

Mixture	OAC, %	Density, g/cm ³	G _{mm} , g/cm ³	Stability, kN	Flow, mm	AV, %	VMA, %	VFA, %
SCRB requirement				min. 7	2.0-4.0	3.0-5.0	min. 13	
Control (CL)	4.6	2.32	2.426142	10.57	3.25	4.02	13.14	69.36
H1L	4.7	2.32	2.432	10.31	3.1	4.3	13.5	66
H1.5L	4.8	2.32	2.428	10.25	2.8	4.3	13.3	67
H2L	4.9	2.319	2.424	11.19	3	4.35	13.36	67.4
H2.5L	5	2.3	2.42	11.5	3	4.5	13.7	67
H3L	5	2.3	2.41	11	2.5	4.6	14	67

Table (4-4) Marshall Design properties for Base course

Mixture	OAC, %	Density, g/cm ³	G _{mm} , g/cm ³	Stability, kN	Flow, mm	AV, %	VMA, %	VFA, %
SCRB requirement				min. 5	2.0-4.0	3.0-6.0	min. 12	
Control (CB)	4.3	2.314	2.418251	8.9	2.92	4.29	14	69.35
H1B	4.3	2.312	2.415861	8.77	2.7	4.28	13.99	69.39
H1.5B	4.4	2.307	2.41	9	2.5	4.5	14.3	69
H2B	4.5	2.305	2.406	9.6	2.4	4.2	14.39	70
H2.5B	4.6	2.297	2.403	10.7	2.45	4.39	14.67	70.06
H3B	4.7	2.291	2.4	9	2.3	4.55	15	70.1

4.3.2 Density of asphalt concrete mixtures

The influence of the addition of hydrated lime on the density of the compacted mixes is shown in Figures (4-6), (4-7) and (4-8). It can be seen that the unit mass tends to decrease as the lime content increases. There are two reasons may be related to the decrease. The first one is due to the low density of hydrated lime (2.43 g/cm³) compared with that of the replaced limestone dust (2.71 g/cm³). The second reason is attributed to the increase of air voids. Generally, the addition

of mineral filler tends to increase the viscosity and makes the mixture stiffer. As a result, the degree of compaction may decrease and be insufficient with the rise of hydrated lime content (Fayadh 1987, Al-Suhaibani et al. 1992, Shahrour and Saloukeh 1992, Baig 1995, Tayh and Jabr 2011, Sengul et al. 2011).

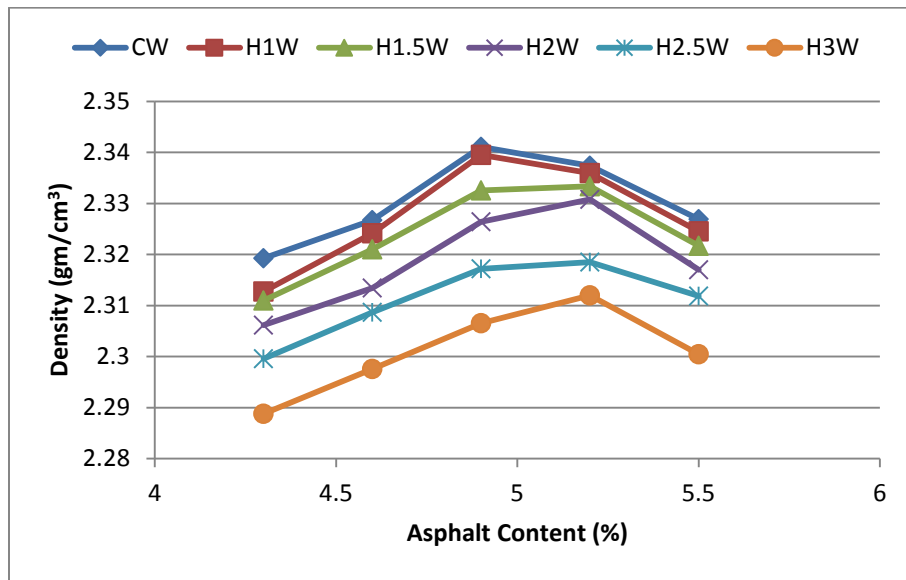


Figure (4-6) Hydrated lime influence on density with respect to AC% for Wearing course

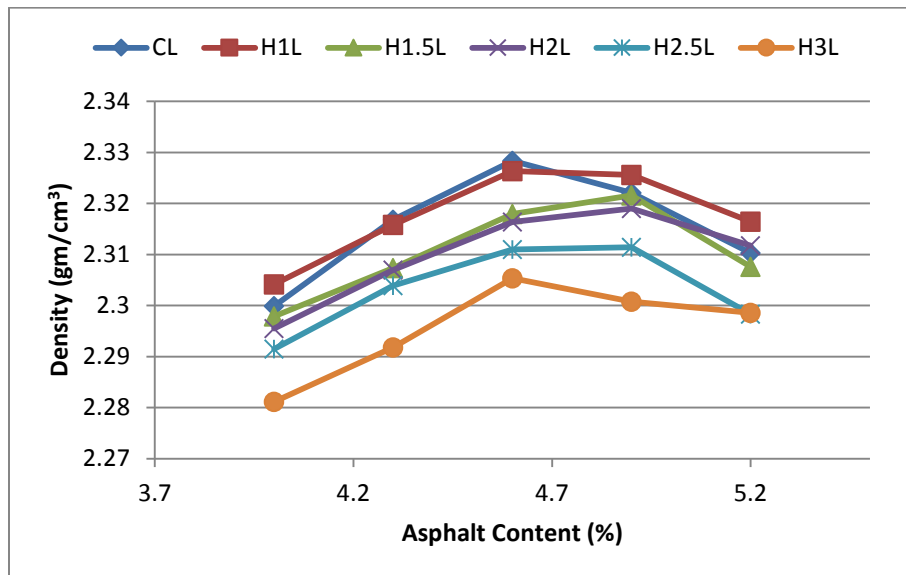


Figure (4-7) Hydrated lime influence on density with respect to AC% for Leveling course

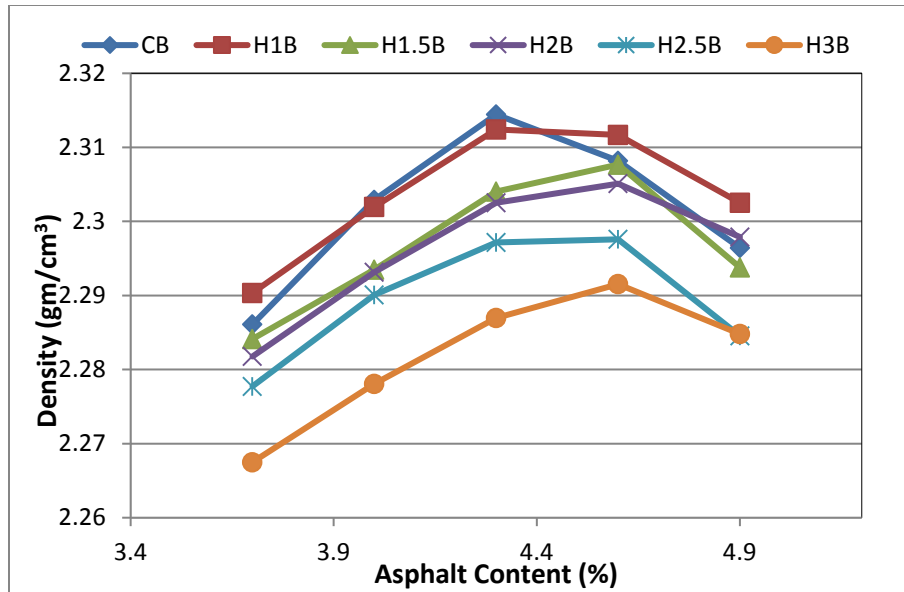


Figure (4-8) Hydrated lime influence on density with respect to AC% for Base course

4.3.3 Marshall Stability

The graphical presentation of data in Figures (4-9), (4-10), and (4-11) exhibits the influence of hydrated lime on the stability of the asphalt concrete mixtures of the W, L and B courses. It can be observed that similar effects are on the mixtures made for different pavement course applications. Initially, the Marshall stability increases with the increase of the hydrated lime content until reaching the maximum value. It can be seen that the maximum stability corresponds to 2% hydrated lime addition to the course W, 2.5% to L course and 2.5% to the course B. The result can be attributed to the fact that hydrated lime is finer than limestone dust. The replacement of the limestone with hydrated lime increases the stiffness of the mixture. On the other hand, because the addition of hydrated lime increases the viscosity of the asphalt cement (Kim et al. 2003, Little and Petersen 2005, Zeng and Wu 2008), a small percentage of hydrated lime has the effect on the improvement of the binding capacity of the mixture. However, when the hydrated lime content is too high, the increase of air voids will result in the decrease of the stability. The results show that the maximum stability value has been increased by 24%, 9%, and 20%, with respect to the control mix, for the mixes H2W, H2.5L, and H2.5B, respectively. This finding is in agreement with the conclusions of some previous research work (Al-Suhaibani et al. 1992,

Albayati 2012, Shahrour and Saloukeh 1992, Baig 1995, Kok and Yilmaz 2009, Tayh and Jabr 2011).

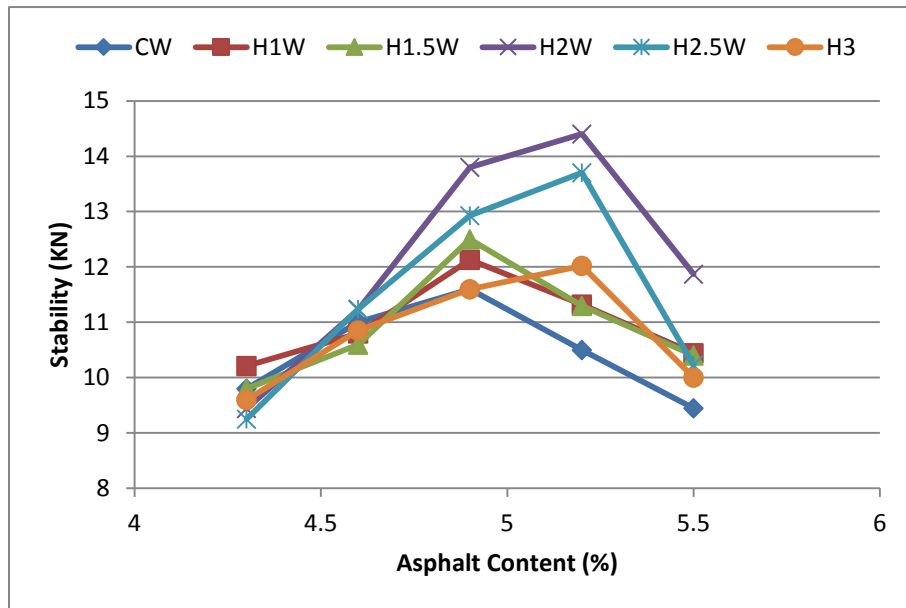


Figure (4-9) Hydrated lime influence on stability with respect to AC% for Wearing course

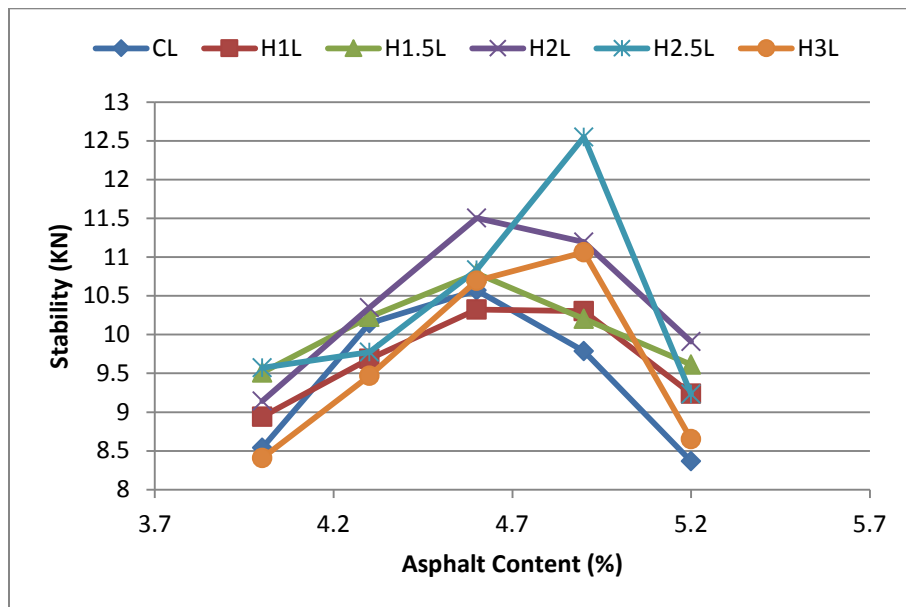


Figure (4-10) Hydrated lime influence on stability with respect to AC% for Leveling course

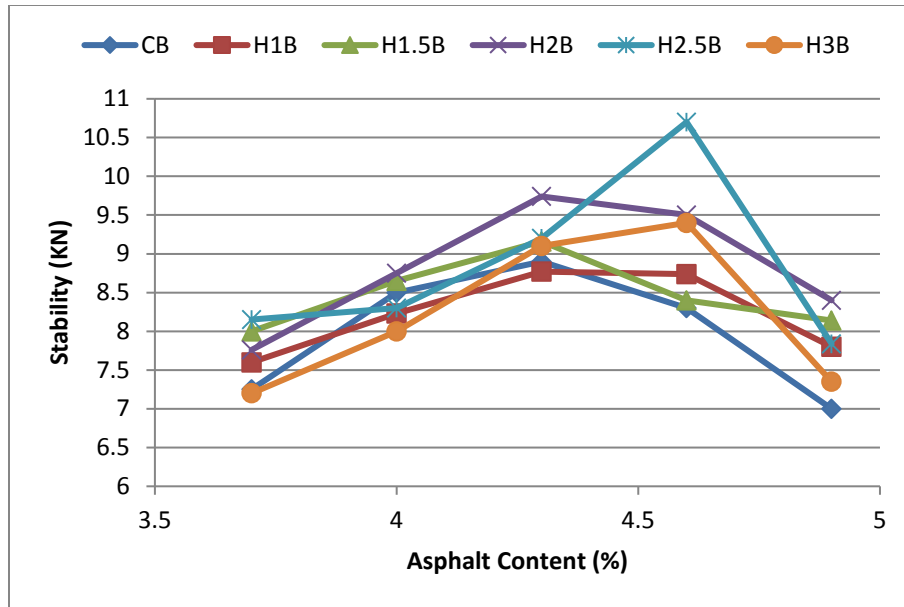


Figure (4-11) Hydrated lime influence on stability with respect to AC% for Base course

4.3.4 Marshall Flow

Marshall flow is the deformation in the specimen that happens during the test and recorded at the point of achieving maximum value of Marshall stability. Figures (4-12), (4-13) and (4-14) indicate that modification of mixtures with hydrated lime exposes a trend of decrease in flow property as hydrated lime increases in the mix. The reduction in flow value is proportionate to the percentage of added hydrated lime, and this is a suggestion for the improvement in rutting resistance in the pavement experiencing high repetitions of traffic load combined with high temperatures. The outcomes are in accord with the findings of other researchers (Peterson 1987, Fayadh 1987, Hossain and Ullah 2011).

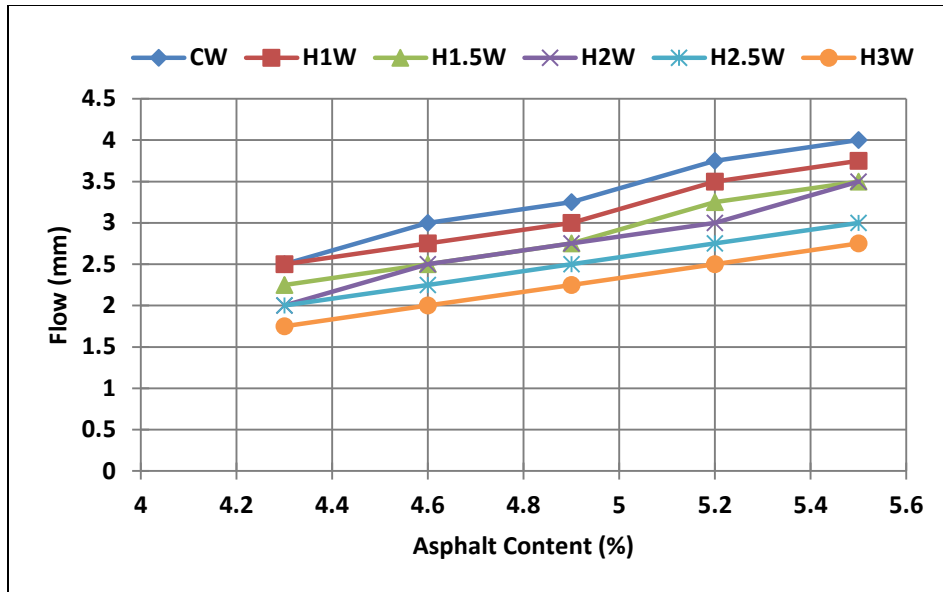


Figure (4-12) Hydrated lime influence on Flow with respect to AC% for Wearing course

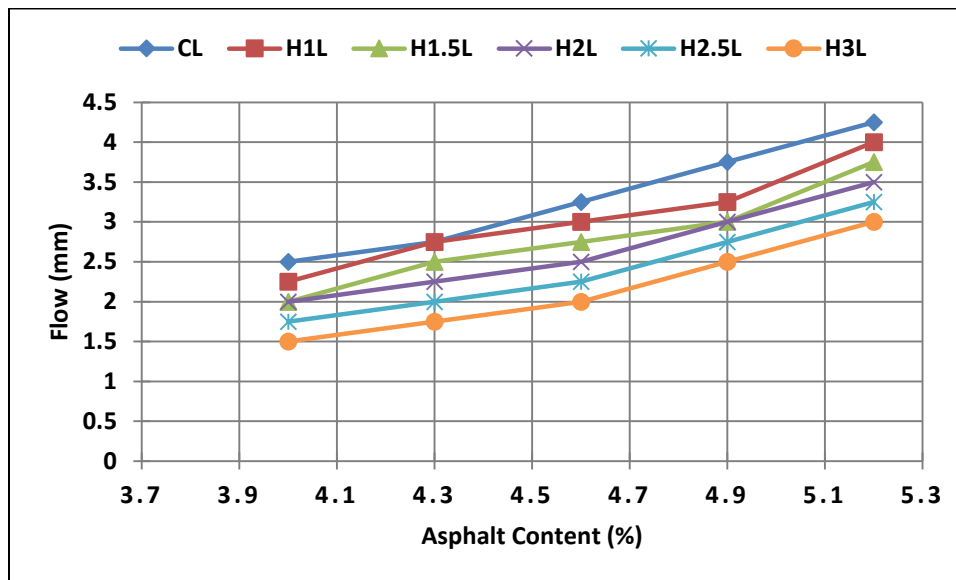


Figure (4-13) Hydrated lime influence on Flow with respect to AC% for Leveling course

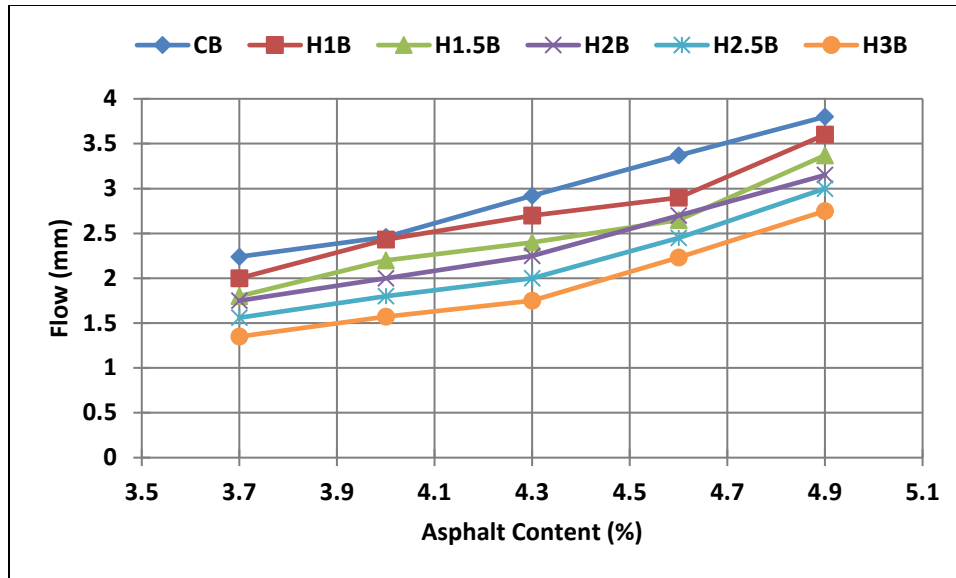


Figure (4-14) Hydrated lime influence on Flow with respect to AC% for Base course

4.4 Influence of Hydrated lime on Volumetric Properties of asphalt mixtures

4.4.1 Air Voids

In the compacted asphalt mixture, the air voids are the volume of air pockets between the aggregate particles that coated with asphalt binder (McGennis et al., 1995). Figures (4-15), (4-16) and (4-17) illustrate that the air void content increases with the increase of hydrated lime content in the range of 0-3% (the curves shift upward in general with the increase of hydrated lime content). The research reported by EuLA (2011) showed that hydrated lime particles have a higher porosity than many other conventional mineral types of filler, which have a porosity value in a range of 60-70% compared the value of 30-34% of the conventional fillers. Figure (4-18) shows the comparison of porosity between hydrated lime particles and other mineral fillers. In the mixing process, the bitumen cement particles will infiltrate into porous hydrated lime particles to produce a stiffer product, known as the mastic, but, meanwhile, the amount of the available asphalt cement particles at the surface of aggregates will decrease. The process results in a relatively high air void content in the mixture. It explains why that with the increase of the asphalt cement content the air void content decreases in an approximately linear relationship for all the mixtures of a certain content of hydrated lime. This is in agreement with the finding of Albayati (2012), who noticed that when the hydrated lime addition is approaching to 2%, the mixtures displayed an increase in

stability. However, beyond this point, the stability decreases as a result of the increase in air void content.

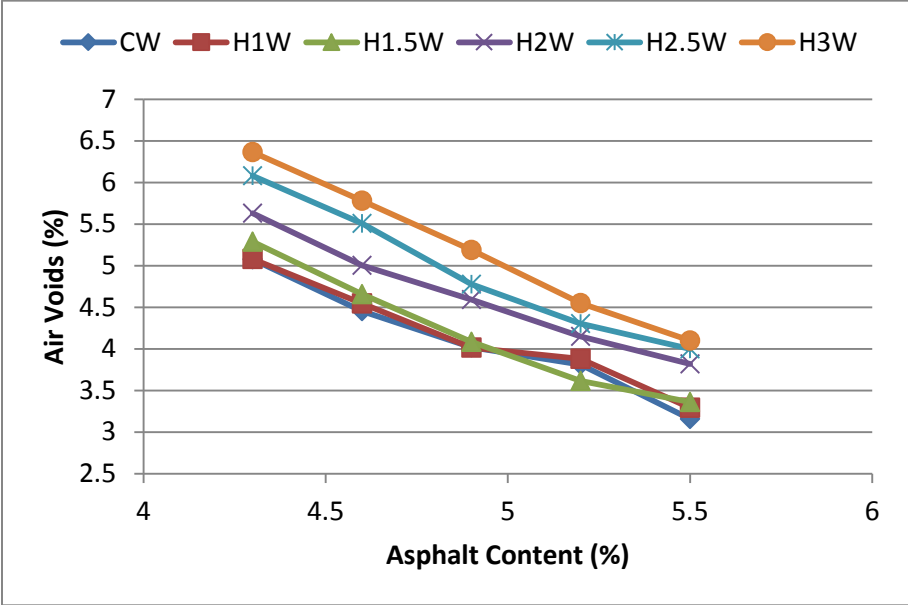


Figure (4-15) Hydrated lime influence on AV% with respect to AC% for Wearing course

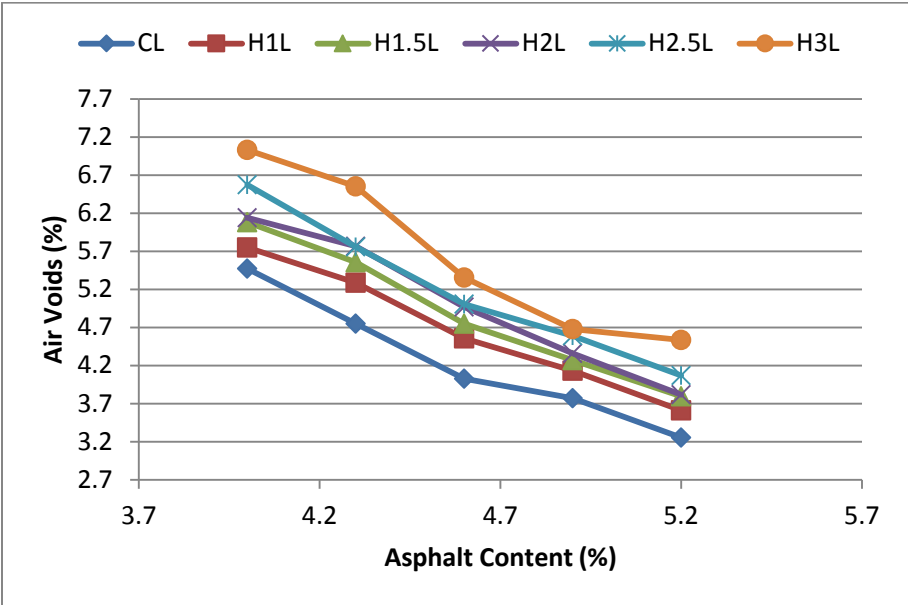


Figure (4-16) Hydrated lime influence on AV% with respect to AC% for Leveling course

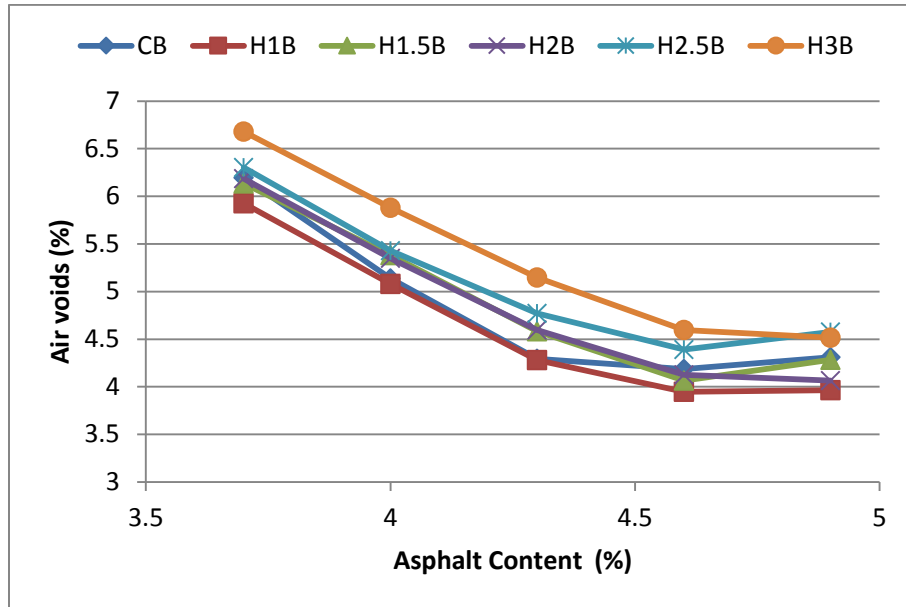


Figure (4-17) Hydrated lime influence on AV% with respect to AC% for Base course

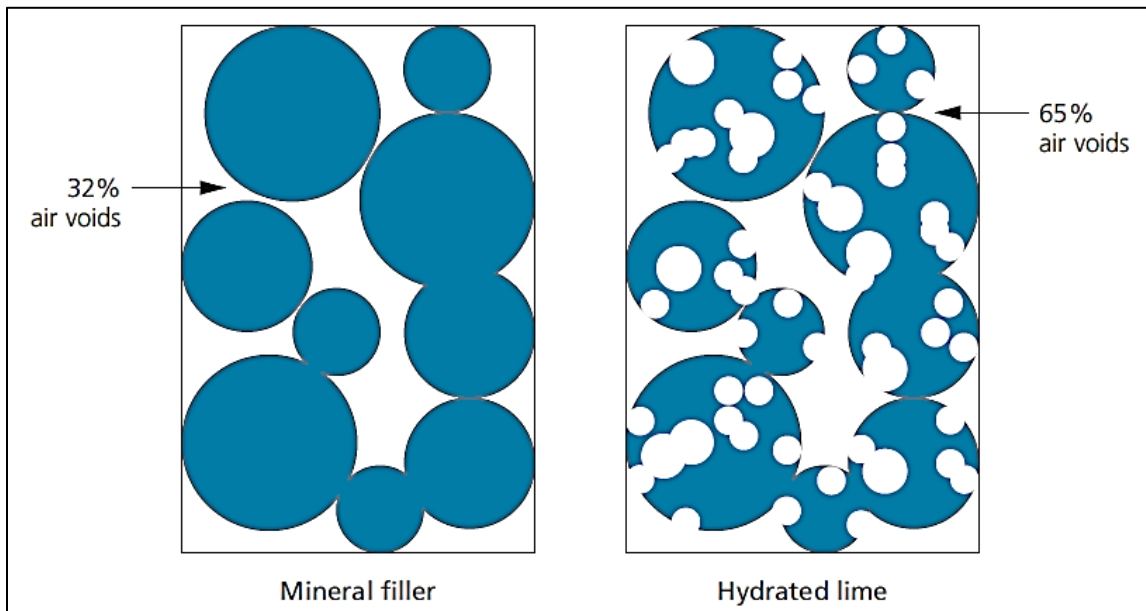


Figure (4-18) Hydrated lime porosity as compared to other mineral fillers (EuLA, 2011)

4.4.2 Voids in Mineral Aggregate (VMA)

The Voids in Mineral Aggregate (VMA) is the space between the aggregate particles in the compacted asphalt mixture that includes the air voids and the effective asphalt cement, which is the remained amount of the total asphalt content after absorption of some of it into the pores of aggregate (McGennis et al., 1995). Figures (4-19), (4-20) and (4-21) illustrate the effect of hydrated lime addition as partial replacement of limestone dust on VMA for W, L and B courses respectively. In general, the VMA increases as the hydrated lime increases in the mix. It is clearer at 2.5 and 3 percent of hydrated lime for all mixtures, in which the increase in VMA is about 1 to 2% as compared to the control mixtures. The increase in VMA may be due to the stiffening of asphalt cement by the addition of hydrated lime, and that leads to stiffer mixtures that present more resistance to compaction. As related to asphalt cement content, it can be seen that the VMA of mixtures begins to decrease with asphalt content increment until reaching the values 4.9%, 4.8% and 4.4% for W, L and B courses respectively. After these values, the voids in mineral aggregate increases until the last value of asphalt cement content.

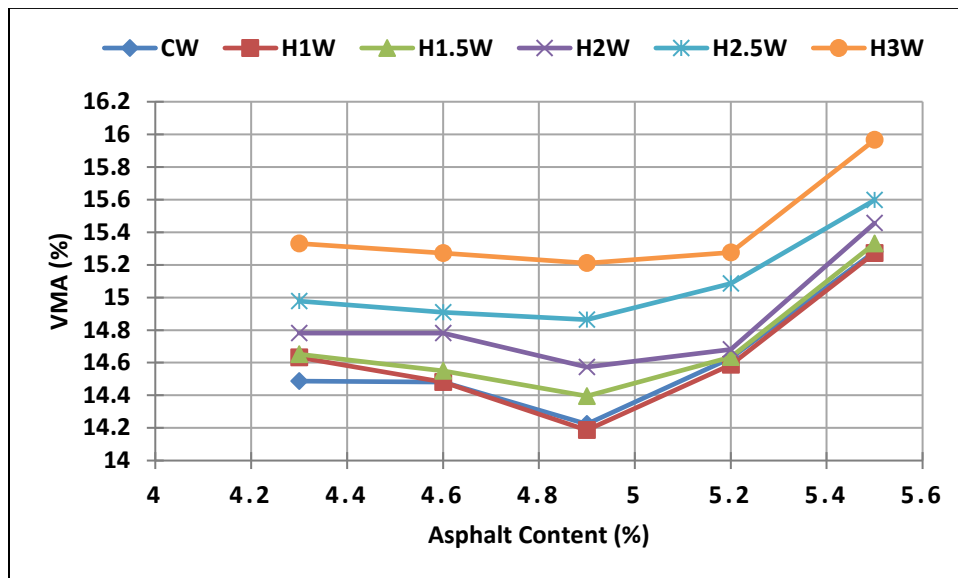


Figure (4-19) Hydrated lime influence on VMA % with respect to AC% for W course

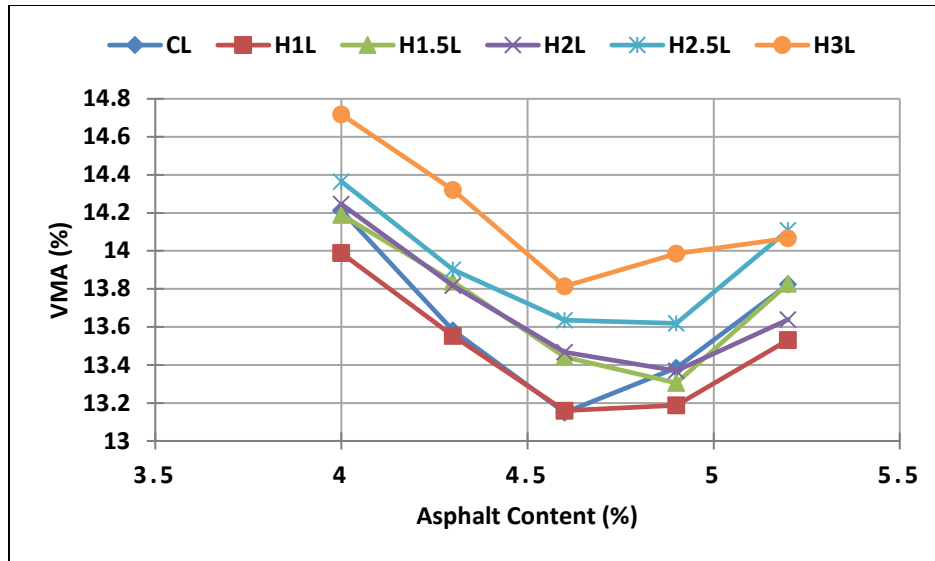


Figure (4-20) Hydrated lime influence on VMA % with respect to AC% for L course

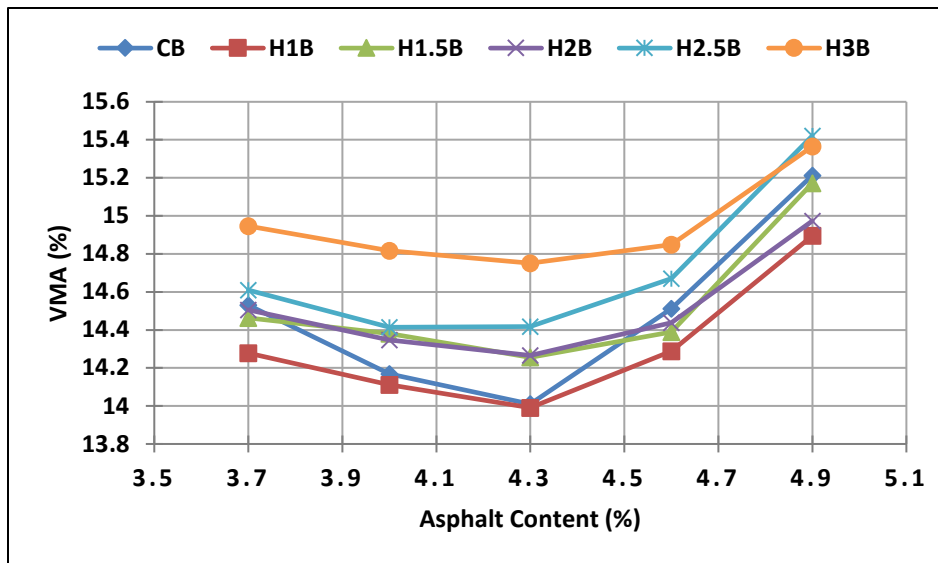


Figure (4-21) Hydrated lime influence on VMA % with respect to AC% for B course

4.4.3 Voids Filled with Asphalt (VFA)

The voids filled with asphalt (VFA) is the part of voids in mineral aggregate (VMA) that occupied by the asphalt cement. This portion represents the effective asphalt volume in the mix. Figures (4-22), (4-23) and (4-24) exhibit the effect of hydrated lime on VFA. For wearing and base courses, it can be seen that the VFA decreased as hydrated lime content increased (starting

from 1.5% until 3%). The VFA for leveling course decreased with hydrated lime addition from 1% until 3%. This could be attributed to the higher volume of hydrated lime particles to occupy in the mix as compared to the ordinary limestone because of its lower density, for each content of asphalt cement.

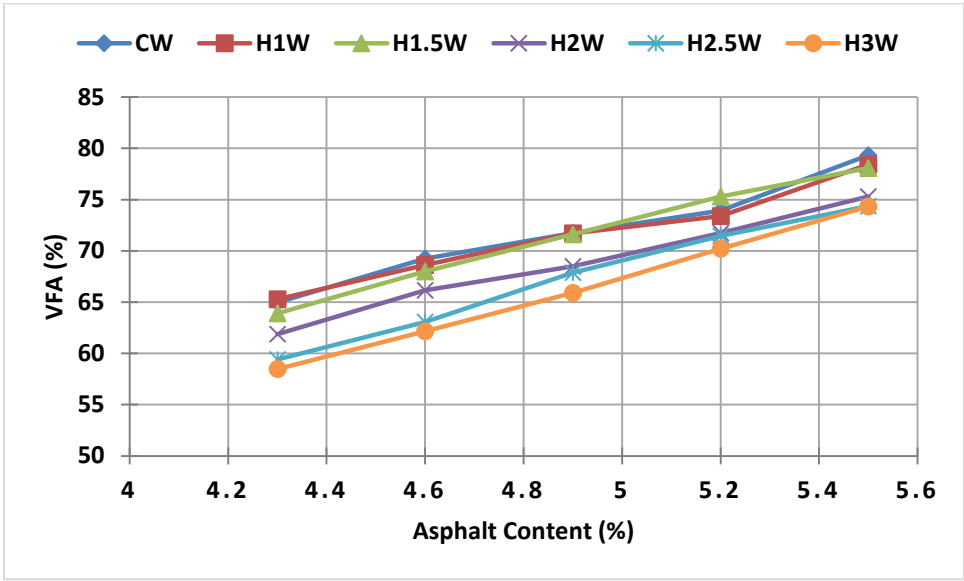


Figure (4-22) Hydrated lime influence on VFA % with respect to AC% for Wearing course

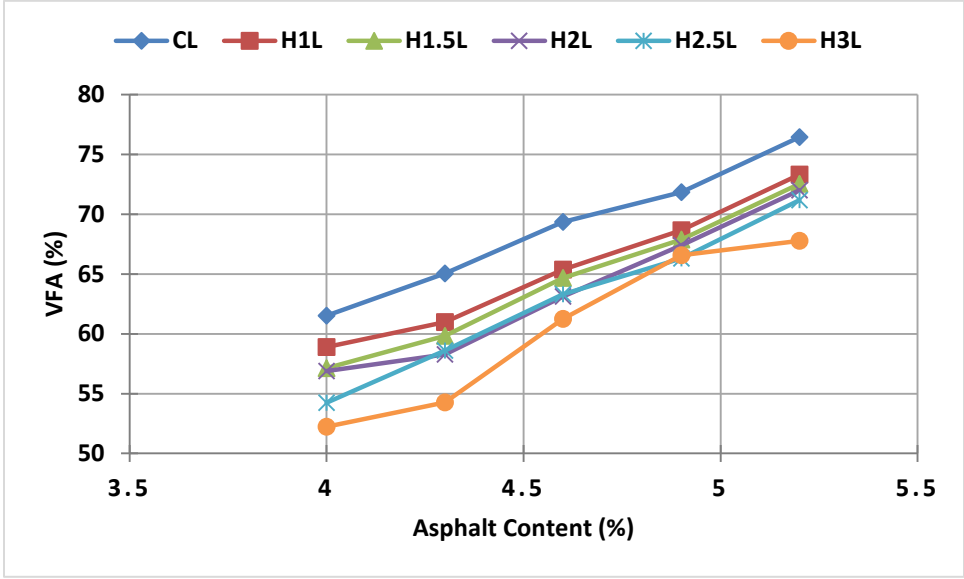


Figure (4-23) Hydrated lime influence on VFA % with respect to AC% for Leveling course

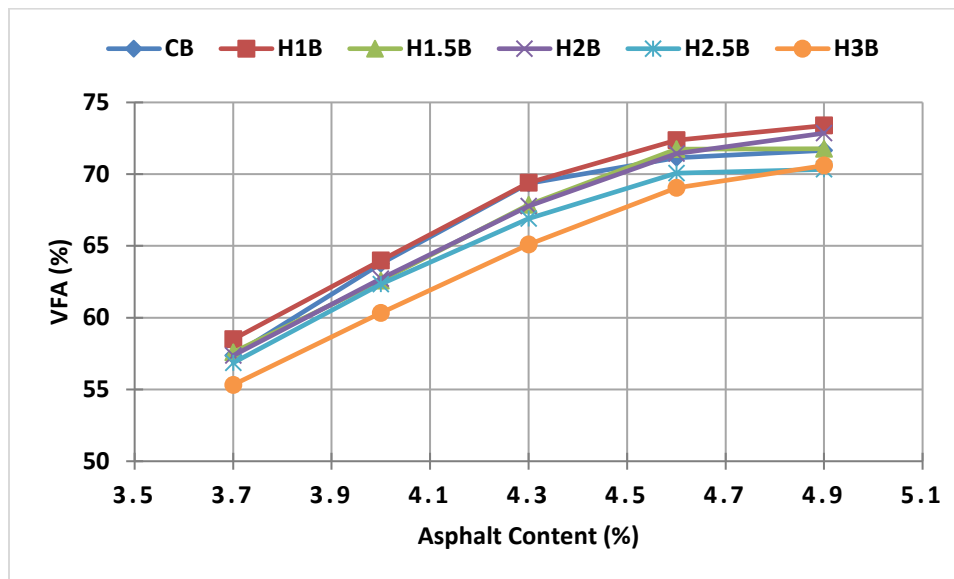


Figure (4-24) Hydrated lime influence on VFA % with respect to AC% for Base course

4.5 Influence of Hydrated lime on Performance related Properties of asphalt mixtures

4.5.1 Hydrated lime Influence on Resilient Modulus (Mr)

The resilient modulus can be worked out in terms of the Eq. (3.6) using the recorded stress-strain relationship. The resilient modulus at different temperatures with respect to the addition of hydrated lime for the course W, L and B mixes are presented in Figures (4-25), (4-26) and (4-27) for 20°C, 40°C and 60°C respectively. It can be seen that relatively high resilient modulus has been achieved by the mixtures of the added hydrated lime with a content in the range of 1.0 to 3.0% at the three temperatures of 20°C, 40°C and 60°C, but, in general, the modulus decreases with the increase of temperature. In detail, the modulus increases with the added content of hydrated lime for all the three types of course mixtures at the low temperature of 20°C. However, for the W and L mixtures, the modulus shows a decrease with the increase in temperature at the high hydrated lime content. Therefore, it can be concluded that the temperature has a significant influence on the HMA performance-related properties. In general, the properties will deteriorate with the increase of temperature. A constructive information from the study is that an optimum 2% hydrated lime content can be used for W and L course application for hot weather conditions, 2.5% content can be used for moderate temperature conditions, and overall, a high content of hydrated lime (such as 3%) will be beneficial for Base course at a wide range of temperature conditions.

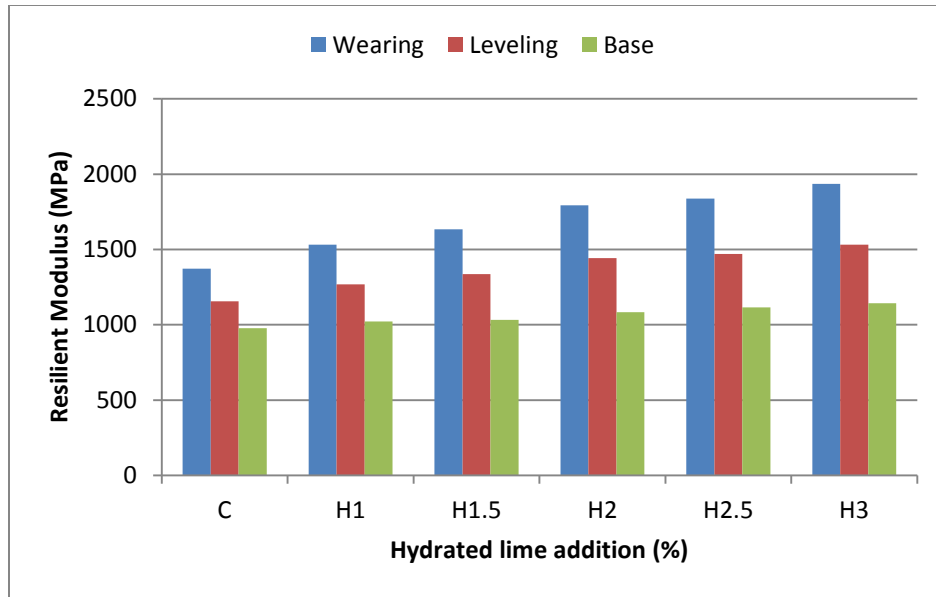


Figure (4-25) Hydrated lime Influence on Resilient Modulus for W, L and B at 20°C

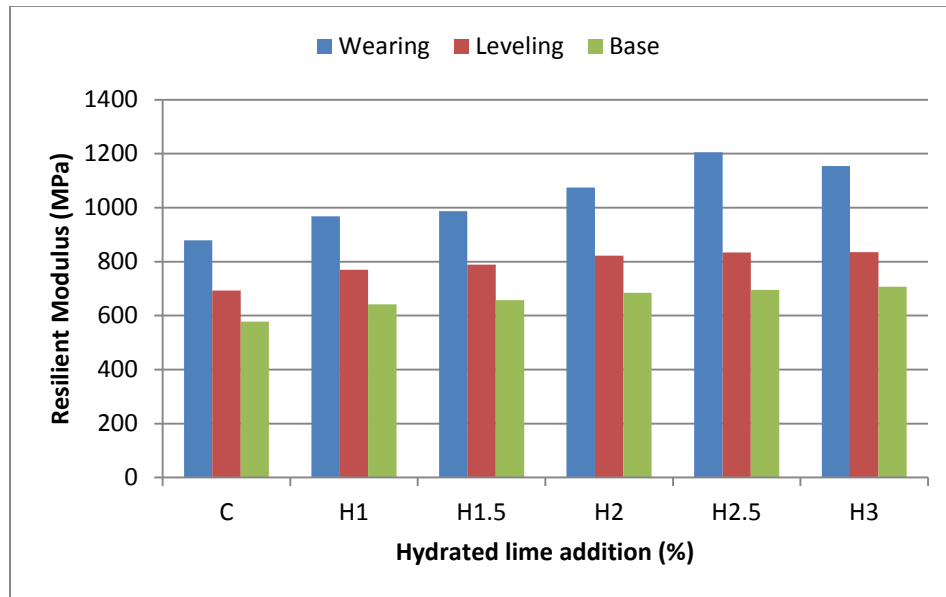


Figure (4-26) Hydrated lime Influence on Resilient Modulus for W, L and B at 40°C

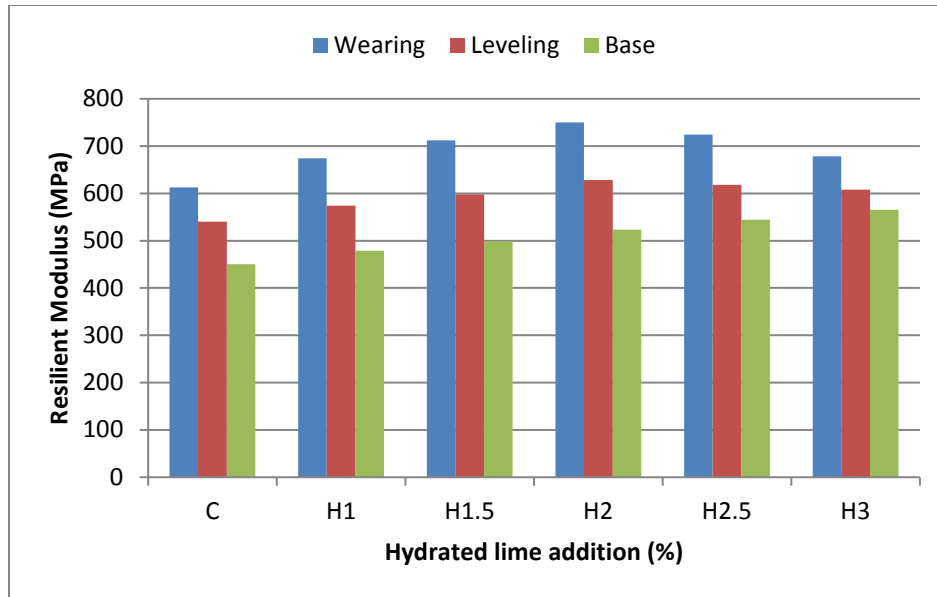


Figure (4-27) Hydrated lime Influence on Resilient Modulus for W, L and B at 60°C

4.5.2 Hydrated lime Influence on Resilient Strain

In the process of permanent deformation test adopted in this study, there are two types of strain that recorded. The first one is the accumulative permanent strain and the second is the resilient strain, which is the recoverable deformation during the unloading period divided by the height of the specimen (Walubita et al, 2013). The resilient strain can be calculated in terms of the Eq. (3.5). The resilient strains at different temperatures with respect to the addition of hydrated lime to the W, L and B mixes are presented in Figures (4-28), (4-29) and (4-30) for 20°C, 40°C and 60°C respectively. Figures exhibit that there is a gradual decrease in resilient strain achieved by adding hydrated lime as partial replacement of limestone filler in the mixtures in the range of 1.0 to 3.0%. In general, the strain increases with the rise in temperature. In detail, at a temperature of 20°C, the strain decreases of about 29% for the H3W as compared to CW, and for H3L the reduction percent from the strain of CL is 24.4% while for H3B, its resilient strain is lower than the control mix (CB) by 14.3%. At 40°C and 60°C of the test, the minimum value of resilient strain recorded at 2.5% and 2% of hydrated lime addition respectively. The decrease in the strain is about 26.9%, 17% and 17% for H2.5W, H2.5L and H2.5B as compared to their control mixtures (CW, CL, and CB) respectively at 40°C. Regarding the test temperature of 60°C, percentages of the drop in the resilient strain as compared to CW, CL and CB are 16.8%, 12.4% and 14.1% for H2W, H2L,

and H2B respectively. However, in comparison of resilient strain for control and modified mixtures at the three temperatures, it can be seen that the temperature has a significant influence on the HMA resilient deformation. In general, the properties will change with the increase of temperature.

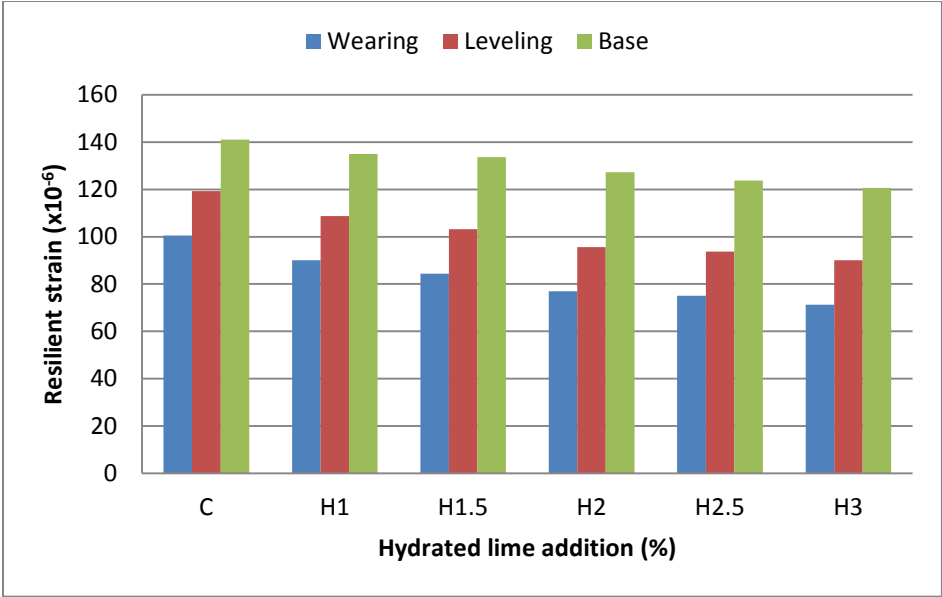


Figure (4-28) Hydrated lime Influence on Resilient Strain for W, L and B at 20°C

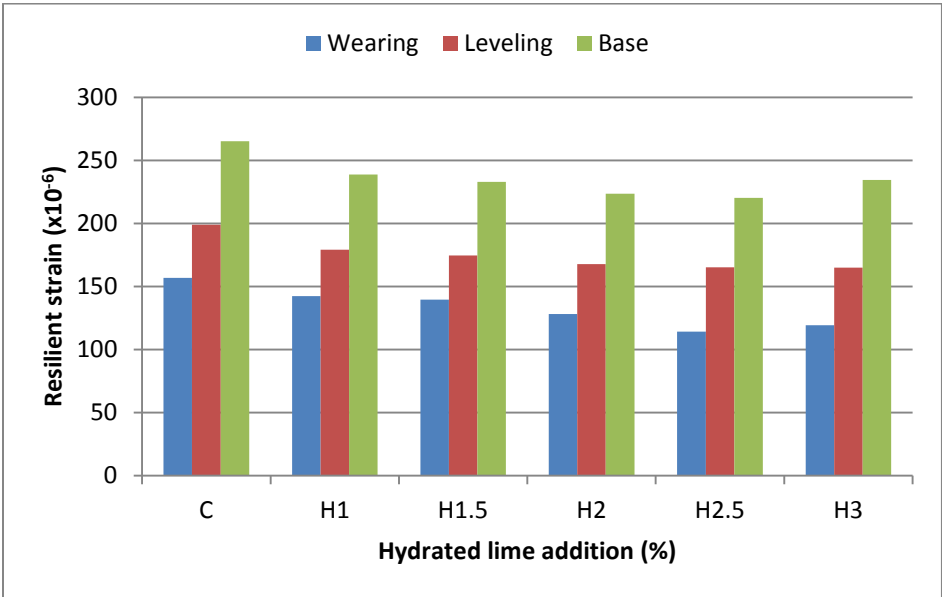


Figure (4-29) Hydrated lime Influence on Resilient Strain for W, L and B at 40°C

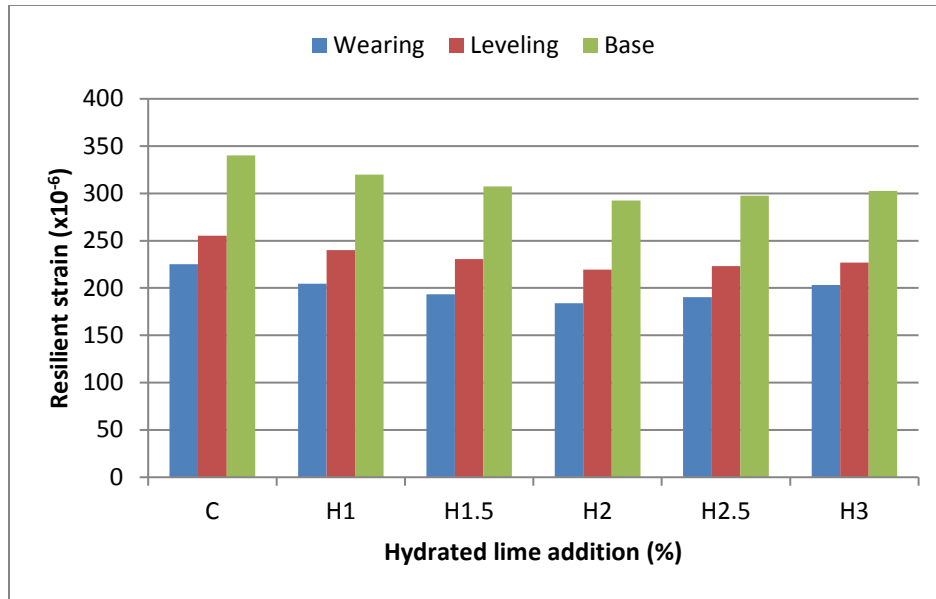


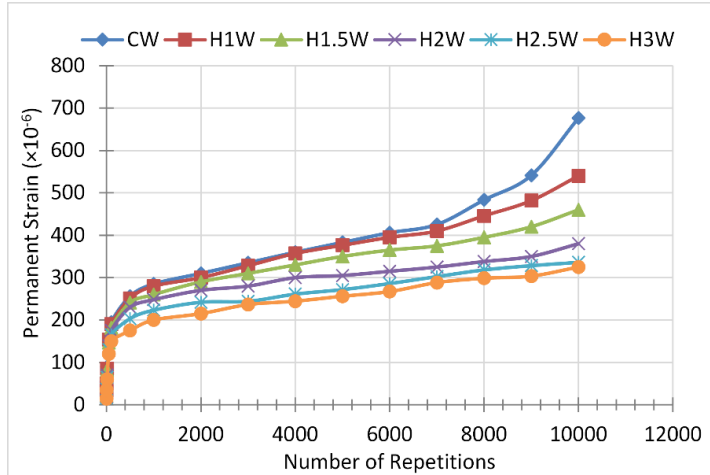
Figure (4-30) Hydrated lime Influence on Resilient Strain for W, L and B at 60°C

4.5.3 Hydrated lime Influence on permanent deformation

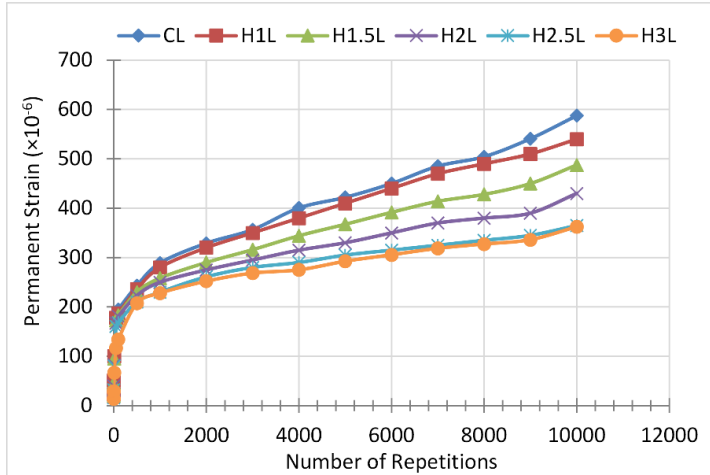
Permanent deformation exhibits itself as a primary distress that happens in the flexible pavement due to heavy and repetitive traffic loads and high temperature. It mainly happens during the hot weather of many countries (hot summer season) including Iraq. In this study, the influence of hydrated lime has been quantified at temperatures of 20°C, 40°C and 60°C describing the range of climate fluctuation throughout the year in Iraq. The test results were obtained using the Equation (3-7) detailed in Chapter 3. Figures (4-31), (4-32) and (4-33) show the permanent deformation of the mixtures under a repeated loading. It can be seen that the addition of hydrated lime improves the capability of the mixtures to resist the deformation at the three temperatures, particularly at the middle temperature of 40°C for the mixtures of W and L (i.e., there has the largest difference between curves). This may be due to the relatively high OAC content of the two types of mixtures, which articulates the effect of the added hydrated lime. For all mixtures, all the curves show a character of three distinctive ranges (Walubita et al. 2013) while the permanent deformation in the secondary middle range shows an approximately linear relationship with the number of the repetition of the applied load in logarithmic scale (Figures (4-34), (4-35) and (4-36)).

Tables (4-5), (4-6) and (4-7) show the parameter results using the Eq. (3-7) to fit the experimental data in the middle phase (secondary portion) of log-log plots of strain versus number of load repetitions for the Wearing, Leveling and Base mixtures.

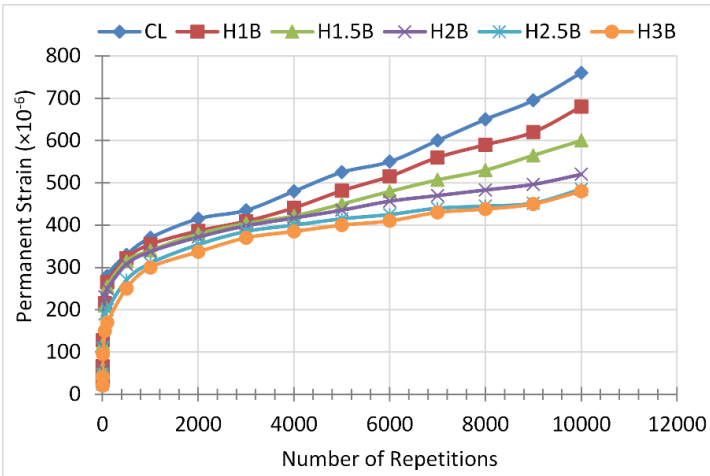
It can be seen that, in general, both the interception (a) and the slope (b) of the linear trend decreases with the increase of the hydrated lime. It means that the addition of the hydrated lime improves the mechanical behavior by increasing the stability of the mixture. It can also be seen that the mixtures 285 of higher hydrated lime contents have a long fatigue life. All the samples of 2.5% and 3% hydrated lime content have the highest number of load repetition before failed in all the studies. These findings are in correlation with the properties observed and discussed before. Little and Petersen (2005) pointed out that hydrated lime is chemically inactive at low temperature, and, as a result, it helps to develop a significant rutting resistance. The results in Figures (4-34), (4-35) and (4-36) show that at a relatively low temperature, such as 20°C, the permanent strain is small for all the mixtures, i.e. both a and b in Tables (4-5) to (4-7) are quite small, and the effect of the variation of the hydrated lime content is not significant (all the lines are very close). However, at a relatively high temperature, such as 40°C and 60°C, the hydrated lime content displays an effective influence, particularly, at 40°C and in the cases of the course W and L, where the effect of the hydrated lime content is evidently pronounced. The results relate to the improvement of the surface bonding between the modified mastic (a compound of asphalt cement and hydrated lime) and aggregate particles, which makes the modified mixture stiffer than the control mixture (containing limestone) at high temperature. However, for base course, because of the relatively large particle size, the effect of the hydrated lime has been reduced by the reduction of the cohesion between the internal microstructure of the mix.



a. Wearing Course

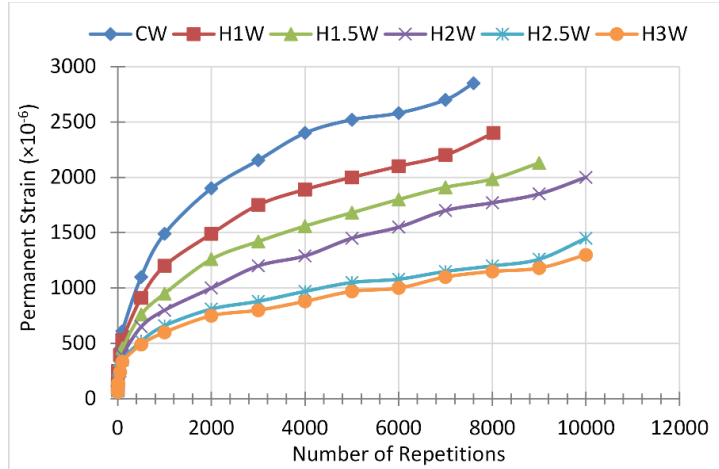


b. Leveling Course

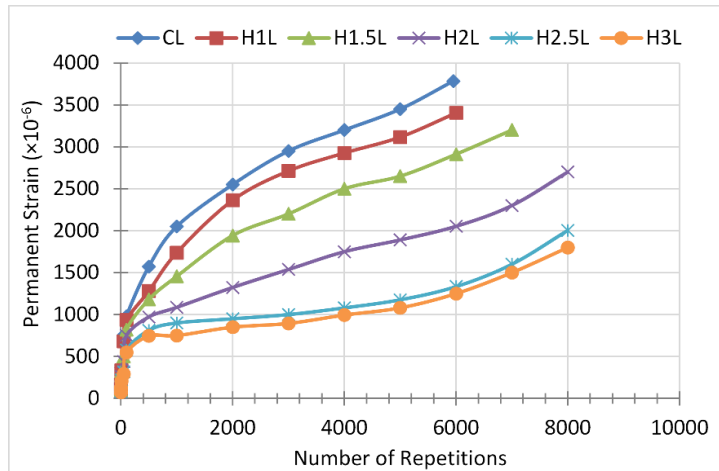


c. Base Course

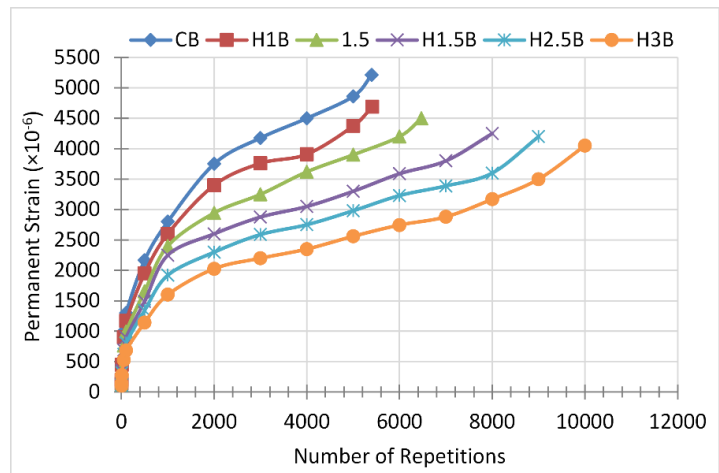
Figure (4-31) Influence of Hydrated Lime on Permanent Deformation at 20°C



a. Wearing Course

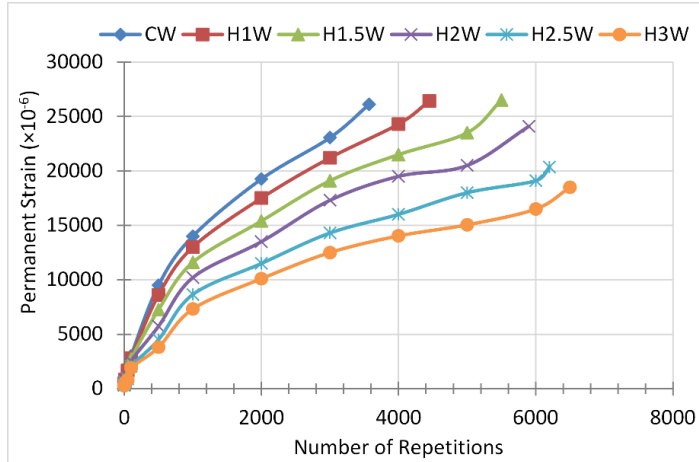


b. Leveling Course

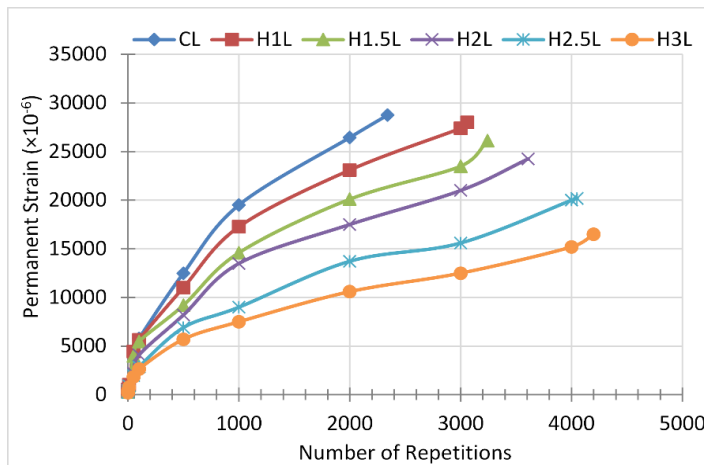


c. Base Course

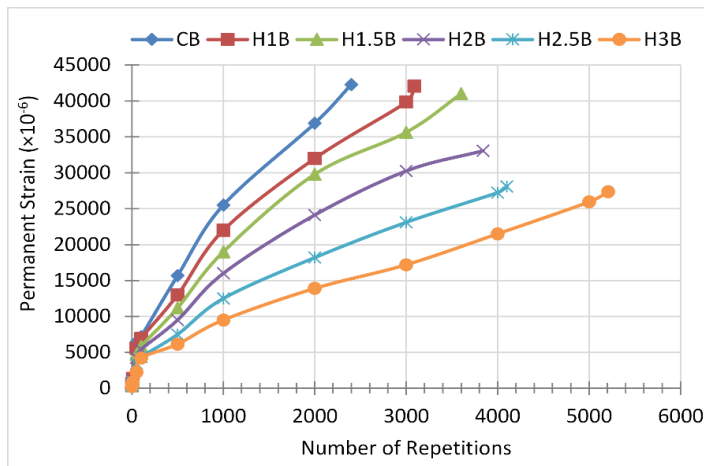
Figure (4-32) Influence of Hydrated Lime on Permanent Deformation at 40°C



a. Wearing Course

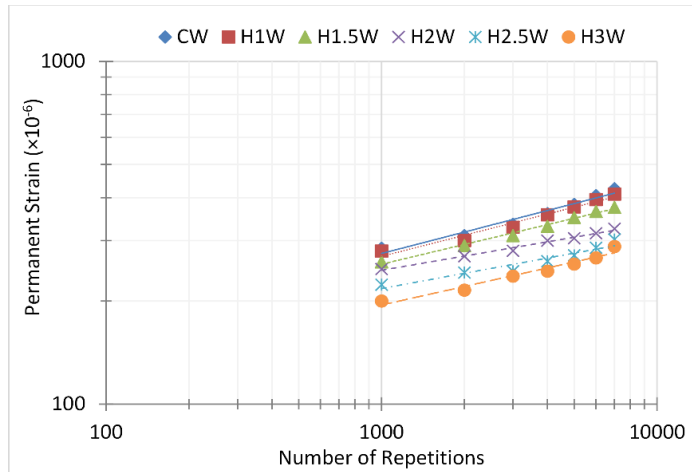


b. Leveling Course

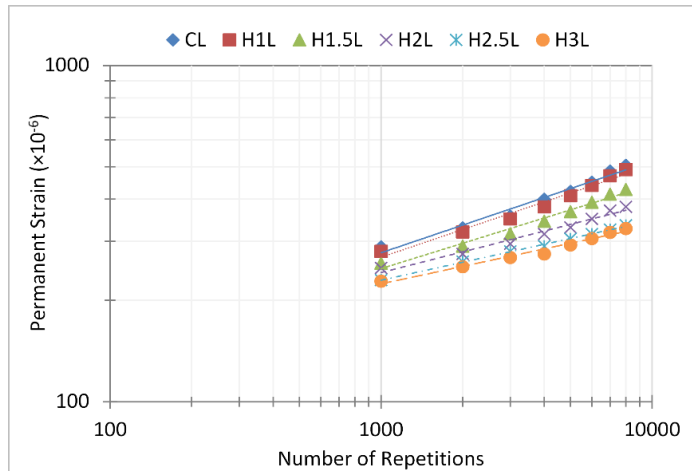


c. Base Course

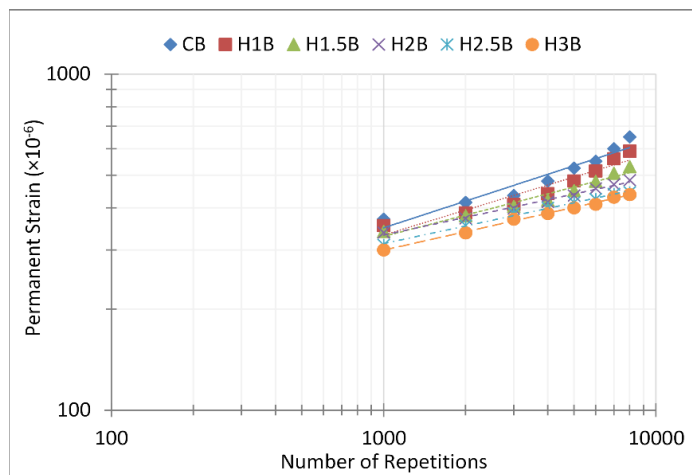
Figure (4-33) Influence of Hydrated Lime on Permanent Deformation at 60°C



a. Wearing Course

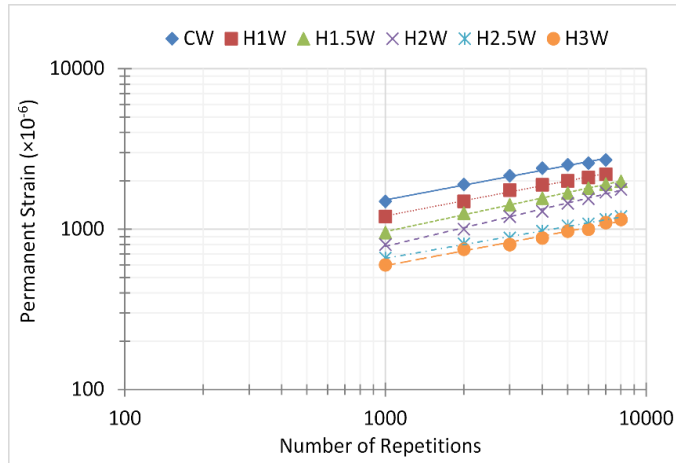


b. Leveling Course

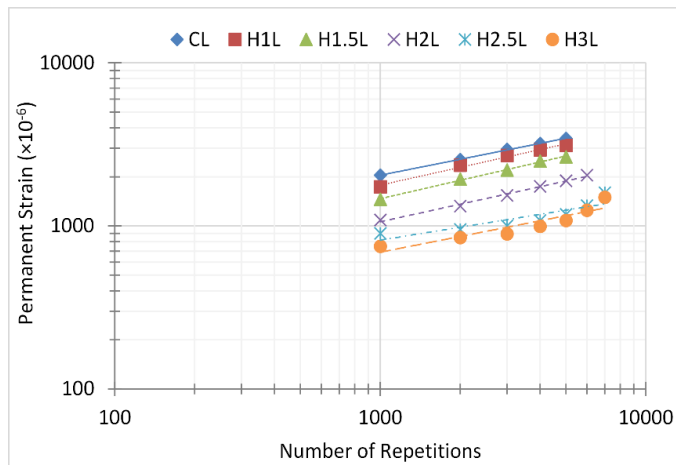


c. Base Course

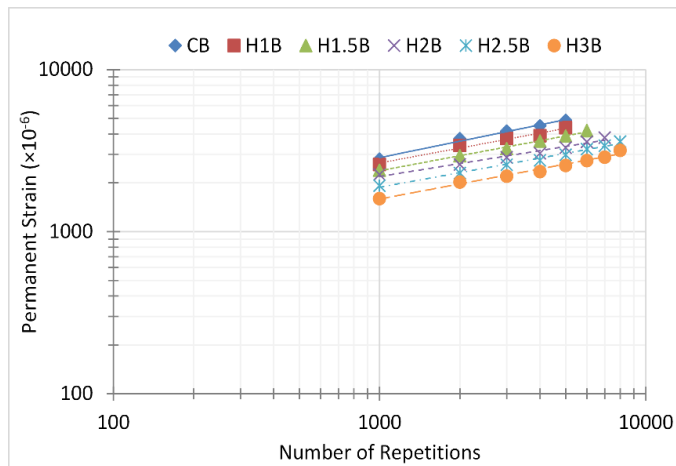
Figure (4-34) Fitting results of permanent deformation for the secondary portion at 20°C



a. Wearing Course

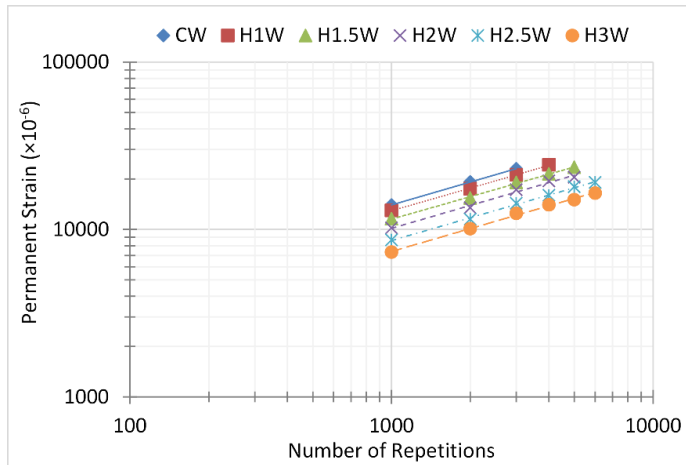


b. Leveling Course

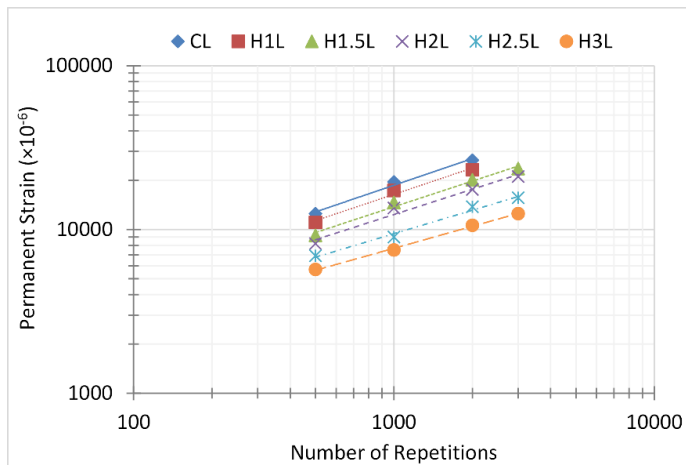


c. Base Course

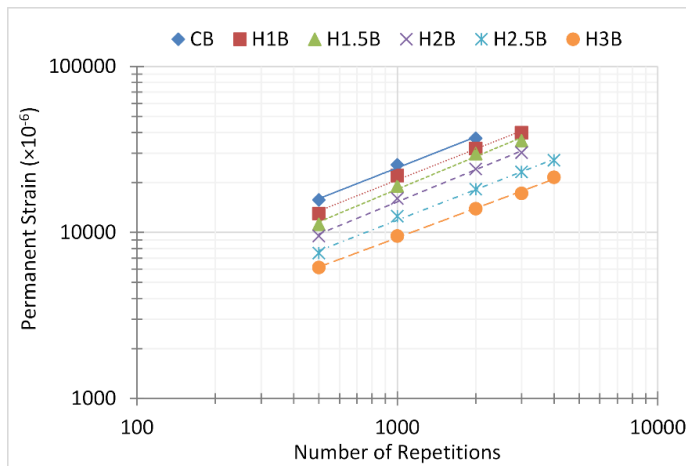
Figure (4-35) Fitting results of permanent deformation for the secondary portion at 40°C



a. Wearing Course



b. Leveling Course



c. Base Course

Figure (4-36) Fitting results of permanent deformation for the secondary portion at 60°C

Table (4-5) The Results of Fitting Parameters using the Eq. (3-7) at 20°C

Mixture	a	b	R ²	Number of repetitions to Failure (N)
CW	65.306	0.2082	0.9648	10000
H1W	65.429	0.2051	0.9665	10000
H1.5W	68.073	0.1918	0.9901	10000
H2W	94.798	0.1379	0.986	10000
H2.5W	78.576	0.1474	0.9183	10000
H3W	56.357	0.1795	0.9583	10000
CL	42.082	0.2729	0.9749	10000
H1L	40.792	0.273	0.976	10000
H1.5L	44.276	0.2499	0.9783	10000
H2L	58.646	0.2052	0.9727	10000
H2.5L	67.507	0.1773	0.9974	10000
H3L	67.998	0.1726	0.9774	10000
CB	56.199	0.2643	0.9332	10000
H1B	60.296	0.2469	0.9201	10000
H1.5B	77.089	0.21	0.9596	10000
H2B	99.475	0.1745	0.991	10000
H2.5B	94.236	0.1738	0.9952	10000
H3B	85.251	0.1819	0.9964	10000

Table (4-6) The Results of Fitting Parameters using the Eq. (3-7) at 40°C

Mixture	a	b	R ²	Number of repetitions to Failure (N)
CW	183.11	0.3065	0.9899	7600
H1W	139.35	0.3129	0.9959	8025
H1.5W	86.636	0.3489	0.9977	9000
H2W	54.034	0.3867	0.994	10000
H2.5W	92.187	0.2844	0.9963	10000
H3W	71.878	0.3054	0.9856	10000
CL	217.93	0.3243	0.9993	5950
H1L	145.45	0.3626	0.9875	6000
H1.5L	110.93	0.3741	0.9963	7000
H2L	89.58	0.3578	0.9924	8000
H2.5L	133.44	0.2626	0.7801	8000
H3L	75.528	0.3203	0.8517	8000
CB	281.73	0.3357	0.9878	5400
H1B	319.08	0.3065	0.979	5410
H1.5B	283.75	0.3076	0.9948	6472
H2B	351.18	0.2649	0.9781	8000
H2.5B	239.39	0.2983	0.9904	9000
H3B	189.53	0.308	0.9842	10000

Table (4-7) The Results of Fitting Parameters using the Eq. (3-7) at 60°C

Mixture	a	b	R²	Number of repetitions to Failure (N)
CW	606.98	0.4545	0.9999	3570
H1W	574.48	0.4508	0.9993	4450
H1.5W	529.96	0.4459	0.9978	5500
H2W	441.59	0.454	0.9899	5900
H2.5W	379.92	0.4514	0.9978	6200
H3W	323.62	0.453	0.9929	6500
CL	444.63	0.5406	0.9884	2340
H1L	409.9	0.5339	0.9851	3060
H1.5L	375.25	0.5214	0.9865	3242
H2L	359.56	0.5118	0.9761	3609
H2.5L	353.49	0.4753	0.9885	4050
H3L	353.82	0.4455	0.9977	4200
CB	344.87	0.6173	0.9938	2400
H1B	287.81	0.6192	0.9921	3090
H1.5B	200.61	0.6528	0.9917	3600
H2B	179.31	0.6436	0.9953	3840
H2.5B	174.43	0.6109	0.996	4100
H3B	161.37	0.587	0.998	5209

4.5.4 Hydrated lime Influence on Fatigue Cracking

Fatigue characteristics evaluation regarding the effect of hydrated lime has been done by adopting the fatigue flexural test mentioned in details in chapter 3. The relationship between strain (ϵ_t) and the number of load repetitions to failure (N_f) takes the power model (Eq. (3-11)). The equation includes the parameters k_1 and k_2 that are the value of N_f when ϵ_t equal to 1 (intercept) and inverse slope of the straight line in the logarithmic relationship respectively. The number of load repetitions needed to complete fracture of specimens was determined and designated as the failure life (N_f). At the initial phase of the flexural fatigue repeated load test, the stiffness modulus and tensile strain (ϵ_t) values were calculated by measuring of the recoverable deflection at the centre point of the specimen beam immediately after 200th load repetition as indicated by Kallas and Puzinauskas (1972) and Huang (2004). As described by Huang (2004), after plotting initial

tensile strain (ϵ_t) and the number of load repetitions to failure (N_f) in log scale, the k_2 (inverse slope) is obtained for the fitted line of relationship. After that the intercept (k_1), in which ϵ_t equal to 1 can be calculated as follows:

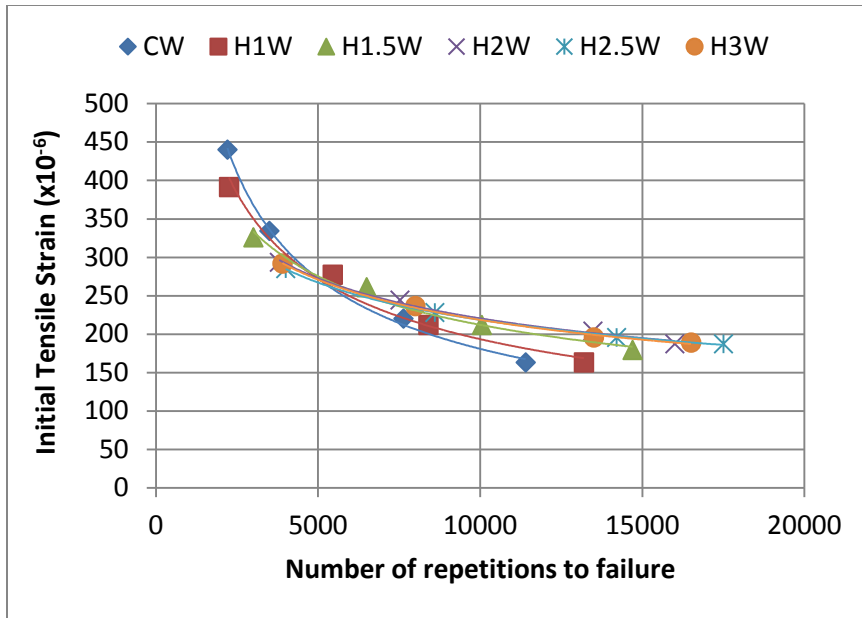
$$k_2 = \frac{\log N_f - \log k_1}{\log 1 - \log \epsilon_t} \quad (4-1)$$

or

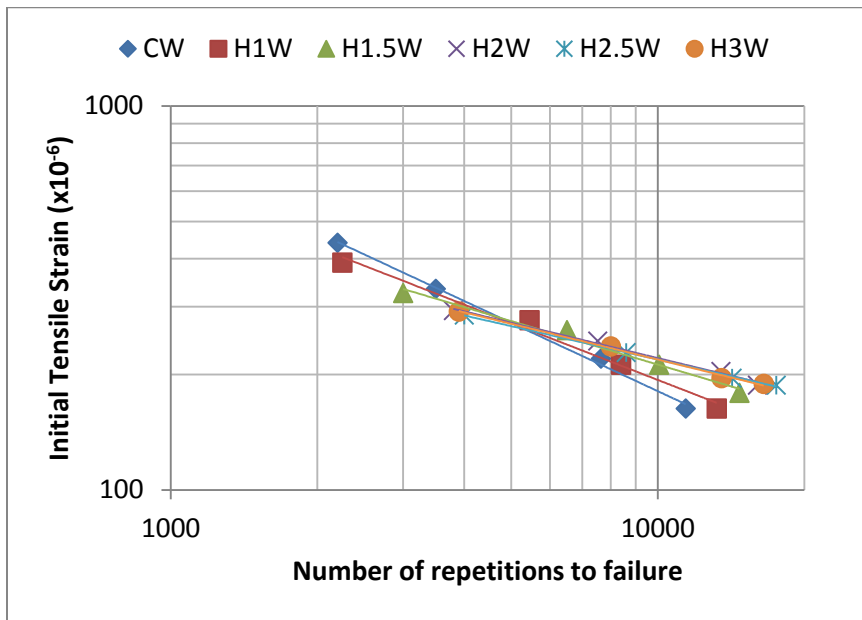
$$\log k_1 = \log N_f + k_2 \log \epsilon_t \quad (4-2)$$

4.5.4.1 Initial Tensile Strain-Fatigue failure Life Relationship

The controlled-stress fatigue tests under repeated loading by means of Pneumatic Repeated Load System (PRLS) resulted in a different optimality in this study. Figures (4-37), (4-38) and (4-39) show the fatigue characteristics of W, L and B courses mixtures as a log-log graphical relationship of the number of load repetitions to failure and the initial tensile strain at a temperature of 20°C for W, L and B.

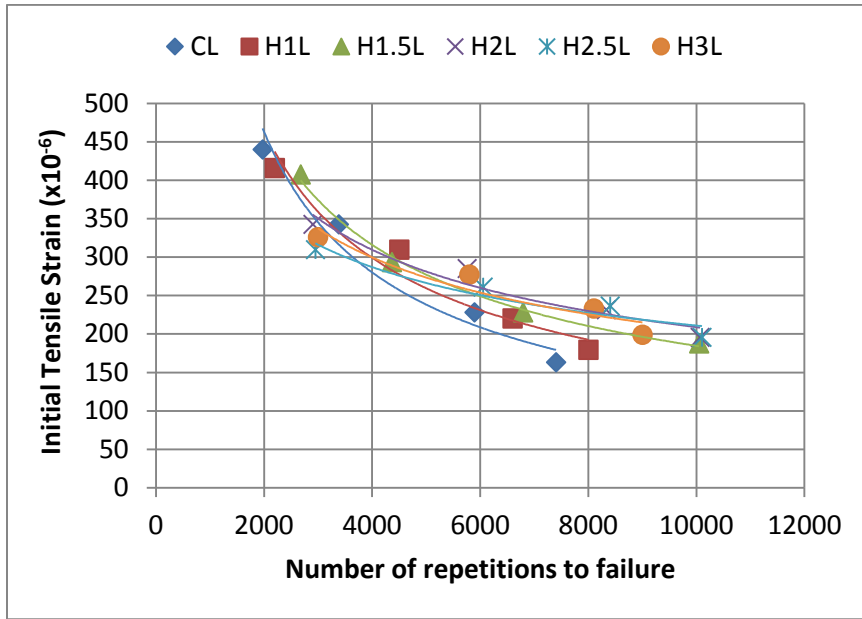


(A) Initial Tensile Strain versus Number of Repetitions to Failure

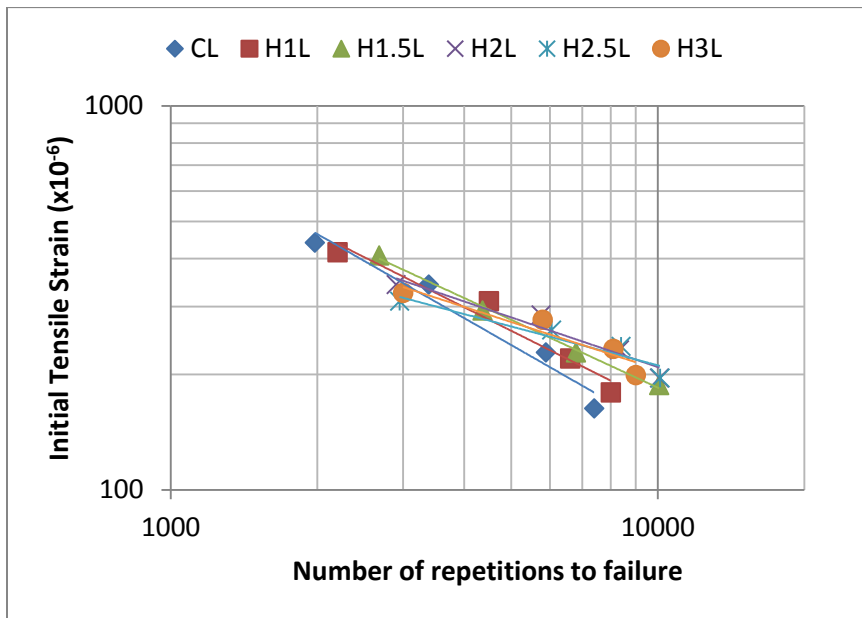


(B) Log-Log Plot of Initial Tensile Strain versus Number of Repetitions to Failure

Figure (4-37) Hydrated lime Influence on fatigue cracking relationship for Wearing course

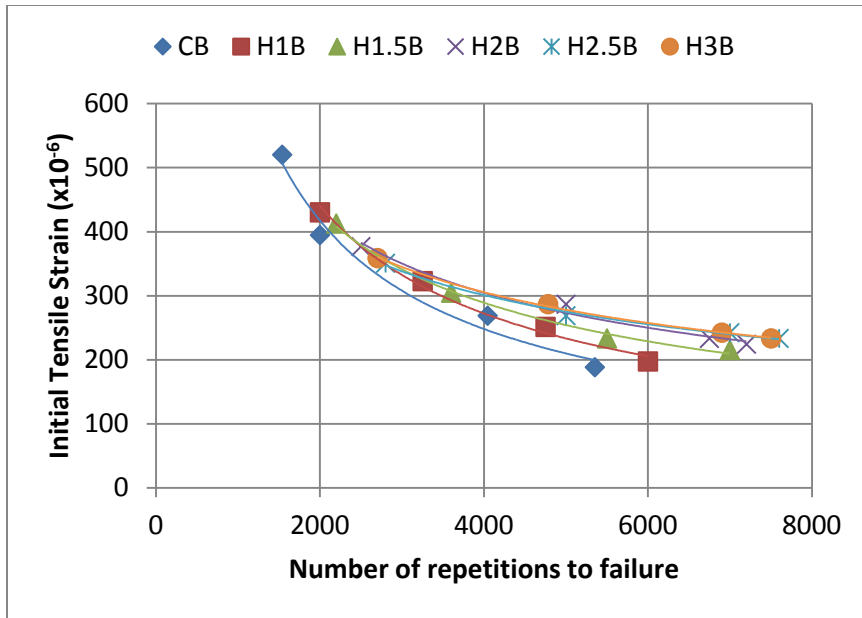


(A) Initial Tensile Strain versus Number of Repetitions to Failure

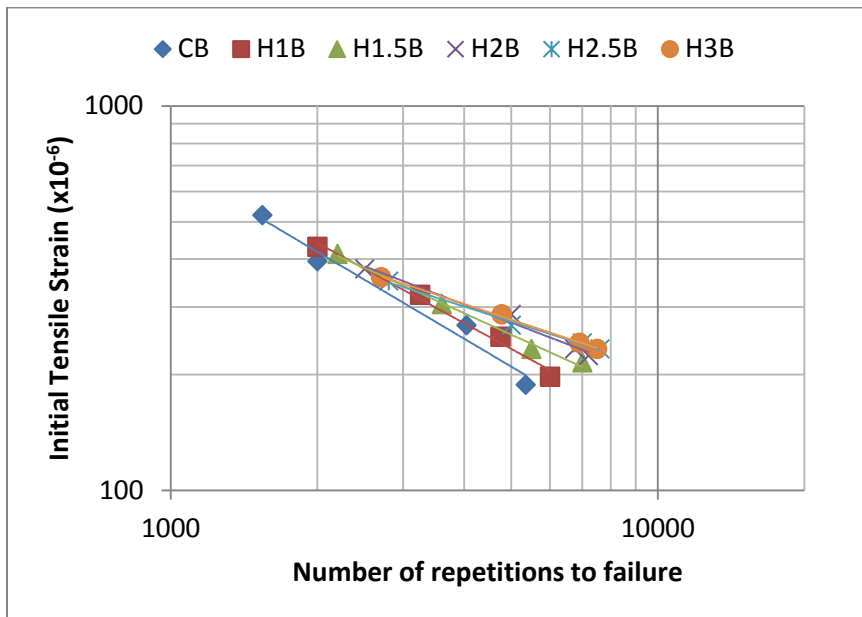


(B) Log-Log Plot of Initial Tensile Strain versus Number of Repetitions to Failure

Figure (4-38) Hydrated lime Influence on fatigue cracking relationship for Leveling course



(A) Initial Tensile Strain versus Number of Repetitions to Failure



(B) Log-Log Plot of Initial Tensile Strain versus Number of Repetitions to Failure

Figure (4-39) Hydrated lime Influence on fatigue cracking relationship for Base course

The fatigue parameters, k_1 and k_2 values, as well as the number of load repetitions to failure related to their corresponding stress level are presented in Tables (4-8), (4-9) and (4-10) for the Wearing, Leveling and Base course mixtures respectively. The parameters k_1 and k_2 can present an indication of the influence of hydrated lime on the fatigue properties of asphalt concrete mixtures. The flatter slope of the fatigue relationship means a higher value of k_2 . In a case of two or more mixtures have the same value of k_1 , the greater value of k_2 gives a possibility of fatigue life increase. In comparison between mixtures, when the slopes of fatigue plots are parallel, which suggests that they have the same value of k_2 , the lower value of k_1 indicates that the mix has a shorter fatigue life. It can be noticed in all mixtures that the resistance to fatigue cracking increases with the decrease in the curve slope. It was found from the output of tests for each mixture that the addition of hydrated lime leads to gradual enhancement of fatigue resistance until the per cent of 2.5. At the 2.5% of hydrated lime, the optimum of performance properties have been achieved and beyond this amount the mixtures became slightly weaker to withstand the fatigue related damage. The mixtures H2.5W, H2.5L, and H2.5B earned an enhancement in their k_2 (inverse slope) value by 104.5%, 115.7%, and 85.6% respectively, as compared to their control mixtures. The wearing mix (H3W) has a reduction in the value of k_2 beyond the mix of 2.5 per cent of hydrated lime (H2.5W) by 6.7%, and there is a small decline observed at H3L, and H3B as well when hydrated lime content increases beyond the value of 2.5 percent for H2.5L and H2.5B mixtures. The reduction in the change in k_2 value after 2.5% of hydrated lime addition is 17.8% and 4.26% for H3L and H3B respectively with respect to the H2.5L and H2.5B mixtures. Tables (4-8), (4-9) and (4-10) summarize the fatigue life equations parameters. There is an indication that k_2 values noticeably gradually increase with respect to hydrated lime addition. The increase in k_2 means a reduction in the slope of S-N curve (relation between tensile strain/stress and the number of load repetitions) and this decline indicates that the material becomes more resistant to fatigue cracking. Moreover, the process of fatigue cracking will take more time than without hydrated lime and eventually this will lead to increase the fatigue life of modified mixtures. Regarding the k_1 values change, it can be noticed that it decreased from 0.004626742 at 0% of hydrated lime to 2.16786×10^{-09} at 2.5% for Wearing course, and 0.050626086 to 1.15199×10^{-07} for Leveling. The value of k_1 for Base course starts with 0.062482667 at control mixture and continues to decrease as well until reaching a minimum value at H2.5B mixture with 7.75256×10^{-06} . The findings are consistent, and in agreement with previous investigations of other researchers pointed that

hydrated lime is capable of strengthening the asphalt mixtures as well as reducing the potential of micro-crack growth (Lesueur and Little,1999, Little and Petersen 2005) and increasing micro-crack healing potential (Little and Petersen 2005).

Table (4-8) Fatigue life parameters using Eq. (3-11) for Wearing mixture

Mixture	Fatigue Equation Parameters			Number of repetition to failure (N_f)			
	$N_f = k_1 \varepsilon_t^{k_2}$			Stress level, N (lb)			
	k_1	k_2	R^2	223 (50)	310 (70)	402 (90)	490 (110)
CW	0.004626742	-1.692047377	0.9964	11400	7632	3500	2200
H1W	0.000295521	-2.028397566	0.9862	13200	8400	5450	2250
H1.5W	1.78429E-06	-2.652519894	0.9848	14700	10050	6500	3000
H2W	1.11427E-08	-3.267973856	0.9928	16000	13475	7520	3800
H2.5W	2.16786E-09	-3.460207612	0.9985	17500	14200	8600	4000
H3W	1.5403E-08	-3.225806452	0.9957	16500	13500	8000	3900

Table (4-9) Fatigue life parameters using Eq. (3-11) for Leveling mixture

Mixture	Fatigue Equation Parameters			Number of repetition to failure (N_f)			
	$N_f = k_1 \varepsilon_t^{k_2}$			Stress level, N (lb)			
	k_1	k_2	R^2	223 (50)	310 (70)	402 (90)	490 (110)
CL	0.050626086	-1.379310345	0.9663	7400	5890	3385	1975
H1L	0.011461435	-1.572327044	0.9585	8000	6600	4500	2200
H1.5L	0.004364545	-1.703577513	0.9957	10051	6790	4364	2678
H2L	2.74277E-05	-2.325581395	0.9357	10070	8331	5756	2900
H2.5L	1.15199E-07	-2.976190476	0.9379	10100	8402	6050	2950
H3L	9.69629E-06	-2.444987775	0.9837	10300	8800	6250	3400

Table (4-10) Fatigue life parameters using Eq. (3-11) for Base mixture

Mixture	Fatigue Equation Parameters			Number of repetition to failure (N_f)			
	$N_f = k_1 \varepsilon_t^{k_2}$			Stress level, N (lb)			
	k_1	k_2	R^2	223 (50)	310 (70)	402 (90)	490 (110)
CB	0.062482667	-1.333333333	0.9746	5350	4045	2000	1540
H1B	0.028738646	-1.443001443	0.9871	6000	4750	3250	2000
H1.5B	0.002936207	-1.733102253	0.9926	7000	5500	3600	2200
H2B	0.000234576	-2.057613169	0.9809	7200	6750	5000	2500
H2.5B	7.75256E-06	-2.475247525	0.9937	7600	7000	5000	2800
H3B	1.87869E-05	-2.369668246	0.9981	7500	6900	4780	2700

4.5.4.2 Hydrated lime Influence on The Parameters of Fatigue Equations

The intercept (k_1) and inverse slope (k_2) of fatigue equations that relates the initial tensile strain (ε_t) and the number of cycles to fracture (N_f) have been influenced by hydrated lime filler partial replacement in the studied asphalt concrete mixes. Figures (4-40) and (4-41) show the influence of hydrated lime on the variation of fatigue equations' parameters (k_1) and (k_2) respectively. It can be seen that k_1 values of control mixtures are 4626.7×10^{-6} , 50626×10^{-6} and 62482.6×10^{-6} for Wearing, Leveling and Base respectively and they decreased until a minimum value at 2.5% of hydrated lime with a slight increase beyond this percentage. It can be found that the decreasing behaviour of k_1 of all mixtures is in a form of polynomial equation to the 3rd degree with a good fitting. Regarding the k_2 values of all mixture, it can be observed that inverse slope values are getting higher due to hydrated lime increment in the mixes. This behaviour can be fitted with a form of polynomial equation to the 4th degree. The output of these figures and equations between hydrated lime and fatigue equation parameters could be useful to describe the influence of hydrated lime on number of fatigue repetitions and tensile strain directly by substitution the equations related k_1 and k_2 with hydrated lime in the main fatigue equation.

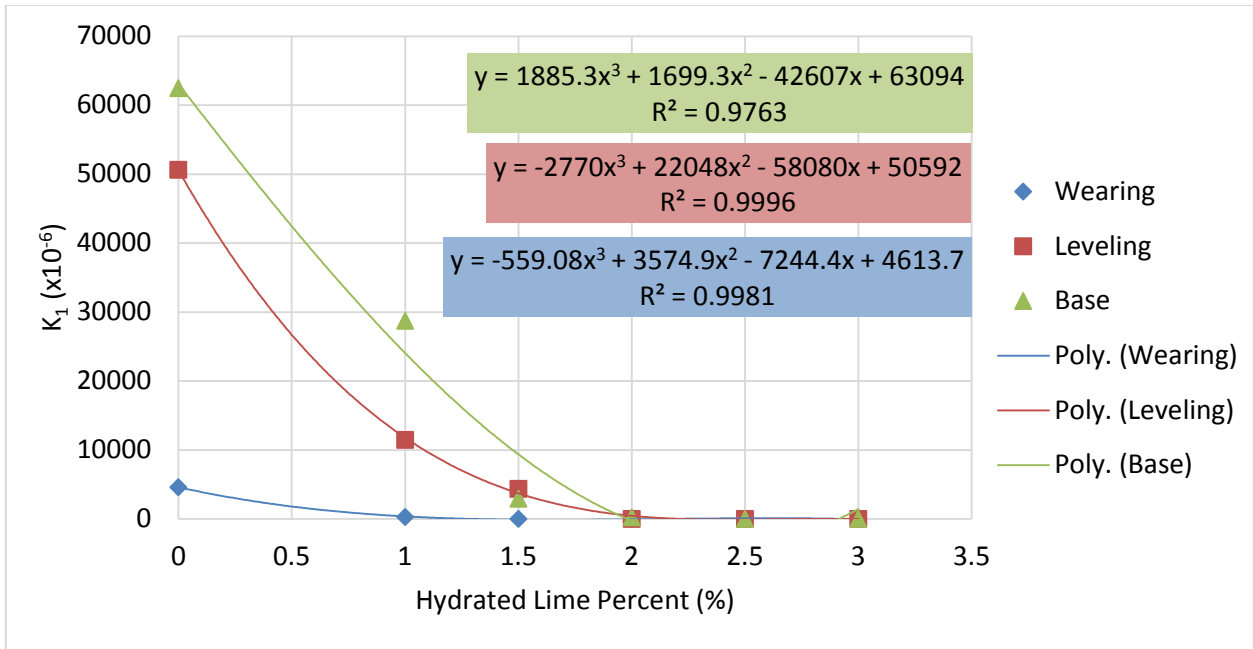


Figure (4-40) Effect of Hydrated Lime on K₁ fatigue parameter of asphalt mixtures

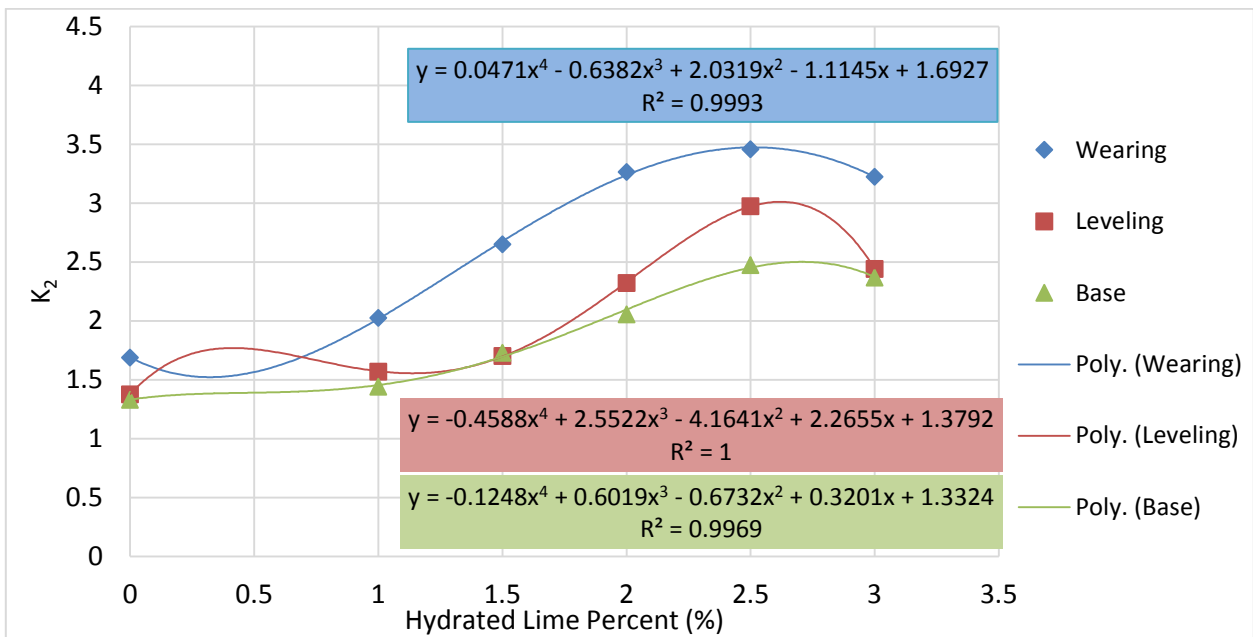


Figure (4-41) Effect of Hydrated Lime on K₂ fatigue parameter of asphalt mixtures

4.5.4.3 Hydrated lime Influence on the Stress level and Number of Load repetitions

Figures (4-42), (4-43) and (4-44) exhibit the relation between the applied stress and number of repetitions to failure for Wearing, leveling and Base respectively. In general, for all control and modified mixtures, the decrease in stress leads to increase in fatigue life. Increasing of hydrated lime percentage in the mixtures leads to rise in their fatigue life until 2.5% of hydrated lime and beyond this percent the repetitions either decreased or at least no significant enhancement. For instance, in the Wearing mix, the control mix (CW) has 11400 repetitions to failure at a level of stress 0.15 MPa while at 0.337 MPa of applied stress the cycles are 2200. The increment in fatigue life continues until an optimum value at the mix (H2.5W) which has 17500 repetitions at 0.15 MPa stress level and decreased to 4000 repetitions at 0.337 MPa. Similarly, the Base course mix on its control mix (CB) the repetitions to failure were 5350 at a level of stress 0.15 MPa and decreased to 1540 cycles at 0.337 MPa of applied stress. For the Leveling course mix, the control mix (CL) repetitions to failure were 7400 at a level of stress 0.15 MPa and decreased to 1975 cycles at 0.337 MPa of applied stress. The increase in fatigue life still until the mix (H2.5L) at 0.15 MPa stress level with 10100 repetitions and decreased to 2950 repetitions at 0.337 MPa and at the same level of stress (0.337 MPa), the fatigue life increased until the mix (H3L) of 3000 repetitions.

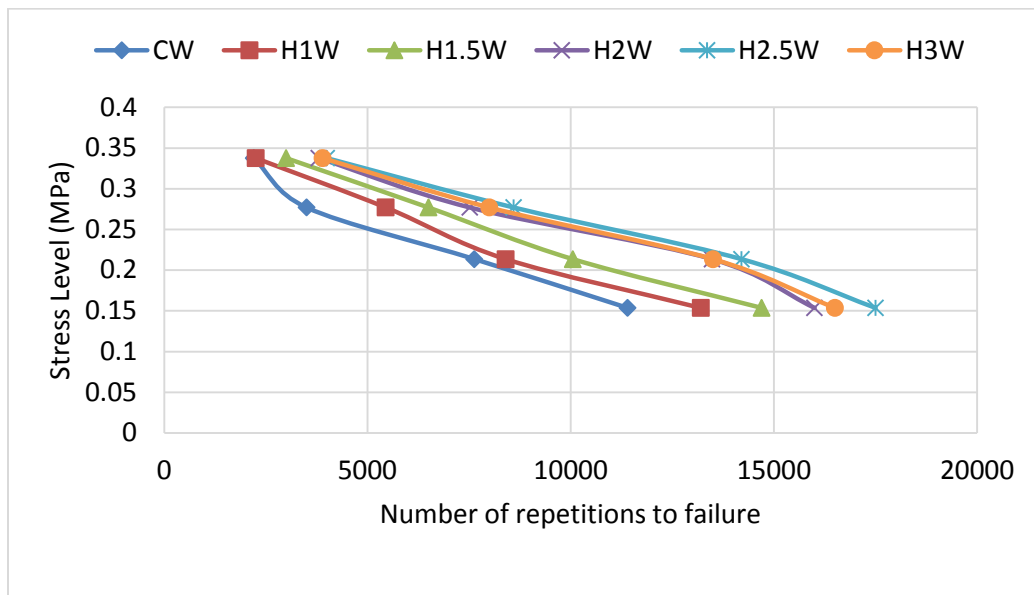


Figure (4-42) Applied stress versus fatigue cycles to failure of Wearing course mixture

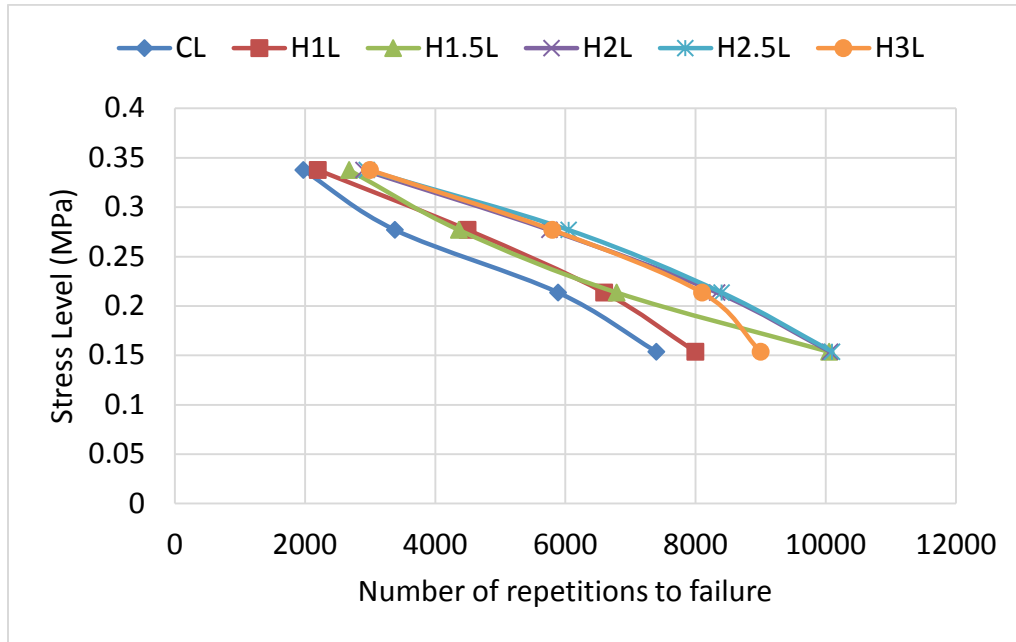


Figure (4-43) Applied stress versus fatigue cycles to failure of Leveling course mixture

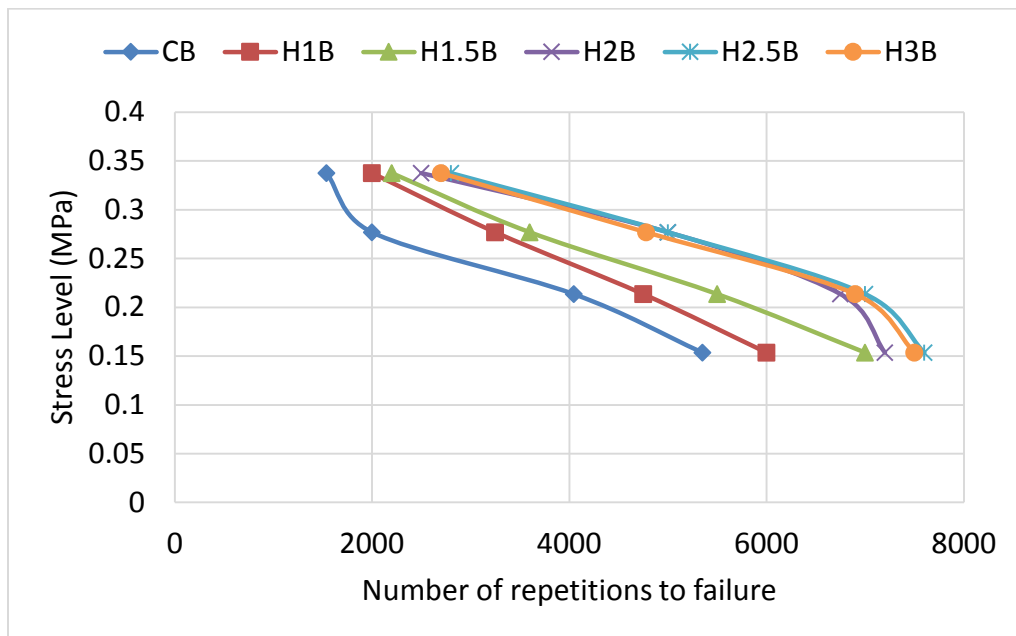


Figure (4-44) Applied stress versus fatigue cycles to failure of Base course mixture

4.5.4.4 Hydrated lime Influence on the Stress level and Initial Tensile Strain

Figures (4-45), (4-46) and (4-47) show the relation between the applied stress and the observed initial tensile strain of Wearing, Leveling and Base mixtures specimens respectively. For each mix, it can be seen that the increase in the stress level of fatigue stress-control test leads to rising in the tensile strain values. For all mixtures behaviour, it can be observed that there is a decrease in the value of strain as well as the trend of changing due to the addition of hydrated lime in which the mixtures performance enhanced by resisting the increasing applied repeated load.

The impact of hydrated lime led to decreasing in tensile strain and affected the relation curve between applied stresses and observed initial tensile strains. The slope of curves increased with each addition of hydrated lime until reaching a maximum slope at a per cent of 2.5 HL. For instance, in the Figure (4-61), the control mix (CW) got strains of 163E-6, 220.1E-6, 334.3E-6, and 440.3E-6 at level stresses of 0.15, 0.21, 0.277 and 0.337 MPa respectively. The strain reduced until the optimum performance is achieved at 2.5% of hydrated lime with a reduction per cent in strain by 11.11%, 31.7%, and 35.18% at the level stresses of 0.21, 0.277 and 0.337 MPa respectively, as compared to the control mix. Similarly, for the Leveling mix and as illustrated in Figure (4-46), the lower values of tensile strain is for the mix (H2.5L) starting with an increase in the strain by 20% and 3.5% at 0.15 and 0.21 MPa of applied stress respectively as compared to the control mix (CL). The saving in the strains that related to the rest of applied stresses started at 0.277 and 0.337 MPa with a reduction rate of 23.8% and 29.6% respectively. For the Base course mixes illustrated in Figure (4-47), it was found the optimum per cent of hydrated lime to enhance its ability to resist the applied stress is 2.5% as well. There was a gradual reduction in tensile strain through out increasing of hydrated lime in the mix causing an increase in the slope of the curves related applied stress and obtained tensile strain. The strain of the mix (H2.5B) initially increased at the level stresses of 0.15 MPa by 23.8% as compared to the control mixture, but at higher stress levels the tensile strain reduced by 10%, 31.8% and 32.6% at 0.21, 0.277 and 0.337 MPa respectively as compared to the control mix (CB).

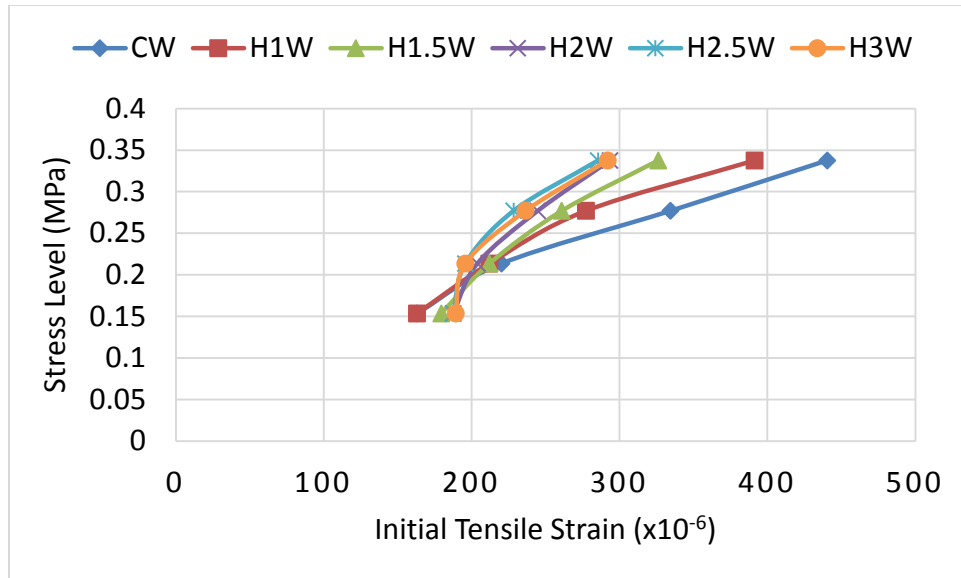


Figure (4-45) Applied stress versus Tensile Strain of Wearing course mixture

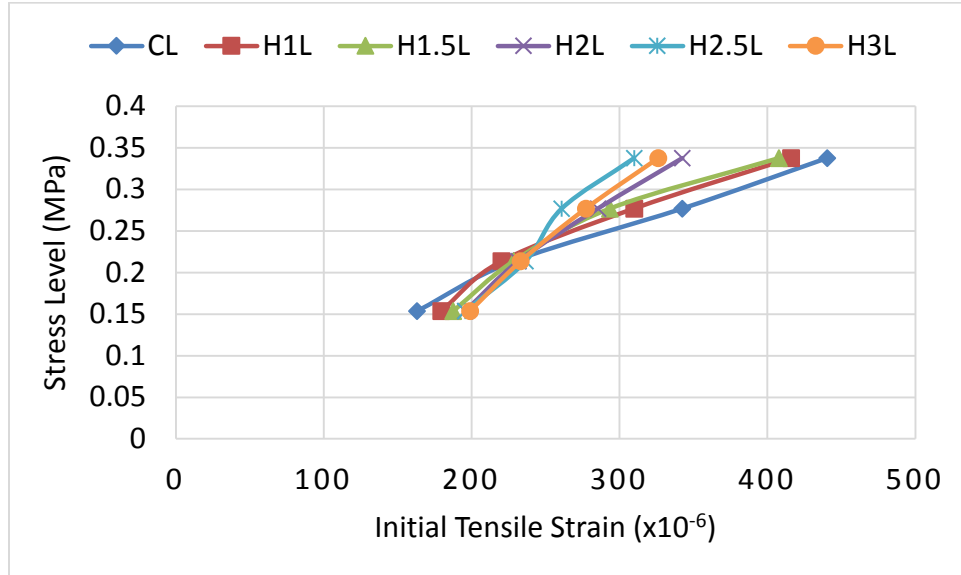


Figure (4-46) Applied stress versus Tensile Strain of Wearing course mixture

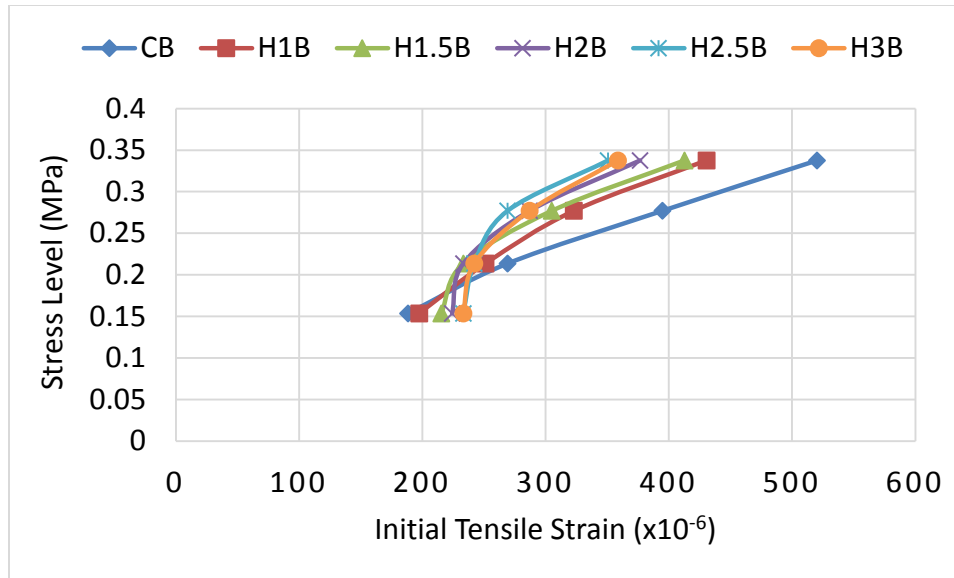


Figure (4-47) Applied stress versus Tensile Strain of Wearing course mixture

4.5.4.5 Hydrated lime Influence on the Average of Fatigue Life

Throughout the laboratory work adopted in this study to evaluate the influence of hydrated lime on asphalt concrete mixtures, it has been observed that the addition of hydrated lime leads to improving the ability of the mixtures to withstand distresses that could happen in pavement. One of these distresses that evaluated in this research is the fatigue cracking. Regarding the test loading and output, it is typically known that there is an inverse logarithmic relationship between the level of stress and the number of repetition to fracture. In other words, the higher the stress, the lower the number of repetition to fracture. The relation between the average value of the number of repetitions to failure and percent of hydrated lime addition is shown in Figure (4-48). The output of the Figure indicates that the mixture with hydrated lime gained better fatigue life than control mixture until reaching an optimum value of hydrated lime. Therefore, the contribution of hydrated lime into the asphalt mixes could be one of the solutions for fatigue damage resistance.

It can be seen that mixtures modified with hydrated lime are more resistant to fatigue cracking for all types of the studied pavement layers by increasing the number of repetition to failure. The hydrated lime addition increases the number of repetition to fracture up to 2.5 percent, and then starts to decrease as lime content increases and this trend is the same for all pavement layers mixtures. For wearing course mixture and at 2.5% of hydrated lime, the average number of load repetitions needed to fracture the specimen is 11075, which is greater than the load repetitions

of CW mix (6183) by about 79.12%. For the leveling course, repetitions of H2.5L mix (6876) are higher than CL mix (4663) by 47.45% and as compared to H2.5W, it is lower than it by about 37.9%. The average value of repetitions to failure for the Base mix increased significantly with increasing the addition percent of hydrated lime until reaching its optimum percentage at the mix H2.5B with 5600 repetitions. It has gained about 73.1% as compared to the average value of CB mix repetitions to fracture (3234), but it is smaller than H2.5L and H2.5W by 18.55% and 49.4% respectively. The variation in the enhancement of number of load repetitions to failure according to mixtures type could be as a result of increasing of coarseness of the mixtures and this happens by changing in the percent passing sieve No.4 (4.75 mm opening). The more coarseness means bigger aggregate particles size (lower surface area) which leads to lower interaction between particles within the mix structure, higher air void and lower percent of asphalt cement (thinner thickness of film coating aggregate particles surface) which act as a binder agent between the aggregate particles . For instance, the Wearing course mix with the lowest coarseness (as compared to the Leveling and Base course mixes) has the highest value of fatigue live cycles among them then the Leveling course and finally the Base mix with the lowest fatigue related number of load repetitions.

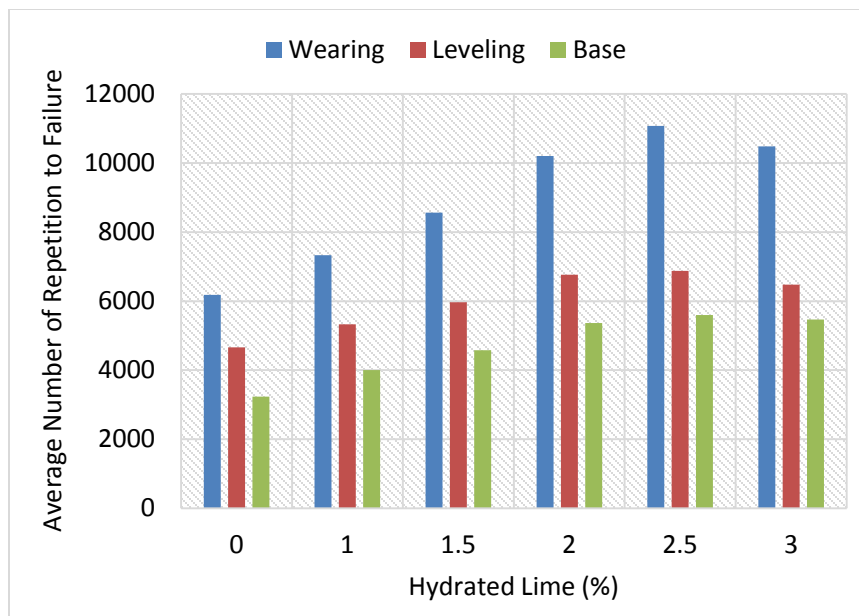


Figure (4-48) Hydrated lime Influence on the average fatigue life of asphalt mixtures

One mechanism that describes hydrated lime’s capability to enhance the fatigue life of asphalt pavements while at the same time strengthening them is named “crack pinning”. The crack pinning is the main mechanism by which the mineral filler particles increase the stiffness of materials. In 1970, Lange introduced the crack pinning theory after recording that for epoxy materials, the fracture energy could be significantly enhanced by the addition of rigid particulate filler. Later, Evans (1972) expanded the work that done by Lange by performing a comprehensive research concentrating on several various perspectives of the crack pinning mechanism. In agreement with the theory, the interactions between the crack front and the second phase dispersion induce the fracture energy of the brittle matrix to rise. While the crack front propagates through the multiphase material, the inclusions prevent or pin the crack front making it bow out in-between the obstructions (filler particles) and creating secondary semi-elliptical defects) until it fractures away from the pinning places. Figure (4-49) shows a schematic of crack pinning mechanism presented by Phillips and Harris (1977).

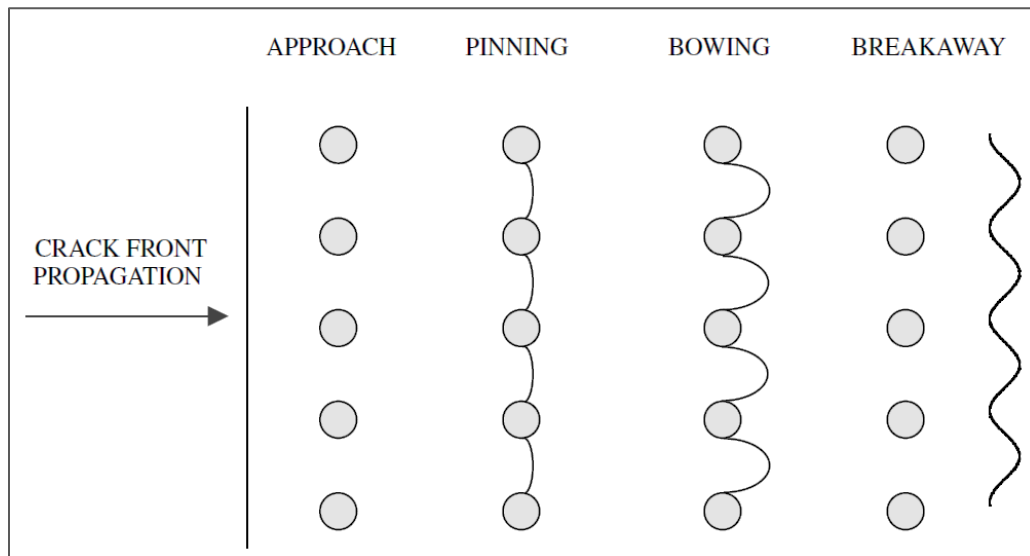


Fig (4-49) Schematic drawing of crack-pinning mechanism (Phillips and Harris, 1977)

The small hydrated lime particles intercept and divert micro cracks while they develop preventing them from combining into macro cracks that can reflect within the pavement course. In addition, as mentioned by (Lesueur and Little, 1999), as a result of the chemical activity of hydrated lime, it adsorbs acidic components from the asphalt cement to its particles' surface, boosting the active volume of the particles causing them more efficient than inert fillers at intercepting the micro cracks.

Based on this observation, it can be concluded that hydrated lime does not perform as an ordinary volume-filling agent only but acts chemically as an active material producing material-specific characteristics. The results from this study about the influence of adding hydrated lime in extending the fatigue life of asphalt concrete mixtures were shared by other researchers and showed similarity (Diab et al., 2013, Diab et.al 2012, Albayati 2012, Lee and Mun, 2012, Aragão et.al 2010, Sebaaly et al 2010, Sequeira 2009, Aragão et al., 2008, Lee 2007, Aragão 2007, Lu 2005, Mohammad et al., 2000, and Baig 1995).

4.5.4.6 Hydrated lime Influence on the average of Initial Tensile Strain

The average initial tensile strain of Wearing, Leveling and Base mixtures specimens as related to hydrated lime influence is illustrated in the Figure (4-50). The increase in the percentage of hydrated lime in each mix produces a gradual reduction in the initial tensile strain. The optimum percent of hydrated lime that gives the minimum average value of initial strain is 2.5% for all the mixtures but with a variable gain percentage among them, and after this hydrated lime percent, the average initial tensile strain increased. To review the influence of hydrated lime on the asphalt concrete mixtures, mixes with no hydrated lime (control) are compared with and the modified mixes at their optimum percent of hydrated lime. The comparison was between the types of asphalt pavement layers at their optimised mixes. For the Wearing layer mix, the average initial tensile strain of the control mix (CW) is 289.45×10^{-6} and decreased to 224.22×10^{-6} at 2.5% of hydrated lime (H2.5W) with a benefit of 22.5%. For the levelling layer mix, the average tensile strain of H2.5L mix is 254.8×10^{-6} , which is lower than CL mix strain (297.6×10^{-6}) by 14.38% and as compared to H2.5W, it is higher than wearing mix strain by about 13.6%. The average value of initial tensile strain for the Base layer mix decreased considerably with the increase in the percentage of hydrated lime until reaching its optimum percentage at the

mix H2.5B with 266.82×10^{-6} . It has gained a reduction of about 22.22% as compared to the average value of CB mix tensile strain (343.06×10^{-6}), but it is higher than H2.5W and H2.5L mixtures by 19% and about 4.71% respectively.

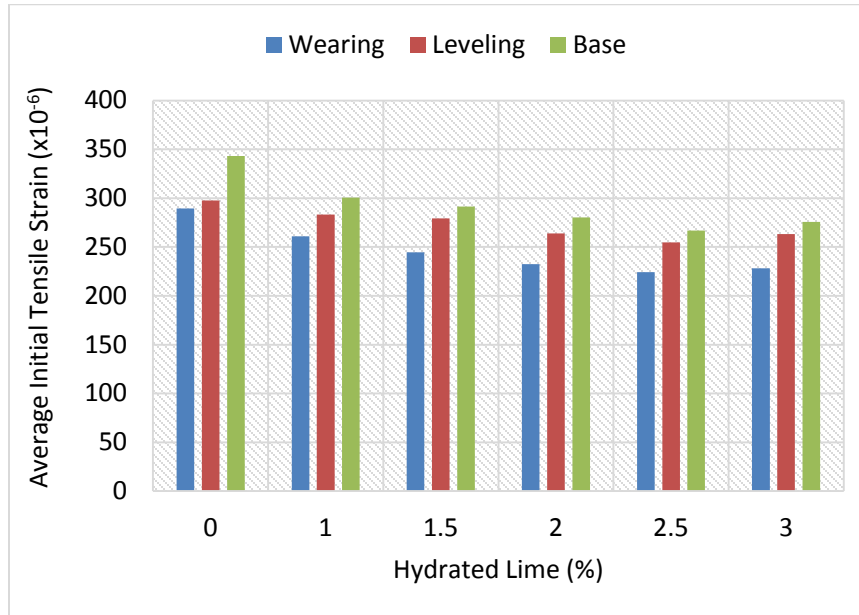


Figure (4-50) Hydrated lime Influence on the average Initial Tensile Strain of asphalt mixtures

4.5.4.7 Hydrated lime Influence on the average of Initial Flexural Stiffness

In the process of flexural fatigue test implemented in this study, the initial flexural stiffness is calculated at the initial stage of loading. Figure (4-51) presents the effect of hydrated lime addition on the initial flexural stiffness of Wearing, Leveling and Base mixtures specimens. For each mix, it can be found that the stiffness increased gradually with the increase in the percentage of hydrated lime in the mix. The optimum percent of hydrated lime that gives the maximum value of initial stiffness is 2.5% for all the mixtures but with a relative differences between them, and after this amount of average initial stiffness reduced. To investigate the effect of changing in hydrated lime percent on mixes, a comparison between control mixes and the mixes with the optimum percent of hydrated lime as well as between the type of asphalt pavement layers has been done and as illustrated in Figure (4-51). In the Wearing layer mix, the average flexural stiffness of the control mix (CW) is 876.8 MPa and became 1076.6 MPa at 2.5% of hydrated lime

(H2.5W) with a benefit of 22.78%. For the leveling layer mix, average flexural stiffness of H2.5L mix is 959.78 MPa, which is higher than CL mix one (863.2 MPa) by 11.18% and as compared to H2.5W, it is lower than wearing mix by about 10.85%. The average value of flexural stiffness for the Base layer mix increased significantly with the increase in the percentage of hydrated lime until reaching its optimum percentage at the mix H2.5B with 883.18 MPa. It has gained about 19.34% as compared to the average value of CB mix initial flexural stiffness (740), but it is smaller than H2.5W and H2.5L by 18% and about 8% respectively.

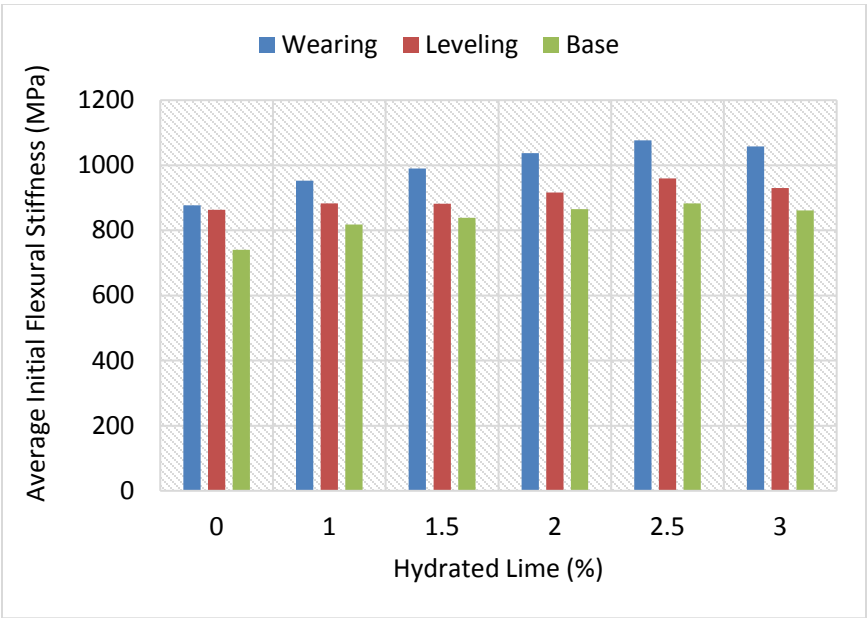


Figure (4-51) Hydrated lime Influence on the average Initial Flexural Stiffness of asphalt mixtures

4.5.5 Hydrated Lime Influence on Moisture Susceptibility

The Average tensile strength ratios (TSR) test result which represent the ratio of tensile strength of the saturated (conditioned) subsets to the dry (unconditioned) subsets of each mixture, are plotted in Figures (4-52), (4-53) and (4-54). These Figures clearly demonstrate that hydrated lime contributed to an increase in TSR when the mixes were subjected to one cycle of freezing and thawing and indicate that mitigation of moisture damage was due to hydrated lime inclusion,

while the mixture with no hydrated lime content experienced lower TSR with same conditioning. Hence, increasing the stiffness due to the addition of hydrated lime typically makes HMA mixtures more resistant to the damage happens due to the presence of moisture. The test results are here listed in Tables (4-11), (4-12) and (4-13), which clearly show the contribution of hydrated lime addition in increasing the TSR for the all asphalt concrete mixtures.

Table (4-11) Influence of hydrated lime addition on TSR of Wearing mixture

Mixture	Tensile Strength, kPa		TSR, %	Gain in TSR, %
	Unconditioned	Conditioned		
CW	980	750	76.53	0
H1W	1050	830	79.04	3.29
H1.5W	1130	945	83.62	9.27
H2W	1150	1000	86.95	13.62
H2.5W	1165	1050	90.12	17.76
H3W	1167	1048	89.80	17.34

Table (4-12) Influence of hydrated lime addition on TSR of Leveling mixture

Mixture	Tensile Strength, kPa		TSR, %	Gain in TSR, %
	Unconditioned	Conditioned		
CL	700	515	73.57	0
H1L	750	560	74.67	1.49
H1.5L	840	680	80.95	10.03
H2L	950	788	84.65	15.06
H2.5L	1000	850	83.90	14.04
H3L	1100	937	80.80	9.83

Table (4-13) Influence of hydrated lime addition on TSR of Base mixture

Mixture	Tensile Strength, kPa		TSR, %	Gain in TSR, %
	Unconditioned	Conditioned		
CB	680	485	71.32	0
H1B	730	540	73.97	3.71
H1.5B	800	600	75	5.15
H2B	920	710	79.89	12.01
H2.5B	990	800	78.065	9.45
H3B	1000	809	77.78	9.049

4.5.5.1 Conditioned and Unconditioned Tensile Strength of mixtures

For the wearing course mix, according to the data shown in the Table (4-11) and Figure (4-52), it can be seen that the addition of hydrated lime has an impact on the moisture damage resistance of the mix. For both dry and conditioned specimens, it is found that the indirect tensile strength approximately in a linear relationship with the hydrated lime percent. As compared to the control mix, CW, the increase in the indirect tensile strength of dry mixes is 70 kPa for H1W and more than two-fold (150 kPa) for H1.5W. The maximum indirect tensile strength has been found in H3W with a gain of 187 kPa as compared to the control mix with just a difference of 2 kPa more than the indirect tensile strength of H2.5W mix. It has been seen that the enhancement rate in the indirect tensile strength for the modified mixtures of the conditioned specimens is higher than that of dry (unconditioned) specimens. For instance, the maximum indirect tensile strength was at 2.5 percent of hydrated lime (H2.5W mix) with an increase of 300 kPa as compared to the control mix, CW. Similarly, there is an increase in the indirect tensile strength of the hydrated lime modified Leveling and Base course mixes. As shown in Figures (4-53) and (4-54) and for the unconditioned set of specimens, H1L and H1B mixes had 750 and 730 kPa respectively with an increase of 50 kPa for each as compared to their control mixes. The increment rate continues until the mixes of 3 percent of hydrated lime, H3L and H3B, maintaining 1100 and 1000 kPa respectively with an improvement in the indirect tensile strength of 400 and 320 kPa as compared to their control mixes. For the conditioned specimens of Leveling and Base mixes and as compared to the control mixes, CL and CB, the maximum values of indirect tensile strength were recorded

at 3% of hydrated lime addition with a gain of 422 kPa and 324 kPa for H3L and H3B respectively. Although, the maximum tensile strength ratio for each of levelling and base course mixes were at 2% of hydrated lime content due to relative ratio differences between conditioned and unconditioned specimens results in each mix as compared to the others. These outcomes prove the influence of hydrated lime as an excellent anti-stripping material.

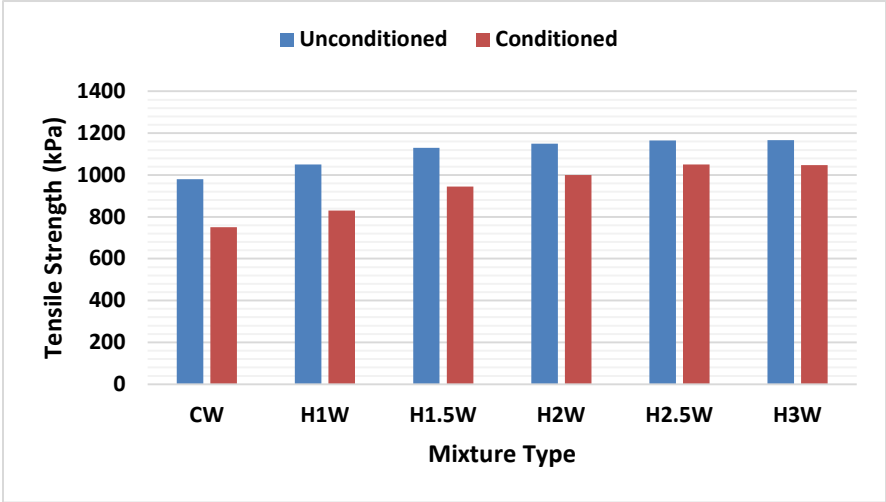


Figure (4-52) Effect of hydrated lime on Controlled and after Freeze-Thaw cycle Tensile Strength of Wearing mixture

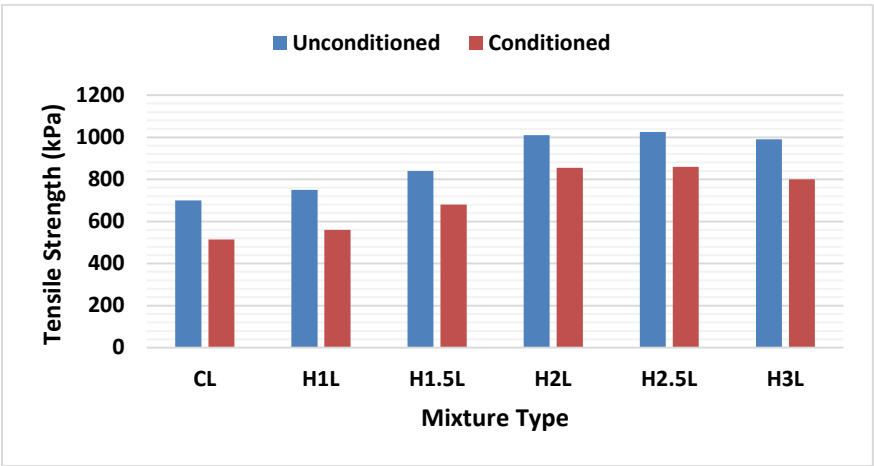


Figure (4-53) Effect of hydrated lime on Controlled and after Freeze-Thaw cycle Tensile Strength of Leveling mixture

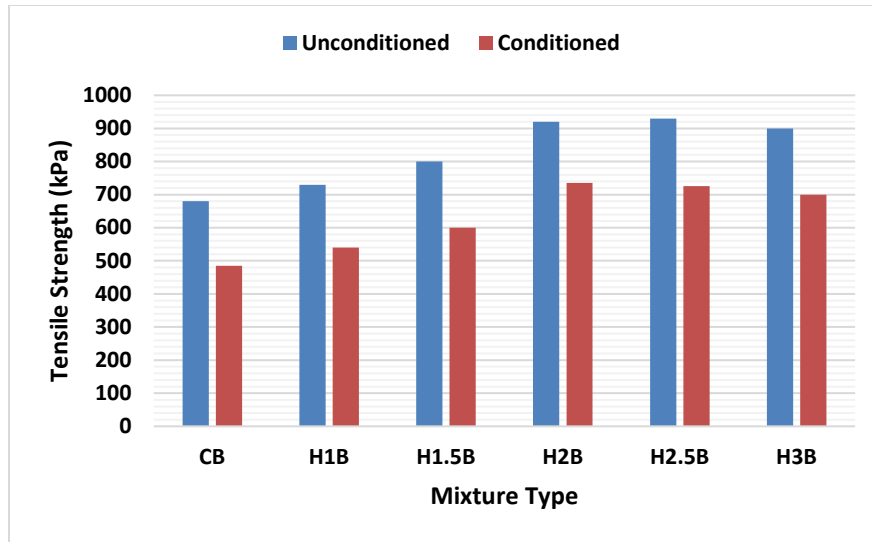


Figure (4-54) Effect of hydrated lime on Controlled and after Freeze-Thaw cycle Tensile Strength of Base mixture

4.5.5.2 Effect of Hydrated Lime Addition on Tensile Strength Ratio (TSR)

Based on the data examined in Figures (4-55) and (4-56), it is clear that hydrated lime contents have an influence on the moisture susceptibility of the asphalt concrete mixes. The indirect tensile strength result for both control and modified mixes approximately have a linear proportional to the increase in hydrated lime content.

For the Wearing course mixture and regarding the introduction of hydrated lime into the mixes, the H2.5W mix shows the highest tensile strength ratio (TSR) value among others. There was a significant improvement in the tensile strength of the mixes with about 3% to 4% rise per each added percentage of hydrated lime to the mix. The optimum percent was 2.5% with a gain of 17.78% in tensile strength ratio as compared to the control mix (CW). Increasing the amount of hydrated lime beyond threshold value of 2.5 percent of 0.5 percent did not appear to enhance the moisture damage resistance any further and exhibited a trend of slight decrease in tensile strength with an increase in the added percentage of hydrated lime. Meanwhile, regarding the Leveling (binder) and Base course mixes, H2L and H2B have the highest tensile strength ratio (TSR) values as compared to all other mixtures by increasing the TSR to 84.65% and 79.89% respectively with tensile strength ratio profit of about 15% for the leveling mix and 12% for the base mix with respect to the control mix. The improvement in TSR can be attributed to an improvement in the adhesion between aggregate and asphalt due to the presence of hydrated lime by interacting with

carboxylic acids in the asphalt and forming insoluble salts that are readily adsorbed at the aggregate surface as stated by (Plancher et al. 1977, Peterson 1987 and Hicks 1991). Such bonding developed between asphalt binder and aggregate leads to mitigate moisture susceptibility in the asphalt mixtures. The result for replacing hydrated lime has a good agreement with similar findings of other researchers (Button et al., 1983, Baig 1995, Atud et al., 2007, Hossain and Ullah 2011, Sengul et al., 2011, Albayati 2012, AlBaiti 2012).

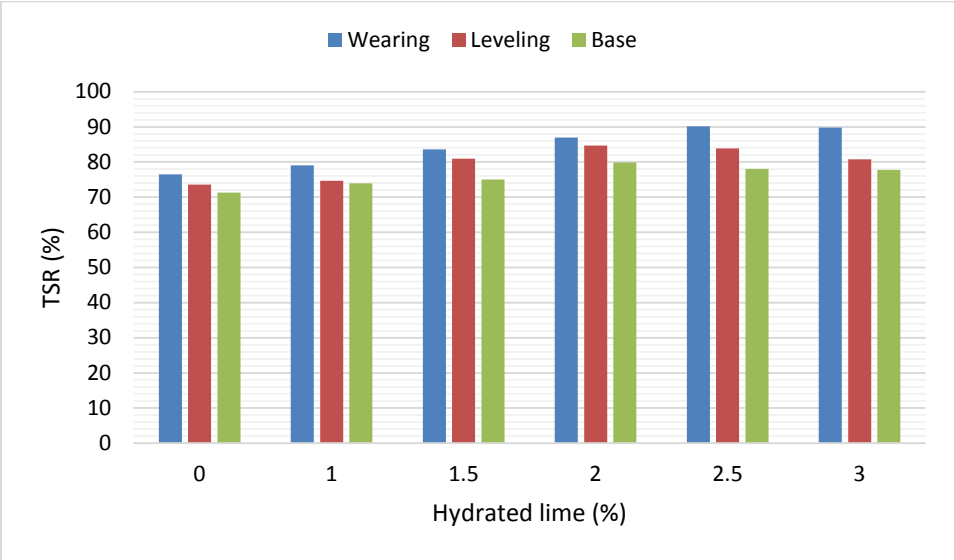


Figure (4-55) Hydrated lime Influence on Tensile Strength Ratio of Asphalt Concrete Mixes

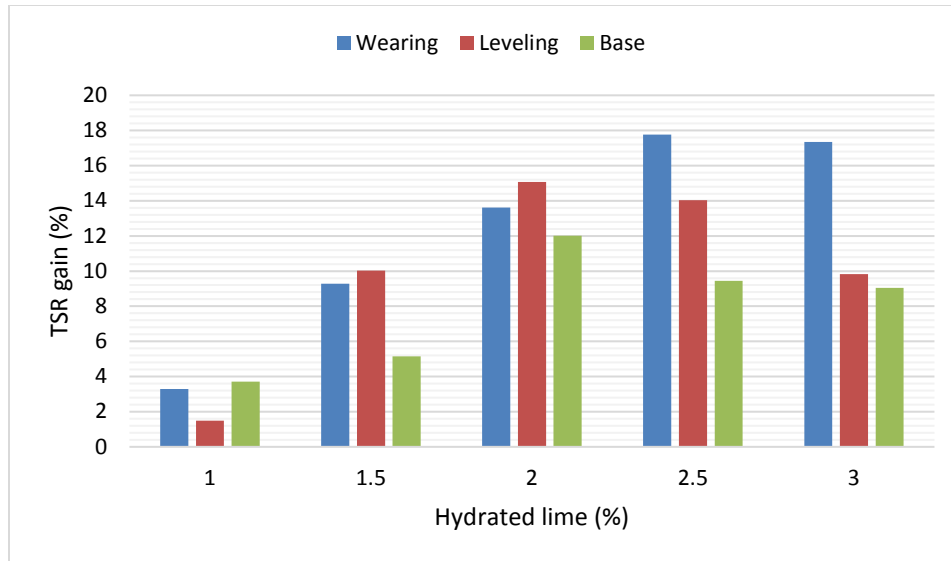


Figure (4-56) TSR Gain of Asphalt Concrete Mixes Due to Hydrated Lime Addition

In the light of the findings from the data presented above, it can be observed that the addition of hydrated lime to the mixtures generally demonstrated positive effects with regard to moisture-damage resistance. Mixtures modified with hydrated lime perform better than control mixtures due to the combined effects of hydrated lime in increasing the stiffness, strength and toughness of mastic that induces better resistance of mastic against changes in internal structure in the presence of moisture. In other words, the addition of hydrated lime benefitted both the condition and uncontended mixtures. The outcomes have a good agreement with similar results of other researchers (Esarwi et al., 2008, Gorkem and Sengoz, 2009, Haung et al., 2010, McCann and Sebaaly, 2003, Hossain and Ullah, 2011, Boyes, 2011, Pinto et al., 2009).

4.6 Summary and Further Discussion

The use of additives is one of the effective techniques adopted to improve pavement mechanical properties. Recently, hydrated lime has been categorized as a major additive in asphalt pavement due to its wide availability and relatively cheap cost. The aim of this chapter is to measure and evaluate the influence of hydrated lime on asphalt mixture performance under varied temperatures of weather and in the application of different pavement courses, i.e. Wearing (or Surface), Leveling (or Binder) and Base. Five different percentages of the hydrated lime additive, namely 1.0, 1.5, 2.0, 2.5 and 3.0%, that applied as partial replacement of the conventional

limestone filler, were investigated. Tests were conducted to evaluate the Marshall and volumetric properties, the resilient modulus, and permanent deformation at three different temperatures, investigate the influence of moisture on the paving mixtures as related to partial replacement of mineral filler with hydrated lime and fatigue characteristics. The experimental results have showed an expected improvement in the mechanical properties of all the designed asphalt concrete mixtures when using the hydrated lime additive. The study revealed that optimum hydrated lime contents for different course applications have been suggested. In details, the use of hydrated lime with a percent of 2 for wearing course and 2.5 percent for leveling and base courses can display the most efficient improvement in the Marshall and volumetric properties. Moreover, 2.5% of hydrated lime enhances resilient modulus and improve the resistance to permanent deformation in the moderate and high temperatures as well as resistance to fatigue cracking and the moisture effect on pavement mixtures.

In general and for the all tests conducted in this study, the results indicated that certain percentage of hydrated lime was effective in improving the Marshall designed properties, increasing the Tensile Strength Ratio (TSR) regarding moisture damage. The hydrated lime also exhibited a significant result concerning enhancement in the ability of mixtures to resist permanent deformation at varying temperatures for Wearing, Leveling (Binder) and Base layers as well as the number of repetitions to failure was increased by replacing 2.5% of ordinary lime content with the hydrated lime.

Hydrated lime improved the properties and performance of the mixtures by stiffening the mix, distributing of small hydrated lime particles in the asphalt helps to strengthen the mix, increasing its resistance to the mechanical failures such as rutting and fatigue cracking. The contributions are synergistic, as is appropriate in a complex system such as asphalt cement, providing interactively to the reduction of moisture sensitivity in the mixtures. Furthermore, based on the National Lime Association (NLA, 2003), it can be noted that mixing hydrated lime with the neat asphalt is not considered to be an acceptable method since the asphalt will coat the hydrated lime particles and isolate them from the aggregate. This behaviour will prevent any chemical interaction between the aggregate and the hydrated lime, such as exchanging of ions with the aggregate surface, agglomeration and flocculation of clay particles, and pozzolanic reactions (NLA, 2006).

The influence of hydrated lime as a filler and its proven capability to withstand damage is due to a complex interaction of influences correlated to the physical/chemical filler effect and the form in which the hydrated lime affects the microstructural characteristics of the asphalt cement beside that it strengthens the asphalt mixtures (Kim et al., 2003 and Little and Petersen, 2005).

The hydrated lime, unlike conventional mineral fillers, chemically reacts with the carboxylic acids and 2-quinolone types that are concentrated in the highly associated, viscosity building components of asphalt, thus efficiently removing them, together with their associated molecular agglomerates, from the asphalt portion of the hydrated lime-asphalt mixture. This result in an improved capability of the asphalt to dissipate stress development in the asphalt, which should enhance the fatigue damage resistance of asphalt concrete mixtures (Little and Petersen, 2005). Based on the outcomes of this chapter, Figure (4-57) summarizes the optimum estimated proportion of hydrated lime addition that could provide the best performance of HMA based on fundamental engineering characteristics of mixtures.

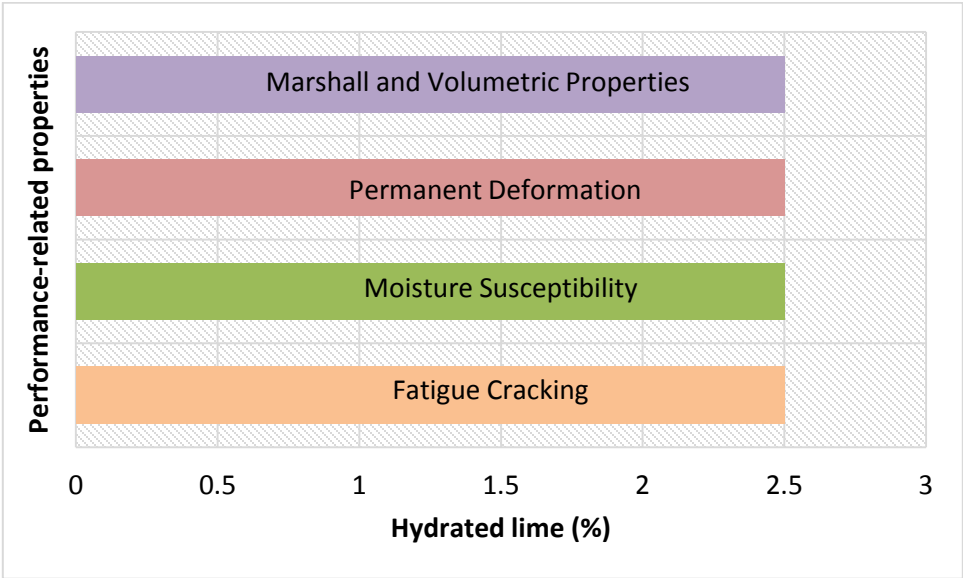


Figure (4-57) Optimum Hydrated Lime Percentage Regarding Pavement Performance as a Replacement of Mineral Filler

Chapter Five

Statistical Modelling of Fatigue Life and Permanent Deformation

5.1 Introduction

The aim of this chapter is to present the specific analysis procedures required to build statistical models that represent two main distresses happen in the asphalt concrete pavement; fatigue cracking and permanent deformation. The models based on the Marshall and volumetric properties as well as performance-related characteristics, regarding fatigue cracking and permanent deformation, as variables observed from the laboratory work with consideration of the hydrated lime effect on asphalt mixtures.

Regression analysis is a statistical methodology that employs the relationship between two or more quantitative variables to predict a response variable behaviour depending on the other variable(s). This method is broadly utilised in business, the social and behavioural sciences, the biological sciences, and many other disciplines (Kutner et al., 2005).

Kutner et al. (2005) stated that regression analysis was firstly found by Sir Francis Galton in the recent part of the nineteenth century. He had investigated the heights of parents and children and remarked that the heights of children of tall and short parents seemed to "revert" or "regress" to the mean value of the group. He counted this behaviour as a regression to "mediocrity." Sir Galton revealed a mathematical description of this form of statistical modelling and considered as a start of regression modelling. The word "regression" still to be used to this day to explain the statistical relationships between variables. The relationship between two variables could take two forms; a functional or a statistical equation. The functional relationship is denoted by a mathematical formula that gives a specific value of the dependent (Y) based on the independent variable (X). Unlike the functional relation, the statistical relationship is not an exact one, and there is a possible error in calculating the output variable. In statistical models, The observed and estimated variables values do not fit exactly on the curve of the developed equation.

There are three major steps required to generate the statistical model: the response variables, mathematical equation, and random errors. The benefits of the mathematical equation

to describe the variables related to pavement structure regarding the influence of hydrated lime on the pavement properties and the type of asphalt concrete layer. The form of the mathematical equation is a multilinear regression equation. Particular linear type of regression equation form used to generate models of fatigue and permanent deformation based on the data collected from experimental tests to represent the best fit of for permanent deformation and fatigue life.

As shown in chapter two, several models have been developed to describe the asphalt concrete performance regarding many variables to predict the fatigue cracking and rutting characteristics. The majority of these models based on laboratory work, properties of paving materials, and other variables, and also used the statistical modelling to reach the final form of models. In this study, the employment of the hydrated lime effect has been assessed to be as an independent variable, inside the model equation, that could be one of the effective factors that are influencing the value of the model's outcome. Two models have been developed; one of them is to predict the number of repetition to fatigue cracking, and the other model is about permanent deformation (rutting) by prediction of the permanent strain in the asphaltic pavement layers. In the permanent strain model, permanent deflection in the pavement can be calculated by multiplying the permanent strain by the asphalt concrete layer depth. The models could be used as failure criteria and to give an impression of the future behaviour of asphalt concrete mixtures.

The basic steps in the process of building a model are the selection of model variables, fitting of model data by a mathematical (regression) equation and validation of the model. These steps were updated throughout the models building process until an appropriate model would have been developed for the dataset. The following procedure has been used in the process of developing models.

In order to perform analysis of data and regression modelling, Statistical Package for the Social Sciences (SPSS) is adopted in this study. SPSS is a Windows-based software that can be employed to achieve insertion and analysis of data and to produce the output as tables and graphs with necessary details. SPSS is capable of management and documentation of huge amounts of data and can perform all of the analyses using many features included in this package. SPSS is widely used in the Social Sciences and the business world (Levesque, 2007).

5.2 Models Development Process

The following steps recommended by many statisticians and researchers (Keller and Warrack, 2000) are considered in this study;

5.2.1 Identifying the Dependent Variables

The analysis or predict variable should be clearly defined.

5.2.2 Listing Potential Predictors

By using the knowledge of the dependent variable, a list of predictors that may be related to the dependent variable should be produced. Although a causal relationship cannot be established, an attempt should be given to including predictor variables that cause changes in the dependent variable, bearing in mind the problems caused by multicollinearity and the cost of gathering, storing, and processing data. It is best to use fewest independent variables that produce a satisfactory model.

5.2.3 Gathering the Required Observations for the Potential Models

A general rule is that there should be at least six observations for each independent variable used in the equation.

5.2.4 Identifying Several Possible Models

The knowledge of the dependent variable and predictor variables should be used to formulate a model. If it is believed that the predictor variable affects the dependent variable, but the form of the relationship is uncertain, it may be helpful to draw a scatter diagram of the dependent variable and each predictor variable to investigate the nature of the relationship.

5.2.5 Using Statistical Software to Estimate the Models

Use ordinary or stepwise regression to determine which variables to be included in the model. If the objective is to determine which variables affect the dependent variable, the multicollinearity should be checked to ensure it is not a problem. If it is, attempt to reduce the number of independent variables.

5.2.6 Determining whether the Required Conditions are satisfied

If the required conditions are not satisfied, attempt to correct the problem. At this point, several “equal” models to choose from may be available.

5.2.7 Using the Engineering Judgment and the Statistical Output to Select the Best Model

This may be the most difficult part of the process. There may be a model that fits well, but another one may be a good predictor, and yet another may feature fewer variables and, thus all above mentioned should be considered to select the best model. Kutner et al. (2005) gave a general strategy for regression modelling which can be useful as modelling process. Figure (5-1) presents the typical steps for modelling suggested by them.

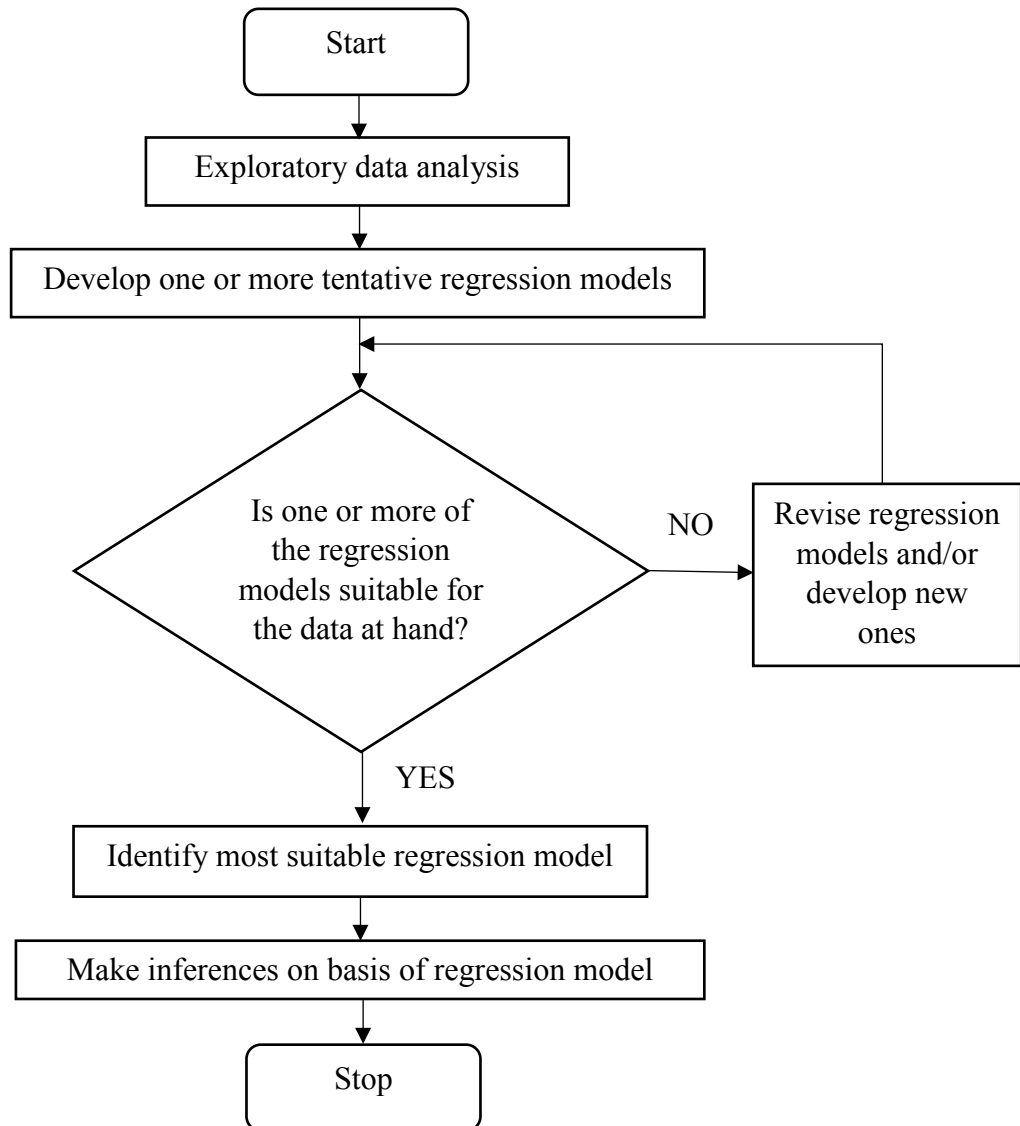


Figure (5-1) Typical Strategy for Regression Analysis (Kutner et al., 2005)

5.3 Predictor and Dependent Variables Identification

The variables used to generate the models in this chapter are the output of the laboratory work adopted in this research regarding the effect of adding hydrated lime as partial replacement of the ordinary lime (limestone). The variables represent the performance-related properties of controlled and modified asphalt concrete layers in the flexible pavement. Affected by environmental and traffic loading conditions adopted in the laboratory to evaluate failure criteria (fatigue cracking and permanent deformation) in pavement, the variables can be defined as:

- HL = Hydrated lime addition percentage as a mineral filler replaced with limestone (%),
- T = Temperature adopted in the laboratory tests (°C),
- D = Density of asphalt concrete mixture (g/cm³),
- AV = Air voids in the mixture (%),
- VMA = Voids in Mineral Aggregate (%),
- VFA = Voids Filled with Asphalt (%),
- OAC = Optimum asphalt content (%),
- N = Number of repetition to failure in permanent deformation,
- ϵ_p = Permanent micro strain at load repetition (N),
- M_r = Resilient Modulus (MPa)
- N_f = Fatigue life at failure repetition (cycle),
- ϵ_t = Initial tensile micro strain,
- MS = Marshall Stability (kN),
- MF = Marshall Flow (mm),
- P4 = Percent passing sieve number 4 of size equal to 4.75 mm (%),
- P200 = Percent passing sieve number 200 of size equal 0.075 μ m (%),

The above variables are initial inputs of the proposed models. Due to the influence of these variables on the models regarding their correlation between each of them and the dependent and among themselves as well, some of them will be eliminated and not appear in the final models.

5.4 Selecting Sample Size

In statistical consulting, the first question frequently asked is "how large should the sample size be?"(Hogg and Tanis, 1988). Kennedy and Neville (1986) stated that there is no direct answer to this question. They mentioned that the large the samples size the greater the cost of testing, but on the other hand the greater the amount of information derived. In other words, there is an apparent influence of the selection of sample size on the accuracy of the model and the random errors ranges resulting from the modelling process. The increment in the size of the sample of the observed data will lead to a reduction in the random errors caused during the model building, and this gives the generated model more reliability.

The following criteria were considered when choosing the size of the sample to generate the model;

- Population parameters required to be assessed,
- The extent of familiarity,
- Diversity of the community,
- The practical application: The difficulty of data collection, and
- The accuracy of final estimates.

To determine the required sample size, (Kennedy and Neville, 1986) presented the following equation to calculate the percent of error according to sample size:

$$E = \frac{CV.t}{n^{0.5}} \quad (5.1)$$

Where:

E= Error of mean,

CV= Coefficient of variation, the ratio between standard deviation (σ) to the mean (μ).

t =T-statistics, which depends on the degree of freedom, which is the number of variables in a study that free to vary (Devore, 2011), and level of significance and,
n = Sample size.

The standard deviation σ is a relation used to measure the amount of variation in a dataset of values (x_1, x_2, \dots, x_N) :

$$\sigma = \sqrt{\frac{1}{N} \sum_{i=1}^N (x_i - \mu)^2} \quad (5.2)$$

The mean value can be calculated as follows:

$$\mu = \frac{1}{N} \sum_{i=1}^N x_i \quad (5.3)$$

There is an obvious effect of the selection of sample size on the accuracy of the model and ranges of random errors resulting from the inaccuracy of the size of the data collected from the laboratory. Thus, affects the ability of the model to work in the required different circumstances. Therefore, when the size of the sample group of practice increases, the random errors formed during the modelling reduces and this gives the generated model more reliability. Based on above, by using the SPSS software, the data collected was separated into two parts by approximately 50 percent to generate the model and 50 percent for the validation process of the model. Table (5-1) shows the percentage of errors for the proposed models as a result of choosing the size of the selected sample to be used in models development process after splitting approximately 50 percent of the data. The error value can be accepted if equal or less than 0.05 achieved (Kennedy and Neville, 1986). It can be seen that the sample sizes are accepted with the presented percent of errors.

Table (5-1) Error of proposed models according to sample size

Model	Sample Size (n)	Coefficient of Variance (CV)	T-statistic value (t)	Degree of Freedom (df)	Error (E)
ln(Nf)	42	0.0664	2.02	41	0.0207
log(εp)	390	0.251	1.96	389	0.0249

5.5 Regression Modelling

The regression modelling is the statistical process used to determine a relation between two variables or more to produce a model. The data set have to be presented well in a model, which should predict the desired variable depending on the other(s) (Montgomery and Peck, 1992). The multiple linear regression is used in the modelling of variables of more than one independent to produce a dependent. The aim of multiple linear regression is to achieve the best model for a selected level of confidence and satisfying the regression modelling assumptions;

- There is no high intercorrelation among predictor variables,
- There is no effective observation or outlier in the data set,
- The error distribution is normal,
- The error distribution mean is zero.

The objective is achieved by selecting a model with the highest adjusted coefficient of determination (R^2) and the lowest mean square error (MSE), of the data (Montgomery and Peck, 1992, Keller and Warrack, 2000). A scatter-plot can show clearly the presence of a relationship between variables, and when the behaviour of this relationship is relatively linear or other forms. Based on the log-log linear relationships of permanent deformation (ϵ_p) and the number of repetitions to failure (N) as well as the number of fatigue repetitions to failure (N_f) and initial tensile strain (ϵ_t), these variables were logarithmically transformed to be entered in multiple linear regression models. Devore (2011) defined the multiple regression model, and the general form of this model is as follows:

$$Y = \beta_0 + \beta_1 x_1 + \beta_2 x_2 + \dots + \beta_k x_k + \epsilon \quad (5.4)$$

Where: Y is the dependent variable, β_0 is constant, β_1 to β_k are the regression coefficients of the independent variables, and the variable ϵ is referred to the random error term in the models represented by the residuals.

In many cases, the correlation matrix will not be able to identify whether multicollinearity is a serious problem because there are many ways for variables to be related (Keller and Warrack, 2000). For example, one variable may be a function of several other variables. Consequently, the

correlation matrix may not reveal the problem thus the stepwise regression may be recognised as a procedure that eliminates correlated independent variables.

The best and communally method usually adopted to find a parameter in the model prediction is the stepwise procedure. The procedure begins by entering a variable that has the smallest significant value; largest F-value SPSS software used $F=3.8$ at significant level 5%, then the software will examine if the variable verifies the condition of remaining in the model or not, after the selection of all variables. To improve the model, the second variable (which have F-statistic greater than F to enter) will examine by comparing with first model (which have the first variable), if it exceeds the standard value the procedure repeated to the end.

In a case of high correlation between two independent variables, one of them have to be cancelled and the other entered into the model equation. When the first variable appears in the model function, the descriptive strength of the second one will be lower, and the F-statistic value will not be sufficiently high to be in the function. In this way, the multicollinearity is minimised, and the process goes on by introducing a predictor variable at the next step. The significant value is calculated for each variable for each step, and a comparison is made with the F value, and in the case of F-statistics of the variable is below this standard, it should be removed from the model. Repetition is possible of the above steps until reaching an equation with no more adding or eliminating variables.

5.6 Checking for Outliers

The data observation values that considerably different from the rest of the observed values are named “outliers”. The data observations that much higher or lower as compared to the vast majority of the data values are considered as outliers as a result of an error or a mistake in the observation process.

The identification of possible outliers can be made by the process of computing the Inter Quartile Range (IQR). In the calculation of Inter Quartile Range, data was sorted from low to high, the third quartile (Q3), which is the value that 75% of observed data values are less than, and the first quartile (Q1), in which 25% of observed data values are lower than, are needed. IQR is the amount of observed data located between Q1 and Q3. In other words, it is the subtraction of Q1 value from Q3 value; i.e. $IQR = Q3 - Q1$. Tukey (1977) found that a data value that lower than the

first quartile minus 1.5 times the interquartile range is a possible outlier. Similarly, the data value that greater than the third quartile plus 1.5 of the interquartile range is also an outlier. Tables (5-2) and (5-3) illustrate the outlier evaluation process for the proposed models and results show that there are no outliers in the input parameters of fatigue and permanent deformation models.

Table (5-2) Explanation of Outlier Evaluation Method for Fatigue Live Model

Variables	Mean	Std. Deviation	Minimum	Maximum	Percentiles			IQR (Q3-Q1)	Upper Threshold (Q3+1.5*IQR)	Lower Threshold (Q1-1.5*IQR)
					Q1 (25 th)	Q2 (50 th)	Q3 (75 th)			
lnNf	8.78	0.607	7.34	9.76	8.1215	8.6206	8.9994	0.8779	10.31625	6.80465
HL	1.6785	0.974	0	3	1	1.5	2.5	1.5	4.75	-1.25
D	2.3154	0.0148	2.29	2.34	2.305	2.316	2.33	0.025	2.3675	2.2675
AV	4.2486	0.196	4	4.6	4.08	4.285	4.39	0.31	4.855	3.615
VMA	14.250	0.6412	13.14	15.4	13.7	14.26	14.67	0.97	16.125	12.245
VFA	69.795	2.0165	66	72.74	69	70.06	71.7	2.7	75.75	64.95
P45	51.428	6.466	44	59	44	50	59	15	81.5	21.5
P200	6.0476	0.854	5	7	5	6	7	2	10	2
MS	10.305	0.8321	8.77	11.5	10.25	10.31	11	0.75	12.125	9.125
MF	2.7992	0.3082	2.3	3.25	2.5	2.8	3.1	0.6	4	1.6
lnEt	5.9596	0.274	5.189	6.429	5.802	6.0003	6.1589	0.3567	6.693898	5.2672
OAC	4.8071	0.2874	4.3	5.3	4.6	4.85	5	0.4	5.6	4

Table (5-3) Explanation of Outlier Evaluation Method for Permanent Deformation Model

Variables	Mean	Std. Deviation	Minimum	Maximum	Percentiles			IQR (Q3-Q1)	Upper Threshold (Q3+1.5*IQR)	Lower Threshold (Q1-1.5*IQR)
					Q1 (25 th)	Q2 (50 th)	Q3 (75 th)			
logN	2.5645	1.30512	0	4	1.699	3	3.6128	1.9138	6.4835	-1.1717
logEp	2.9277	0.7523	1.15	4.62	2.4232	2.7736	3.4386	1.0154	4.9617	0.9001
HL	1.7231	0.98131	0	3	1	2	2.5	1.5	4.75	-1.25
T	37.641	15.8584	20	60	20	40	60	40	120	-40
D	2.3139	0.01331	2.29	2.34	2.305	2.314	2.32	0.015	2.3425	2.2825
OAC	4.8041	0.30621	4.3	5.3	4.6	4.8	5	0.4	5.6	4
AV	4.2669	0.19215	4	4.6	4.08	4.29	4.39	0.31	4.855	3.615
VMA	14.197	0.64814	13.14	15.4	13.7	14.22	14.67	0.97	16.125	12.245
VFA	69.547	1.97079	66	72.7	67.4	69.39	71.47	4.07	77.575	61.295
P45	50.792	6.10663	44	59	44	50	59	15	81.5	21.5
P200	5.9744	0.81083	5	7	5	6	7	2	10	2
MS	10.338	0.90342	8.77	11.5	9.6	10.57	11	1.4	13.1	7.5
MF	2.8024	0.29396	2.3	3.25	2.5	2.8	3	0.5	3.75	1.75
Mr	974.05	387.121	450.3	1935	657.59	835.59	1156.17	498.58	1904	-90.276

5.7 Checking for Normality

The normal distribution is a frequency distribution for a random variable, due to its shape, it is sometimes called bell curve, symmetrical about its mean. It is also named Gaussian after the mathematician Karl Friedrich Gauss. The normal distribution is the most significant and very

widely used in probability and statistics. The majority of the numerical populations have distributions fitting very nearly to the normal distribution curve. For instance, the errors in engineering experiments, tests outputs, many economic measures and indicators and many other social sciences (Devore, 2011, CASELLA and BERGER, 2001).

Devore and Berk (2012) stated that a random variable x could be said to have a normal distribution with parameters μ , the mean, and σ , the standard deviation, where $-\infty < \mu < \infty$ and $\sigma > 0$ if the probability density function is:

$$f(x, \mu, \sigma) = \frac{1}{\sigma\sqrt{2\pi}} e^{-(x-\mu)^2/(2\sigma^2)} \quad -\infty < x < \infty \quad (5.5)$$

The normality check for the distribution of the model's residuals was adopted throughout the process of SPSS software by Kolmogorov-Smirnov and the Shapiro-Wilk tests. The normality can be visually assessed as well throughout examining of Figures (5-3) to (5-5) and (5-7) to (5-9) presented hereafter. The figures show the histograms regarding the frequency distributions of models output residuals as well as scatter plots. It was found that N_f and ε_p models are approximately normally distributed as the frequency closely fitted to the normal distribution curve.

5.8 Multicollinearity

Multicollinearity (collinearity or intercorrelation) is a case when two or more independent variables are correlated with each other. The calculation of correlation coefficients matrix of the predictors in the model is an important statistical method to detect the presence of interrelations among the variables. The purpose of the correlation coefficient is to determine whether there is a significant relationship (i.e., correlation) between two variables. The most commonly used correlation coefficient is the one published by Karl Pearson in 1895, having been developed earlier by Sir Francis Galton. It goes under several names, including Pearson's r , the product-moment correlation coefficient, and Pearson's correlation coefficient. Pearson's r is used to illustrate the relationship between two variables. The correlation between any two variables using Pearson's r will always be between -1 and $+1$. The value of 0 of a correlation coefficient means that there is no relationship between these two variables (Kremelberg, 2011).

Kremelberg (2011) presented an equation to calculate the Pearson's correlation coefficient (r) between two variables. The equation is adopted in the SPSS software and its form as follows:

$$r = \frac{\sum xy - N\bar{x}\bar{y}}{\sqrt{(\sum x^2 - N\bar{x}^2)(\sum y^2 - N\bar{y}^2)}} \quad (5.6)$$

Where: x and y are the variables tested for correlation, \bar{x} and \bar{y} are the mean value of x and y respectively. N is the the number of cases or data pairs.

The influence of the model parameters can significantly appear when a change occurred in any variable involved, and that will lead to a change in the correlation factor between each one of the other variables and another. Through finding a correlation between the internal variables and work on the form in SPSS software, the level of confidence used is 95 percent, and that mean the adopted significance level is 5 per cent. According to the analysis of intercorrelation, each one of the independent variables is inserted into model depending on the importance of it. Based on the way of model building, the variable is tending to take the place of another variable that has less effect on the model. The task is repeated until the survival of the biggest predictor variables; on that specific point is taking into account this interdependence. By using SPSS programme, the correlation matrix was calculated to identify the correlation coefficients of the variables involved in the model building. The decision of the model modification by either adding or removing variables based on the improvement of model adequacy. The bivariate correlation coefficients are found to decide the shape and trend of the relationship between the dependents and predictors variables in the fatigue life and permanent deformation models. Tables (5-4) and (5-5) present the results.

Table (5-4) Correlation Coefficient Matrix for Fatigue (lnNr) model

Pearson Correlations^a, (N=42)

	InNf	HL	D	OAC	AV	VMA	VFA	P45	P200	MS	MF	InEt
InNf	1.000	.135	.196	.390	-.172-	.080	.137	.334	.336	.314	.098	-.294-
HL	.135	1.000	-.709-	.365	.474	.600	-.025-	-.158-	-.172-	.220	-.723-	.648
D	.196	-.709-	1.000	.289	-.792-	-.293-	.373	.746	.750	.193	.778	-.227-
OAC	.390	.365	.289	1.000	-.461-	.381	.361	.825	.833	.755	.219	.557
AV	-.172-	.474	-.792-	-.461-	1.000	-.076-	-.617-	-.804-	-.787-	-.345-	-.602-	.003
VMA	.080	.600	-.293-	.381	-.076-	1.000	.650	.200	.117	.001	-.572-	.516
VFA	.137	-.025-	.373	.361	-.617-	.650	1.000	.563	.481	.026	-.034-	.284
P45	.334	-.158-	.746	.825	-.804-	.200	.563	1.000	.994	.555	.529	.259
P200	.336	-.172-	.750	.833	-.787-	.117	.481	.994	1.000	.597	.577	.243
MS	.314	.220	.193	.755	-.345-	.001	.026	.555	.597	1.000	.405	.420
MF	.098	-.723-	.778	.219	-.602-	-.572-	-.034-	.529	.577	.405	1.000	-.310-
InEt	-.294-	.648	-.227-	.557	.003	.516	.284	.259	.243	.420	-.310-	1.000

a. Selecting only cases for which Approximately 50% of the cases (SAMPLE) = 1

Table (5-5) Correlation Coefficient Matrix for Permanent Deformation (log(ε_p)) model

Pearson Correlations^a, (N=390)

	logEp	HL	T	AV	VMA	VFA	P45	P200	MS	logN	Mr
logEp	1.000	-.070-	.732	.068	-.059-	-.035-	-.144-	-.146-	-.120-	.540	-.678-
HL	-.070-	1.000	.003	.437	.536	-.040-	.023	.020	.358	.070	.225
T	.732	.003	1.000	-.012-	.018	.029	.021	.019	.016	-.106-	-.810-
AV	.068	.437	-.012-	1.000	-.158-	-.646-	-.695-	-.663-	-.229-	.091	-.214-
VMA	-.059-	.536	.018	-.158-	1.000	.693	.274	.183	-.002-	.000	.214
VFA	-.035-	-.040-	.029	-.646-	.693	1.000	.527	.433	-.018-	-.028-	.179
P45	-.144-	.023	.021	-.695-	.274	.527	1.000	.993	.625	-.058-	.431
P200	-.146-	.020	.019	-.663-	.183	.433	.993	1.000	.676	-.056-	.431
MS	-.120-	.358	.016	-.229-	-.002-	-.018-	.625	.676	1.000	.010	.356
logN	.540	.070	-.106-	.091	.000	-.028-	-.058-	-.056-	.010	1.000	.052
Mr	-.678-	.225	-.810-	-.214-	.214	.179	.431	.431	.356	.052	1.000

a. Selecting only cases for which Approximately 50% of the cases (SAMPLE) = 1

5.9 Goodness of Fit

The measures of goodness of fit are aimed to quantify how well the proposed regression model obtained to fit the data. The two measures that are usually presented are the coefficient of determination (R^2) and standard error of regression (SER) (Devore, 2011).

The R^2 value is the percent variation of the criterion variable explained by the suggested model and calculated according to following equation:

$$R^2 = 1 - \frac{SSE}{SST} \quad (5.7)$$

Where:

$$SSE = \sum(y_i - y_i')^2 \quad (5.8)$$

$$SST = \sum(y_i - \bar{y})^2 \quad (5.9)$$

SSE = sum squares of error

SST = total sum of squares

y_i = actual value of response variable for the i^{th} case,

y_i' = value of the regression prediction for the i^{th} case,

\bar{y} = mean of y observed

For more accuracy, several statisticians use the adjusted coefficient of multiple determinations, adjusted R^2 that refer to magnitude increasing of R^2 when new parameter enter the model. The adjusted R^2 is calculated as follows (Devore, 2011):

$$R_{adj}^2 = 1 - \frac{n-1}{n-(k+1)} * \frac{SSE}{SST} \quad (5.10)$$

or

$$R_{adj}^2 = \frac{(n-1)R^2 - k}{n-1-k} \quad (5.11)$$

Where:

$n-(k+1)$ = degree of freedom (Df),

n =number of sample and

k = number of independent variables.

Adjusted R^2 adjusts the proportion of unexplained variation upward [since $(n-1) / (n-k-1) > 1$], which results in $R^2_{adj} < R^2$.

The second parameter SER is estimated using the following equations:

$$SER = \sqrt{\frac{SSE}{n-(k+1)}} \quad (5.12)$$

In general, the less the SER value, the better the proposed regression model. Throughout the regression modelling process, an important step has been done as a significant part of model building, and this part is the Analysis Of Variance or (ANOVA). The analysis of variance refers to a collection of experimental situations and statistical procedures for the analysis of quantitative responses from experimental units. The ANOVA was developed in the first decades of last century by Sir Ronald Fisher, which is why the ANOVA is occasionally called Fisher's ANOVA (Kremelberg, 2011). ANOVA is a statistical procedure that used to examine the equivalence among several means by making a comparison of the variance in a continuous random variable amongst groups relative to variance inside the groups (Larson, 2008). Alternatively, it is used to test the variation of a continuous dependent variable in a single group of respondents who were tested at three or more points in time (Kremelberg, 2011).

There are several versions of the ANOVA that are covered in the SPSS. The first type is called a one-way ANOVA that used for a model of only one categorical independent or predictor variable. The second one is the factorial ANOVA that used when two or more categorical independent or predictor variables in the model. Finally, a repeated measures ANOVA which is applied when the measurement of a dependent variable is repeated over two or more points in time (Kremelberg, 2011).

The results of model summary, Analysis Of Variance (ANOVA), stepwise regression information, for the possible models can be seen in through Tables (5-6) to (5-11).

Table (5-6) Summary of Fatigue life Model (lnNf)

Model Summary^{i,j}				
Model	R	R Square	Adjusted R Square	Std. Error of the Estimate
	Approximately 50% of the cases (SAMPLE) = 1 (Selected)			
1	.390 ^a	.152	.131	.56661
2	.729 ^b	.532	.508	.42653
3	.842 ^c	.710	.687	.34020
4	.888 ^d	.789	.766	.29386
5	.905 ^e	.820	.795	.27532
6	.905 ^f	.820	.800	.27180
7	.927 ^g	.859	.839	.24373
8	.936 ^h	.875	.854	.23244

a. Predictors: (Constant), OAC, b. Predictors: (Constant), OAC, lnEt

c. Predictors: (Constant), OAC, lnEt, HL, d. Predictors: (Constant), OAC, lnEt, HL, D

e. Predictors: (Constant), OAC, lnEt, HL, D, MS, f. Predictors: (Constant), lnEt, HL, D, MS

g. Predictors: (Constant), lnEt, HL, D, MS, VFA,

h. Predictors: (Constant), lnEt, HL, D, MS, VFA, VMA

i. Unless noted otherwise, statistics are based only on cases for which Approximately 50% of the cases (SAMPLE) = 1.

j. Dependent Variable: lnNf

Table (5-7) The Results of ANOVA of Fatigue life Model (lnNf)

ANOVA ^{a,b}						
Model		Sum of Squares	df	Mean Square	F	Sig.
1	Regression	2.309	1	2.309	7.192	.011 ^c
	Residual	12.842	40	.321		
	Total	15.151	41			
2	Regression	8.056	2	4.028	22.141	.000 ^d
	Residual	7.095	39	.182		
	Total	15.151	41			
3	Regression	10.753	3	3.584	30.971	.000 ^e
	Residual	4.398	38	.116		
	Total	15.151	41			
4	Regression	11.956	4	2.989	34.613	.000 ^f
	Residual	3.195	37	.086		
	Total	15.151	41			
5	Regression	12.422	5	2.484	32.776	.000 ^g
	Residual	2.729	36	.076		
	Total	15.151	41			
6	Regression	12.418	4	3.104	42.023	.000 ^h
	Residual	2.733	37	.074		
	Total	15.151	41			
7	Regression	13.013	5	2.603	43.810	.000 ⁱ
	Residual	2.139	36	.059		
	Total	15.151	41			
8	Regression	13.260	6	2.210	40.905	.000 ^j
	Residual	1.891	35	.054		
	Total	15.151	41			

a. Dependent Variable: lnNf

b. Selecting only cases for which Approximately 50% of the cases (SAMPLE) = 1

c. Predictors: (Constant), OAC, d. Predictors: (Constant), OAC, lnEt

e. Predictors: (Constant), OAC, lnEt, HL, f. Predictors: (Constant), OAC, lnEt, HL, D

g. Predictors: (Constant), OAC, lnEt, HL, D, MS, h. Predictors: (Constant), lnEt, HL, D, MS

i. Predictors: (Constant), lnEt, HL, D, MS, VFA

j. Predictors: (Constant), lnEt, HL, D, MS, VFA, VMA

Table (5-8) Stepwise Regression Details of Coefficients of the Fatigue Life (lnNr) Model

Coefficients ^{a,b}							
Model	Unstandardized Coefficients		Standardized Coefficients	t	Sig.	95.0% Confidence Interval for B	
	B	Std. Error	Beta			Lower Bound	Upper Bound
1 (Constant)	4.596	1.482		3.100	.004	1.600	7.592
OAC	.826	.308	.390	2.682	.011	.203	1.448
2 (Constant)	10.199	1.496		6.816	.000	7.173	13.226
OAC	1.700	.279	.804	6.090	.000	1.135	2.264
lnEt	-1.645	.293	-.742	-5.620	.000	-2.237	-1.053
3 (Constant)	14.374	1.474		9.753	.000	11.390	17.358
OAC	1.692	.223	.800	7.602	.000	1.241	2.143
lnEt	-2.437	.285	-1.099	-8.541	.000	-3.015	-1.859
HL	.346	.072	.554	4.828	.000	.201	.491
4 (Constant)	-50.608	17.458		-2.899	.006	-85.982	-15.234
OAC	.750	.317	.354	2.362	.024	.107	1.393
lnEt	-2.543	.248	-1.147	-10.251	.000	-3.046	-2.040
HL	.791	.134	1.267	5.886	.000	.519	1.063
D	29.972	8.031	.732	3.732	.001	13.699	46.244
5 (Constant)	-64.016	17.227		-3.716	.001	-98.955	-29.078
OAC	.097	.397	.046	.244	.809	-.709	.902
lnEt	-2.603	.234	-1.174	-11.140	.000	-3.077	-2.129
HL	.901	.134	1.445	6.750	.000	.631	1.172
D	36.269	7.941	.886	4.567	.000	20.164	52.374
MS	.208	.084	.284	2.480	.018	.038	.377
6 (Constant)	-67.232	10.938		-6.146	.000	-89.395	-45.069
lnEt	-2.600	.230	-1.172	-11.292	.000	-3.066	-2.133
HL	.925	.091	1.482	10.126	.000	.740	1.110
D	37.772	4.941	.923	7.645	.000	27.761	47.783
MS	.221	.062	.303	3.574	.001	.096	.347
7 (Constant)	-52.805	10.817		-4.882	.000	-74.742	-30.868
lnEt	-2.809	.217	-1.266	-12.957	.000	-3.249	-2.369
HL	.865	.084	1.386	10.291	.000	.695	1.036
D	29.526	5.140	.721	5.744	.000	19.101	39.951
MS	.289	.060	.396	4.859	.000	.168	.410
VFA	.076	.024	.253	3.164	.003	.027	.125

**Table (5-8) Stepwise Regression Details of Coefficients of the Fatigue Life (lnN_f) Model
(Cont.)**

Coefficients^{a,b}

Model	Unstandardized Coefficients		Standardized Coefficients	t	Sig.	95.0% Confidence Interval for B	
	B	Std. Error	Beta			Lower Bound	Upper Bound
	8 (Constant)	-47.5	10.600				-4.489
lnEt	-2.850	.208	-1.285	-13.726	.000	-3.271	-2.428
HL	.972	.094	1.557	10.296	.000	.780	1.163
D	27.056	5.036	.661	5.372	.000	16.832	37.280
MS	.272	.057	.372	4.735	.000	.155	.388
VFA	.148	.041	.492	3.638	.001	.065	.231
VMA	-.301	.140	-.317	-2.141	.039	-.586	-.016

a. Dependent Variable: lnN_f

b. Selecting only cases for which Approximately 50% of the cases (SAMPLE) = 1

Table (5-9) Summary of Permanent Deformation Model ($\log \epsilon_p$)

Model Summary^{i,j}

Model	R		R Square	Adjusted R Square	Std. Error of the Estimate
	Approximately 50% of the cases (SAMPLE) = 1 (Selected)	Approximately 50% of the cases (SAMPLE) \approx 1 (Unselected)			
1	.732 ^a		.536	.535	.51289
2	.960 ^b		.922	.921	.21105
3	.970 ^c		.941	.940	.18366
4	.973 ^d		.946	.946	.17532
5	.973 ^e		.948	.947	.17345
6	.975 ^f		.951	.950	.16764
7	.975 ^g		.951	.950	.16742
8	.977 ^h	.971	.955	.954	.16153

a. Predictors: (Constant), T

b. Predictors: (Constant), T, logN

c. Predictors: (Constant), T, logN, MS

d. Predictors: (Constant), T, logN, MS, VMA

e. Predictors: (Constant), T, logN, MS, VMA, HL

f. Predictors: (Constant), T, logN, MS, VMA, HL, P200

g. Predictors: (Constant), T, logN, MS, HL, P200

h. Predictors: (Constant), T, logN, MS, HL, P200, Mr

i. Unless noted otherwise, statistics are based only on cases for which Approximately 50% of the cases (SAMPLE) = 1.

j. Dependent Variable: logEp

Table (5-10) The Results of ANOVA of Permanent Deformation Model ($\log \epsilon_p$)

ANOVA ^{a,b}						
Model		Sum of Squares	df	Mean Square	F	Sig.
1	Regression	118.090	1	118.090	448.922	.000 ^c
	Residual	102.064	388	.263		
	Total	220.155	389			
2	Regression	202.917	2	101.459	2277.825	.000 ^d
	Residual	17.238	387	.045		
	Total	220.155	389			
3	Regression	207.135	3	69.045	2047.035	.000 ^e
	Residual	13.020	386	.034		
	Total	220.155	389			
4	Regression	208.322	4	52.080	1694.479	.000 ^f
	Residual	11.833	385	.031		
	Total	220.155	389			
5	Regression	208.602	5	41.720	1386.711	.000 ^g
	Residual	11.553	384	.030		
	Total	220.155	389			
6	Regression	209.391	6	34.899	1241.814	.000 ^h
	Residual	10.763	383	.028		
	Total	220.155	389			
7	Regression	209.391	5	41.878	1494.031	.000 ⁱ
	Residual	10.764	384	.028		
	Total	220.155	389			
8	Regression	210.162	6	35.027	1342.451	.000 ^j
	Residual	9.993	383	.026		
	Total	220.155	389			

a. Dependent Variable: $\log \epsilon_p$

b. Selecting only cases for which Approximately 50% of the cases (SAMPLE) = 1

c. Predictors: (Constant), T

d. Predictors: (Constant), T, $\log N$

e. Predictors: (Constant), T, $\log N$, MS

f. Predictors: (Constant), T, $\log N$, MS, VMA

g. Predictors: (Constant), T, $\log N$, MS, VMA, HL

h. Predictors: (Constant), T, $\log N$, MS, VMA, HL, P200

i. Predictors: (Constant), T, $\log N$, MS, HL, P200

j. Predictors: (Constant), T, $\log N$, MS, HL, P200, Mr

**Table (5-11) Stepwise Regression Details of Coefficients of the Permanent Deformation
Model ($\log \epsilon_p$)**

Coefficients^{a,b}

Model	Unstandardized Coefficients		Standardized Coefficients	t	Sig.	95.0% Confidence Interval for B	
	B	Std. Error	Beta			Lower Bound	Upper Bound
1 (Constant)	1.620	.067		24.192	.000	1.488	1.752
T	.035	.002	.732	21.188	.000	.032	.038
2 (Constant)	.579	.036		15.891	.000	.507	.651
T	.038	.001	.799	55.822	.000	.037	.039
logN	.360	.008	.624	43.640	.000	.344	.376
3 (Constant)	1.765	.111		15.948	.000	1.547	1.982
T	.038	.001	.801	64.326	.000	.037	.039
logN	.361	.007	.626	50.274	.000	.347	.375
MS				-			
	-.115-	.010	-.138-	11.183	.000	-.136-	-.095-
				-			
4 (Constant)	2.973	.221		13.430	.000	2.538	3.409
T	.038	.001	.802	67.486	.000	.037	.039
logN	.361	.007	.626	52.675	.000	.347	.374
MS				-			
	-.115-	.010	-.139-	11.730	.000	-.135-	-.096-
				-			
VMA				-			
	-.085-	.014	-.073-	6.213-	.000	-.112-	-.058-
5 (Constant)	2.471	.274		9.021	.000	1.933	3.010
T	.038	.001	.802	68.187	.000	.037	.039
logN	.363	.007	.629	53.307	.000	.349	.376
MS				-			
	-.101-	.011	-.122-	9.421-	.000	-.123-	-.080-
				-			
VMA				-			
	-.056-	.017	-.048-	3.370-	.001	-.089-	-.023-
				-			
HL				-			
	-.036-	.012	-.047-	3.052-	.002	-.059-	-.013-

Table (5-11) Stepwise Regression Details of Coefficients of the Permanent Deformation Model ($\log \epsilon_p$) (Cont.)

		Coefficients ^{a,b}						
Model		Unstandardized Coefficients		Standardized Coefficients	t	Sig.	95.0% Confidence Interval for B	
		B	Std. Error	Beta			Lower Bound	Upper Bound
6	(Constant)	1.524	.319		4.771	.000	.896	2.152
	T	.038	.001	.801	70.511	.000	.037	.039
	logN	.361	.007	.626	54.856	.000	.348	.374
	MS	-.026	.018	-.031	-	.148	-.060	.009
	VMA	.002	.019	.002	.095	.924	-.036	.040
	HL	-.080	.014	-.104	-	.000	-.107	-.052
	P200	-.097	.018	-.104	-	.000	-.132	-.061
					5.300			
7	(Constant)	1.553	.104		14.942	.000	1.349	1.757
	T	.038	.001	.801	70.618	.000	.037	.039
	logN	.361	.007	.626	54.931	.000	.348	.374
	MS	-.027	.014	-.032	-	.066	-.055	.002
	HL	-.079	.010	-.103	-	.000	-.098	-.059
	P200	-.096	.015	-.103	-	.000	-.125	-.066
					1.841			
					8.031			
					6.352			
8	(Constant)	1.409	.104		13.590	.000	1.205	1.613
	T	.046	.001	.959	30.877	.000	.043	.048
	logN	.364	.006	.631	57.189	.000	.351	.376
	MS	-.023	.014	-.028	-	.093	-.051	.004
	HL	-.112	.011	-.146	-	.000	-.134	-.090
	P200	-.0177	.021	-.190	-	.000	-.218	-.136
	Mr	.000	.000	.192	5.434	.000	.000	.001
					1.683			
					9.941			
					8.487			

a. Dependent Variable: $\log \epsilon_p$

b. Selecting only cases for which Approximately 50% of the cases (SAMPLE) = 1

5.10 Validation of the Developed Models

5.10.1 Introduction

In the model building process, validation of the developed models is the last step. The objective is to assess the ability of both fatigue cracking and permanent deformation models to predict the number of repetitions to failure as well as the permanent strain in the flexible pavement accurately. The validation of models has been done by using the data that not already used in developing the model.

Regression modelling characterises the relation between a dependent variable (Y) and a group of the predictor (independent) variables (X's). This form of relation between Y and X's is defined by coefficients, which are estimated from a given data set of X's and Y using linear or nonlinear least square (Snee, 1977). Sometimes, regression models provide a misleadingly good estimation of Y for the dependent variables set used to generate the model, but may or may not provide a good prediction of Y for a new data set. Therefore, it is necessary to check the prediction accuracy of a newly developed model. This checking process is called validation (Kennedy and Neville, 1986).

5.10.2 Validation Methods

Neter et al. (1990) and Snee (1977) suggested the following methods for validating of a regression model:

5.10.2.1 Examination of Model Predictions and Coefficients

The checking of model parameters (predictions and coefficients) can be done by comparing them with the physical theory, e.g., to make sure that the model predictions are not negative for a quantity that is positive in theory or that the estimated coefficients do not have wrong signs.

5.10.2.2 Collection of New Data

The purpose of collecting new data is to assess the efficiency of the model made upon earlier dataset by examining it with new data to be applied successfully. When the model can be applicable, this is to confirm that the model is valid for the data further away than the data used in the model building process. The validation of the statistical and physical hypothesis adopted in the prediction of the coefficients of a model are less open to question in the case of the model provides correct predictions for a new set of data. In fact, new data collection gives a general investigation overall model building procedure.

5.10.2.3 Comparison with Previously Developed Models

In some cases, previous empirical results may be helpful in determining whether the selected model is reasonable. Comparisons of the model predictions with previous studies can show whether the developed model can predict this type of distress accurately or not.

5.10.2.4 Data Splitting

A reasonable alternative to the collection of new data is to divide the results obtained into two parts. The first data used in the building of the model and the other one utilised in the validation process to evaluate the adequacy and the ability of the model of prediction. However, it is recommended that data splitting should not be considered unless;

$$N \geq 2P + 25$$

Where:

N = the sample size and

P = the number of coefficients (independent variables) to be estimated.

5.10.2.5 Prediction Sum of Squares (PRESS)

When the splitting of data set being impractical due to small size of data set, the procedure of prediction sum of squares (PRESS) found by Allen (1974) can be adopted as a form of dividing data to assess the predictions' accuracy of the model. In this procedure, one data point is taken away from the data group while the unknown parameters in the model are being estimated. Then the predicted value of the removed point (i.e., predicted using the model developed from the remaining data points) is compared with the real observed value of the response of interest. This procedure is repeated then with a different point removed, and a summary of the differences (e.g., the sum of squared errors or R^2) is employed to assess the model ability under consideration to predict the response of interest rightly. Models with small errors (large R^2) are considered to be good models. The degree of closeness of the prediction errors (or R^2) to that obtained for the full model serves as an indication of the model's prediction power. Good models will have R^2 from the PRESS procedure close to the R^2 for the full model.

5.10.3 Selection of Validation Methods

The literature suggests that all available methods of validation could be used according to the modelling case and data. However, in this study, it is not possible to use all the methods of

validation. Therefore, the applicability of each method regarding the validation of the cracking index model will be discussed, and the most appropriate method of validation will be selected.

The first method (Check on Model Predictions and Coefficients) attempts to make sure that the selected model agrees with the physical theory. This essentially has been already checked during the development process.

The second method (Collection of New Data) suggests that a new data set should be collected.

The third method (Comparison with previously developed regression models) compares the results of a newly developed model with a previously developed model or with a theoretical model.

As per the discussion mentioned above and the nature of the available data, the fourth method (Data Splitting procedure) was selected to assess the predictive ability of fatigue life and permanent deformation models.

The last method (Prediction Sum of Squares) is not necessary because of the available adequate sample size.

5.10.4 Analysis of Error

The residual is an important part of any model (e_i). Residuals are the difference between an observed value of the criterion variable (y_i) and the value predicted by the model (y_i'), ($e_i = y_i - y_i'$). Standardizing residuals is made by subtracting the residuals mean value from each residual and then dividing it by the estimated standard deviation (Devore and Berk, 2012). The following requirements have to be considered (Keller and Warrak, 2000);

- The error distribution is normal,
- The error distribution mean is zero.

For the analysis of error according to the requirements mentioned above and for visual diagnostic, Devore (2011) and Devore and Berk (2012) recommended three types of plots:

1. y_i' on the vertical axis versus y_i on the horizontal axis.
2. e_i on the vertical axis versus y_i' on the horizontal axis.
3. Histogram for the standardised residual versus the frequency.

They found that if the first plot provides points near the line of slope =1 through the point (0, 0), then the proposed regression model accurately predicts independent values of the actual

observed values. Therefore, it is a visual evaluation of the model ability of prediction. If the model is accurate, the second plot of the residuals versus predicted y values should not exhibit a very distinct pattern. Also with the aid of the second plot, one can determine the extreme value of the y_i' , i.e., outliers. The histogram plot of the standardised residual should follow the normal distribution pattern if the underlying assumption of the proposed model is correct, with the mean value of zero. Figures (5-2) and (5-6) present relationships between predicted and observed values of dependent variables for the fatigue life (N_f) and permanent deformation (ϵ_p) models respectively. Figures (5-3), (5-4) and (5-5) show the histogram and scatter plots depicted the distribution of the standardised residual and relation between standardised residual versus standardised predicted value for fatigue life. Similarly, Figures (5-7), (5-8) and (5-9) present histogram and scatter plots of errors of model permanent deformation ($\text{Log } \epsilon_p$). It can be noticed that distribution of errors is normal for each of these models.

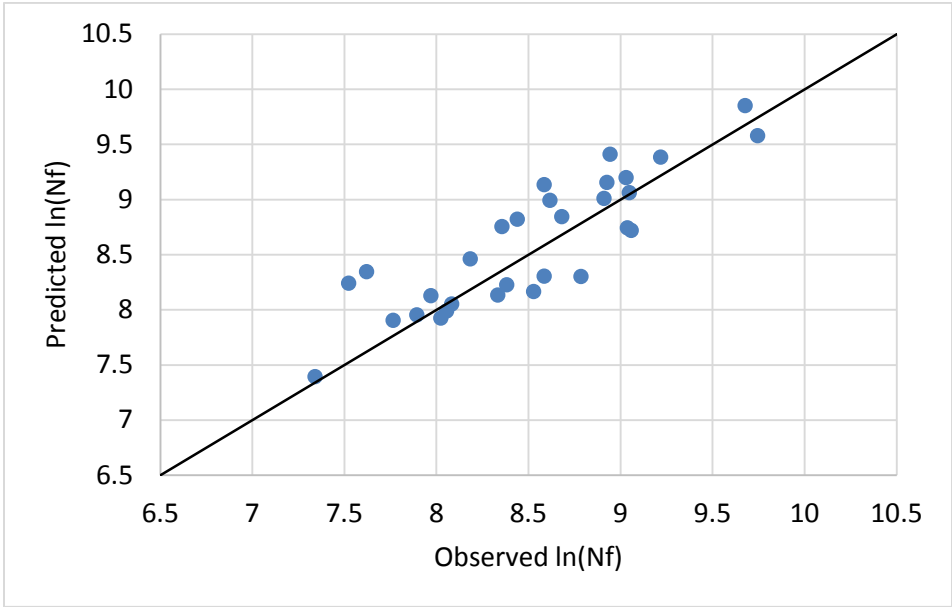


Figure (5-2) Fatigue life model new estimated versus observed values

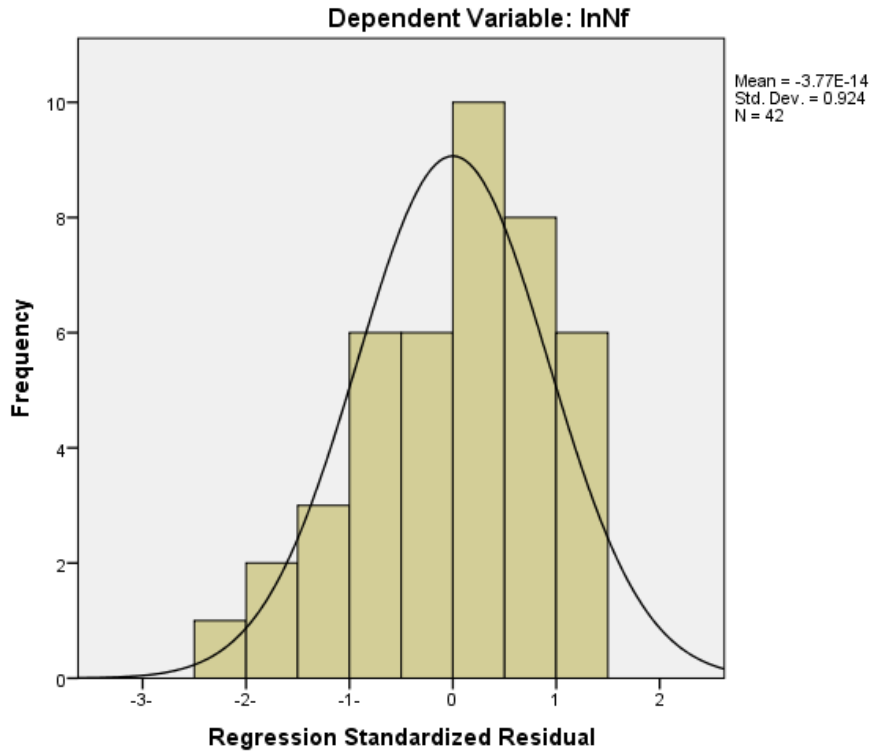


Figure (5-3) Histogram of Regression Standardized Residual of Fatigue Life Model (lnNf)

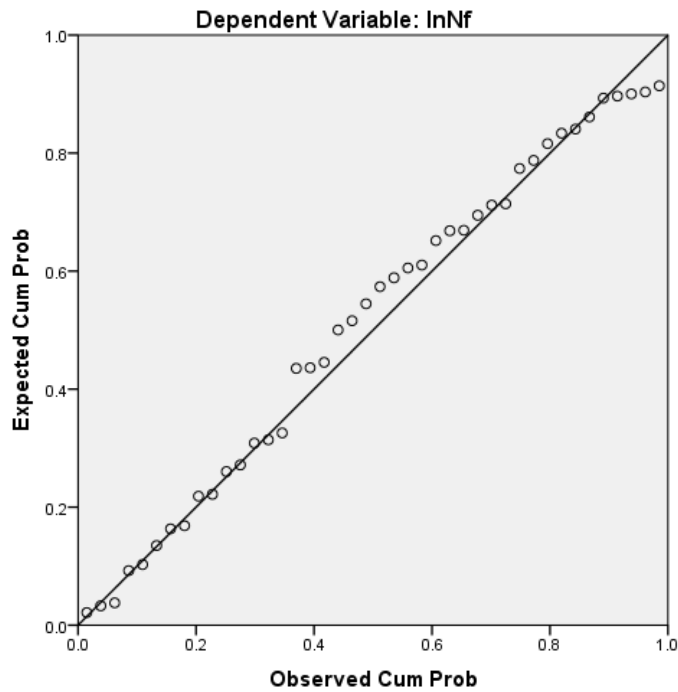


Figure (5-4) Normal Probability Plot of Regression Standardized Residual of Fatigue Life Model (lnNf)

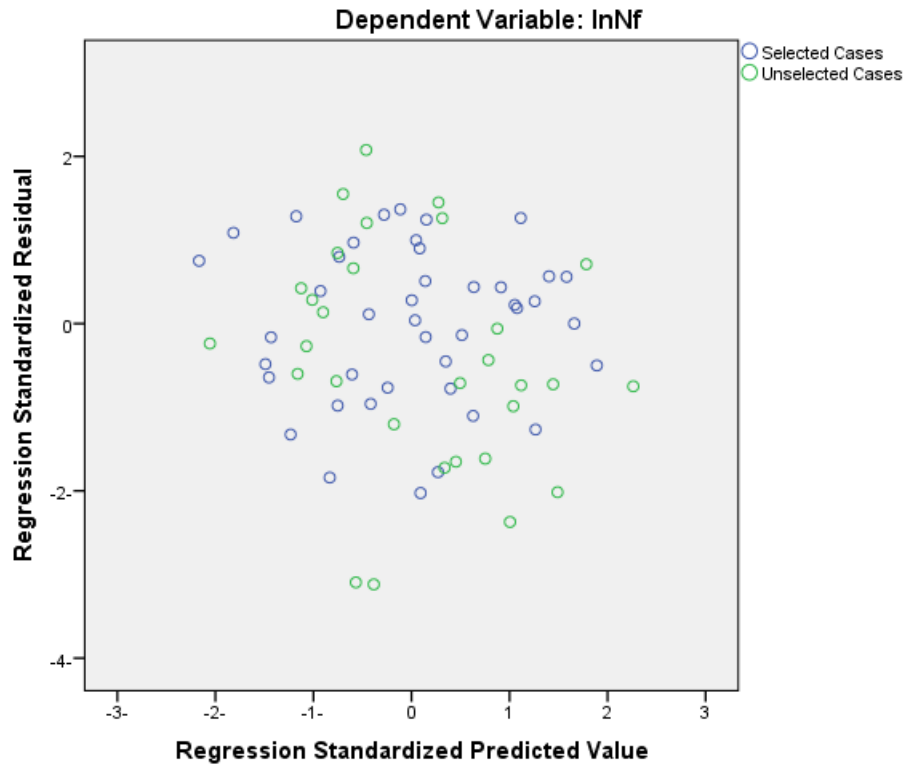


Figure (5-5) Scatter Plot of Regression Standardized Residual of Fatigue Life Model (lnNf)

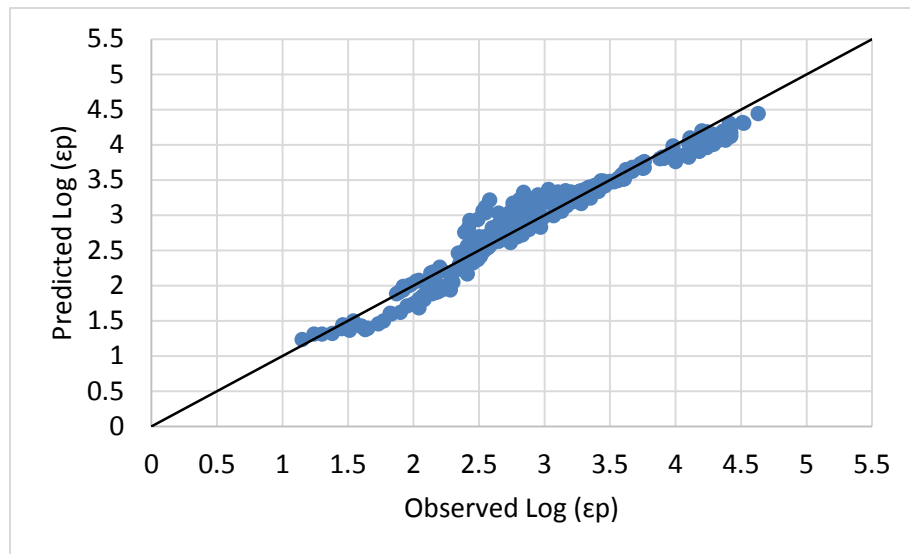


Figure (5-6) Permanent deformation (ϵ_p) model new estimated versus observed values

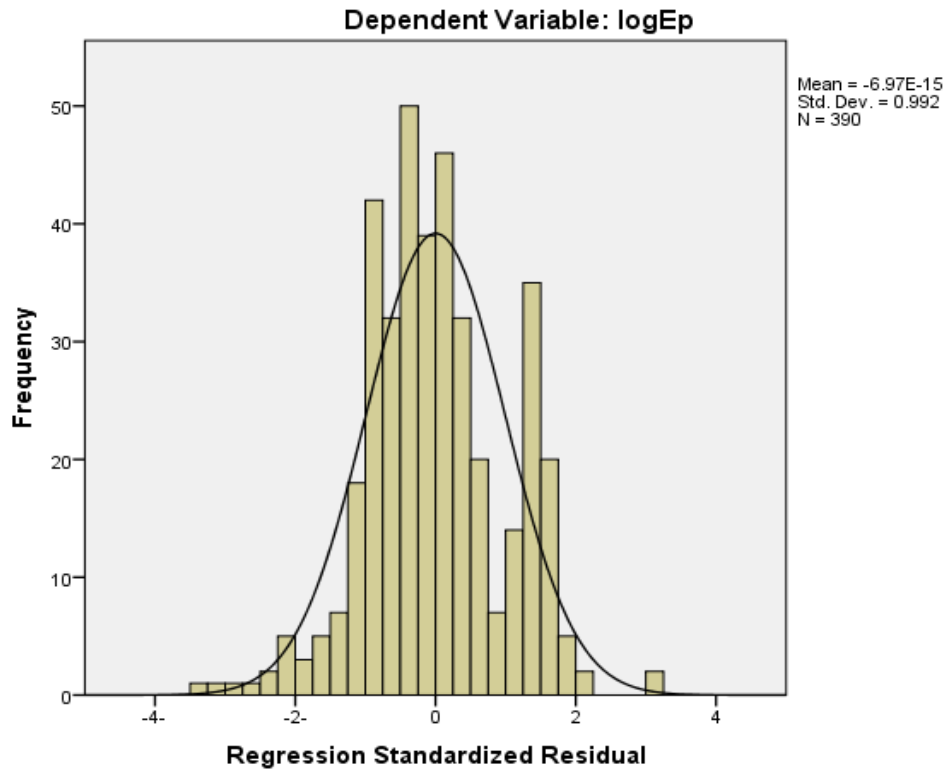


Figure (5-7) Histogram of Regression Standardized Residual of Permanent Deformation Model ($\log \epsilon_p$)

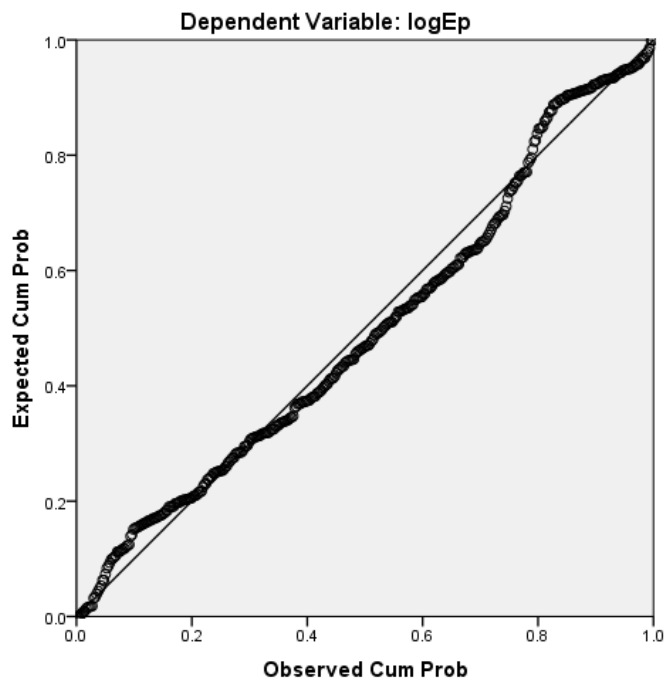


Figure (5-8) Normal Probability Plot of Regression Standardized Residual of Permanent Deformation Model ($\log \epsilon_p$)

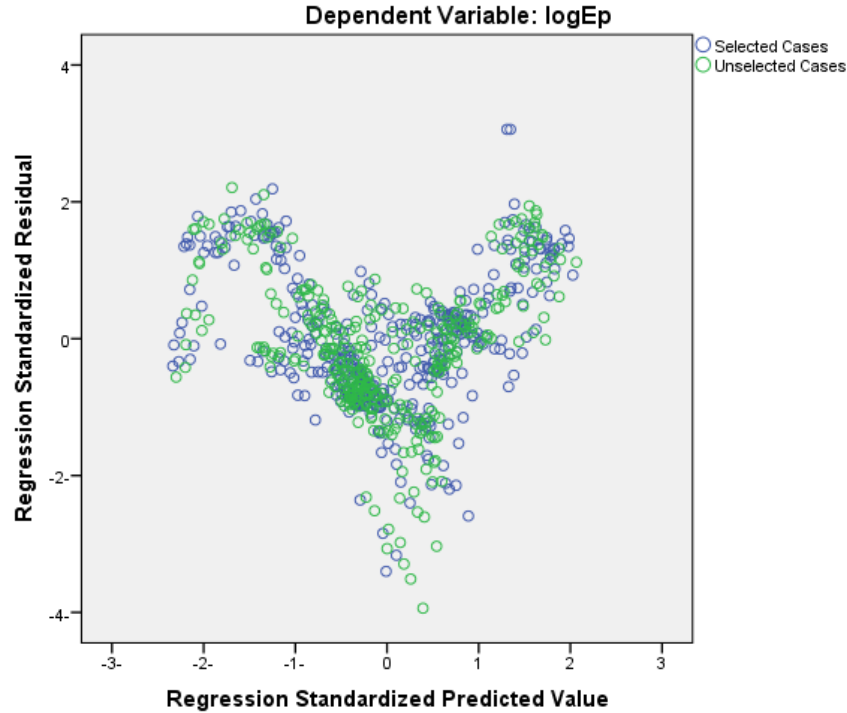


Figure (5-9) Scatter Plot of Regression Standardized Residual of Permanent Deformation Model ($\log \epsilon_p$)

5.10.4.1 Distribution of Error

Figures (5-3) to (5-5) and (5-7) to (5-9) show the histograms and scatter plots of the distribution of errors in the models. They visually explain that the errors in N_f and ϵ_p models are approximately normally distributed with a zero mean value and a standard deviation of 0.924, and 0.992 for N_f , and ϵ_p models respectively.

5.10.4.2 Mean of Error Distribution

For the developed models, mean values of error distribution are calculated, and it is found that the means of error distribution are equal to zero for the models. The results of mean error distribution illustrated in Figures (5-3) and (5-7) as well as Tables (5-12) and (5-13) which present the residual statistics for fatigue life (N_f), and permanent deformation (permanent microstrain, ϵ_p) respectively.

Table (5-12) The Residuals Statistics Summary of the Fatigue Life Model ($\ln N_f$)

	Approximately 50% of the cases (SAMPLE) = 1 (Selected)				
	Minimum	Maximum	Mean	Std. Deviation	N
Predicted Value	7.3324	9.6397	8.5645	.56870	42
Residual	-.47091-	.31766	.00000	.21476	42
Std. Predicted Value	-2.166-	1.891	.000	1.000	42
Std. Residual	-2.026-	1.367	.000	.924	42

Table (5-13) The Residuals Statistics Summary of the Permanent Deformation Model ($\log \epsilon_p$)

	Approximately 50% of the cases (SAMPLE) = 1 (Selected)				
	Minimum	Maximum	Mean	Std. Deviation	N
Predicted Value	1.2107	4.4170	2.9277	.73502	390
Residual	-.54909-	.49425	.00000	.16028	390
Std. Predicted Value	-2.336-	2.026	.000	1.000	390
Std. Residual	-3.399-	3.060	.000	.992	390

5.11 Examination of R-Critical Value

A high value of correlation coefficient R could not be enough to decide that the model gives a good fitting of the data. The correlation between dependent and independent variables is rated to be significant at a chosen level of probability when the calculated value of correlation coefficient (R) overtakes the tabulated value (Saad and Samer, 2014). For fatigue life (N_f) model, the correlation coefficient $R_{\text{calculated}}$ (0.935) is greater than the tabulated critical value ($R_{\text{tabulated}}$) which equal to 0.304 ($n=42$, $df=n-2=40$). Regarding the permanent deformation model (ϵ_p), the correlation coefficient $R_{\text{calculated}}$ is 0.977. It is also greater than the critical tabulated correlation coefficient $R_{\text{tabulated}}$ that equal to 0.087 ($n=390$, $df=n-2=388$). Thus, the null hypothesis that there is no association between the variables is rejected at 95% confidence level. Therefore, there are strong correlations between dependent and independent variables of all developed models.

5.12 Analysis of Results

The stepwise regression using SPSS software served its purpose in drawing attention to dangerous inter-correlation and enabled a selection of variables to be made on a logical basis. The

chosen variables were then entered into a regular multiple regression. The fatigue life and permanent deformation models developed in this study, with their coefficient of determination and standard error of the estimate are displayed in the Table (5-14).

Table (5-14) Summary Results of Developed Models

Model	R ²	SER
$\ln N_f = -47.58 - 2.84997 \cdot \ln E_t + 0.971664 \cdot HL + 27.05582 \cdot D$ $+ 0.271583 \cdot MS + 0.148198 \cdot VFA - 0.30069 \cdot VMA$	0.875	0.23244
$\log \epsilon_p = 1.4092 + 0.0455 \cdot T + 0.36383 \cdot \log N - 0.02349 \cdot MS - 0.1122 \cdot HL -$ $0.01767 \cdot P200$	0.955	0.16153

The coefficient of determination value (0.875) in the fatigue life model ($\ln N_f$) seems to be good especially when the standard error of regression (0.23244) is the lowest among the initially proposed models by the modelling process of SPSS. Also, it can be seen that the dependent variable ($\ln N_f$) increases as the initial tensile strain decreases. The increase in the other independent variables in the model, hydrated lime (HL), the density (D), Marshall stability (MS), the voids filled with asphalt (VFA) and voids in mineral aggregate (VMA), leads to increasing the fatigue life ($\ln N_f$). Regarding the permanent deformation models, the response variable in the first model ($\log N$) has a positive relationship with permanent strain, thus the higher permanent strain, the higher number of load repetitions. A Lower number of load repetitions is expected due to increasing the temperature (T). The increasing in the percent of hydrated lime addition (HL) and percent passing sieve No.200 in the aggregate gradation of the mixtures (P200) leads to enhance the number of load repetitions to failure. The plastic strain model ($\log \epsilon_p$) with a coefficient of determination (0.955) and standard error of regression (0.16153) that conduce to a very good correlation between observed and estimated values of plastic strain. There is only 4.5 percent of observed data variation is unexplained by the model. The model equation indicates that permanent deformation increases when the temperature and the number of load repetitions increase and it decreases with Marshall stability, hydrated lime percent and the percent of passing sieve No.200 decrease. The plots of the observed values versus the estimated values obtained from models as shown in Figures (5-2) through (5-9) illustrate that there are good correlations between the predictors and measured values of the responses variables.

Furthermore, it can be noticed from statistical test and analysis and the figures, that all regression residuals of the data of responses variables in histogram distribution are approximately normally distributed. The scatter plots show as well that scattering are around the line of slope of 45 degrees in normal probability plot and the horizontal line of regression standardised residual. This can confirm that the distributions of these models data are normal. Figure (5-6) presents that some of these data are crowded because all the cycles load repetitions of the specimen are considered in the developed model for permanent deformation, while for fatigue model just the failure cycle is considered.

A study of the correlation coefficient matrix and the variables selected for the regression analysis showed several variables which correlated reasonably well with the dependent variable but did not enter because of a high order of inter-correlation with a variable already selected for the model. Accordingly, it was decided to reduce the number of variables, leaving as few as possible to describe the models.

5.13 Models' Parameters Limitation

The limitations of data set that adopted to develop the fatigue life (N_f) model and permanent deformation models (ϵ_p) are shown in Tables (5-15) and (5-16) respectively. The purpose of presenting the range of the data set used in modelling is not to propose that the efforts of modelling have not been effective. It simply presents an alert about the data limitation.

Table (5-15) Limitation of Fatigue Life ($\ln N_f$) Model variables

	Minimum	Maximum	Mean
N_f	1540.712	17500	6563
ϵ_t ($\times 10^{-6}$)	163	520.19	271
HL	0	3	1.6667
D	2.29	2.34	2.3149
VFA	66	72.74	69.6061
VMA	13.14	15.4	14.1906
MS	8.77	11.5	10.3117

Table (5-16) Limitation of Permanent Deformation ($\log \epsilon_p$) Model variables

	Minimum	Maximum	Mean
ϵ_p	14.12538	42657.95	797.6273
T	20	60	37.3461
N	1	10000	362.0762
MS	8.77	11.5	10.3315
P200	5	7	6.0205
HL	0	3	1.7086

5.14 Summary

In this chapter, two multi-linear regression models were developed representing fatigue cracking and permanent deformation, which are the failure criteria of the Mechanical-Empirical design approach adopted in this study. In the modelling building process, the results of the laboratory work have been used. The results are the asphalt concrete Marshall and volumetric properties and the performance-related properties (fatigue life and permanent deformation) as related to the effect of hydrated lime addition. The output parameters of laboratory work were identified as potential independent variables to be involved in the models. Statistical Package for the Social Sciences (SPSS) is used to complete entry, check and analysis of data and develop the linear regression models. The SPSS results in several models regarding the fatigue cracking and rutting dependent variables, and finally, one model for each dependent has been chosen based on the best results that the model provided as compared to the others. The fatigue life model (N_f) has been made to predict the number of load cycles to fatigue cracking. The model of rutting was developed to predict the permanent strain (ϵ_p) in the asphalt concrete layer. The permanent deformation in asphaltic courses can be estimated by multiplying the strain in each course by the thickness of it and then accumulating the deformations to determine the total rutting depth. Developed models are as follows:

➤ Fatigue Life Model:

$$\ln N_f = -47.58 - 2.84997 \times \ln \varepsilon_t + 0.971664 \times HL + 27.05582 \times D + 0.271583 \times MS + 0.148198 \times VFA - 0.30069 \times VMA \quad (5-13)$$

➤ Rutting Models:

$$\log \varepsilon_p = 1.4092 + 0.0455 \times T + 0.36383 \times \log N - 0.02349 \times MS - 0.1122 \times HL - 0.01767 \times P200 \quad (5-14)$$

Chapter Six

Development of Mechanistic-Empirical Design Approach Using Numerical Modelling

6.1 Introduction

The Analysis of pavement has been turning from empirical to mechanistic techniques. The shortcoming of computational abilities made the pavement design first to be done by empirical approaches in which there is a limitation to a specified set of environmental and material conditions. The design validity depends on these conditions, so if there is any change happen, the design is no more applicable. The influence of the mechanistic design approach depends on the accuracy of the predicted pavement material responses (stresses and strains). The most commonly adopted mechanistic analysis tools are the finite element analysis and multi-layered elastic methods. This chapter consists of an application of a mechanistic approach that based on the review and background mentioned in chapter one and chapter two about the Mechanistic-Empirical (M-E) design process. The Mechanistic-Empirical design approach is adopted by others recently due to its advantages in getting the benefit of empirical approaches, engineering experience and mechanistic responses of paving materials to a group of factors, such as; loading configuration, temperature, climate and pavement material and geometry to achieve as much realistic analysis as can. The process of the adopted mechanistic-empirical approach involving the implementation of hydrated lime addition as a partial replacement of the original filler (Limestone dust) in the design steps has mentioned in the research methodology and illustrated in Figure (6-1). This chapter includes the calculation of input data that needed to determine the optimum thickness of HMA layer in the proposed flexible pavement model regarding the influence of hydrated lime on the asphaltic layer. The influence of hydrated lime is presented by means of the change of important parameters that affect the design output. Also, the chapter involves evaluation and analysis of output and determine the optimum thickness after consideration of pavement distresses (fatigue cracking and permanent deformation) that are the failure criteria of the M-E design method as well as the Miner's hypothesis to determine the critical damage ratio. The critical damage ratio is the ratio between the actual number of repetitions (N_{ESAL}) to the lower value of an allowable number of repetitions of fatigue cracking (N_f) and permanent deformation (N_d). ANSYS

and KENPAVE programmes were used in this process to calculate the stresses and strains and then by using failure criteria models, fatigue life and rutting, allowable load repetitions to failure and tensile and compressive strains in the desired locations calculated for the design of pavement section. In addition, the critical damage rate for each mixture calculated in order to compare and analysis the results to determine the minimum asphalt concrete layer thickness required to withstand loading conditions (damage ratio less than unity).

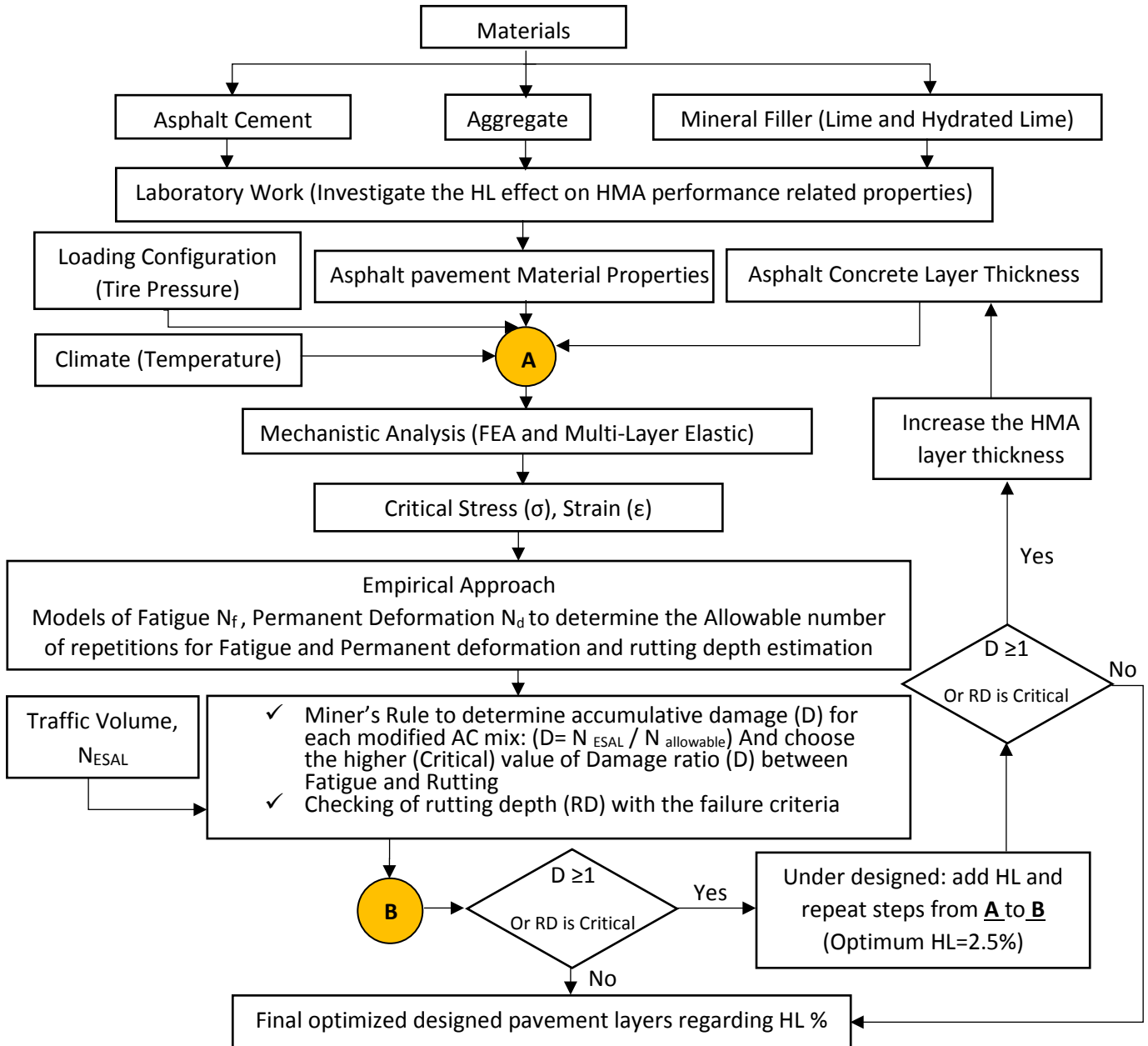


Figure (6-1) Mechanistic-Empirical Design Approach Flow Chart

6.2 Parameters Required For Flexible Pavement Analysis and Design

To design the structure of flexible pavement taking into the accounts the effect of hydrated lime, the following parameters should be estimated:

6.2.1 Traffic Loading

6.2.1.1 Loading Configuration and Dimensions

All the traffic loading types are converted to Equivalent Single Axle Load (ESAL) to simplify the input traffic requirements in accordance with AASHTO load equivalency factors (AASHTO, 1993). The adopted 80kN (18kip) ESAL configuration is shown in Figure (6-2). The required traffic information needed to estimate the 80kN (18kip) ESAL are the Annual Average Daily Traffic (AADT) and the traffic composition at the start of the analysis period. These values are obtained from the actual traffic counts on the existing pavement, where the fatigue life and permanent deformation prediction criteria to be performed. For the newly constructed pavement, traffic information can be obtained from nearby highways with similar travel patterns.

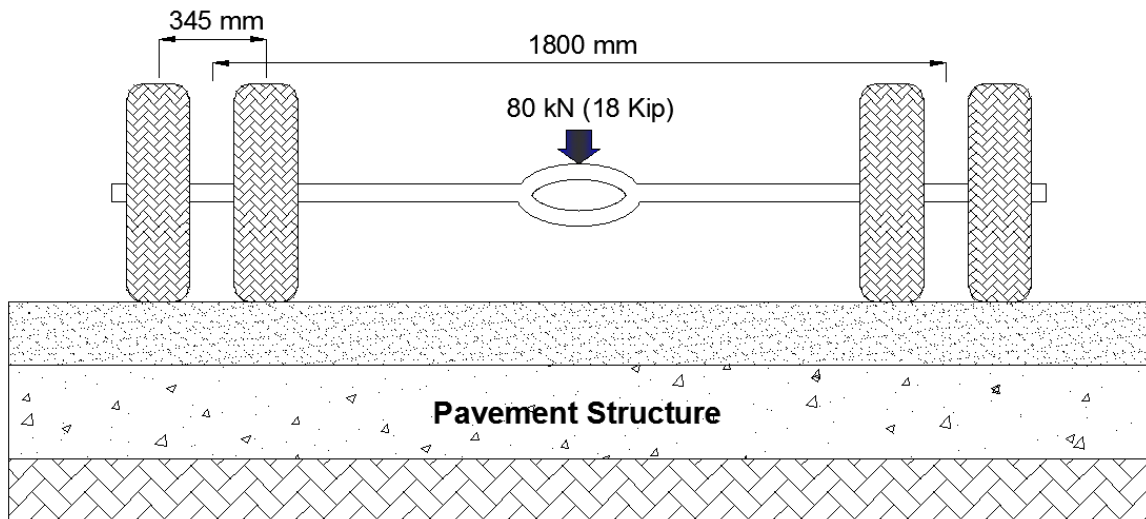


Figure (6-2) 80 kN (18-kip) ESAL Configuration

The procedure for determining the 80kN (18-kip) ESAL is summarised as follows (Huang, 2004):

- Estimate the number of the vehicle of various kinds, such as passenger cars (PC), single unit trucks, involving buses, and various unit truck types that could be in the proposed or existed facility.

- Determine the number of each type of vehicles on the design lane during the first year of analysis. It is calculated according to the following equation:

$$n_i = 365 \times AADT \times P_i \times D_d \times L_d \quad (6-1)$$

Where:

n_i = Number of vehicles type (i) on the design lane during the first year,

AADT = Annual Average Daily Traffic,

P_i = Percentage of i th vehicles in the AADT,

D_d = Directional distribution factor, which is usually assumed to be 0.5 unless the traffic in two directions is different and

L_d = Lane distribution factor. For two-lane highway, the lane distribution factor is 1 whereas for multilane highways its value ranges from 0.85 to 0.70 for two and three lanes in each direction, respectively.

- Determine the Equivalent Axle Load Factor (EALF) for each vehicle type. An equivalent axle load factor (EALF) defines the damage per pass to a pavement by the axle in question relative to the damage per pass of a standard axle load, usually the 80kN (18kip) single-axle load (Huang, 2004). The values of EALF for different vehicle types are presented elsewhere (AASHTO, 1993).
- For a given analysis period, the Asphalt Institute (AI, 1981) and the AASHTO design guide (AASHTO, 1986 and 1993) recommend the use of traffic over the entire design period to calculate the total growth factor according to the following relationship (Huang, 2004):

$$G_f = \frac{(1+r)^Y - 1}{r} \quad (6-2)$$

Where:

G_f = Total Growth factor,

r = Annual growth rate (decimal) and

Y = Analysis period (years).

- ESAL calculation: The total number of ESAL were calculated by multiplying the number of vehicles of each type during the first year (n_i) by the EALF and the growth factor (G_f) and sum the values determined to obtain the 18-kip ESAL applications during the analysis period. Table (6-1) shows the worksheet for the estimation of N_{ESALS} .

Table (6-1) Worksheet Proposal for Estimating the 80-kN ESAL Applications

<ul style="list-style-type: none"> • Road: 2-lane road • Traffic Analysis Period = 15 years • Assumed current AADT = 2500 (during the first year) • Directional distribution factor = 50 % • Lane distribution factor = 100% • Percentage of Trucks = 45% • Annual growth rate = 4 % 					
Vehicle type	Percentage of <i>ith</i> vehicles (P_i), %	Number of vehicles/lane per year (n_i)	Equivalent Axle Load Factor (EALF)	Growth Factor (G_f)	ESAL Applications
Passenger-vehicles (PCU)	55	250937.5	0.0008	20.02	4019.015
Single-unit trucks:					
2 axle, 4 tire	10	45625	0.003	20.02	2740.238
2 axle, 6 tire	10	45625	0.21	20.02	191816.6
3 axle or more	5	22812.5	0.61	20.02	278590.8
Tractor semitrailers and combinations:					
4-axle or less	5	22812.5	0.62	20.02	283157.9
5-axle	10	45625	1.09	20.02	995619.6
6-axle or more	5	22812.5	1.23	20.02	561748.7
Total	100	456250			2317693
The Estimated Design ESAL Applications = 2.318×10^6					

6.2.1.2 Contact Area between the Tire and Pavement

In the mechanistic approach of design, it is important to identify the contact area between the tire and pavement surface, so the axle load can be considered to transfer into each tire and distributed uniformly over the contact area. The dimensions of contact area rely on the contact pressure. In the pavement design, the contact pressure is usually found to be equal to the tire pressure (Huang, 2004). As heavier axle loads have higher tire pressures and more destructive impacts on pavements, the use of tire pressure as the contact pressure is accordingly on the safe side. Heavier axle loads are always applied on dual tires (Huang, 2004). Figure (6-3a) presents the approximate shape of the contact area for each tire, which is comprised of a rectangle and two half circles. By letting the length L and width $0.6L$, the area of contact is as follows:

$$A_c = \pi(0.3L)^2 + (0.4L)(0.6L) = 0.5227L^2, \text{ or}$$

$$L = \sqrt{\frac{A_c}{0.5227}} \quad (6-3)$$

In which A_c is the contact area between the tire and pavement that can be acquired by dividing the applied load on each tire by its pressure. The contact area exhibited in Figure (6-3a) was adopted earlier by Portland Cement Association (PCA) in 1966 for the design of rigid pavements. In 1984, the PCA proposed a method based on the finite element approach in which a rectangular contact area is assumed. The length of the rectangular area is $(0.8712L)$, and width is $(0.6L)$, which has the same area of $0.5227L^2$, as displayed in (6-3b). These contact areas are not axisymmetric and cannot be applied to the layered theory. In the flexible pavement design by using the layered theory, it is assumed that the contact area of each tire is circular. This hypothesis is not entirely correct, although the error obtained is considered to be small as compared to the realistic contact area (Huang, 2004). The contact area adopted in this study depends on the applied load on each tire. As the loading system is 80 kN (18 Kip) and there are dual tires on each side of the axle, the load on each tire is 20 kN. The pressure of the tire is 600 kPa (87 psi). Therefore, by dividing the load by the pressure, the contact area between tire and pavement will be 0.03334 m^2 . Regarding

determination of the dimensions of the contact area for finite element approach and multi layered theory, the radius of contact area for the multi-layered theory is 10.3 cm and for the finite element method will be according to Equation (6-3).

$$L = \sqrt{\frac{0.03334}{0.5227}} = 0.2525 \text{ m}$$

Therefore, the dimensions of the rectangular equivalent area are:

Length = 0.8712 * 0.2525 = 0.22 m

Width = 0.6 * 0.2525 = 0.15 m

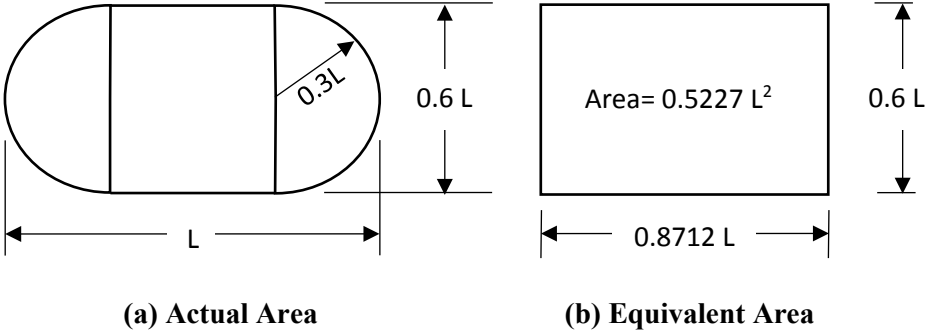


Figure (6-3) Dimensions of the Contact Area between Tire and Pavement (Huang, 2004)

6.2.2 Temperature Consideration

6.2.2.1 Asphalt Concrete Pavement Temperature as related to Air Temperature

Pavement temperature has been found to be in a strong relation with air temperature, solar radiation as well as other variables, but only the air temperature is readily available (Shtawi, 1984). The ambient temperature has a negligible influence on the stiffness of unbound materials (subbase and subgrade layers) as compared to asphalt concrete mixtures. Temperature strongly affects the elastic and plastic properties of asphalt concrete due to the physical characteristics of the binder component in the mixture (asphalt cement) that makes it susceptible to temperature variation and that leads to change in the mechanical behaviour of the asphalt concrete mix as a whole structure.

In this study, the model is shown in Equation (6-4) that developed by (Albayati and Alani, 2015) was used for prediction of pavement temperature. In the model, the pavement layer temperature is a function of the air temperature and the depth below the pavement surface. They conducted a field measurement of air temperature and the temperature in the asphalt pavement at various depths. They made a comparison between their model and two models that widely used in the pavement engineering community, Witczak (1972) and SHRP (1994). They found that the majority of temperature values predicted by Witczak model were higher than the measured values. For the Superpave model (SHRP, 1994), the predicted temperatures were much higher than the measured ones by about 20°C at low temperatures of pavement (20's°C), while at higher temperatures of pavement (about 60°C), the difference between predicted and measured temperatures became lower to be about 12°C. According to the outcome, their model had to be more realistic for pavement temperature estimation.

Based on the available information and the characteristics of materials and the standards that the laboratory tests based on as well as the need for application of Mechanistic-Empirical design for more accuracy in estimation of pavement structural responses affecting failure criteria in Iraq, the city of Baghdad in Iraq will be the case study in this chapter. Regarding the ambient temperature, the Iraqi Meteorological Organization and Seismology (IMOS) provide on their website the Climatic Atlas of Iraq that in which the Mean Annual Air Temperature (MAAT) is about 23°C in Baghdad. Figure (6-4) shows the contour distribution of MAAT of Iraq.

$$T_{pave} = 1.217 \times T_{air} - 0.354 \times Z \quad (6-4)$$

Where:

T_{pave} = Design pavement temperature (°C).

T_{air} = Design air temperature (°C).

Z = Depth of pavement in cm below the pavement surface.

6.2.2.2 Prediction of Resilient Modulus as related to Temperature and Depth

In the experimental work of this study, the resilient modulus of each mixture (wearing, levelling and base courses) was determined at 20°C, 40°C and 60°C. As stated in Chapter 4, the application of hydrated lime into the mixtures enhanced the resilient modulus values of them. Furthermore, it has been noticed that there is a significant effect of temperature on the resilient modulus of each paving mix so that their characteristics will deteriorate with the rise of temperature. Figures (6-5), (6-6) and (6-7) show the influence of temperature on wearing, levelling and base course mixtures as related to hydrated lime addition.

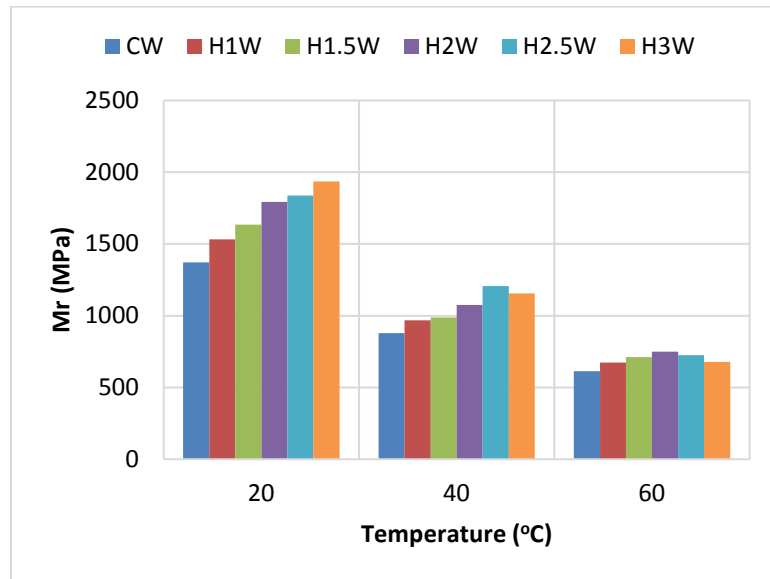


Figure (6-5) Temperature Effect on the Resilient Modulus of Wearing Course Mixtures

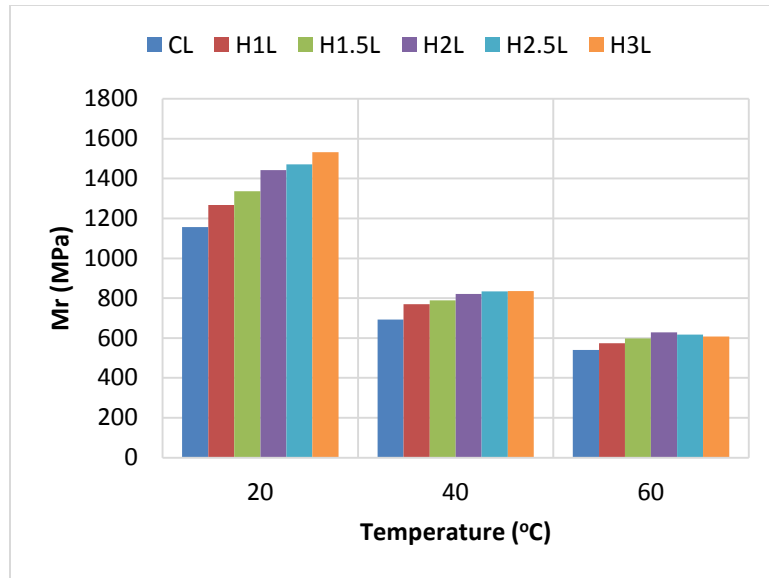


Figure (6-6) Temperature Effect on the Resilient Modulus of Levelling Course Mixtures

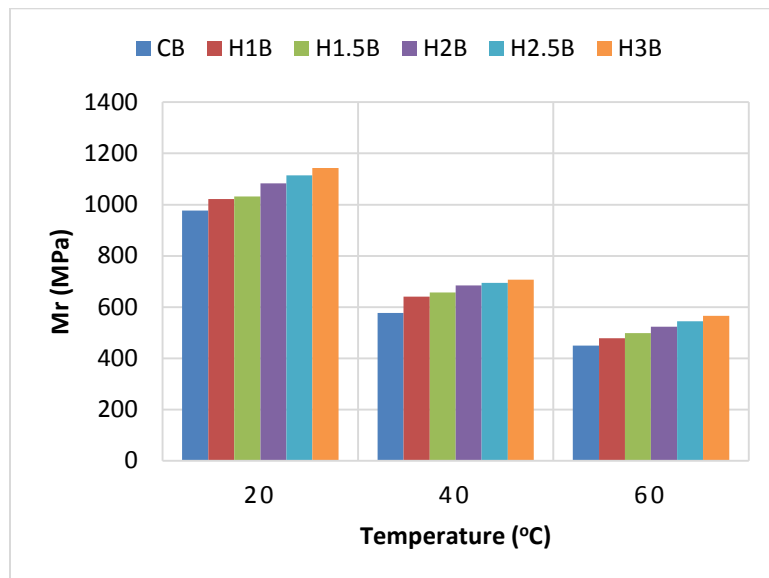


Figure (6-7) Temperature Effect on the Resilient Modulus of Base Course Mixtures

For analysis and design purpose and after determination of the optimum addition per cent of hydrated lime into the asphalt concrete mix (2.5%), the control and the hydrated lime modified mixtures for each type of pavement course have been considered in this chapter. The Figures (6-8) and (6-9) present the relation between the resilient modulus and temperature for each mix at 0% of hydrated lime (control) and 2.5% of hydrated lime (optimum) respectively. As seen in the Figures, the best fit form of equations that relates the resilient modulus of mixtures with temperature is a polynomial equation of the second degree with a correlation coefficient (R^2) of 1. This behaviour can be found in both of control (no hydrated lime) mixtures and the optimised mixtures (modified with 2.5% of hydrated lime). The predicted equations could be useful to calculate the resilient modulus of flexible pavement at a specific asphalt concrete layer depth due to changing of temperature with respect to pavement depth.

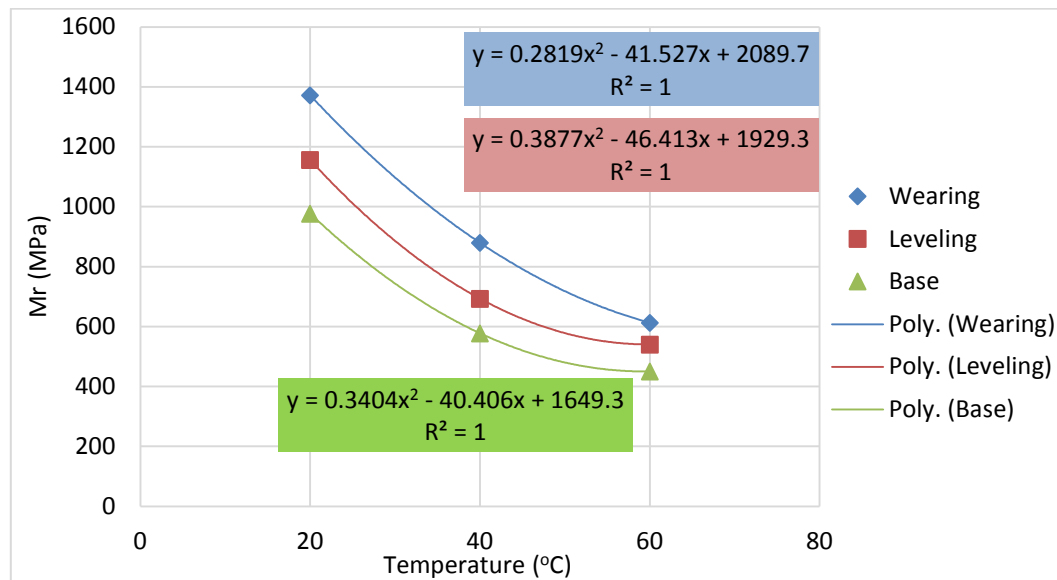


Figure (6-8) Influence of Temperature on the Resilient Modulus of Control Mixtures

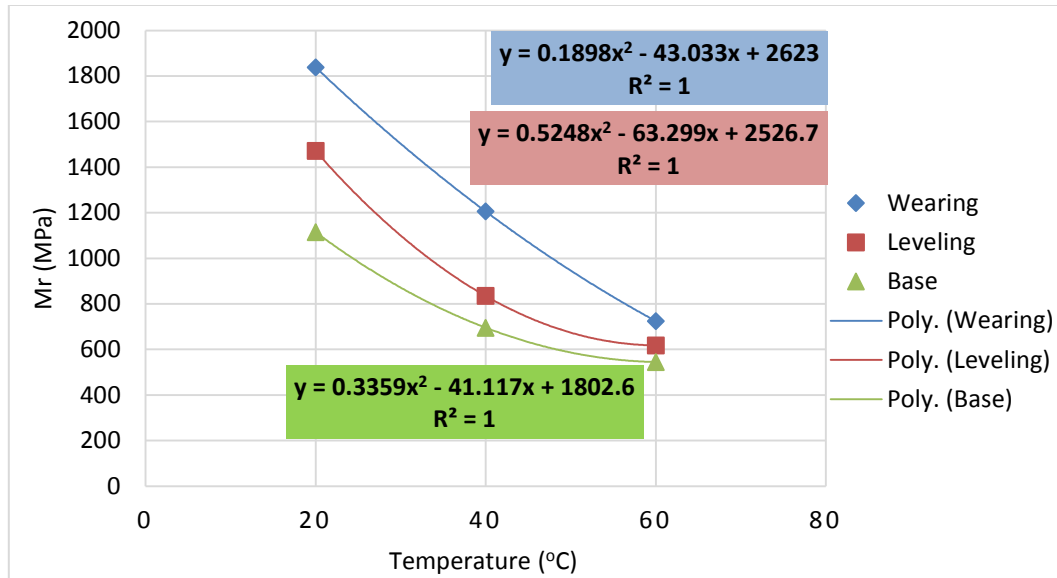


Figure (6-9) Influence of Temperature on the Resilient Modulus of Modified Mixtures (2.5% of Hydrated Lime)

After consideration of air temperature to find the pavement temperature at a specific depth (Equation (6-4)), the resilient modulus of the pavement asphalt concrete layer can be estimated based on the following suggested equations that relate resilient modulus of pavement layer with pavement temperature:

1) For Control Mixtures:

a) Wearing Course:

$$M_r = 0.2819 \times T_{pave}^2 - 41.527 \times T_{pave} + 2089.7 \quad (6-5)$$

b) Levelling (Binder) Course:

$$M_r = 0.3877 \times T_{pave}^2 - 46.413 \times T_{pave} + 1929.3 \quad (6-6)$$

c) Base Course:

$$M_r = 0.3404 \times T_{pave}^2 - 40.406 \times T_{pave} + 1649.3 \quad (6-7)$$

2) For Hydrated Lime Optimized Mixtures:

a) Wearing Course:

$$M_r = 0.1898 \times T_{pave}^2 - 43.033 \times T_{pave} + 2623 \quad (6-8)$$

b) Levelling (Binder) Course:

$$M_r = 0.5248 \times T_{pave}^2 - 63.299 \times T_{pave} + 2526.7 \quad (6-9)$$

c) Base Course:

$$M_r = 0.3359 \times T_{pave}^2 - 41.117 \times T_{pave} + 1802.6 \quad (6-10)$$

Where:

M_r = resilient modulus of mixture (MPa),

T_{pave} = pavement temperature (°C).

6.2.3 Material Response Properties

In the process of design and analysis of asphalt pavement structure, either by finite element analysis method or the axisymmetric multi-layer elastic method, it is necessary to determine resilient modulus and Poisson's ratio of the pavement material, which define the stiffness of the material. These properties are needed for the calculation of the stresses, strains and deflections response in the pavement system under the application of traffic loading.

The methods used to obtain materials response properties for the different pavement layers, asphalt concrete, subbase and subgrade are described below:

- **Asphalt Concrete Layers**

The resilient modulus values of asphalt concrete layers are found from the repeated load test on controlled and modified mixtures. Table (6-2) displays the output of Equations (6-5) to (6-10) to determine the Resilient Modulus (M_r) of controlled and optimised asphalt concrete mixtures at various depth values. The optimum value of the hydrated lime is 2.5% as a partial replacement of limestone dust for the application of wearing, leveling and base courses.

Table (6-2) Resilient Modulus of Asphalt Concrete Mixtures at Various Depths

Depth (cm)	Air Temp. (°C)	Pave Temp. (°C)	Resilient Modulus (MPa)					
			Control Mixtures			Modified Mixtures		
			Wearing	Leveling	Base	Wearing	Leveling	Base
1	23	27.637	1157.335	942.7106	792.5982	1578.667	1178.15	922.8112
2	23	27.283	1166.555	951.6033	800.284	1590.211	1190.355	930.8361
3	23	26.929	1175.845	960.5931	808.055	1601.802	1202.691	938.9453
4	23	26.575	1185.206	969.6801	815.9115	1613.441	1215.159	947.1386
5	23	26.221	1194.638	978.8643	823.8532	1625.127	1227.758	955.4161
6	23	25.867	1204.141	988.1457	831.8802	1636.861	1240.489	963.7778
7	23	25.513	1213.714	997.5242	839.9926	1648.642	1253.352	972.2237
8	23	25.159	1223.358	1007	848.1902	1660.471	1266.346	980.7538
9	23	24.805	1233.072	1016.573	856.4732	1672.348	1279.471	989.3681
10	23	24.451	1242.858	1026.243	864.8415	1684.272	1292.729	998.0665
11	23	24.097	1252.713	1036.01	873.2951	1696.244	1306.117	1006.849
12	23	23.743	1262.64	1045.874	881.8341	1708.263	1319.637	1015.716
13	23	23.389	1272.637	1055.836	890.4583	1720.33	1333.289	1024.667
14	23	23.035	1282.705	1065.895	899.1679	1732.445	1347.072	1033.702
15	23	22.681	1292.843	1076.05	907.9627	1744.607	1360.987	1042.822
16	23	22.327	1303.052	1086.303	916.8429	1756.817	1375.033	1052.025
17	23	21.973	1313.332	1096.654	925.8084	1769.074	1389.211	1061.313
18	23	21.619	1323.683	1107.101	934.8592	1781.379	1403.521	1070.685
19	23	21.265	1334.104	1117.646	943.9954	1793.731	1417.961	1080.141
20	23	20.911	1344.595	1128.287	953.2168	1806.131	1432.534	1089.681

Table (6-2) Continued

Depth (cm)	Air Temp. (°C)	Pave Temp. (°C)	Resilient Modulus (MPa)					
			Control Mixtures			Modified Mixtures		
			Wearing	Leveling	Base	Wearing	Leveling	Base
21	23	20.557	1355.158	1139.026	962.5236	1818.578	1447.238	1099.306
22	23	20.203	1365.791	1149.862	971.9157	1831.073	1462.073	1109.015
23	23	19.849	1376.494	1160.795	981.3931	1843.616	1477.04	1118.807
24	23	19.495	1387.269	1171.826	990.9558	1856.206	1492.139	1128.685
25	23	19.141	1398.114	1182.953	1000.604	1868.844	1507.369	1138.646
26	23	18.787	1409.029	1194.178	1010.337	1881.529	1522.731	1148.691
27	23	18.433	1420.016	1205.5	1020.156	1894.262	1538.224	1158.821
28	23	18.079	1431.072	1216.919	1030.06	1907.043	1553.848	1169.035
29	23	17.725	1442.2	1228.435	1040.049	1919.871	1569.605	1179.333
30	23	17.371	1453.398	1240.049	1050.124	1932.746	1585.492	1189.715
31	23	17.017	1464.667	1251.759	1060.284	1945.669	1601.512	1200.181
32	23	16.663	1476.007	1263.567	1070.529	1958.64	1617.662	1210.732
33	23	16.309	1487.417	1275.472	1080.859	1971.658	1633.945	1221.367
34	23	15.955	1498.898	1287.474	1091.275	1984.724	1650.359	1232.086
35	23	15.601	1510.449	1299.574	1101.776	1997.838	1666.904	1242.889
36	23	15.247	1522.071	1311.77	1112.363	2010.999	1683.581	1253.776
37	23	14.893	1533.764	1324.064	1123.035	2024.207	1700.389	1264.748
38	23	14.539	1545.528	1336.454	1133.792	2037.464	1717.329	1275.803
39	23	14.185	1557.362	1348.942	1144.634	2050.767	1734.401	1286.943
40	23	13.831	1569.267	1361.527	1155.562	2064.119	1751.604	1298.167

The second response property is the Poisson ratio (ν). It is defined as the ratio of the lateral strain to the axial strain. By measuring the axial and lateral strains during the resilient modulus test, the Poisson ratio can be determined. The influence of Poisson ratio on the asphalt pavement evaluation and performance prediction is comparatively slight. Therefore, it is usual to assume a reasonable value in performance prediction instead of determining it from actual tests (Southgate et. al., 1977). Table (6-3) shows the range and typical Poisson ratios values for paving materials.

Hence, typical values of Poisson ratios of the asphalt concrete layer, the subbase layer, and the subgrade soil were assumed according to Table (6-3).

- **Subbase Layer**

The Shell oil company researchers (Claessen et al. 1977) developed the method adopted for the estimation of the resilient modulus of the subbase granular material. The subbase resilient modulus, in this approach, is assumed to be a function of the resilient modulus of subgrade according to the following relationship:

$$M_{R(subbase)} = K \times M_{R(subgrade)} \quad (6-11)$$

Where: $K = 0.2 h^{0.45}$

h = the thickness of subbase layer in mm

M_R = the resilient modulus in psi

The relationship is applicable in the range $2 < k < 4$.

- **Subgrade layer**

Similarly, the subgrade resilient modulus was estimated using the relationship developed by the Shell investigators (Claessen et. al. 1977). The relationship is based on the correlation between dynamic in-situ tests for the subgrade resilient modulus, and the corresponding laboratory measured CBR value (California Bearing Ratio), CBR value for the subgrade soil can be obtained according to standard test procedure of ASTM D-1883, the relationship is given below:

$$M_{R(subgrade)} = 1450CBR \quad (6-12)$$

Where M_R is the subgrade resilient modulus expressed in psi, and CBR value for the subgrade soil is expressed as a percentage.

Table (6-3) Poisson Ratios for Different Paving Materials (Southgate et. al., 1977)

Material	Range	Typical Value
Asphalt concrete	0.30 - 0.40	0.35
Unstabilized granular subbase and base	0.30 - 0.45	0.4
Silty subgrade	0.35 - 0.45	0.45
Clay subgrade	0.4 – 0.5	0.5

6.2.4 Miner's hypothesis

The expected traffic or load cycles, n , for a given design life is considered to calculate a damage factor under particular conditions (i.e., particular truck load and configuration along with in situ pavement and climatic conditions). The damage ratio, the ratio of traffic loading repetitions to the number of repetitions to failure, for each condition is typically added to the others using Equation (6-13), where the failure criteria are reached when the sum of ratio approaches unity (Miner, 1945):

$$D = \sum \frac{n_i}{N_i} \quad (6-13)$$

Where

n_i = Traffic load repetitions

N_i = Load repetitions to failure

6.3 Finite Element Analysis

The Finite element (FE) modelling techniques have considerably increased the capability to express models of physical phenomena correlated to various structural complexities since they substitute the real structural continuum member with an equivalent member comprised of discrete elements that joined with nodes. Dividing the whole original structure into a finite number of elements will facilitate having fairly more easily understood the behaviour of the model than the actual continuum system.

This section manifests the finite element modelling of a flexible pavement structure using ANSYS Ver.12 (ANSYS 2009) software package. In general, the outcomes and techniques would be quite similar using other FEA programmes. Nevertheless, every programme has its individual analysis methods, features nomenclature and specific elements that require being applied suitably.

In this study, a 3-dimensional finite element model made to simulate a section of a flexible pavement. In general, the model includes dimensions of pavement layers, material properties, all the elements, nodes, loading configuration, boundary conditions, and other characteristics that were utilised to describe the physical system. Comparisons between finite element results and those from the Multi-Layered Elastic Theory (MLET), by KENPAVE programme are shown.

6.3.1 Finite Element Modelling of Pavement Structure

The geometric dimensions of the pavement structural components are required as structure input parameters for the mechanistic analysis. The structure of the flexible pavement adopted in this study consists of five layers, three of them represent the asphalt concrete layer, and they are the wearing, leveling (binder) and base course, the other two layers are the granular subbase and compacted subgrade soil. The dimensions of the model are 4000 mm width on the transverse side of the driving direction, and 2000 mm in parallel with the driving direction with a subgrade depth of 2500 mm and subbase thickness of 300 mm with a thickness of the whole asphalt concrete ranged from 180 mm to 240 mm. Based on iterations and calculations, it was found that the results of displacements, stresses and strains are converging. More explicitly, when the dimensions increased beyond than that mentioned above, it will consume much more time of processing, and there will be no significant change in the results. Figure (6-10) shows the structure assumed in the study. Asphalt concrete layer thickness is not fixed, and iterations may be done to reach optimum thicknesses with the addition of hydrated lime.

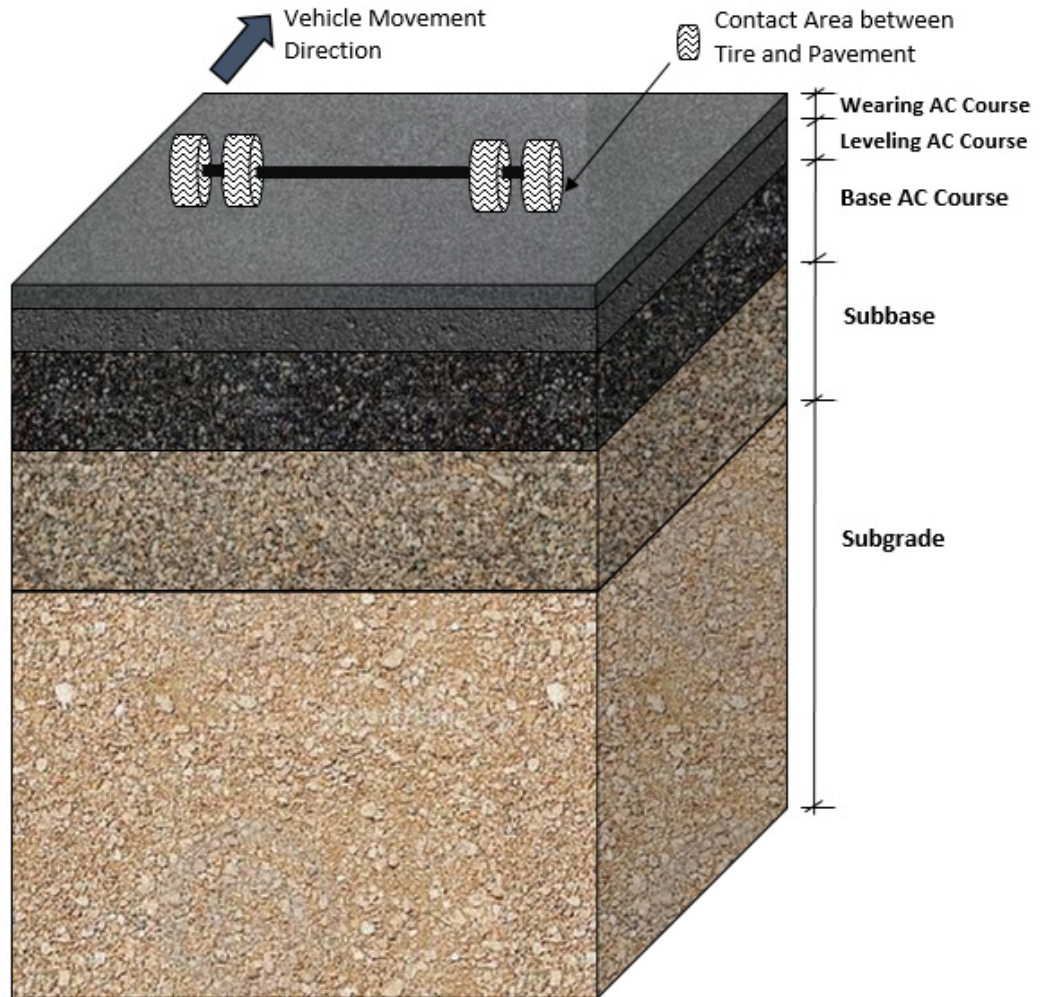


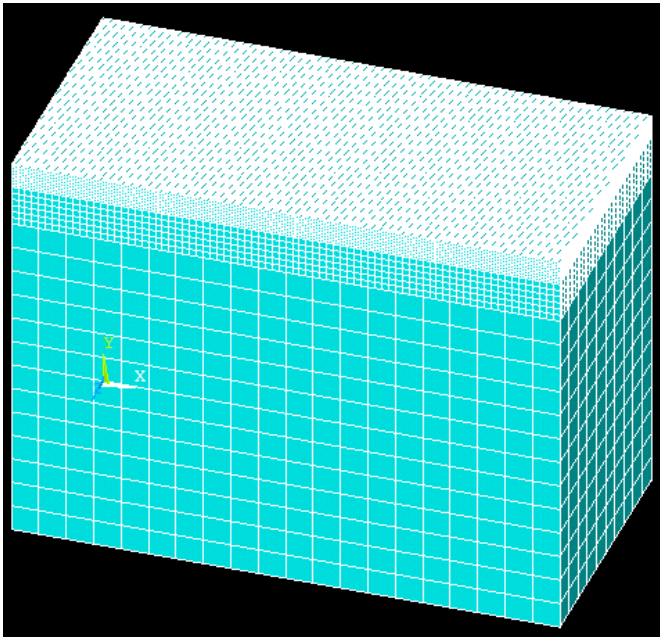
Figure (6-10) Pavement Structure and Loading Configuration for FE Analysis

In the Finite Element Analysis (FEA), the step after creating of model structure and material properties is the meshing of the model structure, and then applying of loading and boundary conditions. After that, stresses and strains are determined at integration points within the structure elements. The selection of a proper mesh density is an essential step in the FE modelling. A convergence of results is achieved if a satisfactory number of elements are used in the structure of a model, and the mesh sensitivity study is the way to decide the sufficient density of the mesh. The adequate number of elements can be achieved at the point when an increment in the mesh density has a negligible influence on the results. Hence, in the finite element modelling, a convergence study was carried out to determine an appropriate mesh density.

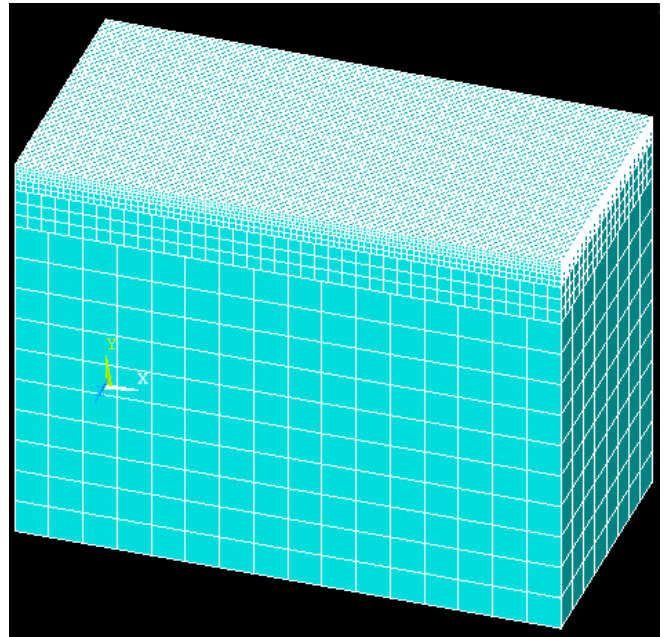
The comparisons between the results obtained from KENPAVE software and the ANSYS software results of the several different element sizes was performed. For the Wearing Course, the trial sizes of elements were 20mm, 25mm and 50mm, and regarding the Leveling Course, the elements sizes were 20mm, 30mm, 40mm, 45mm, 80mm and 90mm. The trial elements sizes of Base course were 20mm, 40mm, 50mm, 55mm, 90 mm, 100mm and 110mm, while the subbase layer's elements sizes were 50mm, 100mm and 150mm. The sizes of elements for the subgrade layer were 200mm and 250mm. The comparison shows that due to change in the depth of the asphalt concrete layer (wearing, levelling and base courses) for each model, the elements sizes explained in Table (6-4) gave the best convergence of the FE results. In general, the proper element size is the half of each of the asphalt concrete layer thickness and 100mm for the subbase layer while for the subgrade layer the element size was 250mm. The Figure (6-11) presents the three different mesh densities for the case of (a 40mm thickness for Wearing course, 60mm for Leveling course and 80mm for Base course). The difference was in the element size so that the first try was 20 mm of element width and then the element size was equal to half of the asphalt concrete layers thickness, and finally when the element size is equal to each of asphalt concrete layer thickness. The subbase layer's element size was 50mm, 100mm and 150mm (half of the layer thickness). While the element size of the subgrade layer was 200mm, 250mm and 250mm for the trials a, b and c respectively as seen in Figure (6-11).

Table (6-4) The Adequate Element Size for each Layer in the Pavement Model

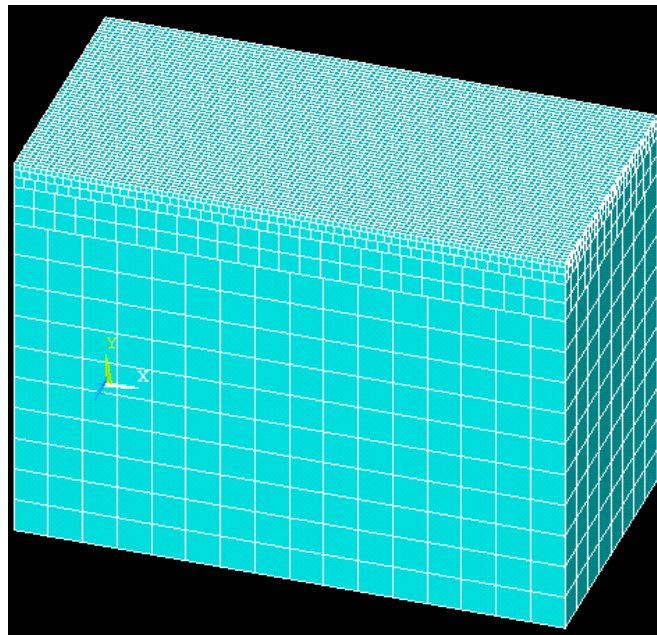
Layer Type		Thickness (mm)	Element Size (mm)	Number of Elements
Asphalt Concrete	Wearing	40	20	40000
		50	25	25600
	Leveling	60	30	17778
		70	35	13061
		80	40	10000
		90	45	7901
	Base	80	40	10000
		90	45	7901
		100	50	6400
Granular Subbase		300	100	800
Subgrade		2500	250	1280



a) FE model with 20 mm elements size for asphalt concrete layer thickness



b) FE model with the size of an element equal to half of asphalt concrete layer thickness



b) FE model with the size of an element equal to asphalt concrete layer thickness

Figure (6-11) Mesh Density of FE Model in ANSYS

- **Loading Configuration and Boundary Conditions**

The loading configuration was made by converting all types of traffic loads and sets into an Equivalent Single Axle Load (ESAL) according to AASHTO guide for pavement design. This loading system is one axle with dual tires on each side. The total axle load is 80kN (18Kip). Therefore, the load is 20kN on each tire, and pressure is 0.6 MPa, and the imprint (contact) area between tire and pavement surface is of 220mm by 150mm with a spacing of 125mm between the dual tires. Figure (6-12) shows the finite element pavement model in ANSYS

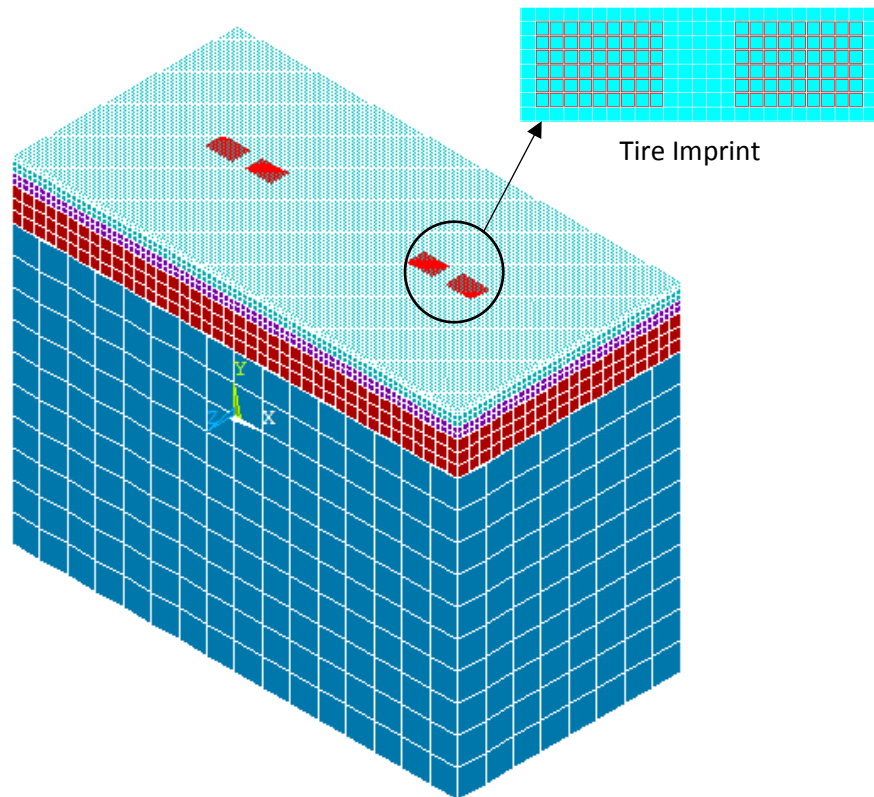
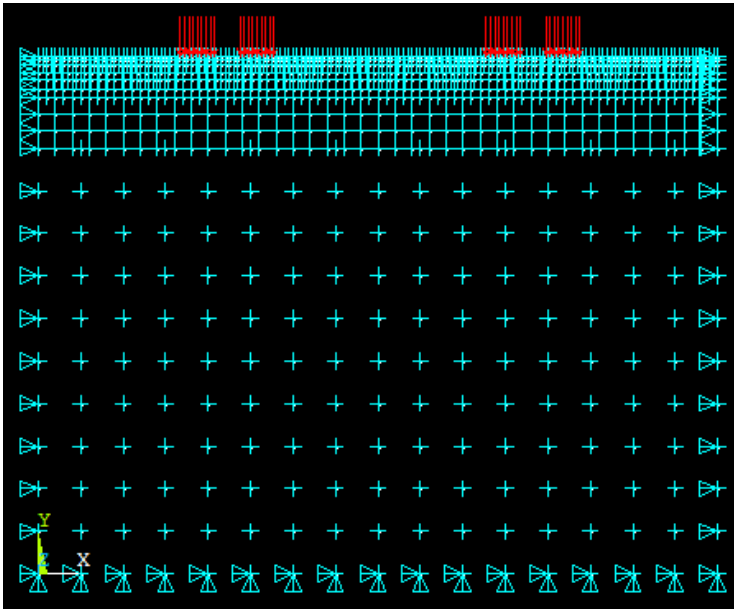
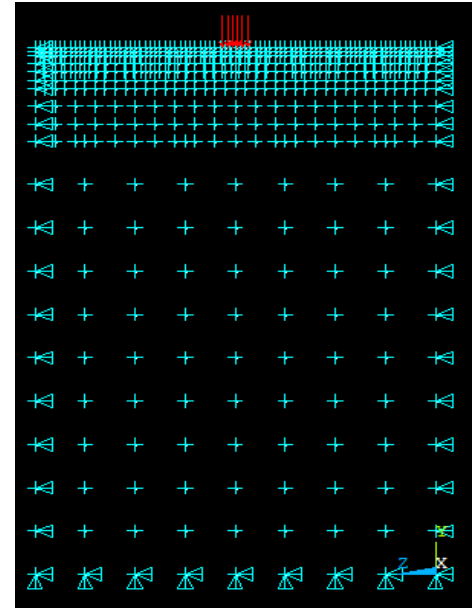


Figure (6-12) FEM of the Pavement Structure with Loading Configuration

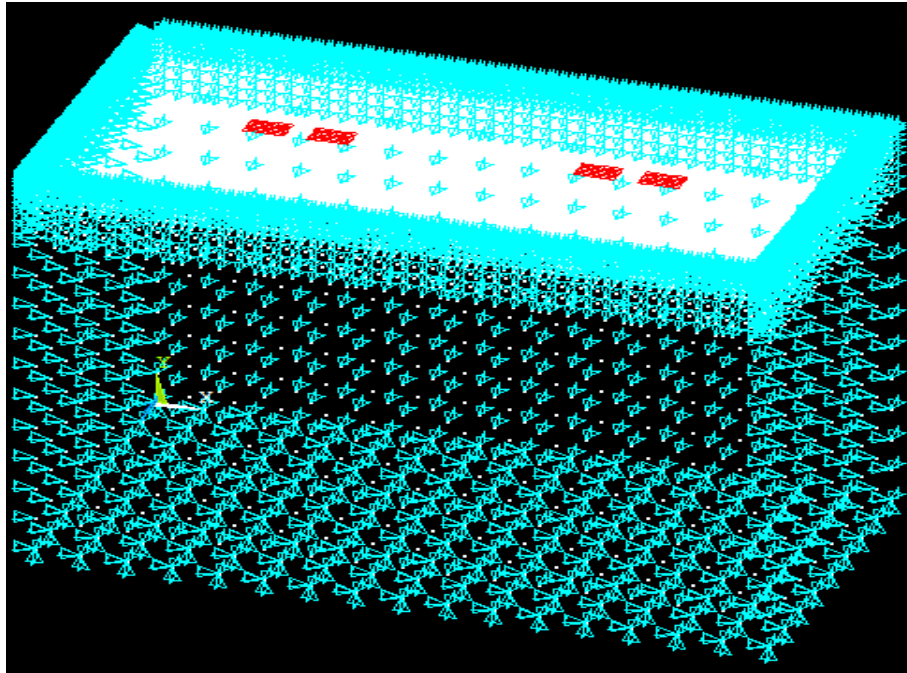
Regarding the boundary conditions of the pavement model, the displacements at the bottom of subgrade layer are restrained, which means that the nodes of the elements at the bottom of the layer cannot move in the vertical and horizontal directions. At the both vertical edges of the model sides that parallel and perpendicular to the vehicle movement direction, the displacement in the horizontal direction is restricted, but it is permitted in the vertical direction. The interface between the layers of the pavement assumed to be fully bonded, so there is no slipping permitted. Figure (6-13) shows the boundary conditions applied to the pavement model.



a) Front View of Model



b) Side View of Model



c) Isometric View of the Model

Figure (6-13) Boundary Conditions of the pavement Model

- **Element Types and Material Properties**

In the Mechanistic-Empirical Pavement Design Guide (M-E PDG), the FEM adopted that the asphalt concrete layer is modelled as a linearly elastic material with stiffness given by the mixture dynamic modulus (NCHRP, 2004). Therefore, the experimental values of the modulus of elasticity (M_r) and the assumed values of the Poisson's ratio (ν) were used to identify the isotropic properties of the asphalt concrete layers of the structural flexible pavement model adopted in this study.

The SOLID45 element is selected to model the pavement structure. The element has eight nodes, and each node has three translational degrees of freedom in nodal x , y and z directions as shown in Figure (6-14). It has plasticity, hyperelasticity, stress stiffening, creep, large deflection, and large strain capabilities (ANSYS 12, 2009).

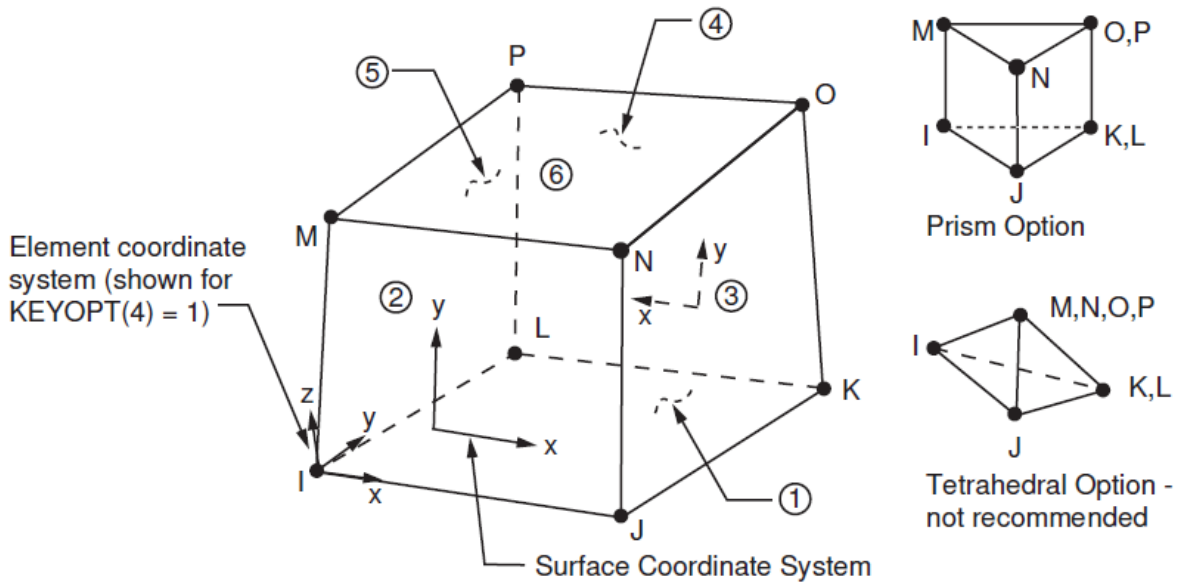


Figure (6-14) SOLID45 Element Geometry (ANSYS 12, 2009)

To simulate interfacial behaviour, CONTA174 elements were used to represent the bonding surface between the pavement layers in the model. CONTA174 is used to represent contact and sliding between 3-D “target” surfaces (TARGE170) and a deformable surface, defined by this element. The element is applicable to 3-D structural and coupled field contact analyses.

This element is located on the surfaces of 3-D solid or shell elements with mid-side nodes. It has the same geometric characteristics as the solid or shell element face with which it is connected. Contact occurs when the element surface penetrates one of the target segment elements (TARGE170) on a specified target surface. Coulomb and shear stress friction is allowed. This element also allows separation of bonded contact to simulate interface delamination (ANSYS 12, 2009).

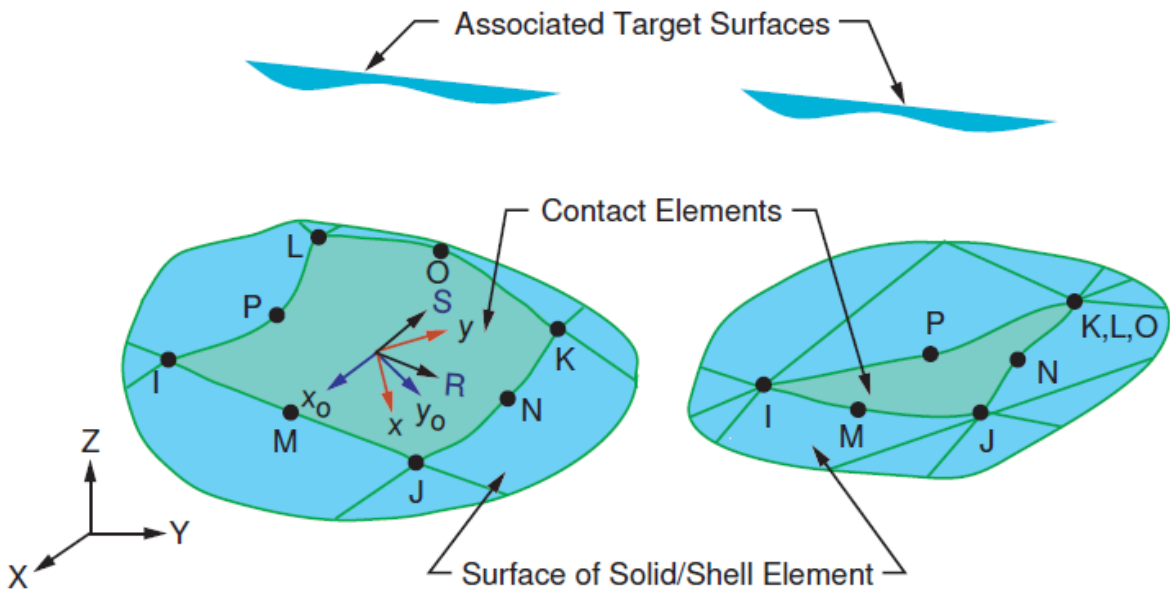


Figure (6-15) CONTACT174 Element geometry (ANSYS 12, 2009)

TARGE170 element is used to represent various 3-D “target” surfaces for the associated contact elements. The contact elements themselves overlay the solid, shell, or line elements describing the boundary of a deformable body and are potentially in contact with the target surface, defined by TARGE170. This target surface is discretized by a set of target segment elements (TARGE170) and is paired with its associated contact surface via a shared real constant set (ANSYS 12, 2009).

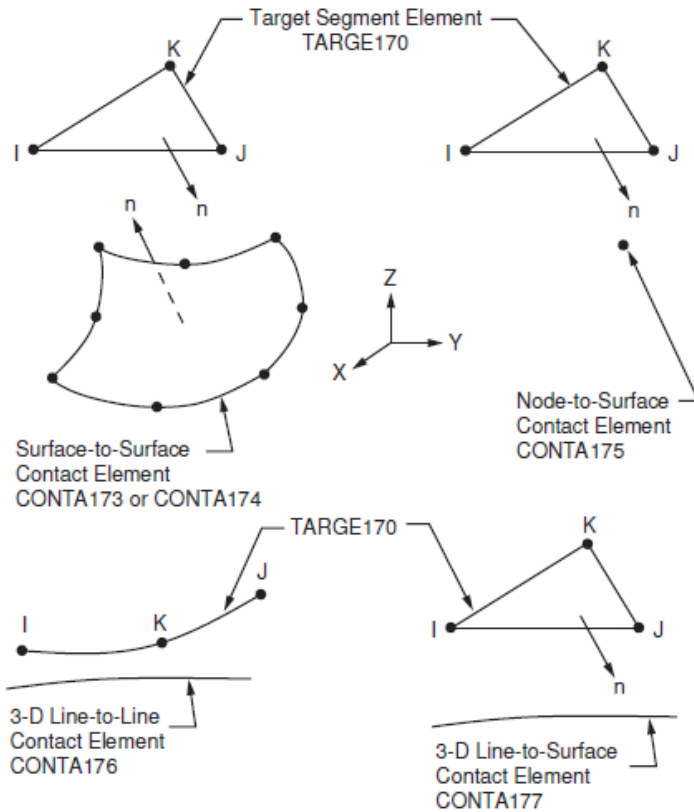


Figure (6-16) Targe170 Element geometry (ANSYS 12, 2009)

In nonlinear solution, the total load applied to a finite element model is divided into a series of load increments called load steps. At the completion of each incremental solution, the stiffness matrix of the model is adjusted to reflect nonlinear changes in structural stiffness before proceeding to the next load increment. The ANSYS programme uses Newton-Raphson equilibrium iterations for updating the model stiffness. Newton-Raphson equilibrium iterations provide convergence at the end of each load increment within tolerance limits. Figure (6-17) shows the use of the Newton-Raphson approach in a single degree of freedom nonlinear analysis (Kachlakev et al., 2001).

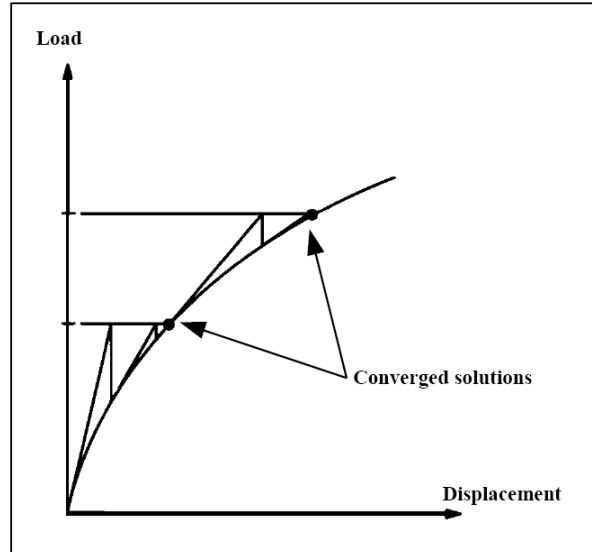


Figure (6-17) Newton-Raphson Iterative Solution (2 Load Increments) (ANSYS 1998)

Prior to each solution, the Newton-Raphson approach assesses the out-of-balance load vector, which is the difference between the restoring forces (the loads corresponding to the element stresses) and the applied loads. Subsequently, the program carries out a linear solution, using the out-of-balance loads, and checks for convergence. If convergence criteria are not satisfied, the out-of-balance load vector is re-evaluated, the stiffness matrix is updated, and a new solution is attained. This iterative procedure continues until the problem converges. In this study, for the reinforced concrete solid elements, convergence criteria were based on force and displacement, and the convergence tolerance limits were initially selected by the ANSYS programme.

6.3.2 FEA Results Comparison with Multi-Layer Elastic Theory

The finite element modelling is a numerical analysis method for achieving approximate solutions to a large-scale of engineering problems. Despite formerly developed to investigate the stresses in airframe structures, it has since been extended and implemented to deal with a wide range of continuum mechanics (Huebner et al., 2001). The finite element modelling approach offers the best method of analysis for multilayered pavement systems. Three-dimensional and two-dimensional or axisymmetric finite element models have different element formulation and

consider different directional components of stresses and strains. Three-dimensional finite element analysis can consider all three directional response components and should predict more accurate pavement responses (Kim et. al, 2009). In a continuum problem (e.g., one that involves a continuous surface or volume) the variables of interest commonly hold remarkably several values because they are functions of each general point in the continuum. For instance, the stress in a specific element in the pavement structure cannot be solved with one simple equation since the functions that define its stresses are specified to its particular location. Though, the finite element approach can be used to divide a continuum, such as the pavement volume, into small discrete volumes (elements) so that each one of these volumes has its own numerical solution instead of an exact closed-form solution for the total pavement volume. Besides, using a layered elastic analysis computer programme will provide calculating the theoretical stresses, strains, and deflections at any point in a pavement structure. Nevertheless, there are a few critical locations that are often used in pavement analysis. The finite elements approach allows for extremely powerful graphical displays of the values of the above responses at any point with a contour distribution based on either elemental or nodal solution. The FEM technique runs with a more complicated numerical model than the layered elastic approach; therefore it makes fewer assumptions (Pavementinteractive.org, 2017).

However, the results of the pavement modelling still need to be verified with results from either laboratory work, in which it is impossible to make such a model in laboratory conditions and requirements, or compared with field results, and these kind of information are not available due to limitation of time and research funding and facilities. The third option is to compare the results gained by the implementation of finite element modelling using the general purpose software ANSYS ver.12 with another software used for pavement analysis and design. The software is KENPAVE, and it adopts the multi-linear elastic theory in the calculation of pavement response.

KENPAVE is a software developed by Huang (2004). The first version was at 1993 named KENLAYER that worked in MS-DOS system. The software can be applied to flexible pavements with no joints. The backbone of KENPAVE is the solution for an elastic multilayer system under a circular loaded area and the determination of the pavement response (stress, strain and deflection) at predetermined points within the pavement structure. Damage analysis can be made by dividing the applied number of repetitions to the allowable number of repetitions for a specific period. The

damage caused by fatigue cracking and permanent deformation can be calculated for several periods, in each period, loading is summed up to evaluate the design life. The same pavement model parameters adopted in ANSYS, such as dimensions of structural section, layers modulus of elasticity, loading configuration and bonding between pavement layers were used as input to run the KENPAVE programme to determine the required stresses and strains at predetermined points within the pavement structure for the prediction purpose. The parameters used for verification are vertical stress, vertical strain, horizontal strain and finally vertical displacement. The verification parameters represent the main response factors that the M-E design approach rely on for mechanistic analysis of pavement structure. Figure (6-18) show the multi-layer system of KENPAVE in cylindrical coordinates.

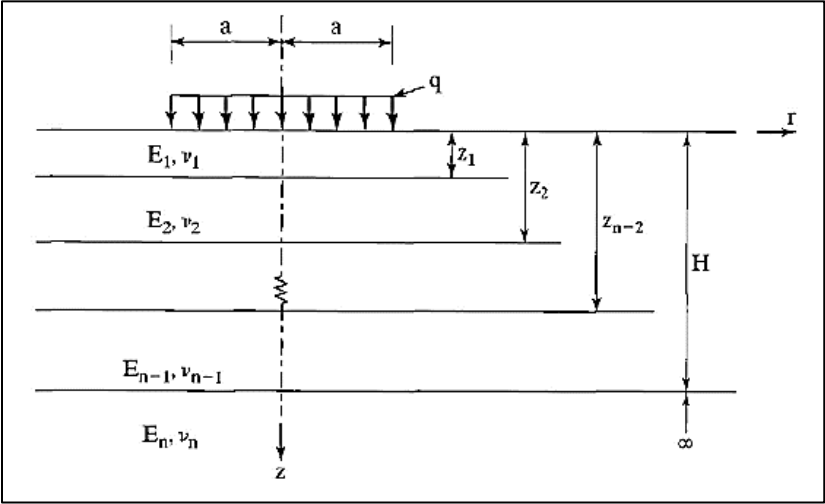


Figure (6-18) The n-layer system in cylindrical coordinates (Huang, 2004)

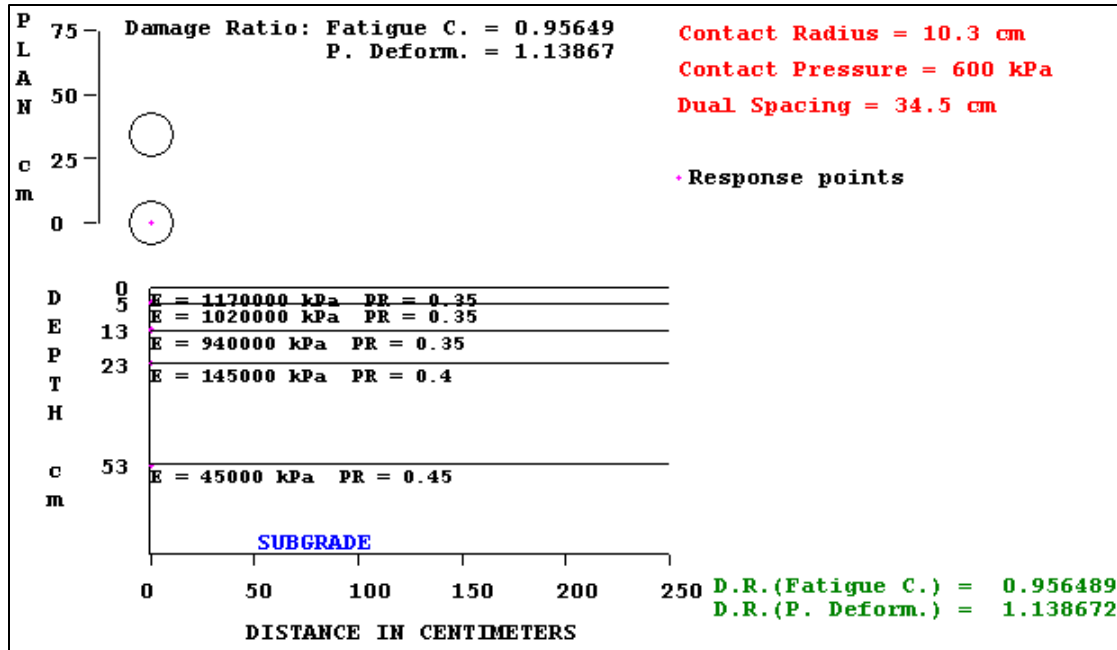
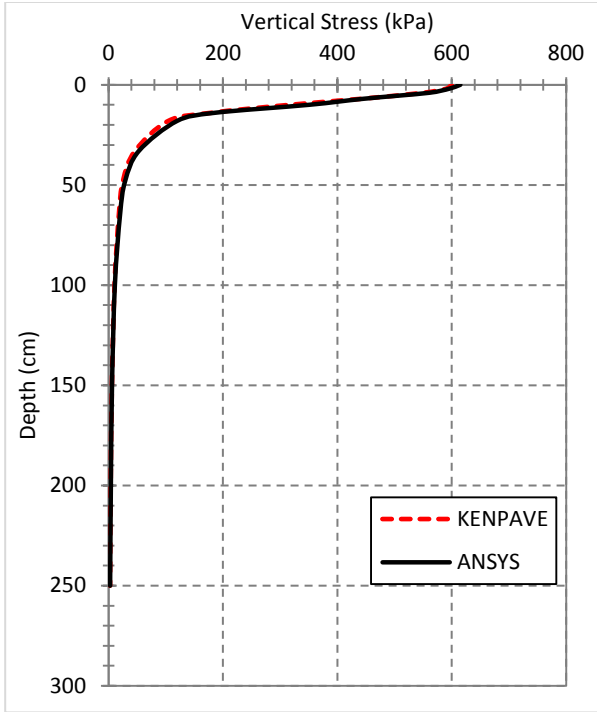


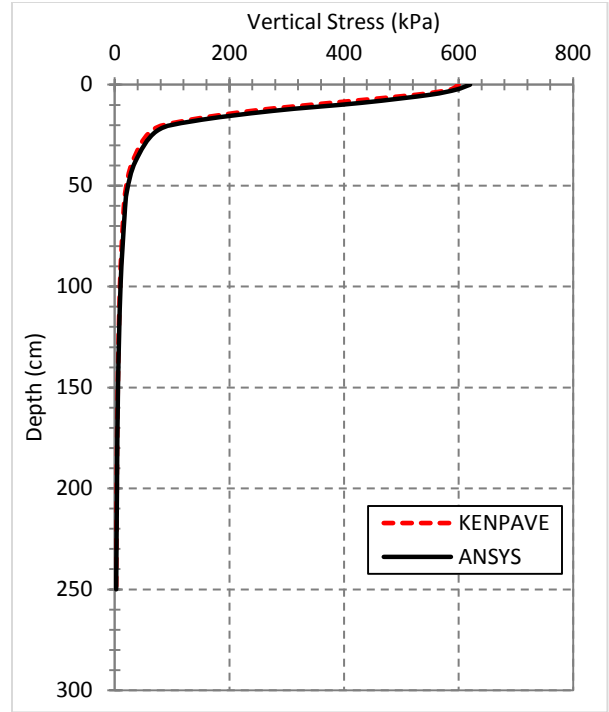
Figure (6-19) Graphical Information of KENPAVE Inputs and Results
(Case: 0% of HL, 230mm HMA Thickness)

6.3.2.1 Vertical Stress

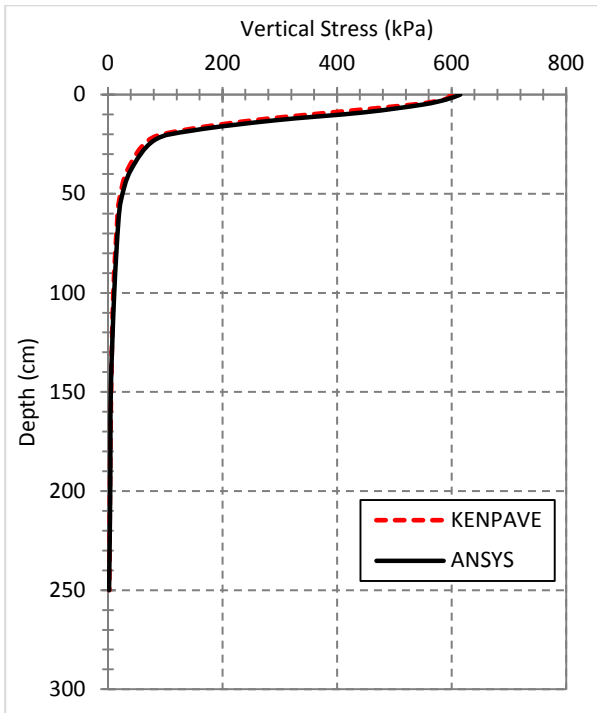
The results of the vertical stress under tire pressure are presented in the Figure (6-20). The Figure shows the vertical stresses for two cases of thickness and each case was studied for two mixtures of asphalt concrete; the control mixtures (without hydrated lime) and optimised mixtures (mixtures with 2.5% of hydrated lime replaced with mineral filler). The case one of the thicknesses of asphalt concrete layer is of 180mm in total (40mm for wearing, 60mm for leveling and 80mm for the base course) and the second case is of the total thickness of 230mm (50mm for wearing, 80mm for leveling and 100mm for the base course). Acceptable agreement between FE and multi-layer elastic approaches is found. The maximum difference between the vertical stresses at is a range of 10% to 14% within the asphalt concrete layer and 13% to 16% at the point between asphalt concrete and subbase layer and below for the case of the thickness of 180mm of the asphalt concrete layer. Regarding the case of the thickness of 230 mm for the asphalt concrete layer, the maximum difference was about 14% in the asphaltic layer and 15% within the subbase layer.



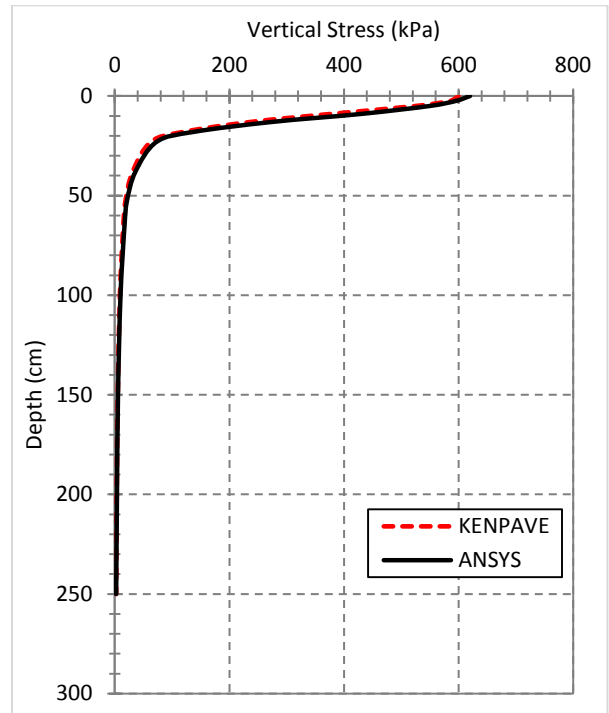
a) For Control Mixes at 180mm of AC Layer



b) For Modified Mixes at 180mm of AC Layer



c) For Control Mixes at 230mm of AC Layer

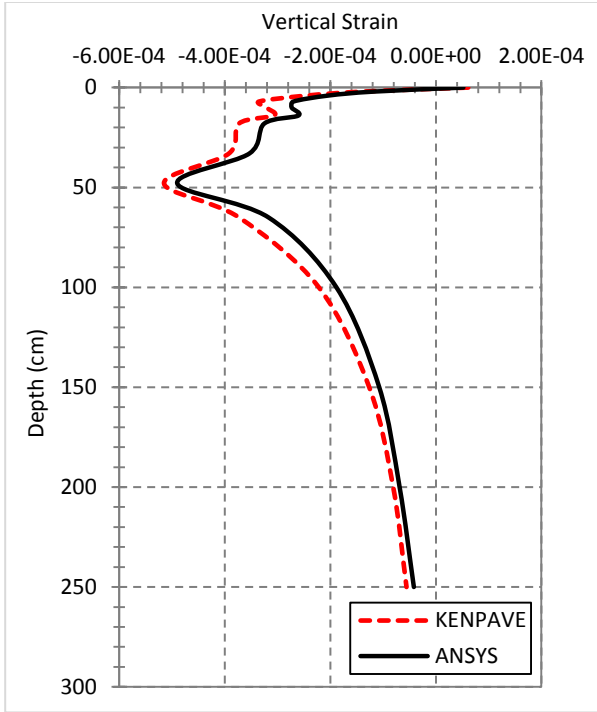


d) For Modified Mixes at 230mm of AC Layer

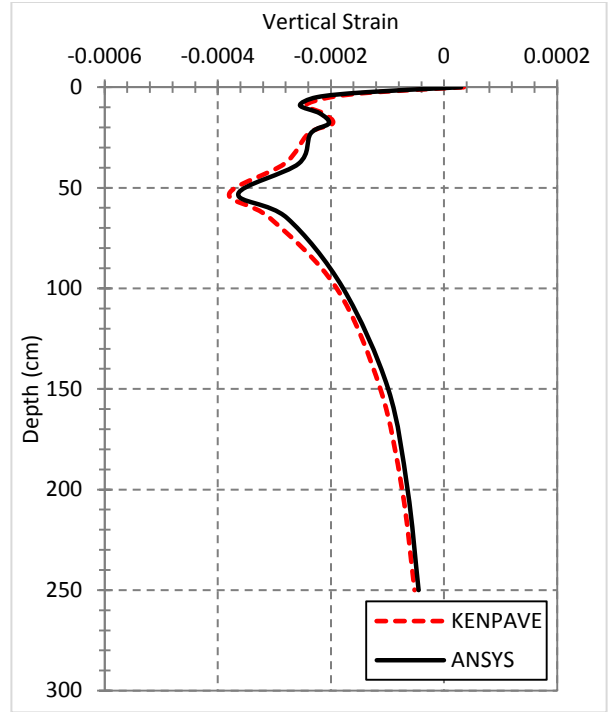
Figure (6-20) Vertical Stress Distribution for Control and Hydrated Lime Modified Mixtures at Different AC Thicknesses

6.3.2.2 Vertical Strain

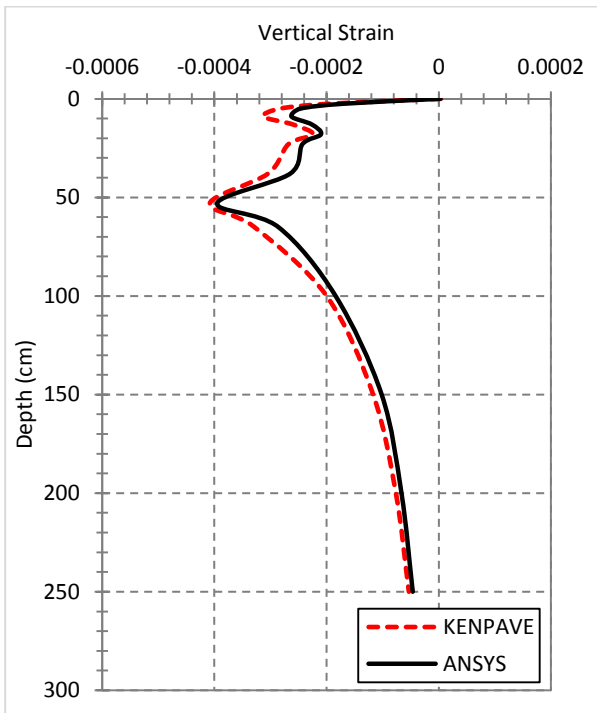
The same cases studied for the verification of vertical stress at the FE and Multi-layered elastic modelling were evaluated for the vertical strain in the pavement. The results are shown in the Figure (6-21). Good agreement was noticed between FE and multi-layer elastic approaches. For the case of HMA total thickness of 180mm, the maximum difference between the two methods for the vertical strain is about 12% to 19% within the asphalt concrete layer and 5% to 10% within the subbase and subgrade layers. For the modified asphalt concrete pavement and at the thickness of 180mm, the difference between the FEM and MLEM for the vertical strain is about 6% to 16% within the asphalt concrete layer and 3% to 13% in the depth below the asphalt concrete layer that involves the subbase and subgrade layers. Regarding the case of the thickness of 230 mm of the asphalt concrete layer, the difference between the finite element and multi-layer elastic approaches was up to 17% for both pavement models of control and modified mixtures in the asphaltic layer. Furthermore, the difference in the vertical strain in the lower layers was about 4% to 15% for the control mixes model and in a range of 6% to 17% for the modified mixtures model within the subbase and subgrade layers.



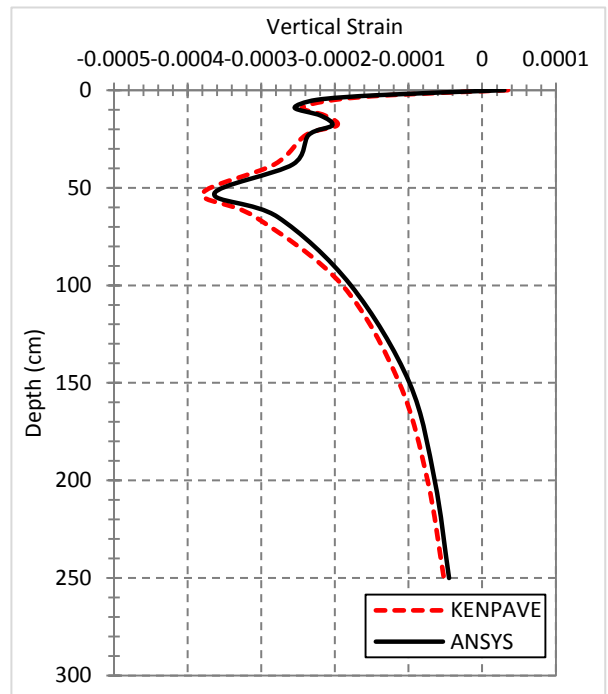
a) For Control Mixes at 180mm of AC Layer



b) For Modified Mixes at 180mm of AC Layer



c) For Control Mixes at 230mm of AC Layer

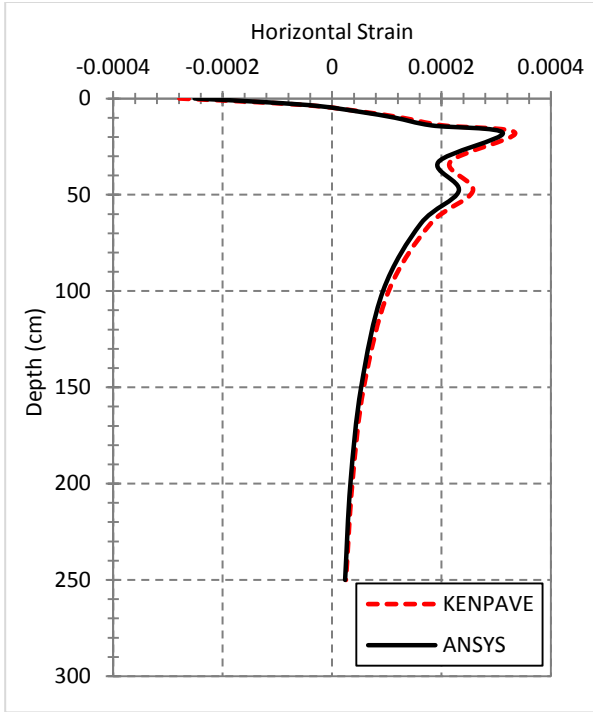


d) For Modified Mixes at 230mm of AC Layer

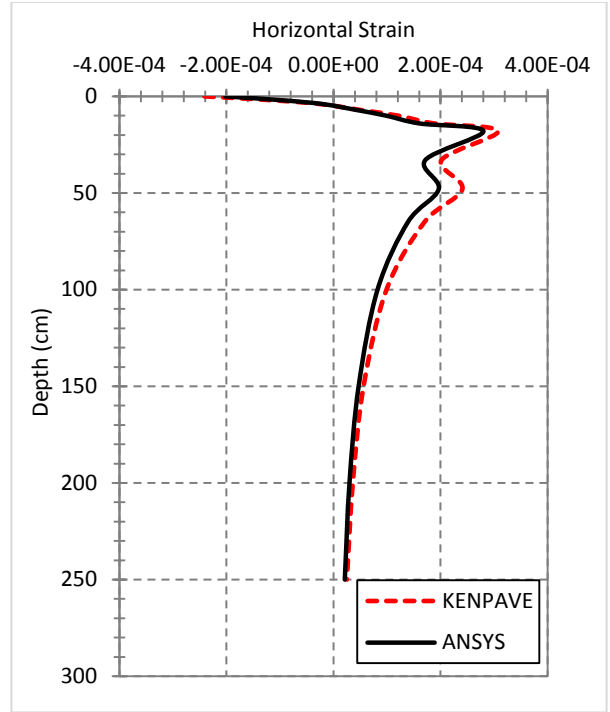
Figure (6-21) Vertical Strain Distribution for Control and Hydrated Lime Modified Mixtures at Different AC Thicknesses

6.3.2.3 Horizontal Strain

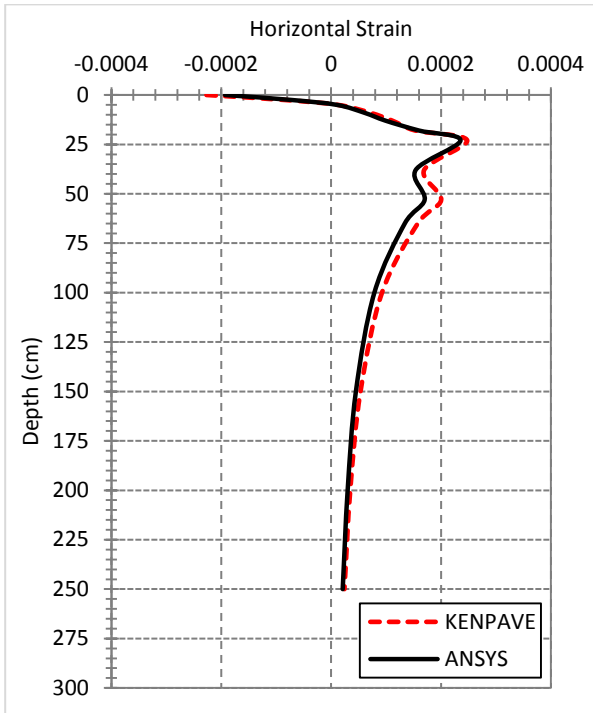
The horizontal tensile strain distribution that obtained by the finite element method using ANSYS package was compared with the values calculated by the Multi-layered elastic modelling using the KENPAVE software. The horizontal strain, as well as the other material responses, were evaluated at points distributed in the pavement model to assess the behaviour of stresses, strains and displacements at variable depths within the pavement model. The response points were 14 starting from the top of the surface of asphalt concrete surface course where the depth is zero until the depth of 2500mm, including the maximum critical value of horizontal tensile strain located at the bottom of the third asphalt concrete course (Base course) of the asphaltic layer. The comparison results can be seen in the Figure (6-22). There was an acceptable agreement between finite element and multi-layer elastic approaches. In the case of asphalt concrete of total thickness of 180mm, the variance between the two procedures for the control mixtures model is about 10% within the asphalt concrete layer and 6% to 10% within the subbase and subgrade layers. In the model of modified asphalt concrete pavement, the difference between the two methods for the horizontal tensile strain is about 16% to 17% within the asphalt concrete layer and 15% to 18% for the layers below the asphalt concrete layer including the subbase and subgrade layers. In the case of the total thickness of 230 mm of the asphalt concrete layer, the variance between the finite element and multi-layer elastic approaches was in the range of 4% to 15% for control pavement models and up to 13% for the model of modified asphaltic layer. The difference in the horizontal strain in the lower layers (subbase and subgrade) was about 13% to 15% for the control mixes model and in a range of 10% to 15% for the modified mixtures model.



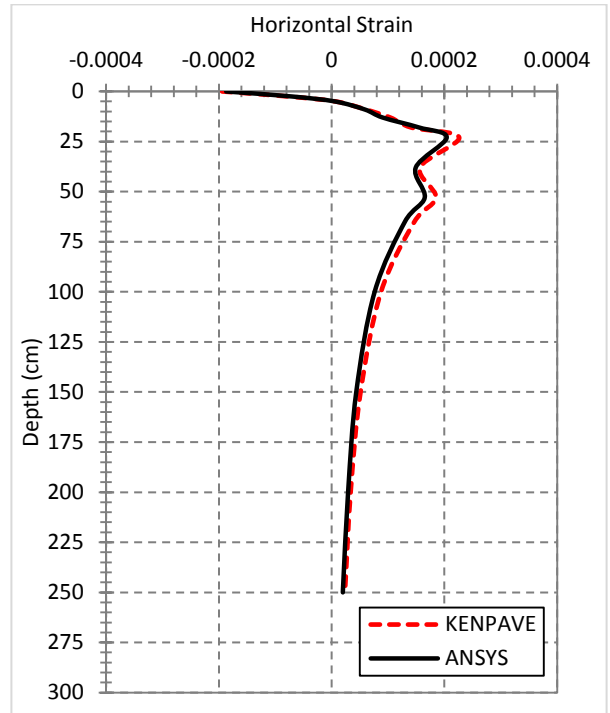
a) For Control Mixes at 180mm of AC Layer



b) For Modified Mixes at 180mm of AC Layer



c) For Control Mixes at 230mm of AC Layer



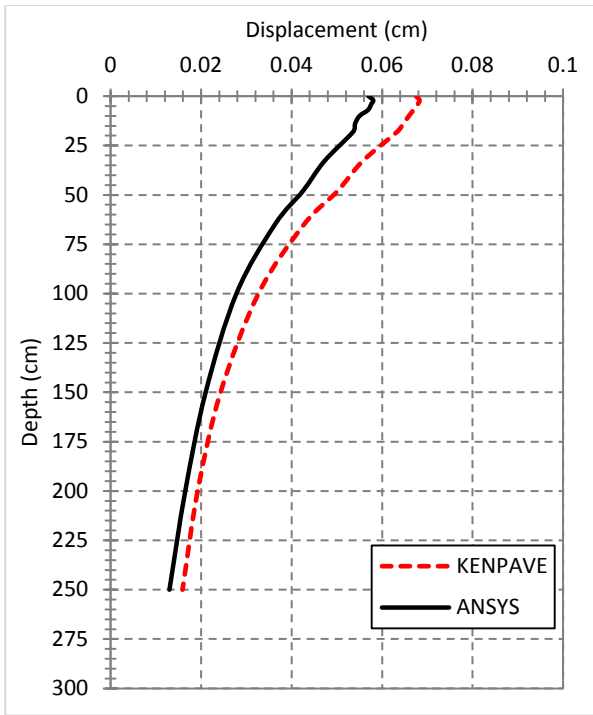
d) For Modified Mixes at 230mm of AC Layer

Figure (6-22) Horizontal Strain Distribution for Control and Hydrated Lime Modified Mixtures at Different AC Thicknesses

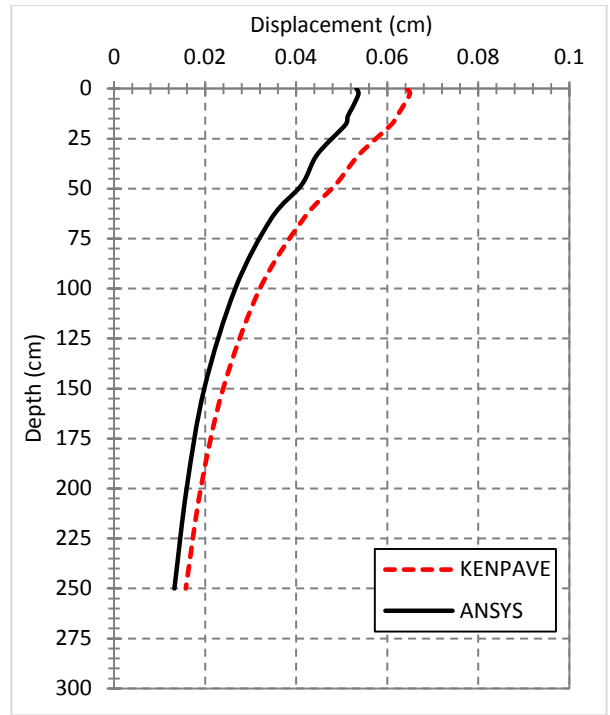
6.3.2.4 Vertical Displacement

The final pavement mechanistic response studied for verification between the finite element, and multi-layered elastic modelling methods is the vertical displacement. A comparison made between the vertical displacement distribution estimated by the ANSYS package and the displacements that found by KENPAVE software. The comparison outcomes can be viewed in the Figure (6-23). The comparison revealed that there is a satisfactory agreement between finite element and multi-layer elastic approaches

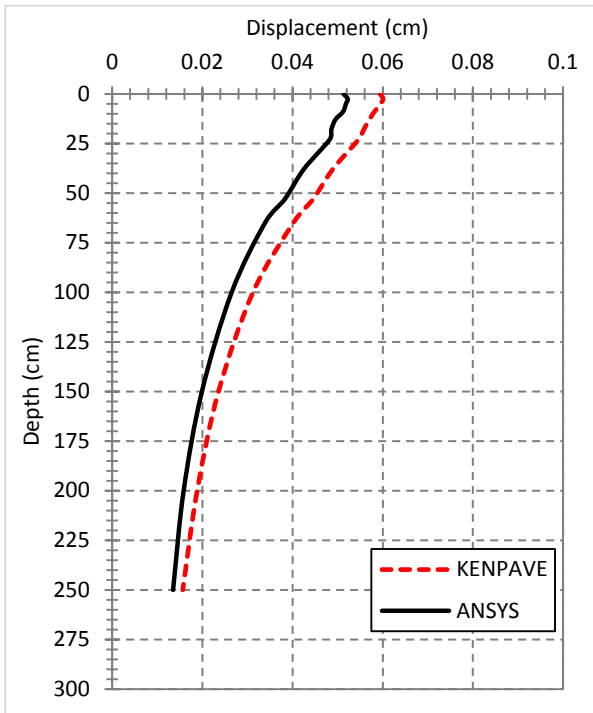
Regarding the case of asphalt concrete total thickness of 180mm and for the control mixes model, the variance between the two methods for vertical displacement is about 13% to 15% in general and for the hydrated lime modified model was about 15% to 17%. For the same case of asphaltic layer thickness with a modification asphalt concrete mixtures with an optimal percent (2.5%) of hydrated lime, the difference between the two techniques for the vertical displacement is about 15% to 17%. In the case of the total thickness of 230 mm of the asphalt concrete layer, the variance between the finite element and multi-layer elastic methods was in the range of 11% to 15% for control pavement models and ranged from 16% to 19% for the model of modified asphaltic layer. The variance percent between the two methods represents how many vertical displacements estimated by ANSYS are lower than the displacements calculated by KENPAVE. The small differences in the calculated values of pavement responses between the two programmes could be related to the difference in the boundary conditions and the theory assumptions of each approach as well as the difference in the loading configuration.



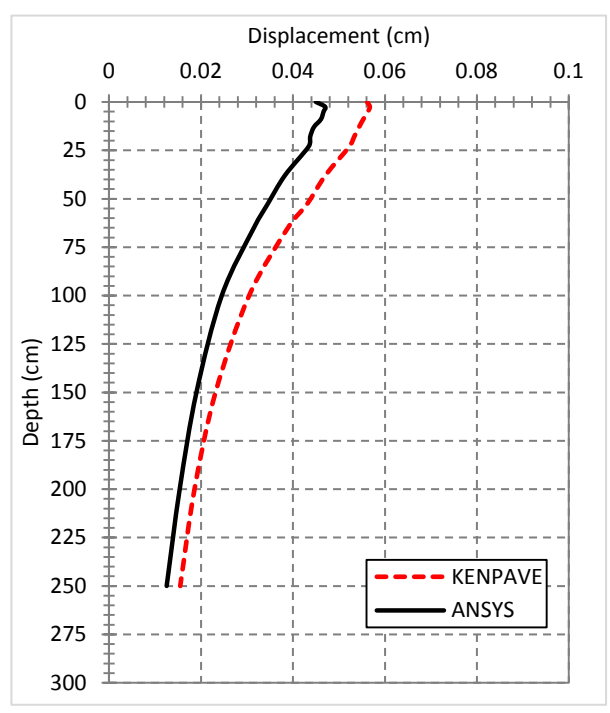
a) For Control Mixes at 180mm of AC Layer



b) For Modified Mixes at 180mm of AC Layer



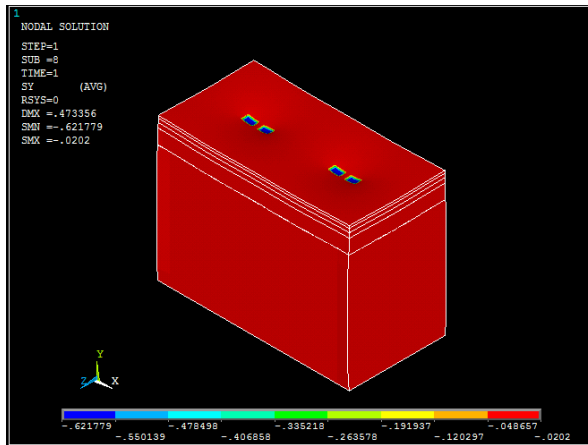
c) For Control Mixes at 230mm of AC Layer



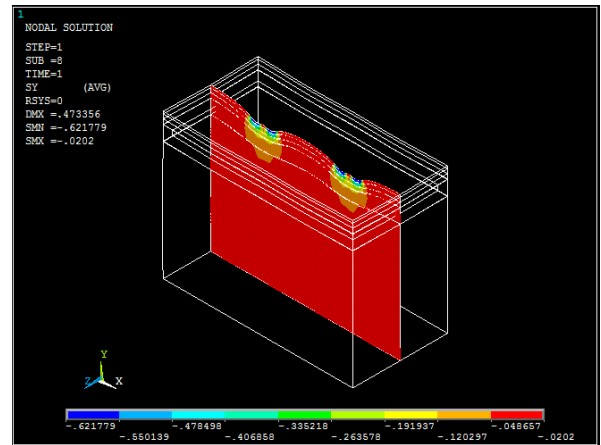
d) For Modified Mixes at 230mm of AC Layer

Figure (6-23) Vertical Displacement Distribution for Control and Hydrated Lime Modified Mixtures at Different AC Thicknesses

Contours of vertical stress distribution, vertical displacement, vertical strain and horizontal strain using FEA by ANSYS software are shown in Figures (6-24) to (6-27) respectively for the case of pavement model of modified HMA layer at the thickness of 230 mm.

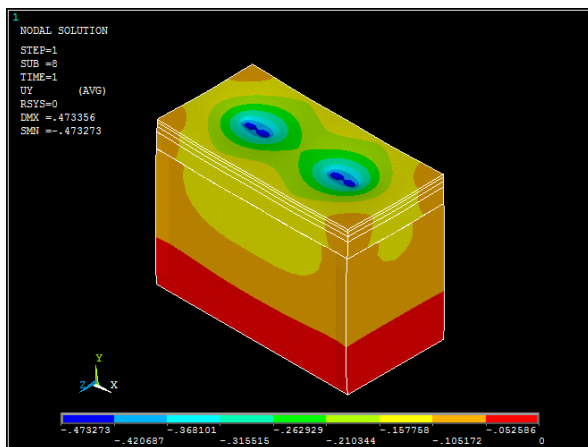


a) The Whole Model

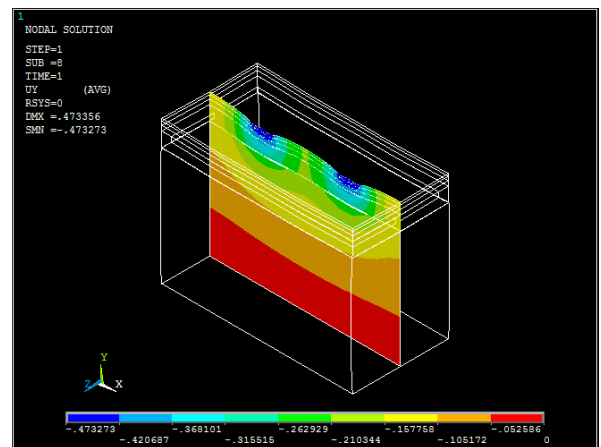


b) Section of Model

Figure (6-24) Vertical Stress Contour Distribution

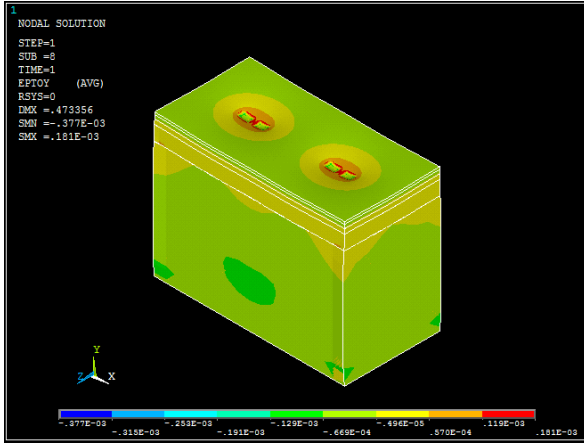


a) The Whole Model

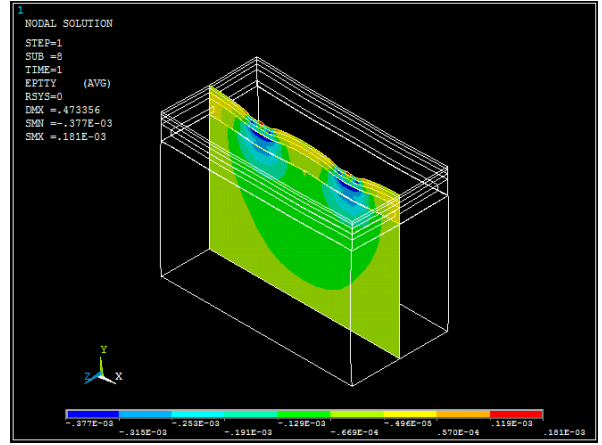


b) Section of Model

Figure (6-25) Vertical Displacement Contour Distribution

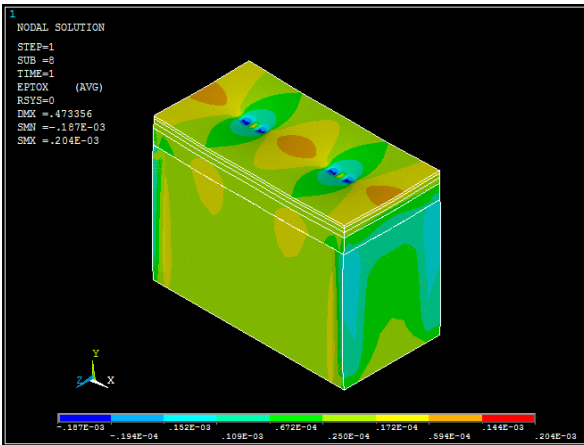


a) The Whole Model

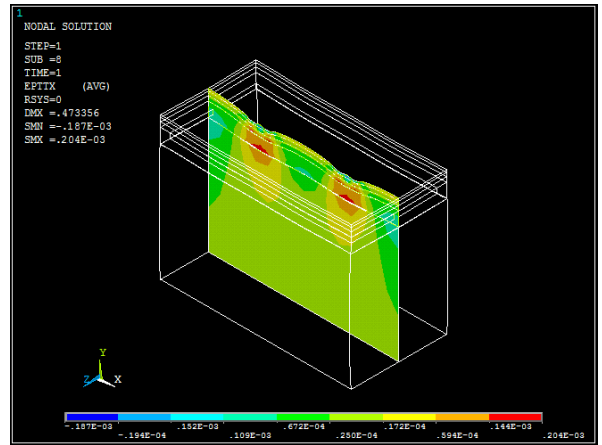


b) Section of Model

Figure (6-26) Vertical Strain Contour Distribution



a) The Whole Model



b) Section of Model

Figure (6-27) Horizontal Strain Contour Distribution

6.4 Mechanistic-Empirical Analysis Procedure Summary

The following procedure has been used to find the maximum tensile strain (fatigue cracking) and vertical strain (rutting):

- Input parameters for this analysis include traffic loading, pavement structure, material properties, and the desired response location. The Equivalent single axle load (ESAL) loading is 18 kip (80 kN) applied through an axle including a double set of tires. In this study, it is assumed that the spacing between dual wheels is 345mm (13.5 in.) and tire pressure of 0.6 MPa (87 psi).
- Resilient modulus of each course of asphalt concrete layers is varied as related to the change in the percentage of hydrated lime, temperature and depth of pavement. The values are presented in the Table (6-2). For a CBR value of 4.5% of the compacted subgrade, the resilient modulus (M_r) is equal to 45 MPa (6525 psi), as a result of equation (6-12). Moreover, the resilient modulus of subbase layer (M_r subbase) is 145 MPa (21000 psi) resulting from equation (6-11).
- Typical value of Poisson's ratio has been used as presented in Table (6-3)
- The critical stress and tensile strain have been found in the points beneath the asphalt pavement layer and stress and vertical compressive strain at the upper of Subgrade layer.
- Calculate the fatigue repetitions to fracture (N_f) after finding the tensile strain at the bottom of HMA layer according to Asphalt Institute (AI) fatigue equation that adopted by KENPAVE:

Fatigue Model:

$$N_f = 0.0796 \times \epsilon t^{-3.291} \times E^{-0.854} \quad (6-14)$$

- Similarity, permanent deformation (rutting) load repetitions to failure (N_d) to be found based on the determination of compression related strain on the upper of the subgrade.

Rutting Model

$$N_d = 1.365 \times 10^{-9} \times \epsilon_c^{-4.447} \quad (6-15)$$

Where:

N_f = the number of repetitions to failure,

ϵ_t = horizontal strain on the bottom of HMA.

E = resilient modulus of asphalt concrete layer,

N_d = axle load to rut depth criteria, 0.5 inch

ϵ_c = vertical strain on the upper face of the subgrade.

- Damage ratio using Miner's law is conducted to find the critical value (larger).

Based on the above, the material properties of the evaluated flexible pavement layers are to be used as inputs of finite element modelling by ANSYS and multi-layer elastic method by KENPAVE. These inputs used to estimate the pavement design life and the optimum thickness of asphalt concrete layer regarding the variation in the resilient modulus of asphalt concrete layer due to the effect of hydrated lime addition. The input variables are:

- Load configuration: A static load of 80kN (18-kip ESAL) (single axle with dual tires, each tire pressure is 600 kPa, (87 psi), and the radius of the tire is 103 mm (4 in.), the spacing between the dual tires is 345 mm (13.56 in).
- The Estimated Number of repetitions (ESAL): 2.318×10^6 , according to calculations in the worksheet illustrated in Table (6-1).
- The number of layers in the pavement section: 5 (three of them are the Wearing, Leveling and Base courses that represent the asphalt concrete layer, and then the Subbase, and finally the Subgrade layer).
- The other needed properties such as resilient modulus, layers' thicknesses, and Poisson's ratio are summarised in the Table (6-5).

Table (6-5) Material properties of proposed pavement structure layers

Layer No.	Layer Type		Thickness, mm	Resilient Modulus, MPa	Poisson's Ratio	Material Characteristics
1	Asphalt Concrete	Wearing	varied	varied	0.35	Isotropic and linear elastic
2		Leveling	varied	varied	0.35	Isotropic and linear elastic
3		Base	varied	varied	0.35	Isotropic and linear elastic
4	Subbase		300	145	0.4	Isotropic and linear elastic
5	Subgrade		3000 (for ANSYS)	45	0.45	Isotropic and linear elastic
			Infinite (for KENPAVE)			

6.5 The Results of Mechanistic-Empirical Analysis

Mechanistic procedures have been adopted to determine the optimum thickness of asphalt concrete layer in the flexible pavement regarding the influence of partially added hydrated lime as filler. One of the main input parameters used in analysis and design through ANSYS and KENPAVE programmes is the resilient modulus. The hydrated lime effect on the resilient modulus plays the main role in thickness optimisation as it enhances the HMA layer stiffness and improves the ability of the pavement to withstand tension and compression stresses. Therefore, the maximum (critical) damage ratio decreases with increasing of hydrated lime percentage for the same layer thickness and that leads to needing lower thickness to reach a damage ratio beneath unity. The Table (6-6) shows the FEA and MLET output of design parameters influenced by hydrated lime addition.

Table (6-6): Mechanistic-Empirical Critical Outputs of the Analysis of Pavement Model

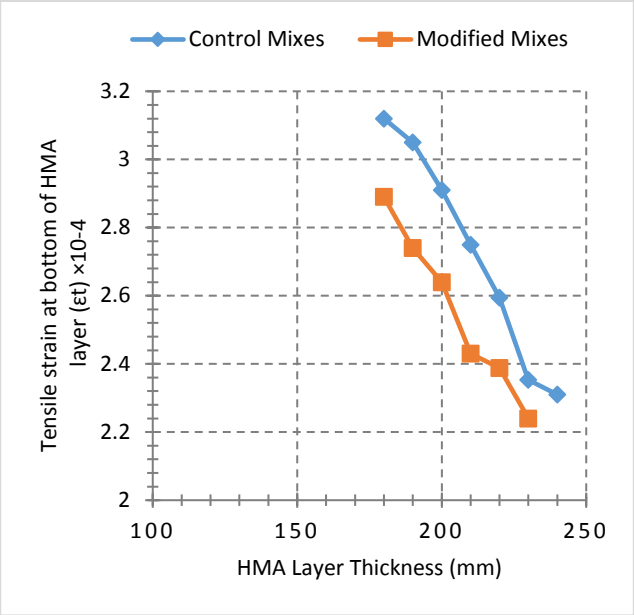
Asphalt Concrete layer thickness (mm)			HL (%)	Tensile strain at the bottom of HMA layer (ϵ_t), $\times 10^{-4}$		Fatigue load repetitions (N_f), $\times 10^6$		Compressive Strain at the top of Subgrade layer (ϵ_c), $\times 10^{-4}$		Rutting load repetitions (N_d), $\times 10^6$		Maximum Damage Ratio		
Trial Case	Each Course	Total		ANSYS	KENPAVE	ANSYS	KENPAVE	ANSYS	KENPAVE	ANSYS	KENPAVE	ANSYS	KENPAVE	
1	W	40	180	0	3.12	3.3329	1.174	0.9448	-4.9	-5.1	0.897	0.7181	2.582	3.228
	L	60		2.5	2.89	3.076	1.333	1.086	-4.55	-4.846	1.250	0.9429	1.853	2.458
	B	80												
2	W	50	190	0	3.05	3.145	1.265	1.144	-	-4.902	0.925	0.8964	2.505	2.586
	L	60		2.5	2.74	2.871	1.576	1.352	-4.53	-4.587	1.275	1.206	1.816	1.921
	B	80												
3	W	50	200	0	2.91	2.942	1.449	1.398	-4.65	-4.666	1.134	1.117	2.042	2.075
	L	70		2.5	2.64	2.695	1.768	1.653	-	-4.365	1.528	1.506	1.516	1.539
	B	80							4.351					
4	W	50	210	0	2.75	2.776	1.736	1.684	-	-4.461	1.392	1.367	1.664	1.696
	L	70		2.5	2.43	2.4315	2.322	2.3181	-	-3.96	2.369	2.329	0.997	0.999
	B	90							3.945					
5	W	50	220	0	2.595	2.616	2.084	2.029	-	-4.262	1.710	1.677	1.355	1.382
	L	80		2.5	2.388	2.394	2.440	2.420	-	-3.9	2.570	2.494	0.949	0.929
	B	90							3.874					
6	W	50	230	0	2.353	2.475	2.863	2.423	-3.95	-4.081	2.355	2.036	1.105	1.138
	L	80		2.5	2.24	2.262	2.990	2.895	-3.74	-3.797	3.008	2.812	0.775	0.824
	B	100												
7	W	50	240	0	2.31	2.346	3.043	2.892	-	-3.909	2.555	2.468	0.907	0.94
	L	90												
	B	100							3.879					

As presented in the Table (6-6), many trials have been made to reach the optimum thickness of HMA layer. The trial process began with 180mm thickness and 0 % of hydrated lime. The first trial showed that the damage ratio is much greater than unity (2.58 in FEA and 3.22 in MLET analysis). After modification of the asphaltic layer (Wearing, Leveling and Base courses) with the

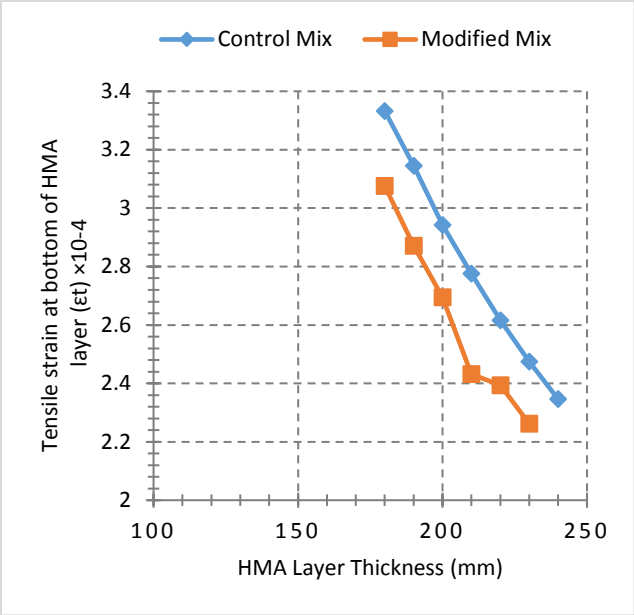
optimum percent of hydrated lime (2.5%) the damage ratio decreased to (1.85 in FEA and 2.4 in MLET). However, the damage ratio value still higher than required and that led to trying greater thicknesses with a step of 10 mm at two percentages of hydrated lime modification; 0% which represents control mixtures and the percent of 2.5 in which the asphalt concrete modified at optimum value. After many iterations of changing asphalt concrete layer thickness and the addition of hydrated lime, it can be found that the optimum thickness of asphalt concrete layer was 210 mm when the calculated damage ratio became lower than 1 for the model of modified mixtures (at 2.5% of hydrated lime). The damage ratio at an optimum thickness (210 mm) was found under unity for both analysis techniques, the finite element analysis and the multi-layer elastic theory and their damage ratios were very close in value.

6.5.1 Critical Pavement Responses as Related to HMA Thickness and Lime Influence

Figures (6-28) illustrates the effect of hydrated lime addition on the critical value of the horizontal tensile strain at the bottom of the asphaltic layer with respect to its thickness in the flexible pavement.



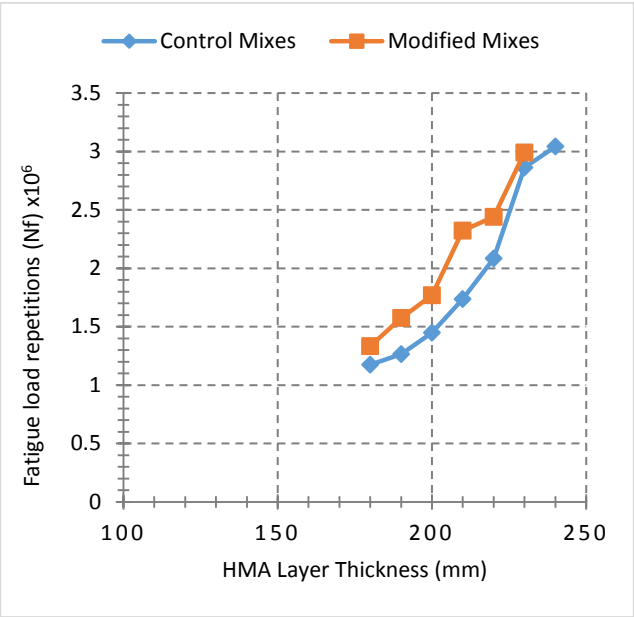
a) Outputs of FEA by ANSYS



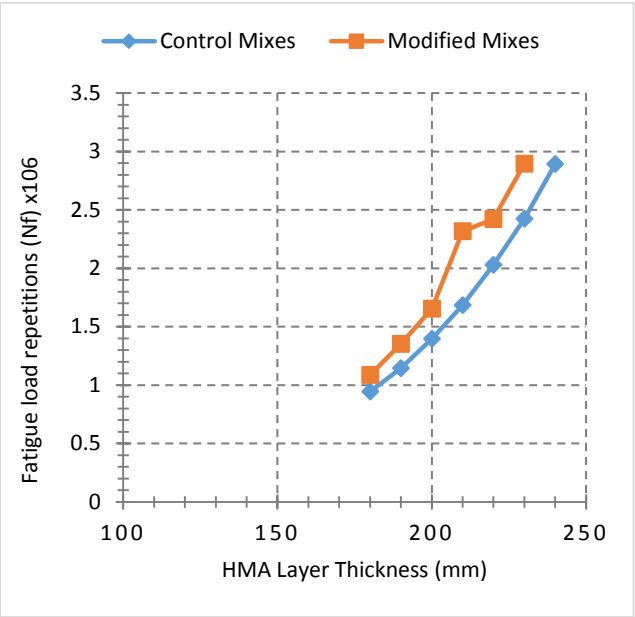
b) Outputs of MLET by KENPAVE

Figure (6-28) HMA layer thickness versus tensile horizontal strain regarding HL Percent Effect

As shown in the Figure (6-28), the tensile strain located beneath HMA layer decreased with the increase of asphalt concrete thickness in both analysis approaches, the finite element and multi-layer elastic theory and that was for the control and modified mixes. In the same thicknesses of HMA and due to the effect of hydrated lime partial addition as mineral filler, a reduction rate in the tensile strain at the model of the asphaltic layer thickness of 180 mm was about 7.3% and 7.7% for FEA, and MLET approaches respectively. The rate of reduction increased until reaching the maximum difference at the asphalt concrete thickness of 210 mm with a rate of 11.63% and 12.4% for FEA and MLET techniques respectively. The accumulated rate of reduction in tensile strain from the pavement model initial thickness (180 mm) until the optimum thickness (210 mm) was 38.4% and 37.22% in the analysis carried out according to FEA and MLET techniques respectively.



a) Outputs of FEA by ANSYS

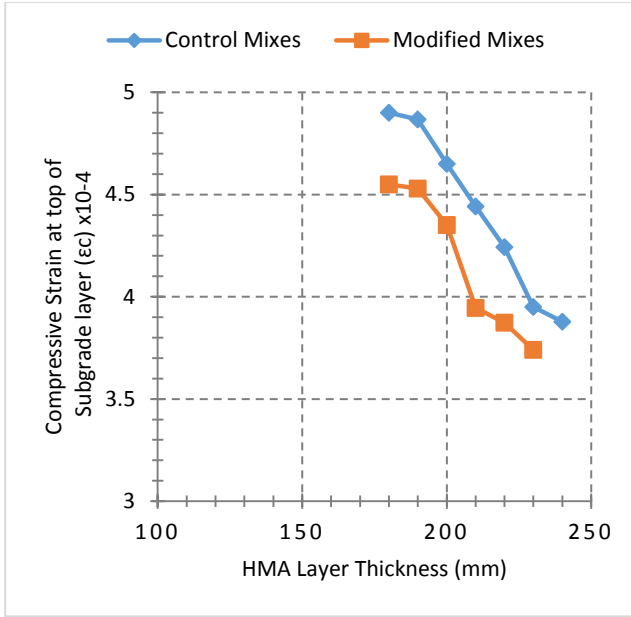


b) Outputs of MLET by KENPAVE

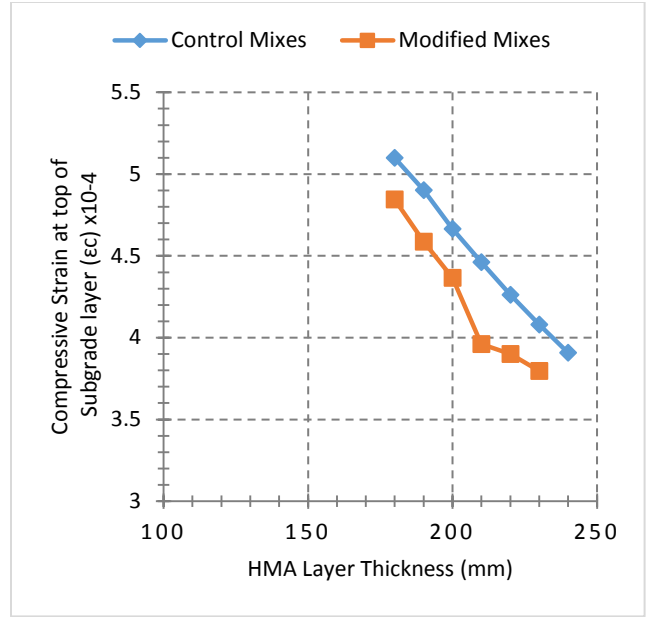
Figure (6-29) HMA layer thickness versus fatigue load repetitions regarding HL Percent effect

As shown in Figure (6-29), the allowable number of load repetitions to fatigue failure rises as the asphalt concrete layer thickness increases. The addition of hydrated lime leads to a gradual increment of fatigue load repetitions in two ways; the first one is within the same thickness of the layer, and the other phase is throughout the proposed thicknesses from 180 mm to 230 mm, which is the thickness beyond the optimum HMA thickness (210 mm). In 180 mm thickness, by adding 2.5% of hydrated lime, the enhancement of load repetition as compared to the pavement model of control mixes was 13.5% estimated by ANSYS and 14.9% by KENPAVE. The fatigue life significantly increased with each iteration of adding hydrated lime and increasing HMA thickness so the enhancement rate at the point of 210 mm was 33.75% and 37.65% for FEA and MLET approaches respectively. The accumulated fatigue life increased from the first iteration thickness (180 mm) until the optimum thickness (210 mm) was 93.9% and 89% for FEA and MLET techniques respectively.

Figure (6-30) shows the relationship between HMA layer thickness and the compression related strain over the subgrade layer for the finite element analysis and multi-layer elastic theory methods and regarding hydrated lime addition that clearly affects this relationship. It can be seen that the strain decreases when thickness increases. Furthermore, the hydrated lime addition decreases the amount of strain for each thickness value. For instance, the vertical strain decreased by about 7.1% and 5% for FEA and MLET approaches respectively at the 180 mm thickness. Also, a gradual increase in the reduction rate was recorded reaching an accumulated value of 31% estimated by ANSYS and 29% by KENPAVE in the thickness of 210 mm. The increase in the asphaltic layer thickness leads to the applied stress being more declined at the top of subgrade layer, so the reduction in vertical strain continued when asphalt concrete layer thickness was being more than the optimum thickness with or without hydrated lime addition.

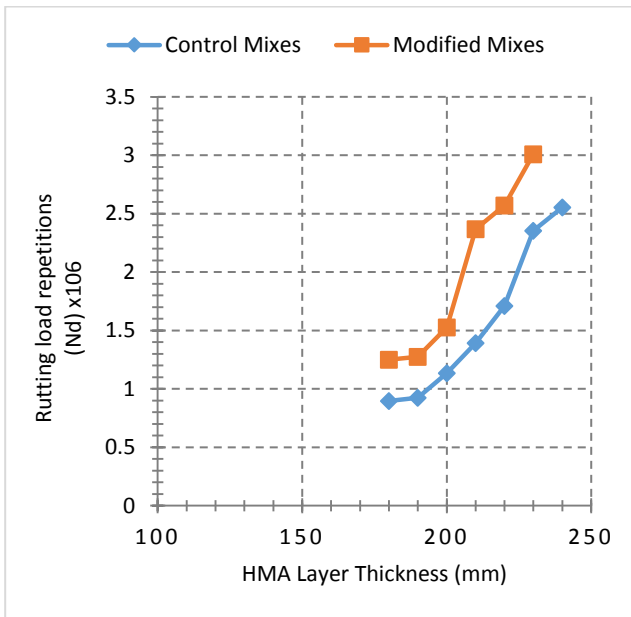


a) Outputs of FEA by ANSYS

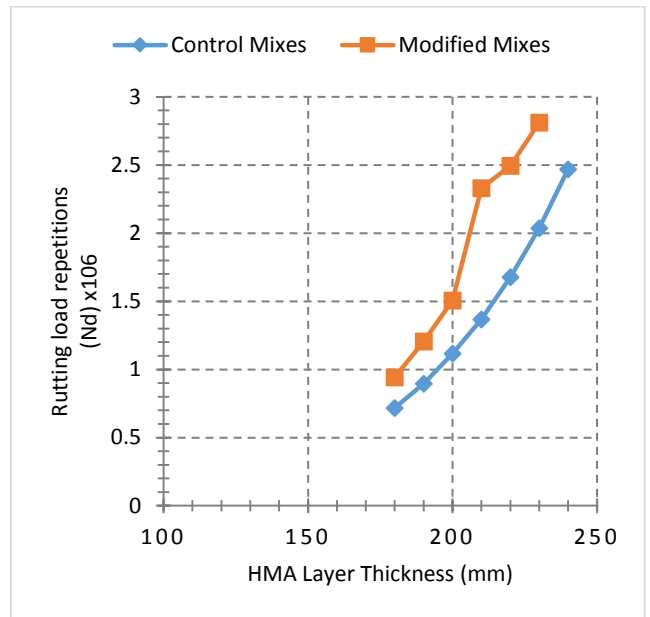


b) Outputs of MLET by KENPAVE

Figure (6-30) HMA layer thickness versus compressive vertical strain regarding HL Percent Effect



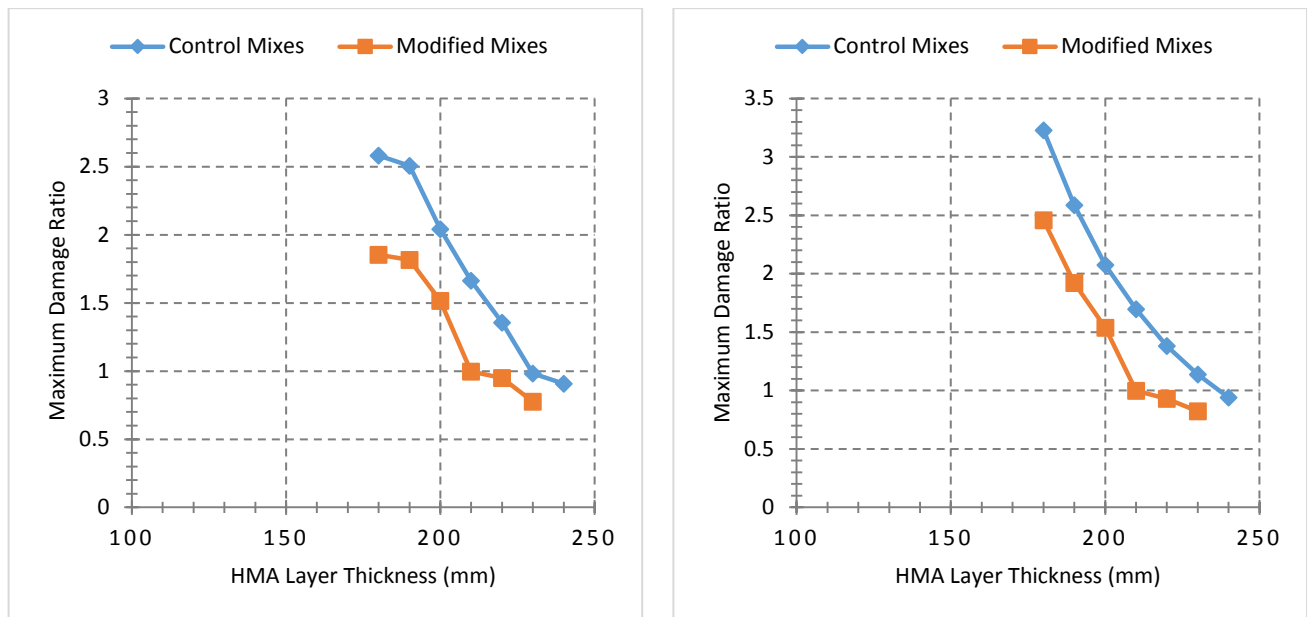
a) Outputs of FEA by ANSYS



b) Outputs of MLET by KENPAVE

Figure (6-31) HMA layer thickness versus rutting load repetitions regarding HL Percent Effect

Figure (6-31) illustrates that there are two factors affecting the allowable load repetitions to permanent deformation failure. The first one is the thickness of the hot mix asphalt layer and the second one is the hydrated lime partial replacement percentage. The increase in both of hydrated lime and thickness leads to enhance the rutting load repetitions. It can be found that the hydrated lime addition to the mix significantly increases the number of load repetitions for the same thickness of the asphaltic layer, especially in 210 mm thickness. For instance, the increase percent in repetitions for the thickness of 210 mm was about 70% in both FEA and MLET methods. The accumulation in rutting load repetitions from the first iteration thickness of 180 mm up to the optimum thickness of 210 mm was 182% and 171% at FEA and MLET procedures respectively.



a) Outputs of FEA by ANSYS

b) Outputs of MLET by KENPAVE

Figure (6-32) HMA layer thickness versus maximum damage ratio regarding HL Percent Effect

In this mechanistic design approach, the final and important indicator of proper design procedure according to requirements and limits is the damage ratio, which is the ratio between the supplied load repetitions (ESAL) and the minimum (critical) allowable load repetitions to failure (the lower value of N_f or N_d). For an adequate design output, the damage ratio should not be equal

to or greater than unity (1) because the expected traffic load repetitions will be equal to (critical) or higher than allowable (maximum) traffic loads that the pavement structure can withstand.

As shown in Figure (6-32), the iterations began from a thickness of 180 mm with control and modified mix with an optimum percent of hydrated lime (2.5%) and the damage ratio is far from unity. The damage ratio was decreasing as a result of two factors, the first one is the addition of hydrated lime as partial replacement of mineral filler which enhanced the modulus of elasticity of asphalt concrete mixtures and the second factor is the increasing of asphaltic layer thickness to withstand the applied load. The damage ratio reduction reached the required value (being under unity) at the thickness of 210 mm of HMA layer modified by hydrated lime, while for the same thickness (210 mm), the damage ratio without the addition of hydrated lime was still more than one. The optimum thickness of the non-modified asphalt concrete layer that equivalent to the modified HMA thickness (210 mm) was 240 mm, in which the damage ratio became lower than one. As an advantage of the implementation of hydrated lime in pavement design, it can be found that there is a profit of about 30 mm in pavement thickness by comparing the damage ratio value of the estimated optimum thickness of asphaltic layer modified with hydrated lime to the thickness of control (non-modified) asphalt concrete layer. In details, the total thickness of 210 mm of asphalt concrete layer (that includes wearing, leveling and base courses) with 2.5% of hydrated lime gives almost the same value of damage ratio that 240 mm thickness at 0% of hydrated lime provides. Accordingly, the profit percentage in the asphalt concrete thickness is about 12.5%.

6.5.1.1 Asphalt Concrete Courses Thicknesses Related to Pavement Critical Responses

As mentioned before, the asphalt concrete layer of the pavement model comprises three courses, and they are wearing, leveling (binder) and base. During application of the Mechanistic-Empirical design approach, the iteration process of asphalt concrete layer thickness to reach the optimum total thickness was achieved by increasing the thickness of each asphalt concrete course within the whole HMA layer of 1cm increment in each try. Figures (6-33) and (6-34) illustrate the effect of increasing of the wearing, leveling and base courses thickness as well as the addition of hydrated lime on the critical (maximum) tensile strain at the bottom of the asphaltic layer and the fatigue life respectively. The analysis was performed utilising ANSYS FE model and compared using KENPAVE software. For all courses, it can be seen that the general trend of material behaviour is decreasing of tensile strain with the increase in asphalt concrete thickness of each

course, and for the same thickness, the tensile strain decreased because of hydrated lime addition to the mixes. As in Figure (6-34), fatigue life increased for all mixes with the addition of hydrated lime in the same thickness as well as increasing of asphalt concrete courses thicknesses.

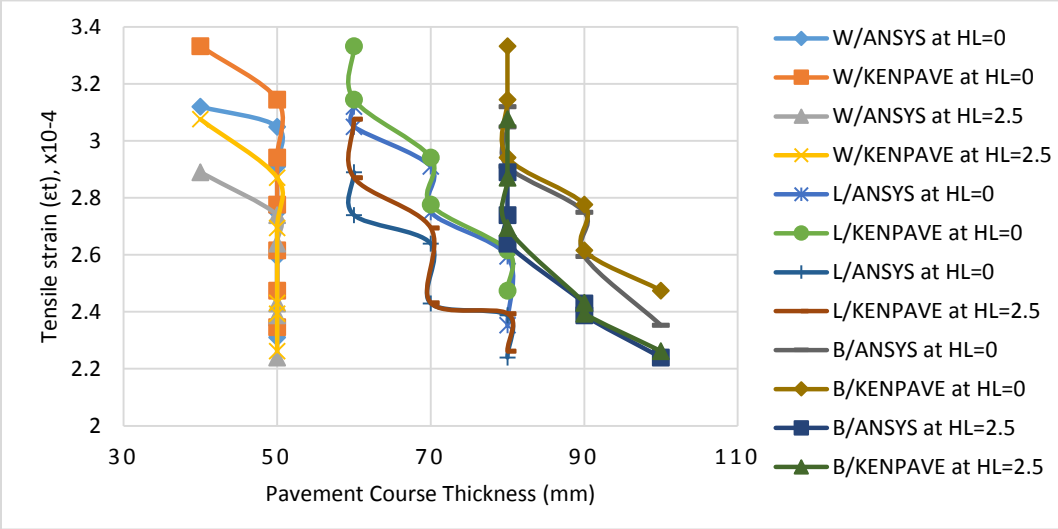


Figure (6-33) Effect of Thickness of Each Course on Tensile Strain

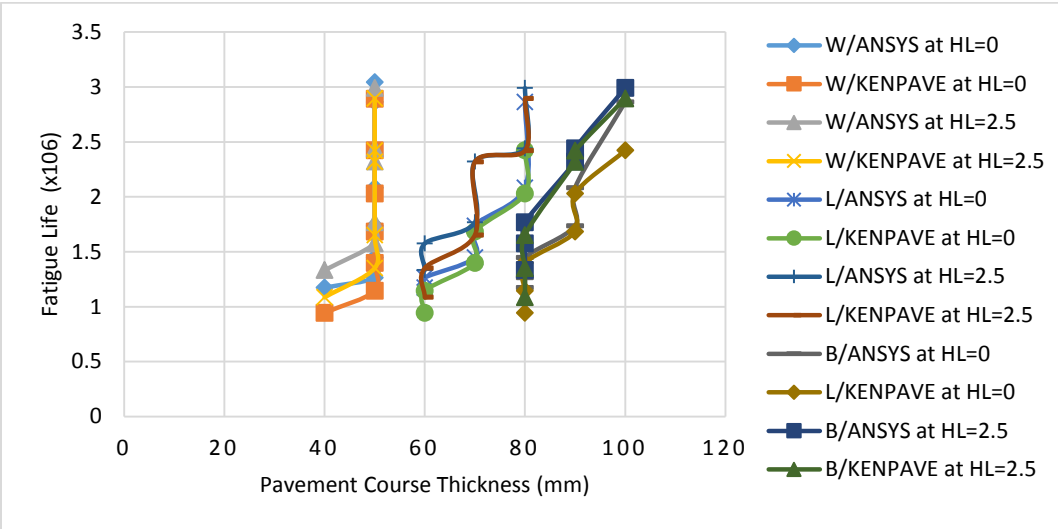


Figure (6-34) Effect of Thickness of Each Course on Fatigue Life

Similarity, Figures (6-35) and (6-36) show that addition of hydrated lime and increasing of thickness of each HMA course within the total asphaltic layer leads to decreasing of critical compressive strain and the allowable number of load repetitions to rutting respectively.

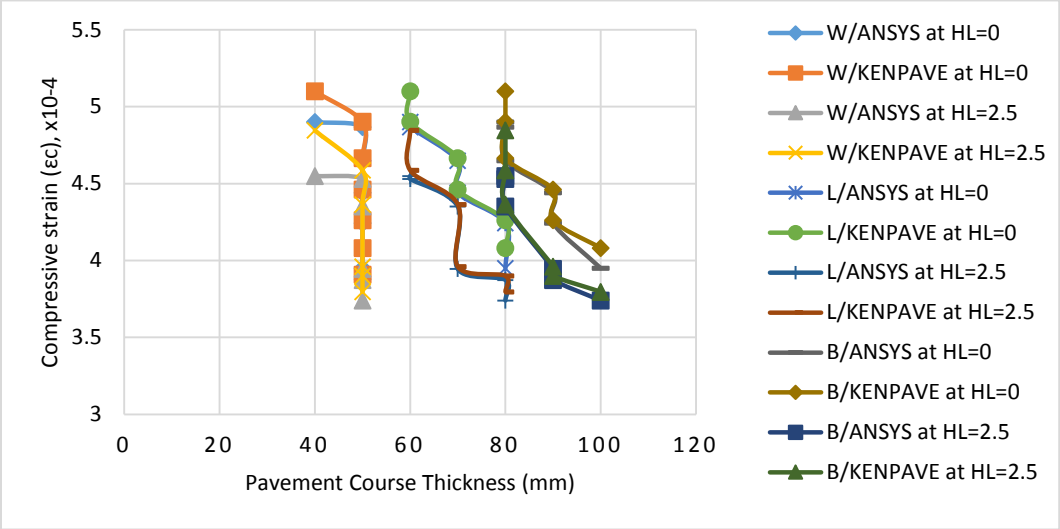


Figure (6-35) Effect of Thickness of Each Course on Compressive Strain

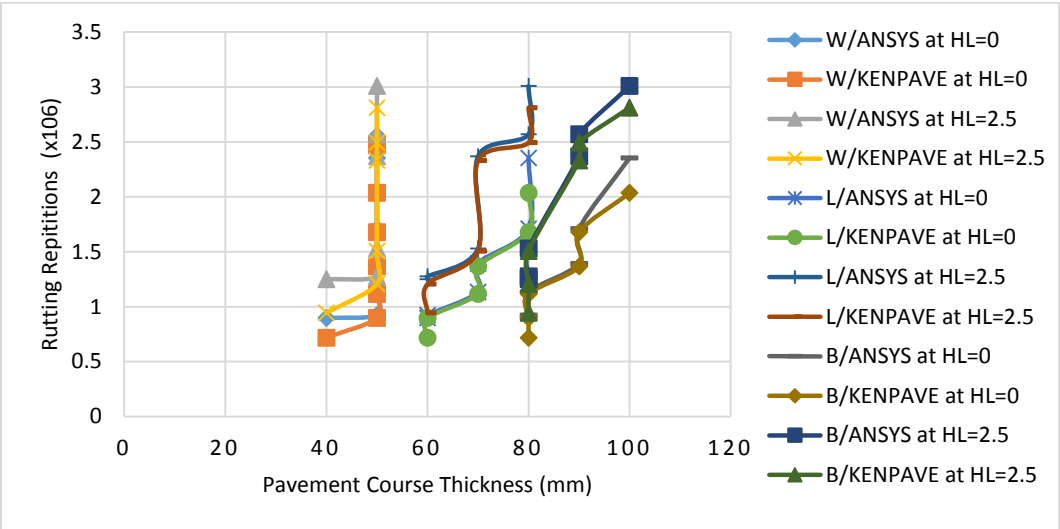


Figure (6-36) Effect of Thickness of Each Course on Repetitions to Rutting

Figure (6-37) that demonstrates the damage ratio related to critical pavement responses versus the thickness of each asphalt concrete course within the HMA layer. The iterations initiated at a total thickness of 180 mm (W=40, L=60, and B=80) for control and modified mix with the optimum hydrated lime percent (2.5%) and ended after 7 attempts at the thickness of 240mm (W=50, L=90, and B=10). It can be observed that the damage ratio of all of the pavement courses decreased with the addition of hydrated lime as well as thickness increase in each course.

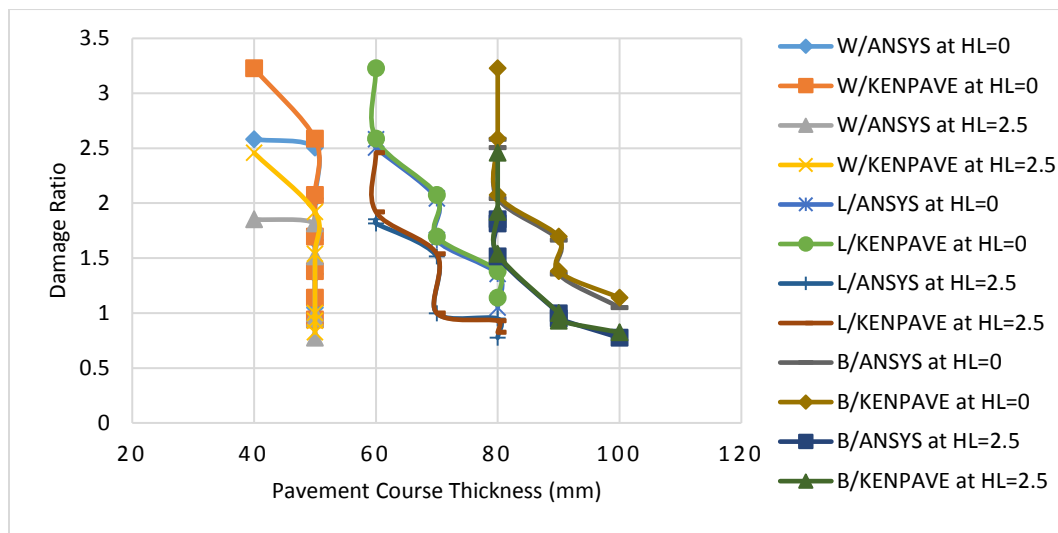


Figure (6-37) Effect of Thickness of Each Course on Damage Ratio

6.5.1.2 Asphalt Concrete Courses Thicknesses Related to Total HMA Thickness

As mentioned before, the asphalt concrete layer comprises three courses, and they are wearing, leveling (binder) and base. It could be useful to evaluate the relation between the asphaltic courses thicknesses and the total asphalt concrete thickness. Figures (6-38) shows the ratio of each course thickness to the total thickness of asphalt concrete layer. It can be found that the ratio of wearing course thickness to the total thickness ranged from 20.8% to 26.3%, and the average value is nearly the same as the ratio (23.8%) at the optimum total thickness of asphalt concrete layer (210 mm). The ratio of course thickness to the total layer thickness for the leveling course is ranged from 31.5% to 37.5% with 33.33% at the optimum layer thickness. For the base course, the ratio range is relatively small (40% to 44.4%) with an average of about 42.2% found to be closer to the thickness ratio of the layer thickness of 190 mm and 210 mm. At the optimum thickness of asphalt

concrete layer, the ratios of asphalt pavement courses to the total thickness are 23.8%, 33.33% and 42.8% for the wearing, leveling and base courses respectively.

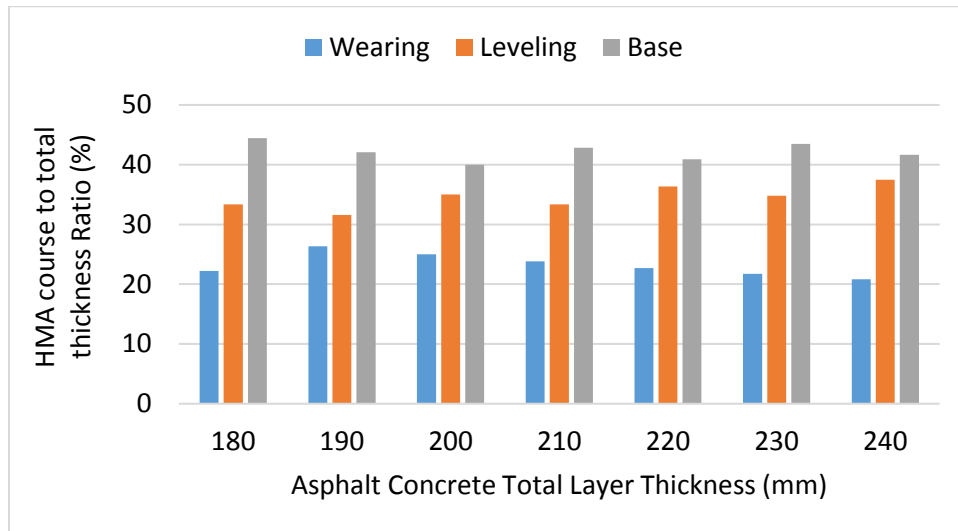


Figure (6-38) The Ratio of Each Course Thickness to The Total Layer Thickness

6.5.2 Fatigue Life and Permanent Deformation Developed in This Study

▪ Fatigue Life

The fatigue life of a prototype pavements should be much greater than for laboratory specimens due to the fact that wheel loads on actual pavements do not apply at the same location and have longer rest periods, both of which increase the fatigue life. Also, for thicker pavements, it takes more repetitions for cracks to appear on the surface to be considered as failure (Huang, 2004). In order to apply the laboratory fatigue test results to predict in-situ fatigue performance, it is necessary to apply a shift factor. Shift factor of 10 means that the damage to a lab test sample caused by one repetition is equivalent to the same damage caused by 10 load repetitions as accumulated in an asphalt pavement. Pell (1987) indicated that the shift factor could vary from 5 to 700. Variations in materials characteristics, test techniques, field conditions and the pavement structural models suggest that a wide variety of shift factors is expected. It is important to apply an appropriate shift factor so that the predicted distress can match field observations (Huang, 2004).

The fatigue life was investigated for the control and lime modified asphalt concrete mixtures in this study, and laboratory equations, as well as statistical models, were made based on the materials characteristics and performance-related properties of asphaltic mixtures. In the FEA of the pavement model in this chapter, the maximum (critical) horizontal tensile strain was found at the bottom of the lowest asphalt concrete course (Base) in the asphaltic layer. Therefore, the properties of this mix were adopted to find the fatigue life of the model. Regarding the application of appropriate shift factor (SF) to an allowable number of load repetitions to fatigue failure generally requires local calibration to field conditions, which is beyond the scope of this thesis. Based on the pavement material properties of the model, the loading configuration and tests outputs, a comparison was made between fatigue life estimated by the model developed in chapter five (Equation (5-13) in this study and the fatigue life estimated by the Asphalt Institute (AI) model (Equation (6-6), which is already calibrated to involve a shift factor of 18.4. The comparison was made to decide a suitable shift factor for the model at the optimum amount of hydrated lime (2.5%). It was found that a value of 84.55 can be applied as a shift factor. As mentioned before, the critical (maximum) tensile strain was at the bottom of Base course, so the properties of the mixture is applied to find fatigue life of the pavement model according to developed fatigue model (Equation (5-13) for the case of the optimum thickness of asphalt concrete layer (210 mm) that modified with optimum lime content:

$$\ln N_f = -47.58 - 2.84997 \times \ln \varepsilon_t + 0.971664 \times HL + 27.05582 \times D + 0.271583 \times MS + 0.148198 \times VFA - 0.30069 \times VMA$$

$$N_f = 27416$$

And by applying a shift factor of 84.55

$$N_f = 2318023 \text{ which greater than expected Traffic } (N_{ESAL})$$

Where:

$$\varepsilon_t = 0.000243, HL = 2.5\%, D = 2.297 \text{ g/cm}^3, MS = 10.7 \text{ kN}, VFA = 67\%, VMA = 13.7\%$$

▪ Permanent Deformation

Permanent deformation is one of the major distresses happen in the flexible pavements. Therefore, it is important to find the rut depth (RD) in the pavement and investigate its influence in the process of Mechanistic-Empirical Approach to assess pavement responses and find the optimum thickness of the asphaltic layer.

The rut depth calculation depends on the summation of plastic strain and the thicknesses of pavement layers during the analysis period Harold and Van (1994). SHRP model by Harold and Van (1994) (Equation (2-19)) calculates the rut depth by multiplying the permanent strain of each pavement layer by its thickness to find the permanent deformation in it and then the summation of the deformation of all layers to determine the total permanent deformation (rut depth).

As mentioned in chapter two, there are three types of permanent deformation that may happen in the asphalt pavement; the first one is wearing rutting occurs due to lack of coated aggregate particles in the pavement surface layer and leads to loose material along the wheel path. The second one is the structural failure due to inadequate asphaltic and subbase layers thicknesses that lead to transfer higher loading stresses to the subgrade without reaching the value that the subgrade layer can withstand. The third type is related to the asphaltic layer instability due to high vehicle tire pressure and axle load repetitions that lead to condensation and lateral displacement of material within the pavement asphaltic concrete layers. To find rut depth (RD) in the asphalt concrete, firstly the amount of permanent strain should be obtained from Equation (5-14), which is developed in chapter five.

$$\log \varepsilon_p = 1.4092 + 0.0455 \times T + 0.36383 \times \log N - 0.02349 \times MS - 0.1122 \times HL - 0.01767 \times P200$$

Based on the AASHTO guide (1993), rutting is classified according to severity level as exhibited in Table (6-7).

Table (6-7) Rut Depth Criteria According to AASHTO (1993)

Mean Rut Depth, mm (in.)	Severity Level
6 – 13 ($\frac{1}{4}$ - $\frac{1}{2}$)	Low
> 13 – 25 ($> \frac{1}{2}$ - 1)	Medium
> 25 (> 1)	High

Throughout calculation of permanent deformation for each trial thickness of the asphaltic layer in the pavement model, it was found that the rut depth value significantly depended on the hydrated lime addition to the mixtures. The range of rut depth of non-modified models was about 6 mm to 7 mm, while after modification with the optimum value of hydrated lime, the rut depth reduced to half and was ranged from 3 mm to 3.6 mm and this is a significant improvement in resisting the rutting. For instance, in the case of the asphaltic layer thickness of 230 mm (50 mm Wearing, 80 mm Leveling, and 100 mm Base course), the rut depth for the model of control mixes was 6.9 mm, and for the modified mixes the total rut was 3.6 mm. The results and according to AASHTO 1993 criteria indicate that severity of these rutting depths classified as low level even without the impact of hydrated lime. However, the modification with hydrated lime gave an additional factor of safety to withstand the loads causing rutting and minimise its effect on the flexible pavement structure. The Table (6-8) shows the rut depth (RD) results for each asphalt concrete layer thickness for control and lime modified mixtures.

Table (6-8) Rut Depth Prediction in Asphaltic Layer of Pavement Model (N= N_{ESAL}= 2318000)

Asphalt Concrete layer thickness (mm)		Input Parameter of Permanent Strain Model Including N and HL			Permanent Strain (ϵ_p)		Rut Depth, RD (mm)		Total Rut Depth (mm)	
Total	Each Course	Pave Temp. (°C)	Marshall Stability (kN)	Passing sieve No. 200 (%)	Control	Modified	Control	Modified	Control	Modified
180	W 40	27.23	11.6	7	0.0369	0.01937	1.47	0.77	5.9	3.09
	L 60	25.51	10.57	6	0.0339	0.01782	2.03	1.06		
	B 80	23	8.9	5	0.0297	0.0156	2.38	1.24		
190	W 50	27	11.6	7	0.0360	0.0189	1.8	0.94	5.85	3.06
	L 60	24	10.57	6	0.0290	0.0152	1.74	0.91		
	B 80	22.68	8.9	5	0.0288	0.0151	2.3	1.2		
200	W 50	27	11.6	7	0.0360	0.0189	1.8	0.94	6.35	3.32
	L 70	25.3	10.57	6	0.0332	0.0174	2.32	1.22		
	B 80	22.32	8.9	5	0.0277	0.0145	2.21	1.16		
210	W 50	27	11.6	7	0.0360	0.0189	1.8	0.94	6.54	3.43
	L 70	25.3	10.57	6	0.0332	0.0174	2.3	1.22		
	B 90	22	8.9	5	0.0268	0.0140	2.41	1.26		
220	W 50	27	11.6	7	0.0360	0.0189	1.8	0.94	6.69	3.5
	L 80	24.8	10.57	6	0.0315	0.01654	2.52	1.32		
	B 90	21.8	8.9	5	0.0262	0.01377	2.36	1.23		
230	W 50	27	11.6	7	0.0360	0.01891	1.8	0.94	6.9	3.6
	L 80	24.8	10.57	6	0.0315	0.01654	2.52	1.32		
	B 100	21.61	8.9	5	0.0257	0.0135	2.57	1.35		
240	W 50	27	11.6	7	0.0360	0.0189	1.8	0.94	7.05	3.69
	L 90	24.6	10.57	6	0.0309	0.0161	2.78	1.45		
	B 100	21.2	8.9	5	0.0246	0.0129	2.46	1.29		

6.6 Summary and Further Discussion

Some points are summarised based on the analysis and results of this chapter:

- The horizontal tensile strain located beneath HMA layer and vertical compressive strain at the top of subgrade layer decreased due to two causes. The first one is the increase of the thickness of the hot mix asphalt layer and the second reason is the addition of hydrated lime as a partial replacement of the mineral filler percentage. The accumulated decrease rate in tensile strain from 180 mm HMA thickness up to the optimum thickness (210 mm) was 38.4% and 37.22% in FEA and MLET techniques respectively. For the compressive strain, the reduction rate accumulation reached a value of 31% estimated by ANSYS and 29% by KENPAVE at the thickness of 210 mm.
- It can be found that the hydrated lime addition to the mix significantly increases the fatigue and permanent deformation number of load repetitions for the same thickness of the asphaltic layer. For instance, the improvement in the of fatigue life at the HMA thickness of 210 mm was 33.75% and 37.65% for FEA and MLET approaches respectively and increased from the first iteration thickness of 180 mm until the optimum thickness of 210 mm by 93.9% and 89% for FEA and MLET techniques respectively. The enhancement percent in permanent deformation repetitions for the thickness of 210 mm was about 70% at both of FEA, and MLET approaches. The accumulation in rutting load repetitions thickness of 180 mm up to the optimum thickness of 210 mm was 182% and 171% at FEA and MLET techniques respectively.
- The optimum thickness of asphalt concrete layer is 210 mm at hydrated lime addition percent of 2.5, which contributed a damage ratio that less than one in both finite element analysis and multi-layer elastic theory approaches.
- At the optimum thickness of asphalt concrete layer (210mm), the ratios of asphalt pavement courses to the total thickness of HMA layer are 23.8%, 33.33% and 42.8% for the wearing, leveling and base courses respectively, and they were approximately equal to the average values of each pavement course. The ratios could be an indication of the relation of each course thickness to the total thickness of the whole asphalt concrete layer.
- There is a profit of about 12.5% in the asphalt concrete thickness of the studied model due to hydrated lime addition. The thickness of 210 mm with 2.5% of hydrated lime gave almost the same value of damage ratio that the thickness of 240 mm at 0% of hydrated

lime (control mixes) provided. The 12.5% profit in asphaltic layer thickness could save a cost of flexible pavement construction. For instance, the profit in the asphalt concrete layer thickness in the case studied in this chapter is 0.03 m. To construct a new flexible pavement road of a length of 1 km and two lanes (the width of the lane is 3.65 m, so the total width is 7.3 m) by adopting the pavement layers thicknesses and material properties of the case study in this research, there will be a gain of about 219 m³ of asphalt concrete mix (about 503700 kg since the density of the asphalt concrete mix is about 2.3 g/cm³ (2300 kg/m³)).

Chapter Seven

Conclusions and Recommendations

From the materials and testing programme, the investigation of results, statistical analysis, design proposal, and numerical modelling, the following points are concluded together with recommendations and future research works.

7.1 Conclusions

1. The hydrated lime has been successfully used in asphalt concrete mixtures for a long time, and it is still an active research area as explained by the high number of recent publications. As observed in the literature review, the efficiency of hydrated lime has been confirmed in improving the asphalt concrete pavement resistance to the major distresses that could occur in it such as rutting, fatigue cracking and moisture damage. In this study, the hydrated lime was added in a dry form (adding dry lime to dry aggregate) prior to binder addition and mixing process. The addition of hydrated lime was in six contents; 0%, 1.0%, 1.5%, 2.0%, 2.5% and 3.0% by total weight of aggregate as a partial replacement of limestone dust.
2. The conclusions that based on the results of experimental work are as follows:
 - 2.1 The hydrated lime addition has a significant effect on the consistency of asphalt-filler mix;
 - Regarding the penetration test, the increasing in hydrated lime amount leads to decreasing the penetration, for instance, adding of 2.5% of hydrated lime results in a reduction in penetration of about 24% of penetration at 1% of hydrated lime addition percentage to the asphalt cement. An approximated average of reduction rate in the penetration can be concluded as 4.7 at hydrated lime increment rate of 1%.
 - The rising in the hydrated lime percent leads to increase in softening point value. The softening point at 3% of hydrated lime is greater than softening point temperature degree when hydrated lime is 0% by about 27%. It can be noticed that the increment rate of the temperature is about (4°C to 5°C) for every 1% of hydrated lime replacement. Accordingly, the higher the addition percent of hydrated lime, as a partial replacement with the mineral filler, the higher consistency and stiffness of the lime modified asphalt cement.

- 2.2 Hydrated lime enhances Marshall Properties as well as reflects the demand of mixture for more asphalt cement by increasing the optimum asphalt content. Mixtures with 2, 2.5 and 2.5% of hydrated lime of the Wearing, Leveling, and Base mixes respectively, have more desirable properties. They gained higher stability, low flow and maintained suitable air voids. The extra amount of hydrated lime negatively affected the volumetric properties of mixtures.
- 2.3 Mixtures modified with hydrated lime perform better than control mixes due to the combined effects of hydrated lime in increasing the mix stiffness, strength and toughness of mastic that induces better resistance against degradation.
- 2.4 The addition of hydrated lime as a filler substitution material led to progressive enhancement of fatigue resistance until the percent of 2.5. Beyond this amount of hydrated lime, the mixtures were weaker to withstand the fatigue related damage.
- 2.5 The addition of more hydrated lime content to the mixes up to 2.5% has shown an increase in resilient modulus for the mixes for temperature sequence of 20°C, 40°C, and 60°C. In 3% lime addition percentage, there is a slight decrease in stiffness at 40°C and 60°C. At 20°C, the resilient modulus values steadily increase as more hydrated lime content added until the last addition percentage (3%). It can be concluded that the temperature is a significant factor affecting HMA performance-related properties such as stiffness since mixtures became stiffer at the lower temperature and vice versa. Nevertheless, the influence of hydrated lime is obvious in enhancing the properties of mixtures to withstand temperature significance.
- 2.6 Regarding the moisture susceptibility of evaluated mixtures, the H2.5W mix shows the highest tensile strength ratio (TSR) among others. There was a significant improvement in the tensile strength of the mixes of about 3% to 4% rise per each percent of hydrated lime added to the mix. The optimum percent was 2.5% with a gain of 17.78% in tensile strength ratio as compared to the control mix (CW). Increasing the amount of hydrated lime beyond the threshold value of 2.5% did not appear to enhance the resistance to moisture damage any further and exhibited a trend of slight decrease in tensile strength. H2L and H2B mixes produced the highest values of TSR as compared to other mixtures by raising the TSR of H2L and H2B mixes to 84.65% and 79.89% respectively. The gain in tensile strength ratio was about 15% for the leveling mix and 12% for the base mix as compared to the control

mixes. The addition of hydrated lime to the mixtures displayed positive impact concerning moisture damage resistance. Mixtures modified with hydrated lime perform better than control mixtures due to increasing the mixture stiffness and consistency of mastic that induces better resistance against degradation caused by water presence. In addition, the enhancement of the tensile strength was noticed on the uncontended (dry) mixtures as well, as a result of the hydrated lime addition.

2.7 In general, high hydrated lime content (up to 3% in this study) results in an obvious improvement in the resistance to permanent deformation under repeating loads and increases the durability of the mixtures. The improvement is highly pronounced in hot weather conditions. Together with the conclusions above, an optimum 2.5% hydrated lime percentage can be suggested for all practices. The general trends in the tests data showed that the addition of hydrated lime up to 2.5% as a partial replacement of ordinary limestone mineral filler results in a considerable improvement in the performance of asphalt concrete mixes and makes them more durable and higher resistant to distresses.

3. Statistical analysis was performed to investigate the relation between the performance related properties parameters studied in the laboratory work. Two statistical models were developed to predict the number of repetition to fatigue cracking and the permanent strain in the asphaltic layer. These models could be indexes of failure criteria that may be adopted for the Mechanistic-Empirical design method and to give an impression of the future behaviour of asphalt concrete mixtures. In the modelling building, the pavement material properties and performance-related properties variables gained from the laboratory work and affected by hydrated lime addition have been adopted. In the permanent strain model, permanent deflection in the pavement can be calculated by multiplying the output strain of each asphaltic layer by its thickness. The developed models are as follows:

- Fatigue Life Model:

$$\ln N_f = -47.58 - 2.84997 \times \ln \varepsilon_t + 0.971664 \times HL + 27.05582 \times D + 0.271583 \times MS + 0.148198 \times VFA - 0.30069 \times VMA$$

- Rutting Model:

$$\log \varepsilon_p = 1.4092 + 0.0455 \times T + 0.36383 \times \log N - 0.02349 \times MS - 0.1122 \times HL - 0.01767 \times P200$$

4. In the application of Mechanistic-Empirical design method, the mechanistic part of the approach was performed by numerical modelling of pavement structure through using finite element analysis by ANSYS programme and axisymmetric multilayered elastic method by KENPAVE software. The performance analyses and results illustrated that the asphalt concrete layer in the pavement model reached the optimum total thickness of 210 mm. The optimum thickness was for the asphalt concrete pavement layers modified with optimum percent value of hydrated lime (2.5%). The iteration process began with 180 mm of asphalt concrete layer thickness for the asphalt concrete mixtures before and after hydrated lime modification.
5. The reason behind the testing programme conducted in this study is to determine and evaluate the hydrated lime modified HMA pavement mechanical responses to the major distresses (fatigue cracking, rutting and moisture susceptibility) that generally occurred in the pavement. In particular, fatigue cracking and rutting that considered as failure criteria in the M-E design method. The modification of pavement asphaltic mixtures by hydrated lime was a useful step in the M-E design process to reach the optimum thickness of asphalt concrete layer with less thickness as compared to control mixtures.

7.2 Recommendations for Future Research

Based on the findings and conclusions of this study, further studies are recommended to consider the following related approaches:

1. Implementation of hydrated lime effect on the asphalt concrete mixes to develop a framework to design the overlay of flexible pavement. Based on the M-E design method, the determination of overlay thickness relies on the condition of the pavement and its remaining life. Modification of the overlay layer with hydrated lime could give the required life with less layer thickness or extend the design life more than the control overlay mix at the same designed thickness.

2. Prediction of a local pavement adjustment (shift) factor after correlating the developed statistical models of fatigue life and permanent deformation that based on the laboratory test results with actual measurements of the pavement structural responses in the field.
3. Further investigation could be needed for the Mechanistic-Empirical design of pavement to determine the optimum asphalt concrete pavement thickness with respect to hydrated lime influence accompanied by other modification materials like aluminium or carbon fibres, with different types of mineral filler, asphalt cement, and aggregate.

References

- AASHTO, (1986). Guide for Design of Pavement Structures; American Association of State Highway and Transportation Officials. Washington, D.C., USA.
- AASHTO, (1993). Guide for Design of Pavement Structures, American Association of State Highway and Transportation Officials. Washington, D.C., USA.
- AASHTO, 2007, “Standard Specification for Mineral Filler for Bituminous Paving Mixtures.” AASHTO Designation: M 17-07, American Association of State Highways and Transportation Officials, Washington, D.C.
- Adrian R. A. and Samer M. (2000) “Development Of A Pavement Rutting Model From Experimental Data” The University of California Transportation Center University of California at Berkeley. The Journal of Transportation Engineering.
- Ahlvin,R.G.; Ulery, H.H. (1962) “Tabulated values for determining the complete pattern of stresses, strains and deflections beneath a uniform circular load on a homogeneous half space”. Highway Research Board Bulletin 342. Washington D.C.
- Albayati, A. (2012). Mechanistic Evaluation of Lime-Modified Asphalt Concrete Mixtures. 7th RILEM International Conference on Cracking in Pavements. A. Scarpas, N. Kringos, I. Al-Qadi and L. A, Springer Netherlands. 4: 921-940.
- Albayati, A. and Ahmed M., “Assessment the Impact of Different Hydrated Lime Addition Methods on Fatigue Life Characteristic”. Eng. & Tech. Journal, Vol. 31, Part (A), No.21, 2013.
- Albayati, A. H. K. & Alani, A. M. M. 11th – 12th February 2015. Temperature Prediction Model for Asphalt Concrete Pavement. LJMU 14th Annual International Conference on Asphalt, Pavement Engineering and Infrastructure. Liverpool, UK.
- ALLEN, D. M. 1974. The Relationship Between Variable Selection and Data Augmentation and a Method for Prediction. Technometrics, 16, 125-127.
- Al-Suhaibani, AbdulRahman., Al-Mudaiheem, Jamal, and Al-Fozan ,F.(1992) , “ Effect of Filler Type and Content on Properties of Asphalt Concrete Mixes”. In Effects of Aggregates and

- Mineral Fillers on Asphalt Mixtures Performance, SPT 1147 (R. C. Meininger, ed.), ASTM, Philadelphia, Pa., pp. 107–130.
- Angela L. P, Kimley, H.,(2006) “Methodology and Calibration of Fatigue Transfer Functions for Mechanistic-Empirical Flexible Pavement Design”, NCAT Report 06-03, National Center for Asphalt Technology Auburn University, Alabama.
- ANSYS User's Manual. (2009). 12th ed. Canonsburg, PA, ANSYS, Inc.
- ANSYS User's Manual. (1998). 5.5th ed. Canonsburg, Pennsylvania, ANSYS, Inc.
- Asam , K.,R., (2001), ” Laboratory Evaluation of the Effect of Superpave Gradations and Polymer Modified Asphalts on Pavement Performance”, M.Sc thesis , The Faculty of the Fritz J. and Dolores H. Russ, College of Engineering and Technology, Ohio University.
- Aschenbrener, T. and Far, N., (1994). “Influence of Compaction Temperature and Anti- Stripping Treatment on the Results from the Hamburg Wheel-Tracking Device”, Rpt # CDOT-DTD-R-94-9, Colorado Department of Transportation, July 15.
- Asphalt Institute, (1981). “Thickness Design-Asphalt Pavements for Highways and Streets”, Asphalt Institute, Manual Series No.1, College Park, Maryland, USA.
- Asphalt Institute, (1984). Mix Design Methods for Asphalt Concrete and Other Hot-Mix Types. Manual Series No. 2.Lexington, KY.
- ASTM D6926-10, Standard Practice for Preparation of Bituminous Specimens Using Marshall Apparatus, ASTM International, West Conshohocken, PA, 2010.
- ASTM, (2004). “Road and Paving Materials,” Annual Book of ASTM Standards, Volume 04.03, American Society for Testing and Materials,” West Conshohocken, USA.
- Baig, M.G., (1995). “Laboratory Evaluation of Hedmanite and Lime Modified Asphalt Concrete Mixes”, M.Sc., Thesis, civil engineering, King Fahd University of petroleum & Minerals, Dhahran, Saudi Arabia.
- Barksdale, R. (1972). “Laboratory Evaluation of Rutting in Base Course Materials”, Proceedings, Third International Conference on the Structural Design of Asphalt Pavements, London.

- Behiry Ahmed E. Abu El-Maaty, "Fatigue and rutting lives in flexible pavement" *Ain Shams Engineering Journal* (2012) 3, 367–374.
- Bonnaure, F., Huibbers, A.H.J.J., and Booders, A. (1982) "A Laboratory Investigation of the Influence of Rest Periods on Fatigue Characteristics of Bituminous Mixes", *Proceedings, The Association of Asphalt Paving Technologists*, Vol. 51, pp. 104.
- Boussinesq, J. (1885). *Application des potentials a l'étude de l'équilibre et du Mouvement des Solids Elastiques*, Gauthier-Villars, Paris, France.
- Boynton, R. S., (1980) "Chemistry and Technology of Lime and Limestone", 2nd ed., New York (New York, USA): Wiley-Interscience.
- Boyes, A. J. (2011) "Reducing moisture damage in asphalt mixes using recycled waste additives". Doctoral dissertation, California Polytechnic State University, San Luis Obispo.
- Brown, E.R., and S. A. Cross, (1992), "A national Study of Rutting in Hot Mix Asphalt (HMA) Pavements," National Center for Asphalt Technology, USA.
- Burmister D. M. (1945a) "The general theory of stresses and displacements in layered systems. I" *Journal of Applied Physics*, 16, pp. 89–94.
- Burmister D. M. (1945b) "The general theory of stresses and displacements in layered systems. II" *Journal of Applied Physics*, 16, pp. 126–127.
- Burmister D. M. (1945b) "The general theory of stresses and displacements in layered systems. III" *Journal of Applied Physics*, 16, pp. 296–302.
- Burmister, D. M. (1943). "The Theory of Stresses and Displacements in Layered Systems and Applications to the Design of Airport Runways." *Highway Research Record* 23, TRB, National Research Council, Washington, D.C., pp. 126-144.
- Chen, D. H., Zaman, M., Laguros, J., and Soltani, A. (1995). "Assessment of Computer Programs for Analysis of Flexible Pavement Structures." *Transportation Research Record* 1482, TRB, National Research Council, Washington, D.C., pp. 123-133.
- Chen, J., S., Peng, C., H., (1998), "Analyses of Tensile Failure Properties of Asphalt-Mineral Filler Mastics" *ASCE, Journal of Materials in Civil Engineering*.

- Cheng, D., D. N. Little, R. L. Lytton, and J. C. Holste. (2002). Surface Energy Measurement of Asphalt and Its Application to Predicting Fatigue and Healing in Asphalt Mixtures. In Transportation Research Record: Journal of the Transportation Research Board, No. 1810, TRB, National Research Council, Washington, D.C., pp. 44–53.
- Claessen, A., P. Edwards, P. Sommer, and P. Uge, (1977), “Asphalt pavement Design: the SHELL Method,” Proceedings Fourth International Conference on the Structural Design of Asphalt Pavements, the University of Michigan, Ann Arbor, Michigan, USA.
- Collins, R., Johnson, A., Wu, Y. and Lai, J., “Evaluation of Moisture Susceptibility of Compacted Asphalt Pavement Analyzer”, paper submitted to TRB, January 12-16, 1997.
- Crossley, G., A., (1998), “Synthesis and Evaluation of a New Class of Polymers for Asphalt Modification” , M.Sc thesis , Queen's University Kingston, Ontario, Canada.
- Curtis, C. W., R. L. Lytton, and C. J. Brannan. (1992). Influence of Aggregate Chemistry on the Adsorption and Desorption of Asphalt. In Transportation Research Record 1362, TRB, National Research Council, Washington, D.C., pp. 1–9.
- Dawley, C., B. Hogewiede, and K. Anderson, (1990), “Mitigation of Instability Rutting of Asphalt Concrete Pavements in Lethbridge, Alberta, Canada,” Proceedings Association of Asphalt Paving Technologists (AAPT), USA.
- Deacon, J., A. Tayebali, J. Coplantz, F. Finn, and C. Monismith, (1994), "Fatigue Response of Asphalt-Aggregate Mixes, Part III - Mix Design and Analysis", Strategic Highway Research Program Report No. SHRP-A-404, National Research Council, Washington, D.C, pp. 225-279.
- Devore, J. & Berk, K. 2012. Regression and Correlation. Modern Mathematical Statistics with Applications. Springer New York.
- Devore, J. 2011. Probability and Statistics for Engineering and the Sciences, Cengage Learning.
- Eisenmann, J., and A. Hilmer. (1987), “Influence of Wheel Load and Inflation Pressure on the Rutting Effect at Asphalt-Pavements – Experiments and Theoretical Investigations,” Proceedings, Sixth International Conference on the Structural Design of Asphalt Pavements, Vol. I, Ann Arbor, Michigan, USA.

- Epps, J. A., "Hydrated Lime in Hot Mix," Presentation Manual, FHWA, AASHTO, NLA, 1992.
- Esarwi, A.M., Hainin, M.R. and Chik, A.A., (2008) "Stripping resistance of Malaysian hot mix asphalt mixture using hydrated lime as filler". EASTS International Symposium on Sustainable Transportation incorporating Malaysian Universities Transport Research Forum Conference, Universiti Teknologi Malaysia.
- Fayadh, S., S., (1987). "Hydrated lime and Rubber as Additives in Asphalt Paving Mixtures", M.Sc, thesis, civil engineering, University of Baghdad.
- Finn, F., Saraf. C.L., KulKarni, R., Nair, K., Smith, W. and Abdullah, A. (1987). "Development of pavement structural subsystems". National Cooperative Highway Research Program (NCHRP) No. 291, National Research Council, Washington DC.
- Foster, C. R., and Ahlvin, R. G. (1958). "Development of Multiple-Wheel CBR Design Criteria." Journal of the Soil Mechanics and Foundations Division, ASCE, Vol. 84, No. SM2, pp. 1647-1 – 1647-12.
- Gorkem, C. and Sengoz, B., (2009) "Predicting stripping and moisture induced damage of asphalt concrete prepared with polymer modified bitumen and hydrated lime". Construction and Building Materials, 23(6), pp.2227-2236.
- Harichandran, R. S., Yeh, M. S., and Baladi, G. Y. (1989). "MICH-PAVE: A Nonlinear Finite Element Program for Analysis of Pavements." Transportation Research Record 1286, TRB, National Research Council, Washington, D.C., pp. 123-131.
- Harris, B.M. and Stuart, K.D. (1995). "Analysis of Mineral Fillers and Mastics Used in Stone Matrix Asphalt.", Vol. 64, pp.54-95., Journal of the Association of Asphalt Paving Technologists.
- Helwany, S., Dyer, J., and Leidy, J. (1998). "Finite-Element Analyses of Flexible Pavements." Journal of Transportation Engineering, ASCE, Vol. 124, No. 5, pp. 491-499.
- Hicks, R. G. (1970). Factors Influencing the Resilient Response of Granular Materials, Ph.D. Dissertation, University of California, Berkeley, CA.
- Hogg, R.V., and Tanis, E.A. (1988), "Probability and Statistical Inference, Macmillan Publishing Company, 3rd Edition, New York.

- Hopman, P.C., Kunst P.A.J.C , A.,C., Pronk, (1989) “A Renewed Interpretation Method for Fatigue Measurement, Verification of Miner’s Rule” 4th Eurobitume Symposium, Volume 1, , pp 557-561 Madrid.
- Hossain, K. and Ullah, F., (2011) “Laboratory evaluation of lime modified asphalt concrete mixes with respective to moisture susceptibility”. International Journal of Civil & Environmental Engineering IJCEE-IJENS, 11(4), PP 47-54.
- Huang, Y., (2004), “Pavement Analysis and Design”, 2nd Edition, Prentice Hall, Englewood Cliffs, New Jersey, USA.
- Huang, Yang H., (1993) “Pavement Analysis and Design,” 1st Edition, Prentice Hall, Englewood Cliffs, New Jersey, USA.
- Huang, B., Shu, X., Dong, Q. and Shen, J., (2010) “Laboratory evaluation of moisture susceptibility of hot-mix asphalt containing cementitious fillers”. Journal of Materials in Civil Engineering, 22(7), pp.667-673.
- Huebner, K. H., Dewhirst, D. L., Smith, D. E., & Byrom, T. G. (2001). The finite element method for engineers (4th ed.). New York: Wiley.
- Iqbal M. H., (2004), “Influence of Polymer Type and Structure on the Modification of Saudi Asphalt”, MS Thesis, KFUPM, Dhahran, Saudi Arabia.
- J.W. Button and J.A. Epps. (1983). “Evaluation of Methods of Mixing Lime and Asphalt Paving Mixtures.” Texas Hot Asphalt Pavement Association.
- Jamieson, J.S. Moulthrop, and D.R. Jones, (1995). “SHRP Results on Binder-Aggregate Adhesion and Resistance to Stripping,” Asphalt Yearbook 1995, pp. 17-21.
- Jia Ying and Chen Yiling, (2015). "Application of Elastic Layered System in the Design of Road", International Journal of Engineering Research and Applications (IJERA), Vol. 5 - Issue 7, ISSN: 2248-9622.
- Jony,H.,H., (2010) “ Most Distresses Causes in Flexible Pavement For Baghdad Streets At Last Years “ , Engineering and Technology Journal, Vol. 28 , No.18.

- Kachlakev, D., Miller, T., Yim, S., Chansawat, K. and Potisuk, T., (2001). Finite element modeling of concrete structures strengthened with FRP laminates. Final report, SPR, 316.
- Kandhal, P. S., and J.F. Parker, (1998), “Aggregate Tests Related to Asphalt Concrete Performance in Pavements,” NCRP Report 405 National Academy Press Auburn.
- Kavussi, A., Hicks, R.G., (1997), “Properties of Bituminous Mixtures Containing Different Fillers.”, Vol. 66, pp.153-186, Journal of the Association of Asphalt Paving Technologists.
- Keller, G., and Warrack, B. (2000), “STATISTICS for Management and Economies,”5th Edition, USA.
- Kennedy, J.B., and Neville, A.M. [1986], “Basic Statistical Methods for Engineers and Scientists” 3rd Edition, Thomas Y., Crowell Company, USA.
- Kim Yong-Rak, Ban Hokie, Im Soohyok (2010). “Impact of Truck Loading on Design and Analysis of Asphaltic Pavement Structures.” Final Reports & Technical Briefs. Paper 23. Mid-America Transportation Center. University of Nebraska -Lincoln.
- Kim, M. (2007). Three-Dimensional Finite Element Analysis of Flexible Pavements Considering Nonlinear Pavement Foundation Behavior. Ph.D. Thesis, University of Illinois at Urbana-Champaign.
- Kim, M., E. Tutumluer and J. Kwon (2009). "Nonlinear Pavement Foundation Modeling for Three-Dimensional Finite-Element Analysis of Flexible Pavements." International Journal of Geomechanics, ASCE 9(5): 195-208.
- Kim, O. X., Bell, C.A., and Hicks, R. G, (1995), “The Effect of Moisture on the Performance of Asphalt Mixtures”, ASTM STP-899, 1995.
- Kim, Y. R., Little, D. N. & Song, I. (2003)” Effect of Mineral Fillers on Fatigue Resistance and Fundamental Material Characteristics Mechanistic Evaluation”. Transportation Research Record, Journal of the Transportation Research Board ,pp. 1-8 , Transportation Research Record 1832, Transportation Research Board of the National Academies, Washington.
- Kok,B.,V., Yilmaz,M.,(2009), “The effects of using lime and styrene–butadiene–styrene on moisture sensitivity resistance of hot mix asphalt”, Vol.23, PP1999-2006, journal of Construction and Building Materials, Elsevier.

- Kopperman, S., Tiller, G., and Tseng, M. (1986). ELSYM5, Interactive Microcomputer Version: User's Manual, Federal Highway Administration, Washington, D.C.
- Kremelberg, D. 2011. Practical statistics : a quick and easy guide to IBM SPSS statistics, STATA, and other statistical software, Los Angeles, SAGE Publications.
- Kutner, M. H., Nachtsheim, C. J., Neter, J., Li, W. 2005. Applied Linear Statistical Models, McGraw-Hill Irwin.
- Lee ,S.,(2007),” Investigation of the Effects of Lime on the Performance of HMA using Advanced Testing and Modeling Techniques”, PH.D thesis, Civil Engineering, Raleigh, North Carolina , North Carolina State University.
- Lesueur, D . , Little, D. N., (1999), “Effect of Hydrated Lime on Rheology, Fracture and Aging of Bitumen” Transportation Research Record, Journal of the Transportation Research Board ,pp. 93-105, Transportation Research Record 1661, Transportation Research Board of the National Academies, Washington.
- Li, Qiang, Xiao, DannyX, Wang, KelvinC P., Hall, KevinD, Qiu, Yanjun, (2011), "Mechanistic-empirical pavement design guide (MEPDG): a bird's-eye view." Journal of Modern Transportation 19(2): 114-133.
- Little, D. N. and Epps, J.,” The benefits of hydrated lime in hot mix asphalt”, Report for national lime association, 2001.
- Little, D. N., “Laboratory Testing Asphalt Mixtures Incorporating Crushed River Gravel Stockpile Treated with Lime Slurry”, prepared for Chemical Lime Corporation, Texas Transportation Institute, 1994.
- Little, D., N., Peterson, J.,C., (2005) ” Unique Effects of Hydrated Lime Filler on the Performance Related Properties of Asphalt Cements: Physical and Chemical Interactions Revisited” Journal of Materials in Civil Engineering, Vol. 17, No. 2,PP207-218., ISSN 0899-1561/2005/2-207 218, ASCE.
- Little, D., N., Peterson, J.,C.,(2005) , ” Unique Effects of Hydrated Lime Filler on the Performance-Related Properties of Asphalt Cements: Physical and Chemical Interactions

Revisited” Journal of Materials in Civil Engineering, Vol. 17, No. 2, PP207-218., ISSN 0899-1561/2005/2-207–218, ASCE.

Little, D.N. and Jones, D.R., (2003). Chemical and mechanical processes of moisture damage in hot-mix asphalt pavements. In National seminar on moisture sensitivity of asphalt pavements (pp. 37-70).

M. Satyakumar, R. Satheesh Chandran and M.S. Mahesh, “Influence of Mineral Fillers on the Properties of Hot Mix Asphalt”. International Journal of Civil Engineering and Technology (IJCIET), Volume 4, Issue 5, September – October (2013).

Mathew Tom V, Krishna Rao KV, (2009), “Introduction to transportation engineering”. Press, p. 27.1–8 [National Programme on Technology Enhanced Learning, India.

McCann, M. and Sebaaly, P.E., (2003) “Resilient Modulus, Tensile Strength, and Simple Shear Test to Evaluate Moisture Sensitivity and the Performance of Lime in Hot Mix Asphalt Mixtures”. Transportation Research Record 1832, Bituminous Paving Mixtures, pp.9-16.

McGennis, R.B., Anderson, R.M., Kennedy, T.W., and Solaimanian, M., (1995), "Background of Superpave Asphalt Mixture Design and Analysis", Report No. FHWA-SA-95-003, U.S. Department of Transportation.

Millard, R.S. (1993), “Road building in the Tropics”. Transport Research Laboratory State-of-the-art Review 9, HMSO, London.

Miner, M.A., (1945) “Cumulative Damage in Fatigue,” Transactions, American Society of Mechanical Engineers, Vol. 67, pp. A159-A164.

Monismith, C. L. (1966). “Asphalt Mixture Behavior in Repeated Flexure.” Report No. TE 66-66, ITIE, to California Division of Highways, University of California.

Monismith, C., Ogawa, N. and Freeme, C. (1975). “Permanent Deformation Characteristics of Subgrade Soils due to Repeated Loadings”, TRR 537.

Monismith, C.L., Epps, J.A. and Finn, F.N. (1985) "Improved asphalt mix design". Journal of the Association of Asphalt Paving Technologists, Vol. 54, pp. 347-406, pp. 43.

- Monismith, C.L., J.A. Epps, D.A. Kasianchuk, and D.B. McLean (1971), " Asphalt Mixture Behavior in Repeated Flexure", Report TE 70-5, University of California, Berkeley, pp.303.
- Montgomery, D.C., and Peck, E.A. (1992), "Introduction to Linear Regression Analysis,"2nd Edition, John Wiley & Sons, Inc., New York.
- Morris, J. (1973), "The Prediction of Permanent Deformation in Asphalt Concrete Pavements," The Transport Group, Department of Civil Engineering, University of Waterloo.
- National Cooperative Highway Research Program, NCHRP (2002). "Contributions of Pavement Structural Layers to Rutting of Hot Mix Asphalt Pavements", Report No. 468, National Research Council, Washington, D. C. USA.
- National Lime Association, (2006) "Hydrated Lime - A Solution for High Performance Hot Mix Asphalt", Fact Sheet.
- NCHRP (2004), "Mechanistic-Empirical Design of New and Rehabilitated Pavement Structures," NCHRP Project 1-37A Draft Final Report, Transportation Research Board, National Research Council, Washington, D.C.
- NCHRP (2004), "Guide for Mechanistic-Empirical Design of New and Rehabilitated Pavement Structures", Final Document. Appendix II-1.
- Neter, J., Wassermann, W., and Kutner, M.H. (1990). "Applied Linear Statistical Models: Regression, Analysis Of Variance, and Experimental Designs, 3rd Edition, Richard D.Irwin, Inc., Homewood, IL, 1181.
- Pavementinteractive.org (2017) [online] Available at:
<http://www.pavementinteractive.org/article/flexible-pavement-mechanistic-models>.
[Accessed 8 Feb, 2017].
- Pell, P. S. and K. E. Cooper (1975), "The effect of testing and mix variables on the fatigue performance of bituminous materials." Journal of the Association of asphalt Paving Technologists, Vol. 44. pp. 1-37.

- Pell, P.S. (1967). "Fatigue of asphalt pavement mixes." Proceedings, Second International conference on the structural design of asphalt pavements, Ann Arbor, University of Michigan, pp. 310.
- Petersen, J. C., H. Plancher, and P. M. Harnsberger. (1987). Lime Treatment of Asphalt—Final Report. National Lime Association.
- Pinto, I., Ban, H., and Kim, Y., (2009) "Moisture Sensitivity of Hot Mix Asphalt (HMA) Mixtures in Nebraska – Phase II", Report No. MPM-04, Nebraska Department of Roads, Lincoln.
- Plancher, H., and Petersen, J.C. (1976) , "Reduction of Oxidative Hardening in Asphalts by Treatment with Hydrated Lime: A Mechanistic Study". Proc., Association of Paving Technologists, Vol. 45, pp. 1–24.
- Plancher, H., S. Dorrence, and J. C. Petersen. (1977)." Identification of Chemical Types in Asphalts Strongly Absorbed at the Asphalt–Aggregate Interface and Their Relative Displacement by Water". Proc., Association of Asphalt Paving Technologists, Vol. 46, pp. 151–175.
- Prithvi S. Kandhal. (1992). "Moisture susceptibility of HMA Mixes: Identification of Problem and Recommended Solution." NCAT Report No. 92-1.
- Raad, L. and Figueroa, J. L. (1980). "Load Response of Transportation Support Systems." Journal of Transportation Engineering, ASCE, Vol. 16, No. TE1, pp. 111-128.
- Raymond E. Robertson. (1991) "Chemical Properties of Asphalt and Their Relationship to Pavement Performance." SHRP-A/UWP-91-510 Report.
- Roberts, F.,L., Prithvi S, Kandhal, E. Ray Brown, Dah-Yinn Lee, Thomas W. Kennedy. (1996). "Hot mix asphalt materials, mixture design, and construction." Second Edition.
- Roberts, F.,L., Prithvi S, Kandhal, E. Ray Brown, Dah-Yinn Lee, Thomas W. Kennedy. (1996). "Hot mix asphalt materials, mixture design, and construction." Second Edition.
- Saad Issa Sarsam, Samer Muayad Al-Sadik. 2014. Deterioration Model Assessment of Asphalt Concrete Pavement. Research Journal of Modeling and Simulation, 1.

- Sady A. Tayh and Aqeel R. Jabr (2011), "The Effect of Filler Type on the Hot Mix Asphalt Behavior", Eng. & Tech. Journal, Vol. 29, No.9, pp. 1701- 1720.
- Sangyum Lee, Sungho Mun, Y. Richard Kim, Fatigue and rutting performance of lime modified hot-mix asphalt mixtures, Construction and Building Materials, Volume 25, Issue 11, November 2011, Pages 4202-4209, ISSN 0950-0618.
- Savitha T S, R Satheesh Chandran. and M Satyakumar, "Study on Structural Characteristics of Bituminous Mix with Added Hydrated Lime and Phosphogypsum". International Journal of Emerging trends in Engineering and Development. Issue 2, Vol.4 (May 2012).
- Scheaffer, R. L. and McClave, J. T., Probability and Statistics for Engineers. PWSKENT Publishing Company, 3rd ed., 1990. ISBN 0-534-92184-1.
- SCRB/R9 (2003). "General Specification for Roads and Bridges", Section R/9, Hot-Mix Asphalt Concrete Pavement, Revised Edition. State Corporation of Roads and Bridges, Ministry of Housing and Construction, Republic of Iraq.
- Sebaaly, P. E., Hilty, E. and Weizel, D., "Effectiveness of lime in hot mix asphalt pavement". University of Nevada, Reno, 2001.
- Sebaaly, P., E. (2006). "The Benefits of Hydrated Lime in Hot Mix Asphalt." National Lime Association.
- Sengul,C.,E., Aksoy,A., Iskender,E.,Ozen,H., (2011), " Hydrated lime treatment of asphalt concrete to increase permanent deformation resistance", Vol.30, PP139-148, journal of Construction and Building Materials, Elsevier.
- Ševelová, L. ; Florian, A. (2013), 'Comparison of Material Constitutive Models Used in FEA of Low Volume Roads', World Academy of Science, Engineering and Technology, International Science Index 82, International Journal of Civil, Environmental, Structural, Construction and Architectural Engineering, 7(10), 749 - 753.
- Sharrou, A. M., and Saloukeh, G.B., (1992) "Effect of Quality and Quantity of Locally Produced Filler (Passing Sieve No. 200) on Asphaltic Mixtures in Dubai", Effect of Aggregates and Mineral Fillers On asphalt Mixtures Performance, ASTM STP 1147, Richard C. Meininger, Ed., American Society for Testing and Material, Philadelphia.

- Shell (1978), "Shell Pavement Design Manual", Shell International Petroleum Company, Limited, London.
- Shi Chun-xiang, and Guo Zhong-yin (2008). "Mechanical Properties of Asphalt Pavement Structure in Highway Tunnel." *Journal of Shanghai Jiaotong University (Science)* 13(2): 206–210.
- Shoukry, S. N., and Gergis, W. W. (1999). "Performance Evaluation of Backcalculation Algorithm through Three-Dimensional Finite-Element Modeling of Pavement Structures." *Transportation Research Record* 1655, TRB, National Research Council, Washington, D.C., pp. 152-160.
- Sinha, A. K., S. Chandra and P. Kumar (2014). "Finite element analysis of flexible pavement with different subbase materials." *Indian Highways*, Volume: 42, Issue Number: 2, pp 57-66.
- Snee, R.D. (1977) "Experiments in Industry" American Society of Quality Control, Milwaukee, WI.
- Southgate, H. R. Deen, J. Havens, and W. Drake, (1977), "Kentucky Research: A Flexible Pavement Design and Management System," *Proceedings Fourth International Conference on Structural Design of Asphalt Pavements*, Vol. II, the University of Michigan, Ann Arbor, Michigan, USA.
- Strategic Highway Research Program, SHRP (1994), "The Superpave Mix Design System, Manual of Specifications, Tests Methods, and Practices", SHRP-A-379, National Research Council, Washington, D. C., USA.
- Strategic Highway Research Program, SHRP (1994), "The Superpave Mix Design Manual for New Construction and Overlays", SHRP-A-407, National Research Council, Washington, D. C., USA.
- Tayebali, A. A., G. M. Rowe, and J. B. Sousa, (1992), "Fatigue Response of Asphalt-Aggregate Mixtures," *Journal of the Association of Asphalt Paving Technologists*, Vol. 61.
- Thompson, M.R., and Garg, N. (1999). *Wheel Load Interaction: Critical Airport Pavement Responses*, In *Proceedings of the Federal Aviation Administration Airport Technology Transfer Conference*, Atlantic City, NJ.

- Trb.org. (2017). [online] Available at: <http://www.trb.org/NCHRP/NCHRP.aspx> [Accessed 6 Feb, 2017].
- Tukey, J.W. (1977). *Exploratory Data Analysis*. Reading, MA: Addison-Wesley.
- Walid, M. N. (2001) "Utilization of Instrument Response of SuperPave™ Mixes at the Virginia Smart Road to Calibrate Laboratory Developed Fatigue Equations" PhD Dissertation, Virginia University, pp. 168.
- Walubita, L. F., Zhang, J., Alvarez, A. E., and Hu, X. (2013). "Exploring the flow number (FN) index as a means to characterise the HMA permanent deformation response under FN testing." *J. South Afr. Inst. Civ. Eng.*, 55(3), 103–112.
- Wang, J. (2001). *Three-Dimensional Finite Element Analysis of Flexible Pavements*. Master Thesis, the University of Maine, ME
- Witczak M.W., K. Kaloush, T. Pellinen, M. El-Basyouny, and H. V. Quintus, (2002), "Simple Performance Test For Superpave Mix Design," NCHRP Report 465, National Academy Press.
- Witczak, M. (1972). "Design of Full Depth Air Field Pavement", *Proceedings, Third International Conference on the Structural Design of Asphalt Pavements*, London.
- Xiaodi Hu, Shen Zhong & Lubinda F. Walubita (2015). "Three-dimensional modelling of multilayered asphalt concrete pavement structures: strain responses and permanent deformation", *Road Materials and Pavement Design*, 16:3, 727-740.
- Yoder, E. J., Witczak, M. W., (1975), "Principles Of Pavement Design", Second Edition, John Wiley and Sons, Inc. New York.
- Yoon, H. H., A. R. Tarrer and N. R. C. T. R. Board (1988). *Effect of Aggregate Properties on Stripping*, National Research Council, Transportation Research Board.
- Zeng, M., Wu, C., (2008), "Effects of Type and Content of Mineral Filler on Viscosity of Asphalt Mastic and Mixing and Compaction Temperatures of Asphalt Mixture" *Transportation Research Record, Journal of the Transportation Research Board* ,pp. 31-40, *Transportation Research Record 2051*, Transportation Research Board of the National Academies, Washington.

Appendix (A)

The appendix involves Marshall Design Detailed Properties and graphical presentation of Marshall and volumetric characteristics of the Studied Asphalt Concrete Mixtures

Table A-1 Marshall Test Results for the Wearing course

HL	AC %	Density (g/cm ³)	Gmm (g/cm ³)	Stability (kN)	Flow (mm)	Air Voids (%)	VMA (%)	VFA (%)
0	4.3	2.319279	2.443319	9.8	2.5	5.076701	14.48633	64.95524
0	4.6	2.32671	2.435151	11	3	4.453153	14.48127	69.24888
0	4.9	2.341085	2.439101	11.6	3.25	4.01853	14.2235	71.74726
0	5.2	2.337422	2.430078	10.5	3.75	3.812882	14.62788	73.93415
0	5.5	2.326914	2.402802	9.45	4	3.158313	15.28063	79.33126
1	4.3	2.31277	2.436539	10.21	2.5	5.079705	14.63223	65.28412
1	4.6	2.324137	2.434819	10.8	2.75	4.5458	14.48158	68.60978
1	4.9	2.339515	2.437343	12.13	3	4.013715	14.18644	71.70738
1	5.2	2.33595	2.430298	11.32	3.5	3.882158	14.5875	73.38709
1	5.5	2.32457	2.403742	10.44	3.75	3.293698	15.27257	78.4339
1.5	4.3	2.310986	2.439976	9.8	2.25	5.286527	14.65103	63.91704
1.5	4.6	2.321004	2.434387	10.6	2.5	4.657559	14.54976	67.98877
1.5	4.9	2.332536	2.431891	12.5	2.75	4.085504	14.39525	71.61908
1.5	5.2	2.333408	2.42088	11.3	3.25	3.613232	14.63339	75.30831
1.5	5.5	2.321704	2.402448	10.4	3.5	3.360905	15.33037	78.07681
2	4.3	2.306179	2.443825	9.44	2	5.6324	14.78167	61.89605
2	4.6	2.313414	2.435259	11.23	2.5	5.003369	14.7823	66.15297
2	4.9	2.326401	2.438339	13.8	2.75	4.590748	14.57339	68.49911

Table A-1 Continued

HL	AC %	Density (g/cm ³)	Gmm (g/cm ³)	Stability (kN)	Flow (mm)	Air Voids (%)	VMA (%)	VFA (%)
2	5.2	2.330798	2.431671	14.4	3	4.1483	14.68193	71.74553
2	5.5	2.316994	2.408957	11.87	3.5	3.817544	15.45561	75.29995
2.5	4.3	2.29961	2.448482	9.25	2	6.080175	14.97763	59.40495
2.5	4.6	2.30868	2.443248	11.24	2.25	5.50775	14.90986	63.05969
2.5	4.9	2.31722	2.433453	12.93	2.5	4.776464	14.86368	67.86486
2.5	5.2	2.318507	2.422751	13.7	2.75	4.302712	15.08511	71.47709
2.5	5.5	2.311843	2.408141	10.23	3	3.998852	15.59712	74.36161
3	4.3	2.288804	2.444398	9.6	1.75	6.36533	15.33057	58.4795
3	4.6	2.297582	2.438534	10.85	2	5.780194	15.27229	62.1524
3	4.9	2.306516	2.432704	11.6	2.25	5.18715	15.2103	65.89713
3	5.2	2.312002	2.422193	12.02	2.5	4.549225	15.27675	70.22124
3	5.5	2.300483	2.398792	10	2.75	4.098271	15.96563	74.33067

Table A-2 Marshall Test Results for the Leveling course

HL	AC %	Density (g/cm ³)	Gmm (g/cm ³)	Stability (kN)	Flow (mm)	Air Voids (%)	VMA (%)	VFA (%)
0	4	2.299887	2.433002	8.540816327	2.5	5.471207722	14.21285	61.5052
0	4.3	2.316813	2.432308	10.14489796	2.75	4.748385522	13.5815	65.03783
0	4.6	2.328394	2.426142	10.57142857	3.25	4.028935677	13.14951	69.36055
0	4.9	2.32209	2.413053	9.785714286	3.75	3.769637294	13.38466	71.83614
0	5.2	2.310303	2.388036	8.367346939	4.25	3.255114697	13.82433	76.45372
1	4	2.304162	2.444697	8.93877551	2.25	5.748548788	13.98842	58.90493
1	4.3	2.315835	2.445115	9.687755102	2.75	5.287253812	13.55267	60.98737
1	4.6	2.326365	2.437453	10.32244898	3	4.557550282	13.15961	65.36714
1	4.9	2.325616	2.425889	10.30408163	3.25	4.133448113	13.18757	68.65649
1	5.2	2.316424	2.403162	9.23877551	4	3.609338581	13.5307	73.32481
1.5	4	2.297904	2.446707	9.510204082	2	6.081785362	14.18964	57.13924
1.5	4.3	2.307337	2.443113	10.22857143	2.5	5.557501846	13.83738	59.83705
1.5	4.6	2.317936	2.433511	10.79183673	2.75	4.74929949	13.44157	64.66707
1.5	4.9	2.321594	2.425199	10.20408163	3	4.272037442	13.30497	67.89142
1.5	5.2	2.307622	2.398722	9.612244898	3.75	3.797884797	13.82673	72.53231
2	4	2.295528	2.445706	9.142857143	2	6.140495495	14.246	56.8967
2	4.3	2.306988	2.448118	10.34693878	2.25	5.764835225	13.81789	58.27991
2	4.6	2.316396	2.437464	11.50408163	2.5	4.966974913	13.46643	63.11587
2	4.9	2.319	2.424651	11.19591837	3	4.357382342	13.36915	67.4072
2	5.2	2.311763	2.403508	9.912244898	3.5	3.817136766	13.63951	72.01412

Table A-2 Continued

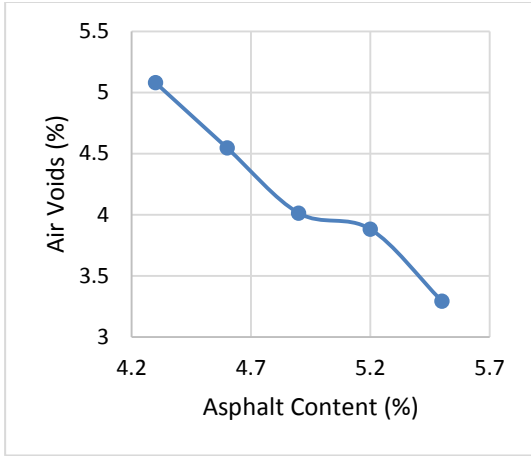
HL	AC %	Density (g/cm ³)	Gmm (g/cm ³)	Stability (kN)	Flow (mm)	Air Voids (%)	VMA (%)	VFA (%)
2.5	4	2.291477	2.452713	9.571428571	1.75	6.57378451	14.36501	54.23752
2.5	4.3	2.303903	2.444634	9.775510204	2	5.756716241	13.90062	58.58662
2.5	4.6	2.311019	2.432759	10.83673469	2.25	5.004188867	13.63469	63.29811
2.5	4.9	2.311443	2.422649	12.55102041	2.75	4.590281271	13.61888	66.29471
2.5	5.2	2.298328	2.39576	9.23152	3.25	4.066824557	14.10897	71.17561
3	4	2.281174	2.453714	8.408163265	1.5	7.031780543	14.71787	52.22284
3	4.3	2.291805	2.452422	9.469387755	1.75	6.549320864	14.32044	54.26593
3	4.6	2.305349	2.435762	10.69387755	2	5.354117457	13.81411	61.24166
3	4.9	2.300763	2.41364	11.06122449	2.5	4.676629936	13.98554	66.56097
3	5.2	2.298607	2.407772	8.653061224	3	4.53382763	14.06613	67.76777

Table A-3 Marshall Test Results for the Base course

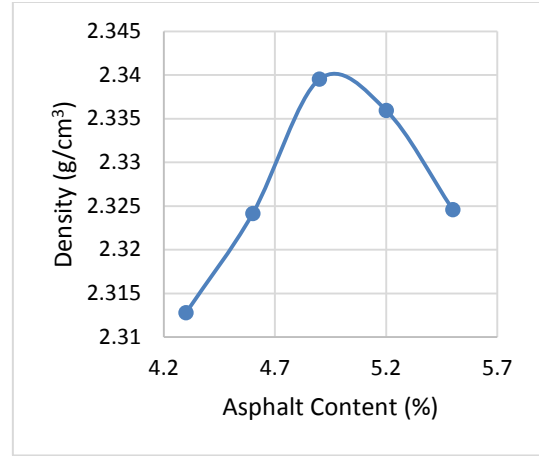
HL	AC %	Density (g/cm ³)	Gmm (g/cm ³)	Stability (kN)	Flow (mm)	Air Voids (%)	VMA (%)	VFA (%)
0	3.7	2.2861	2.43707	7.25	2.24	6.19473384	14.53016	57.36636
0	4	2.302924	2.427598	8.5	2.46	5.135693801	14.16938	63.75499
0	4.3	2.314435	2.418251	8.9	2.92	4.293020038	14.00992	69.35729
0	4.6	2.30817	2.40903	8.3	3.37	4.186747363	14.51153	71.14881
0	4.9	2.296452	2.399932	7	3.8	4.311788834	15.213	71.6572
1	3.7	2.290348	2.434627	7.6	2	5.926123386	14.27759	58.49352
1	4	2.301952	2.42518	8.23	2.43	5.08118985	14.11168	63.99301
1	4.3	2.312418	2.415861	8.77	2.7	4.281827473	13.9908	69.39541
1	4.6	2.311674	2.406665	8.74	2.9	3.946997193	14.28801	72.37545
1	4.9	2.302537	2.39759	7.8	3.6	3.964522708	14.89526	73.38399
1.5	3.7	2.284128	2.433408	8	1.8	6.134606281	14.46361	57.58593
1.5	4	2.293504	2.423974	8.65	2.2	5.382483475	14.38006	62.56981
1.5	4.3	2.30404	2.414667	9.16	2.4	4.581459887	14.25553	67.86187
1.5	4.6	2.307676	2.405483	8.4	2.65	4.066002545	14.38943	71.74313
1.5	4.9	2.293788	2.396421	8.14	3.37	4.282761668	15.17224	71.77239
2	3.7	2.281766	2.43219	7.76	1.75	6.184714188	14.50535	57.36254
2	4	2.293158	2.422769	8.75	2	5.349705234	14.34618	62.70989
2	4.3	2.302509	2.413474	9.74	2.25	4.597729248	14.26566	67.77065
2	4.6	2.305098	2.404303	9.5	2.7	4.126143835	14.43832	71.42227
2	4.9	2.297904	2.395253	8.4	3.15	4.064247075	14.97357	72.8572

Table A-3 Continued

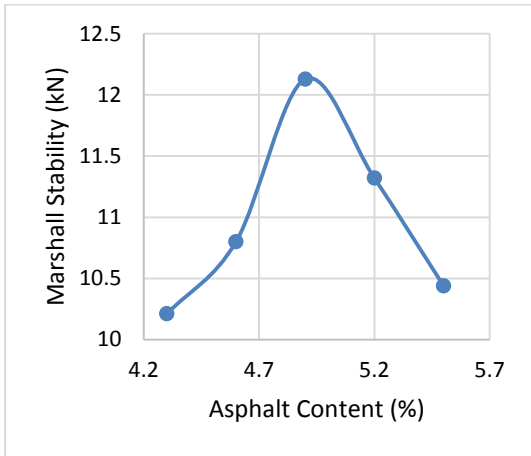
HL	AC %	Density (g/cm ³)	Gmm (g/cm ³)	Stability (kN)	Flow (mm)	Air Voids (%)	VMA (%)	VFA (%)
2.5	3.7	2.27774	2.430973	8.15	1.56	6.303360835	14.60956	56.85453
2.5	4	2.290091	2.421565	8.3	1.8	5.429298821	14.41398	62.33311
2.5	4.3	2.297165	2.412282	9.2	2	4.772120341	14.41789	66.90141
2.5	4.6	2.297586	2.403124	10.7	2.45	4.391700137	14.67054	70.0645
2.5	4.9	2.284549	2.394086	7.84	3	4.575316008	15.42153	70.33163
3	3.7	2.267498	2.429757	7.2	1.35	6.677992902	14.9471	55.32248
3	4	2.278066	2.420362	8	1.57	5.879120561	14.81689	60.3215
3	4.3	2.28697	2.411092	9.1	1.75	5.147957855	14.75119	65.1014
3	4.6	2.291528	2.401946	9.4	2.23	4.597022581	14.84905	69.04165
3	4.9	2.284827	2.392921	7.35	2.75	4.517240644	15.36504	70.60053



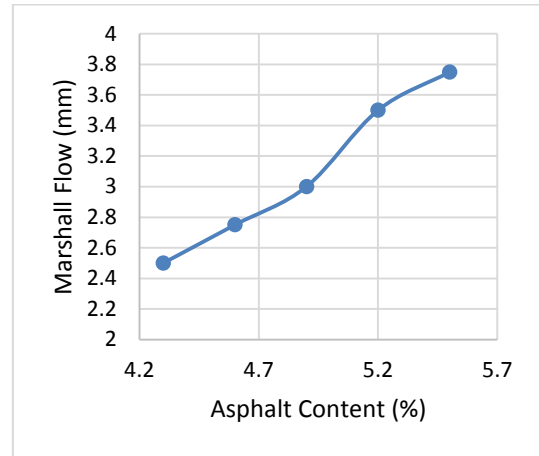
a. Air Voids (AV)



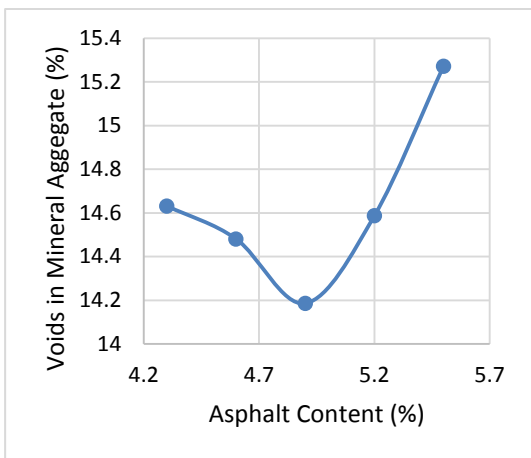
b. Density



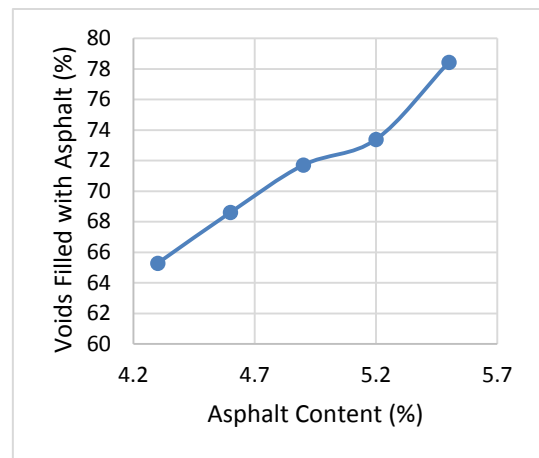
c. Marshall Stability, kN



d. Marshall Flow

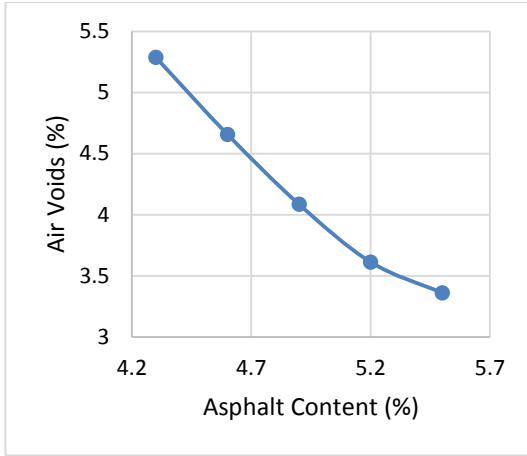


e. Voids in Mineral Aggregate (VMA)

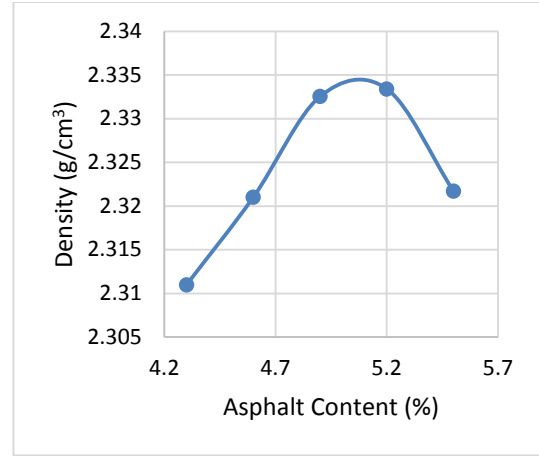


f. Voids Filled with Asphalt (VFA)

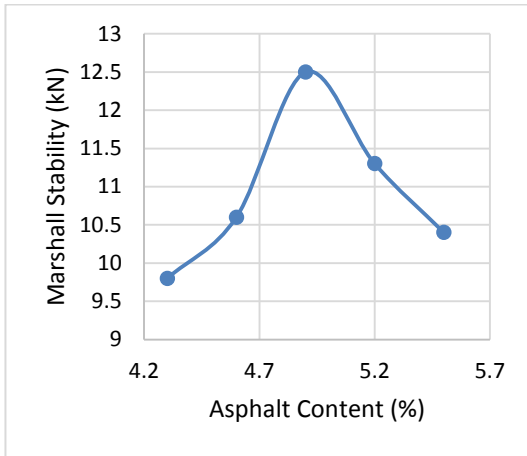
Figure (A-1) Marshall Mix Design Properties for H1W mixture



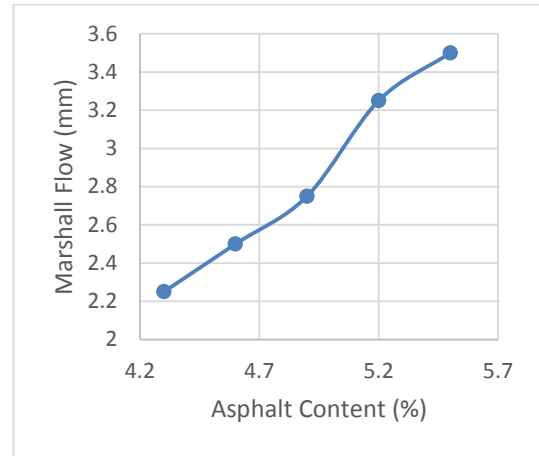
a. Air Voids (AV)



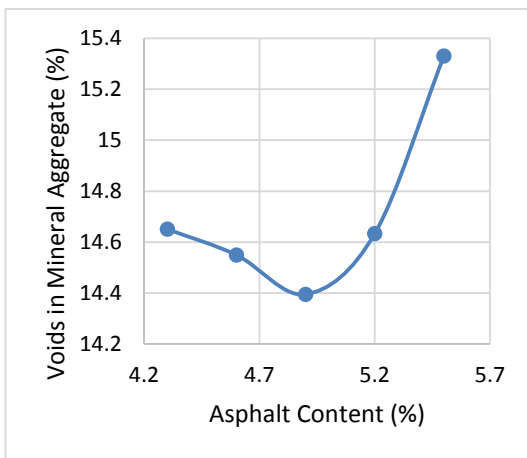
b. Density



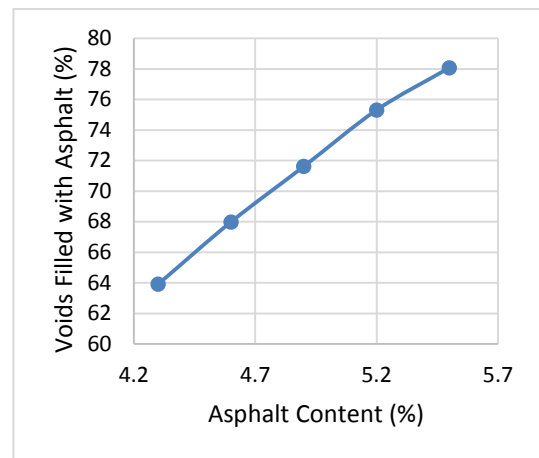
c. Marshall Stability, kN



d. Marshall Flow

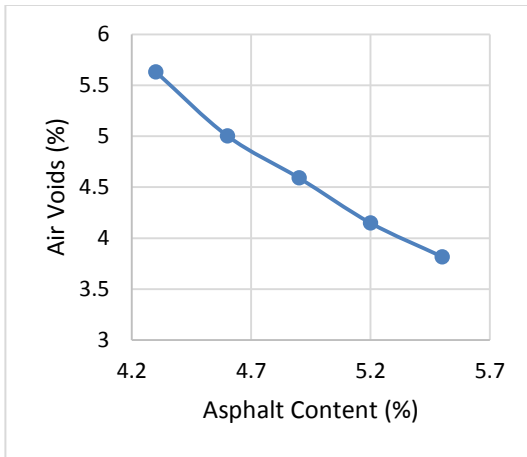


e. Voids in Mineral Aggregate (VMA)

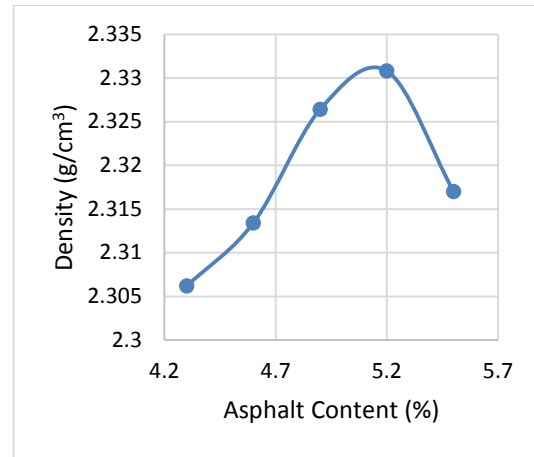


f. Voids Filled with Asphalt (VFA)

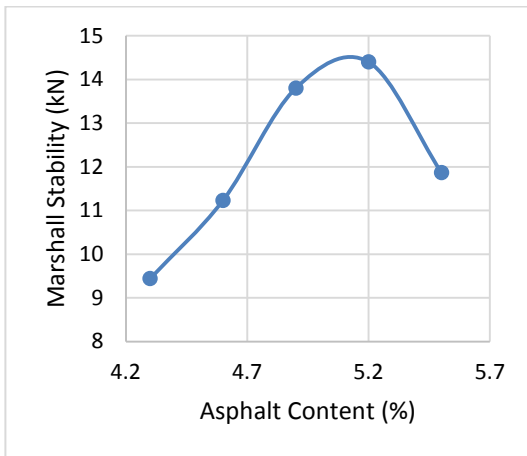
Figure (A-2) Marshall Mix Design Properties for H1.5W mixture



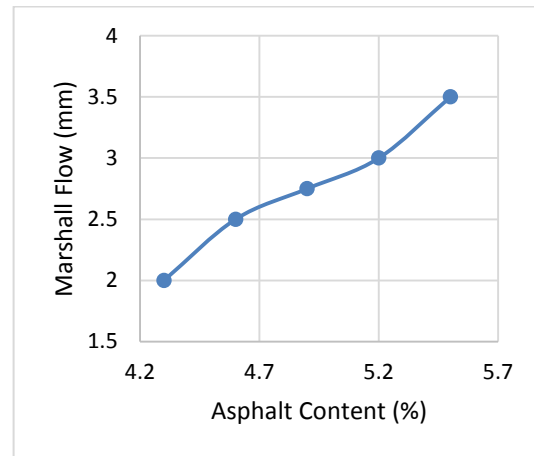
a. Air Voids (AV)



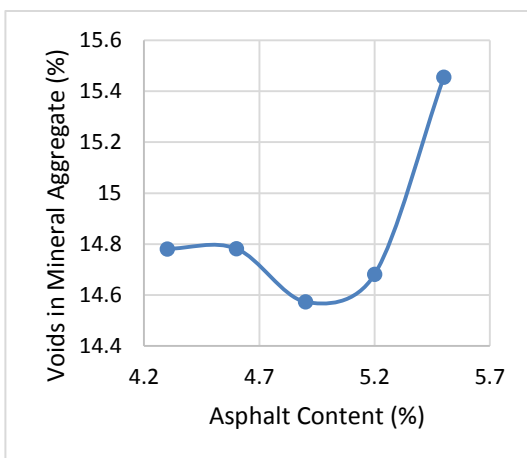
b. Density



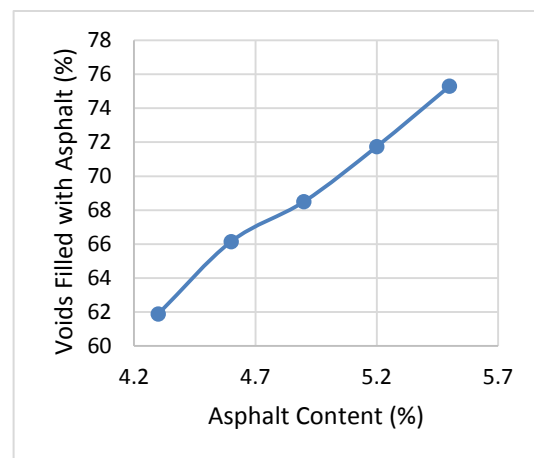
c. Marshall Stability, kN



d. Marshall Flow

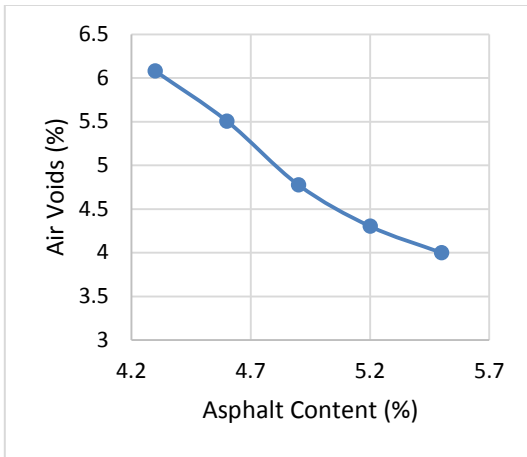


e. Voids in Mineral Aggregate (VMA)

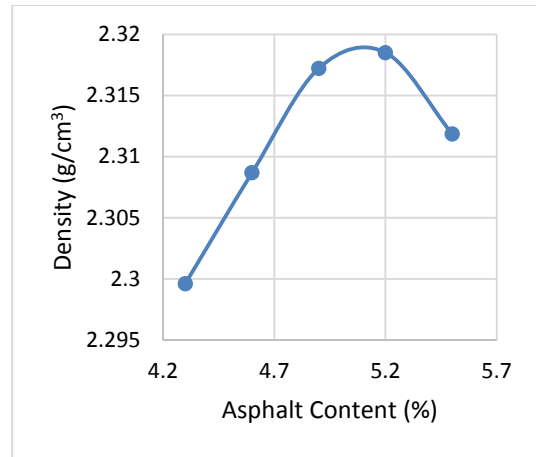


f. Voids Filled with Asphalt (VFA)

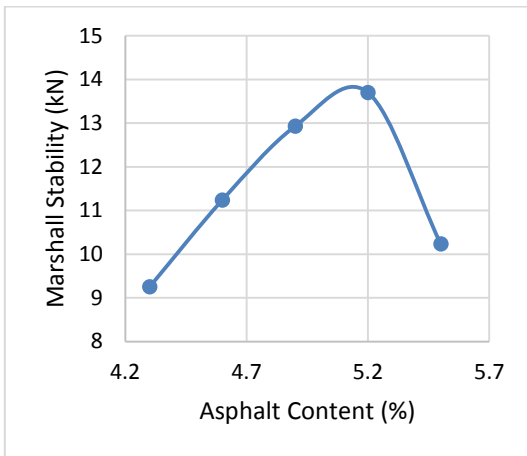
Figure (A-3) Marshall Mix Design Properties for H2W mixture



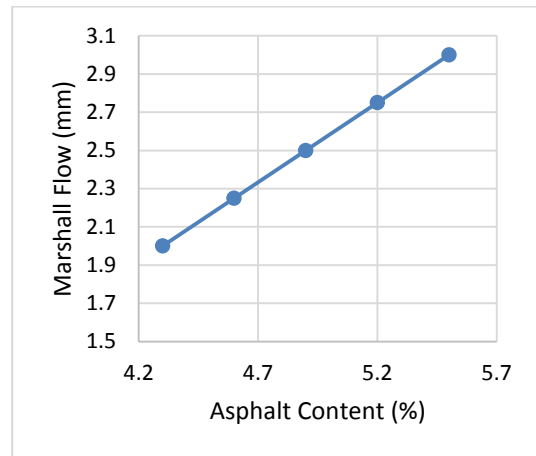
a. Air Voids (AV)



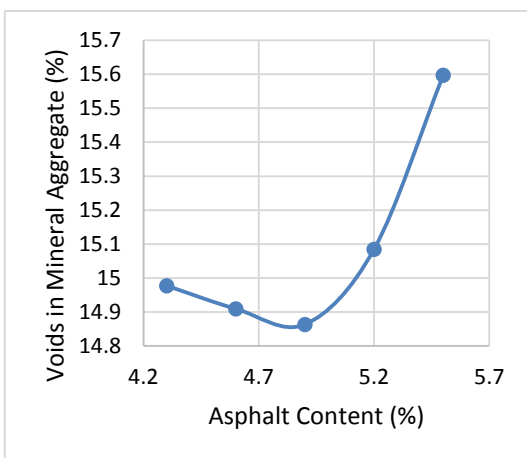
b. Density



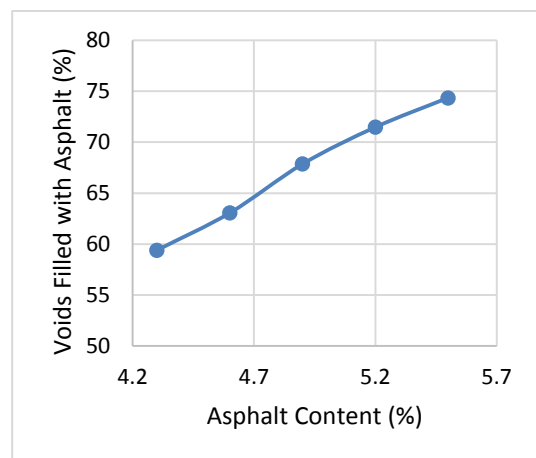
c. Marshall Stability, kN



d. Marshall Flow

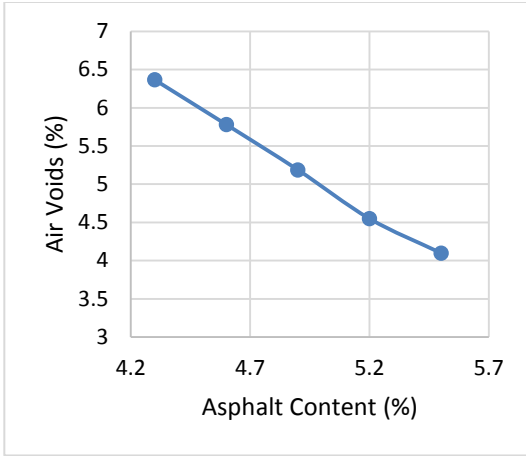


e. Voids in Mineral Aggregate (VMA)

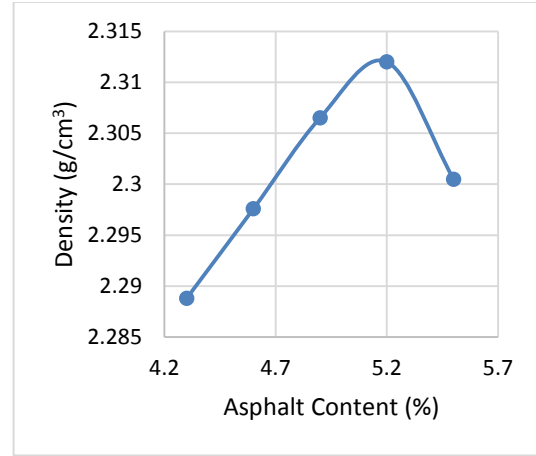


f. Voids Filled with Asphalt (VFA)

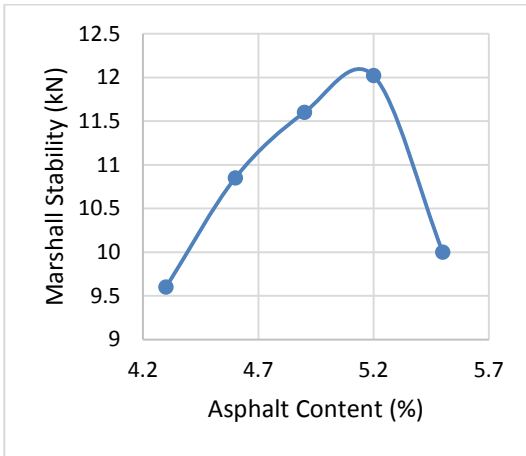
Figure (A-4) Marshall Mix Design Properties for H2.5W mixture



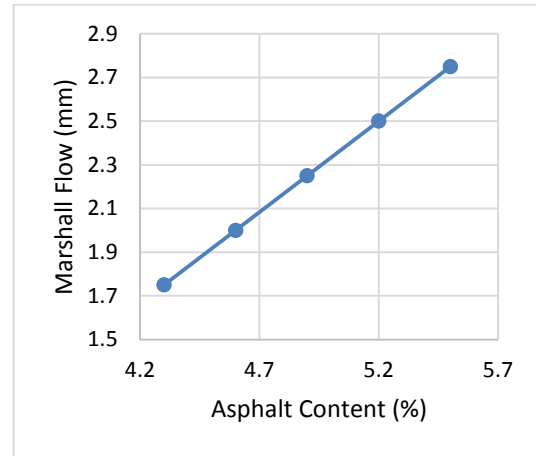
a. Air Voids (AV)



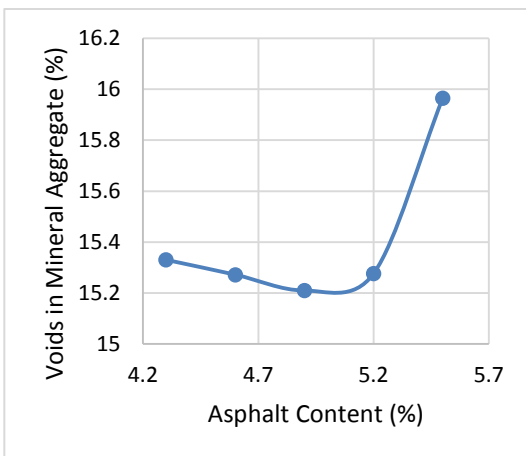
b. Density



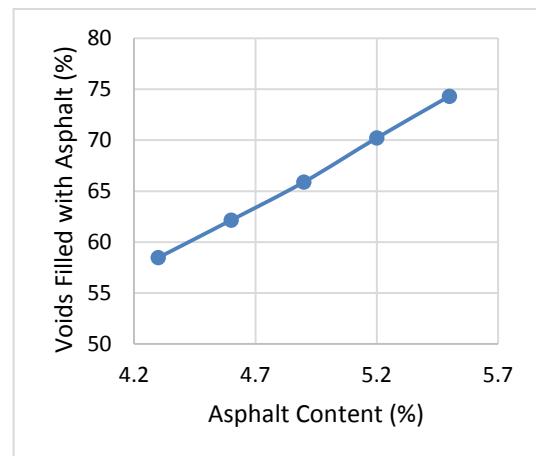
c. Marshall Stability, kN



d. Marshall Flow

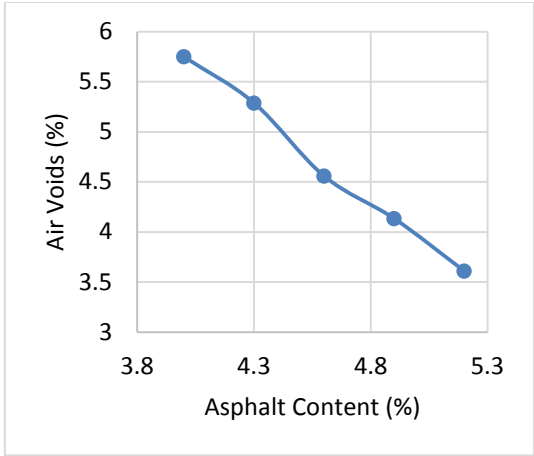


e. Voids in Mineral Aggregate (VMA)

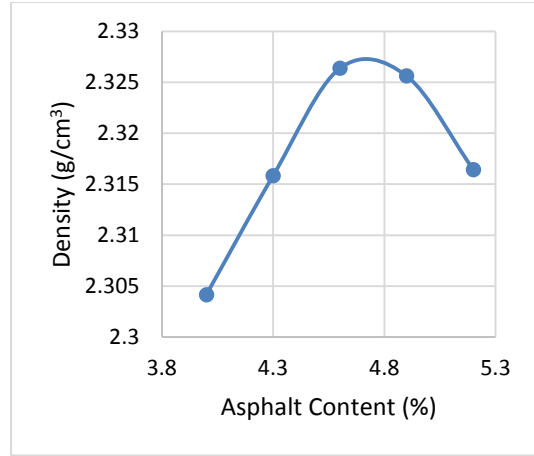


f. Voids Filled with Asphalt (VFA)

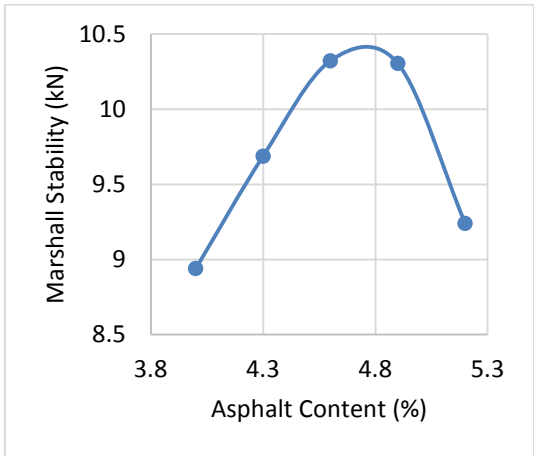
Figure (A-5) Marshall Mix Design Properties for H3W mixture



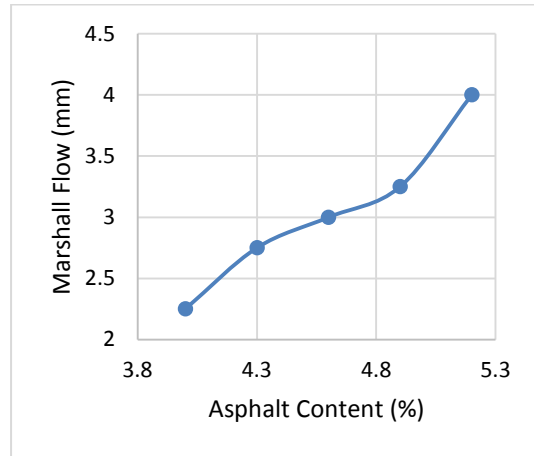
a. Air Voids (AV)



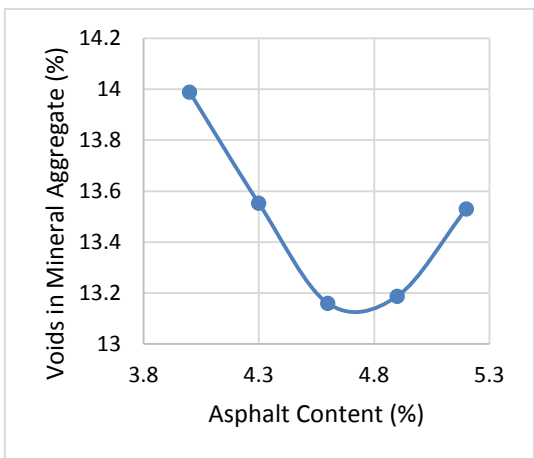
b. Density



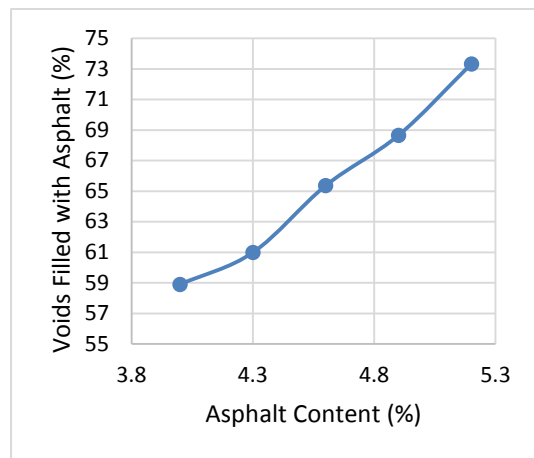
c. Marshall Stability, kN



d. Marshall Flow

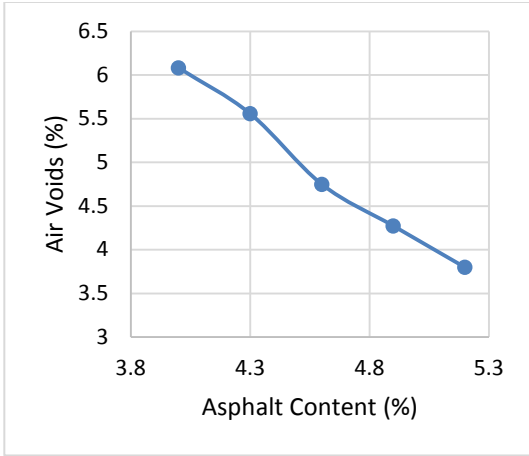


e. Voids in Mineral Aggregate (VMA)

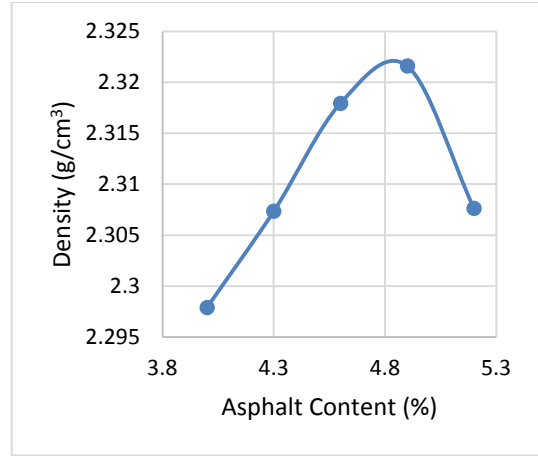


f. Voids Filled with Asphalt (VFA)

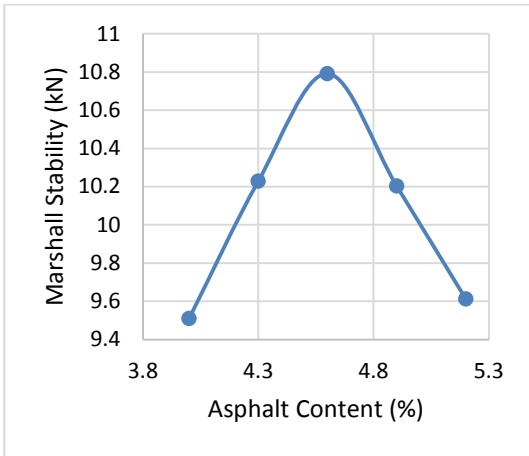
Figure (A-6) Marshall Mix Design Properties for H1L mixture



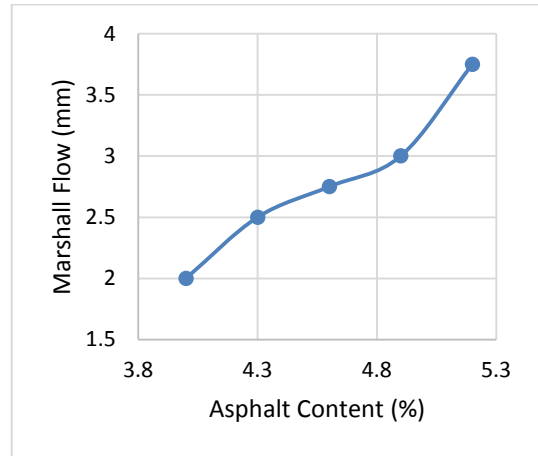
a. Air Voids (AV)



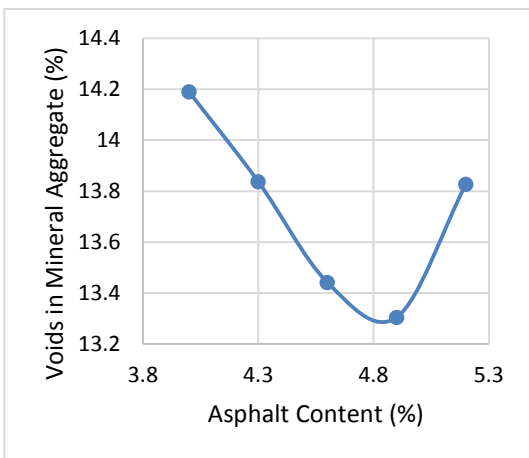
b. Density



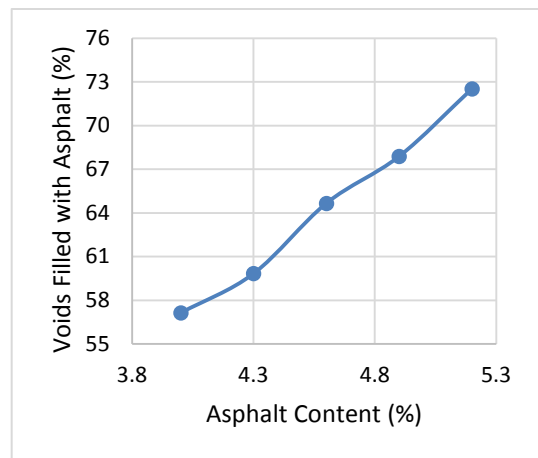
c. Marshall Stability, kN



d. Marshall Flow

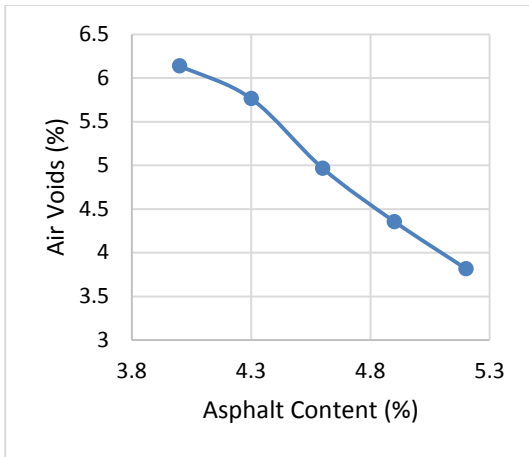


e. Voids in Mineral Aggregate (VMA)

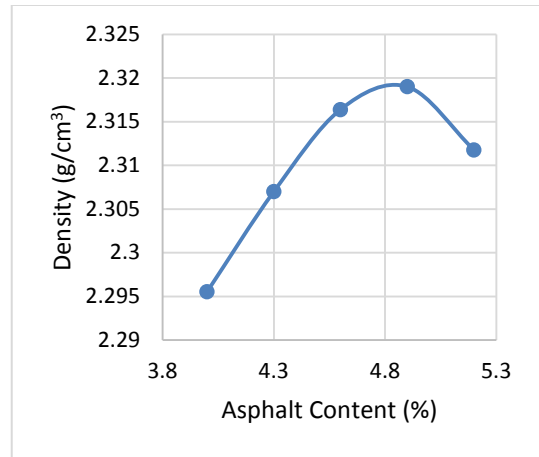


f. Voids Filled with Asphalt (VFA)

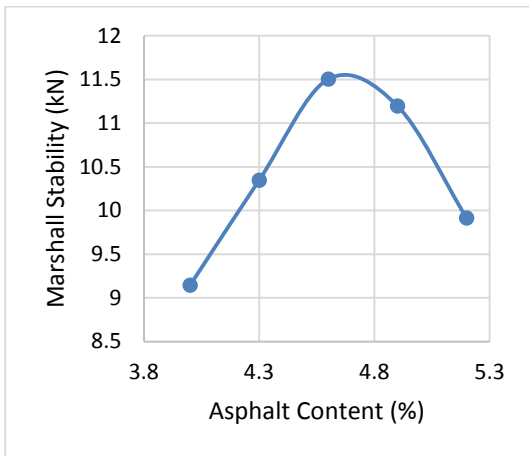
Figure (A-7) Marshall Mix Design Properties for H1.5L mixture



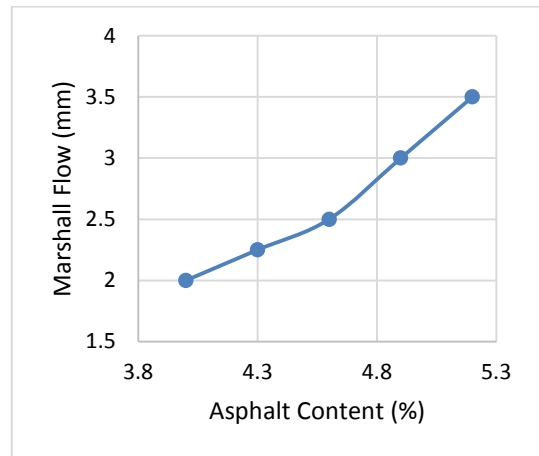
a. Air Voids (AV)



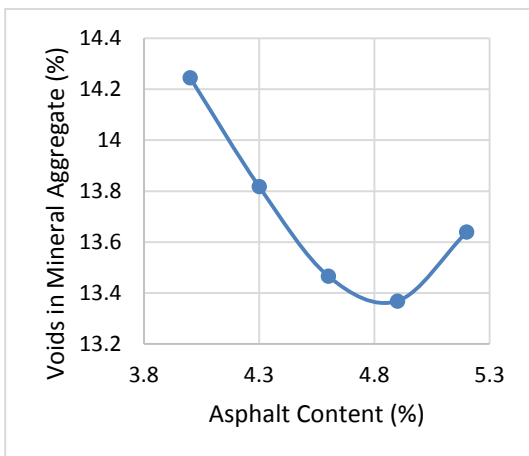
b. Density



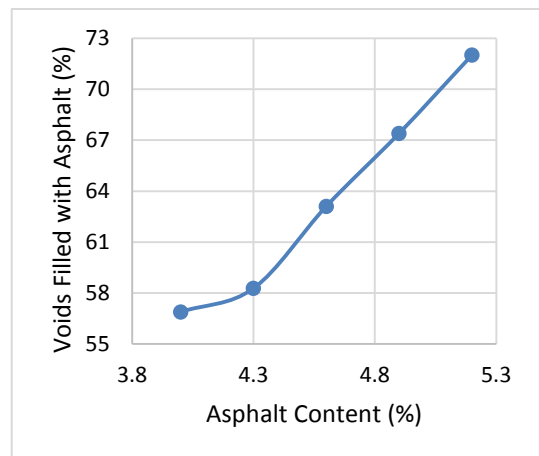
c. Marshall Stability, kN



d. Marshall Flow

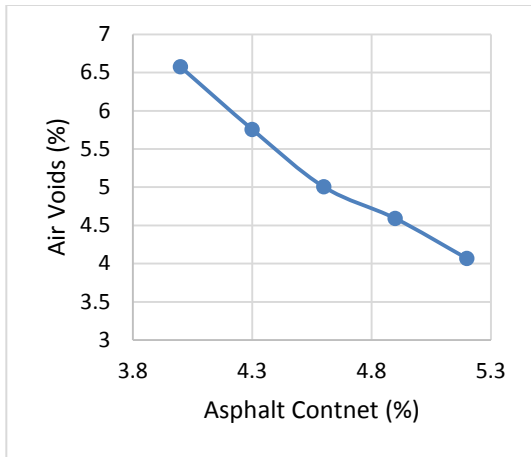


e. Voids in Mineral Aggregate (VMA)

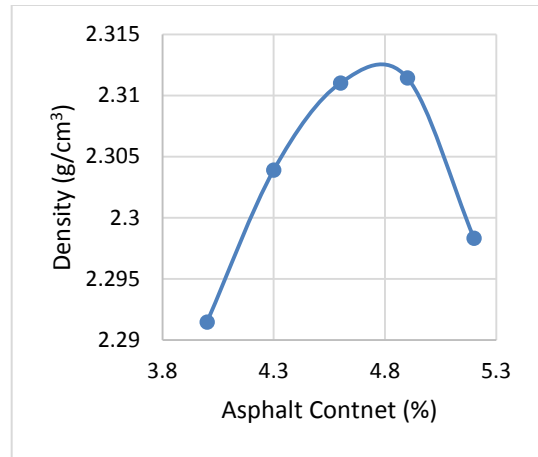


f. Voids Filled with Asphalt (VFA)

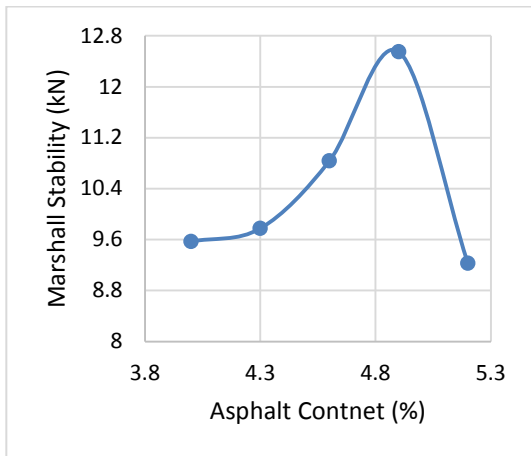
Figure (A-8) Marshall Mix Design Properties for H2L mixture



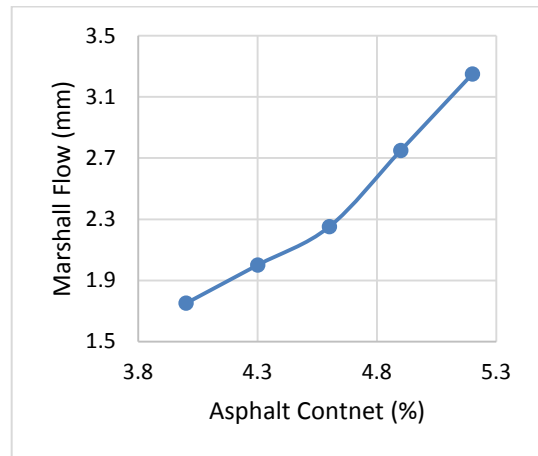
a. Air Voids (AV)



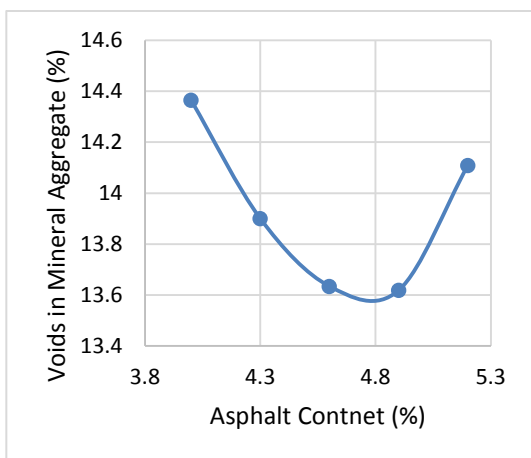
b. Density



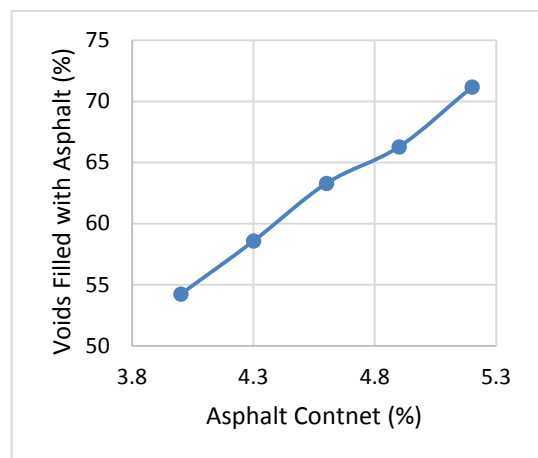
c. Marshall Stability, kN



d. Marshall Flow

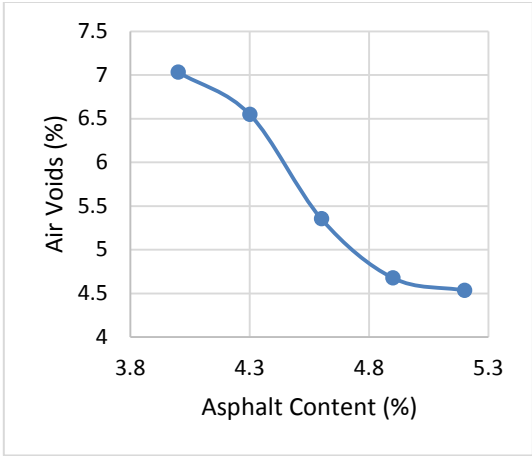


e. Voids in Mineral Aggregate (VMA)

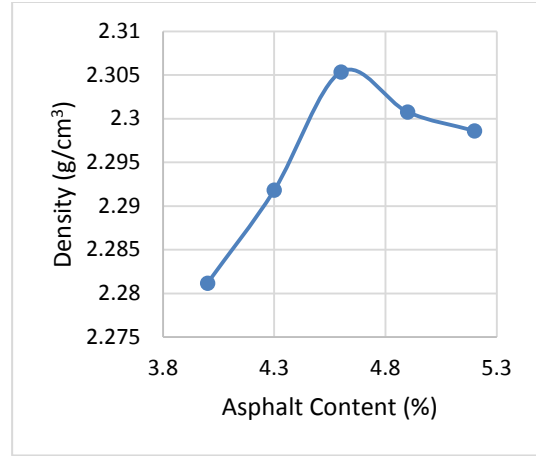


f. Voids Filled with Asphalt (VFA)

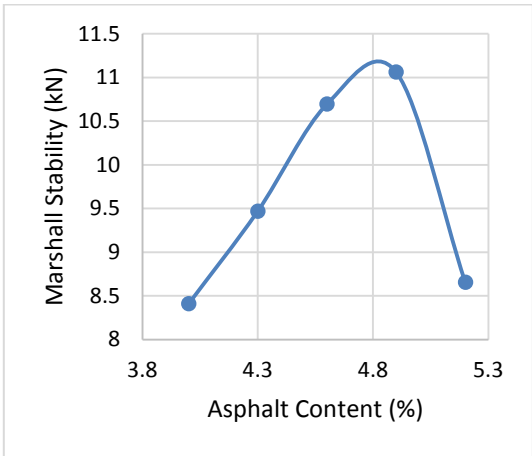
Figure (A-9) Marshall Mix Design Properties for H2.5L mixture



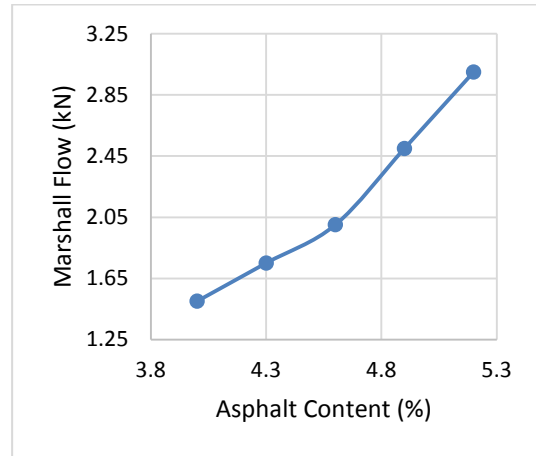
a. Air Voids (AV)



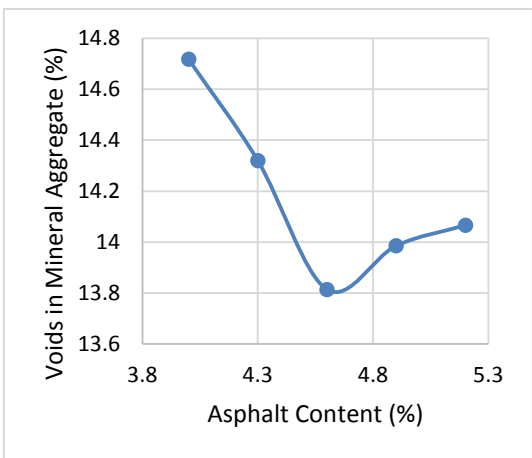
b. Density



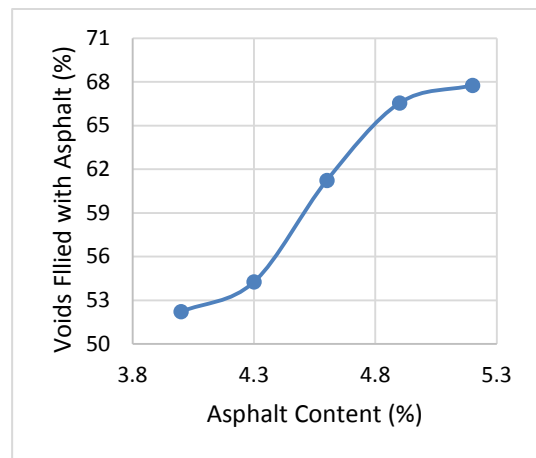
c. Marshall Stability, kN



d. Marshall Flow

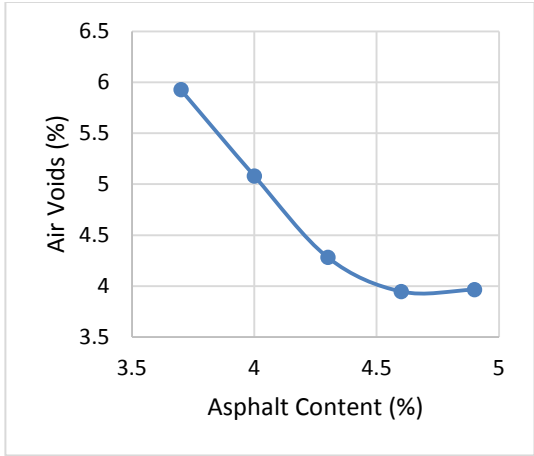


e. Voids in Mineral Aggregate (VMA)

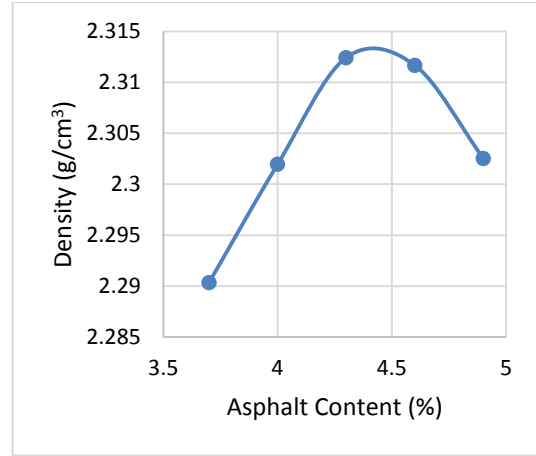


f. Voids Filled with Asphalt (VFA)

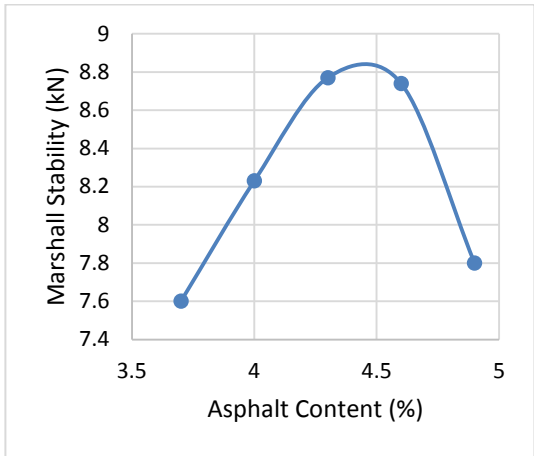
Figure (A-10) Marshall Mix Design Properties for H3L mixture



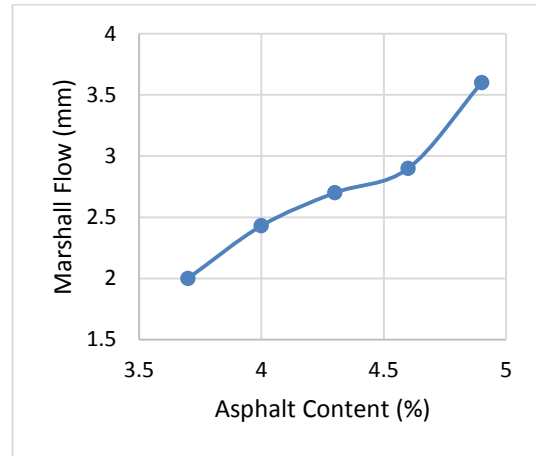
a. Air Voids (AV)



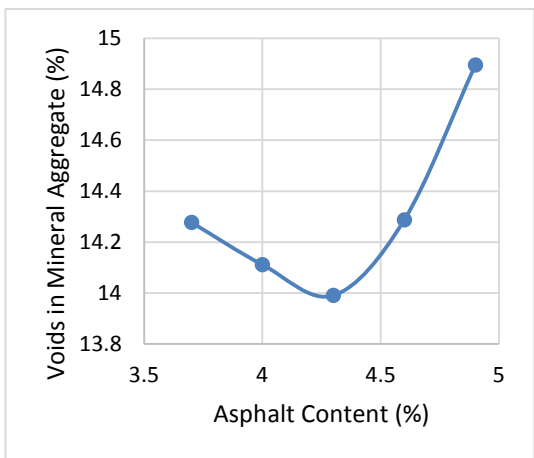
b. Density



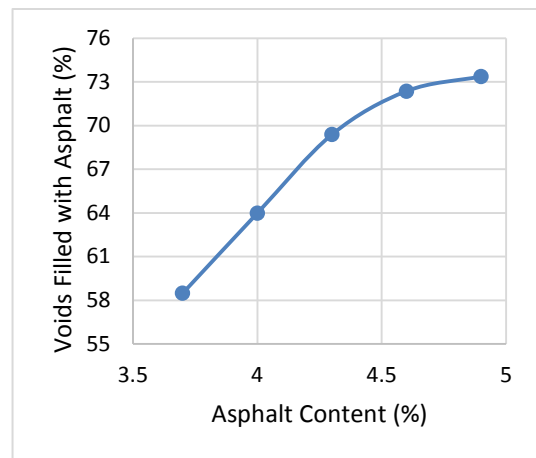
c. Marshall Stability, kN



d. Marshall Flow

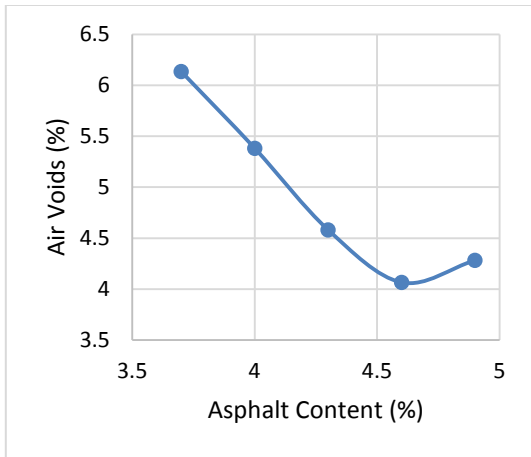


e. Voids in Mineral Aggregate (VMA)

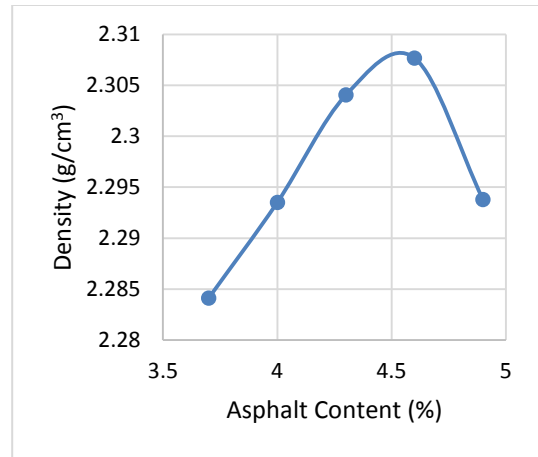


f. Voids Filled with Asphalt (VFA)

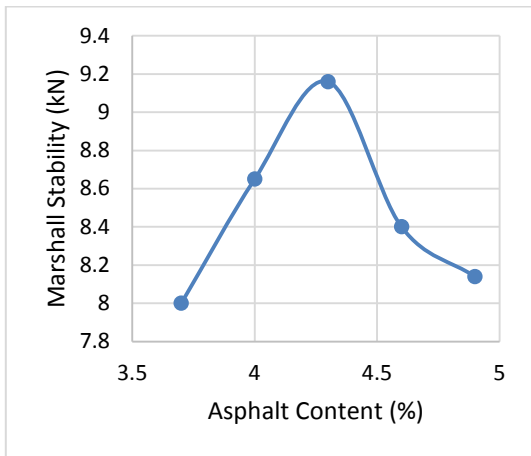
Figure (A-11) Marshall Mix Design Properties for H1B mixture



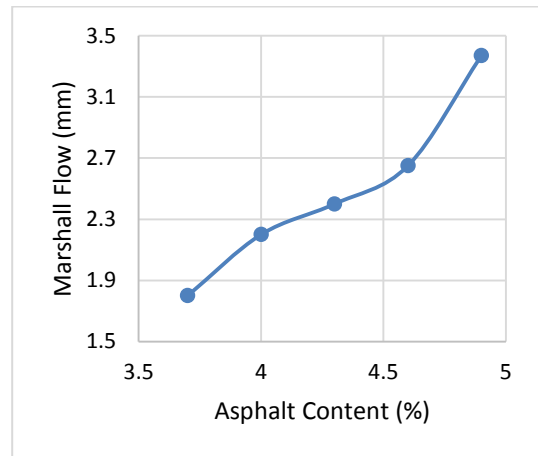
a. Air Voids (AV)



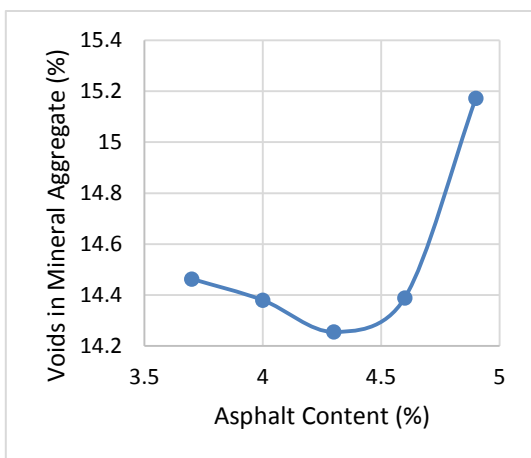
b. Density



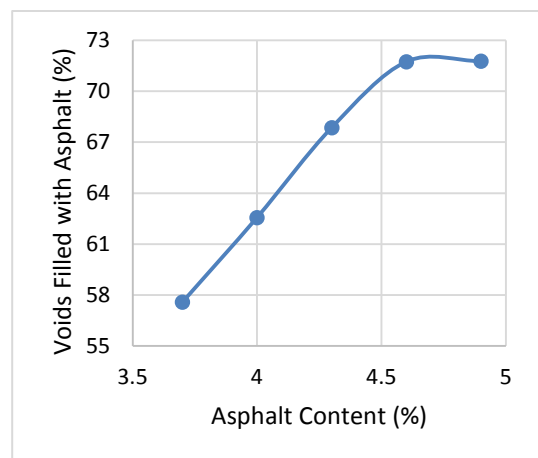
c. Marshall Stability, kN



d. Marshall Flow

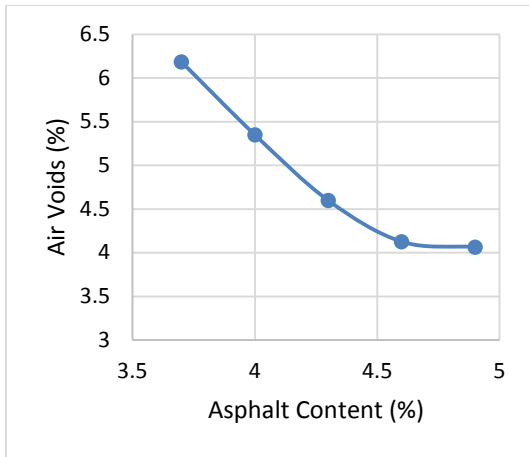


e. Voids in Mineral Aggregate (VMA)

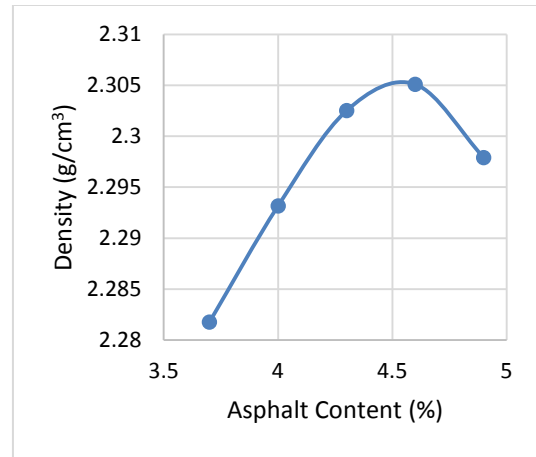


f. Voids Filled with Asphalt (VFA)

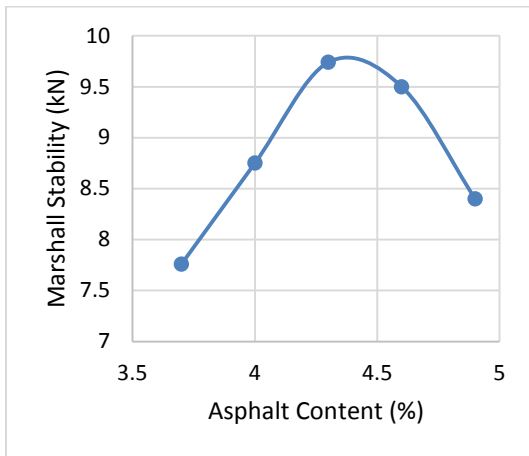
Figure (A-12) Marshall Mix Design Properties for H1.5B mixture



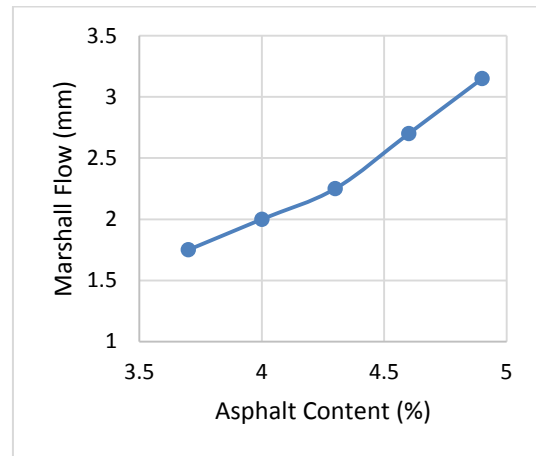
a. Air Voids (AV)



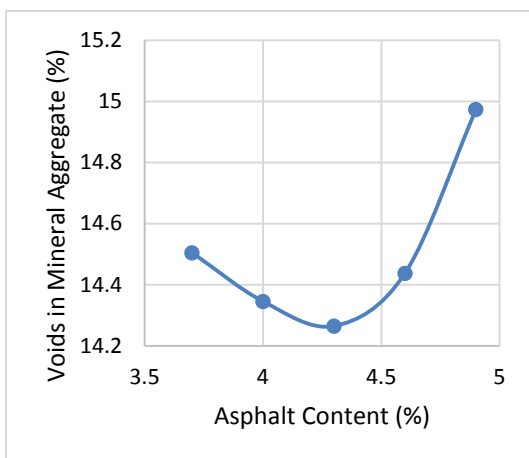
b. Density



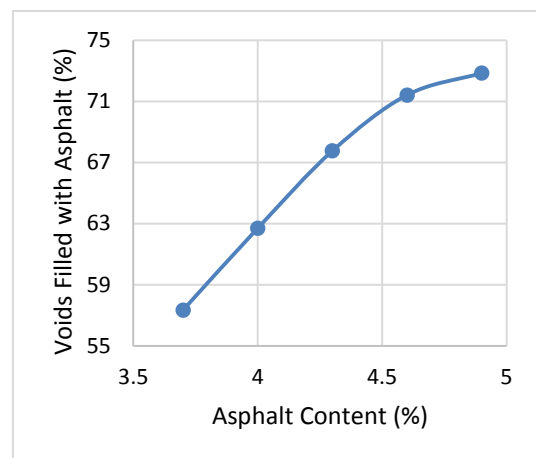
c. Marshall Stability, kN



d. Marshall Flow

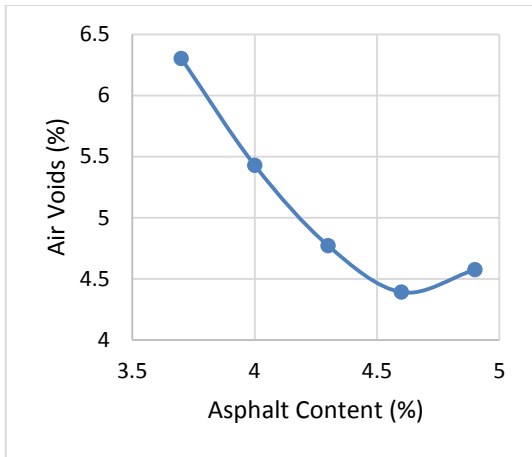


e. Voids in Mineral Aggregate (VMA)

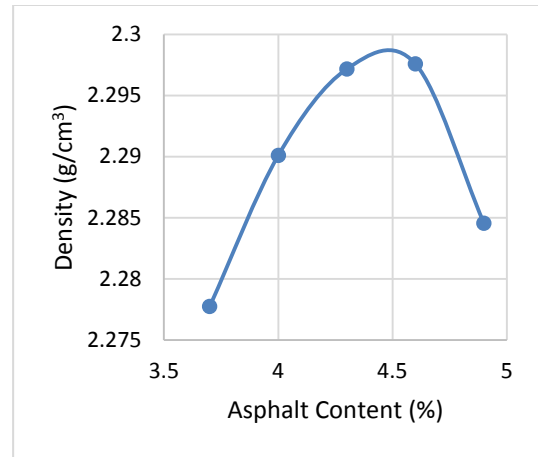


f. Voids Filled with Asphalt (VFA)

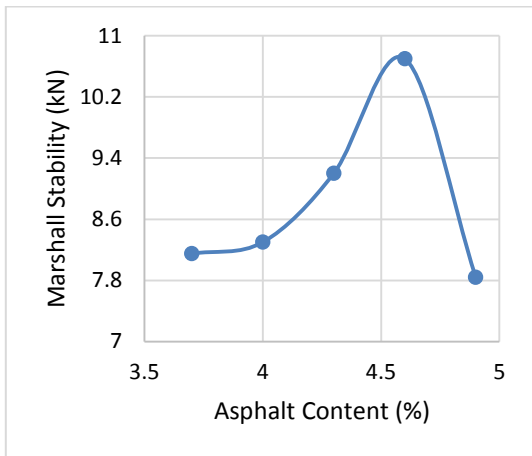
Figure (A-13) Marshall Mix Design Properties for H2B mixture



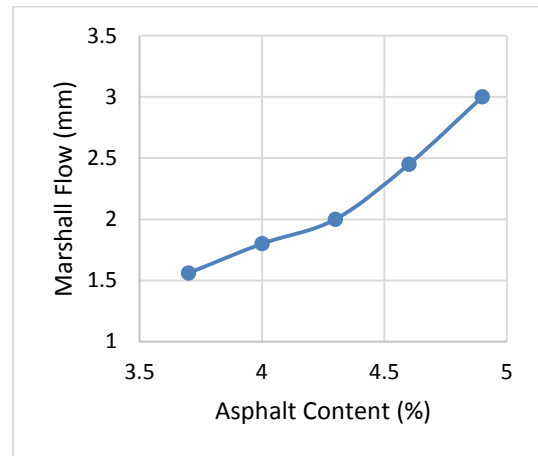
a. Air Voids (AV)



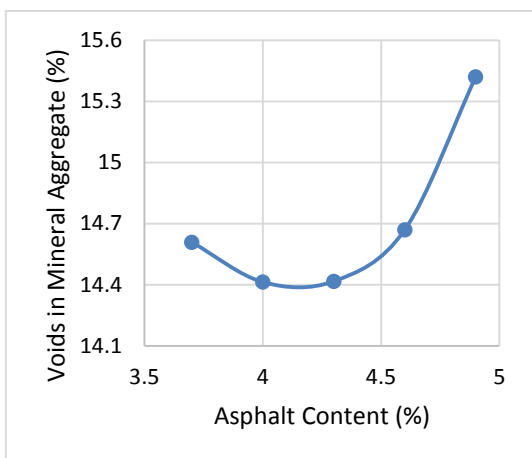
b. Density



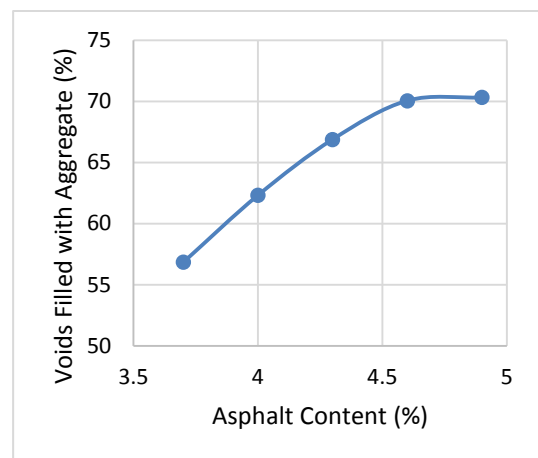
c. Marshall Stability, kN



d. Marshall Flow

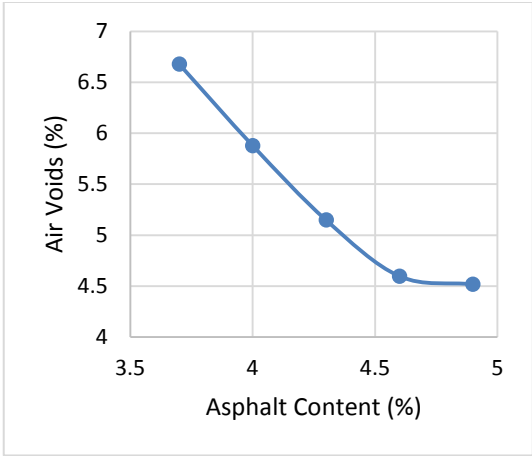


e. Voids in Mineral Aggregate (VMA)

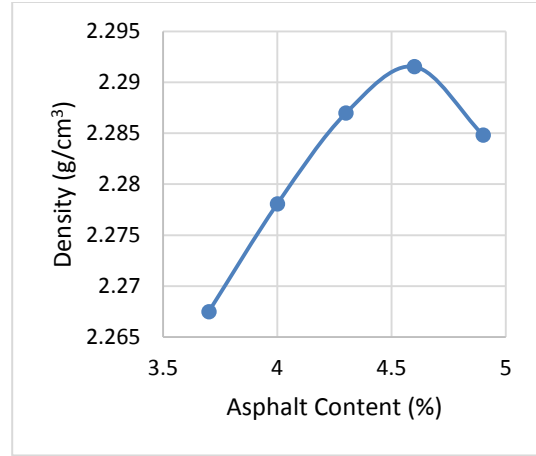


f. Voids Filled with Asphalt (VFA)

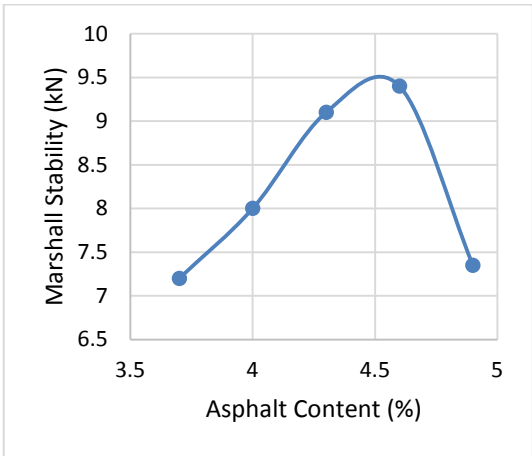
Figure (A-14) Marshall Mix Design Properties for H2.5B mixture



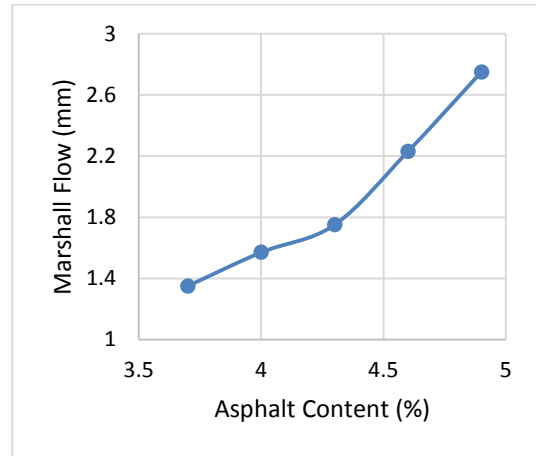
a. Air Voids (AV)



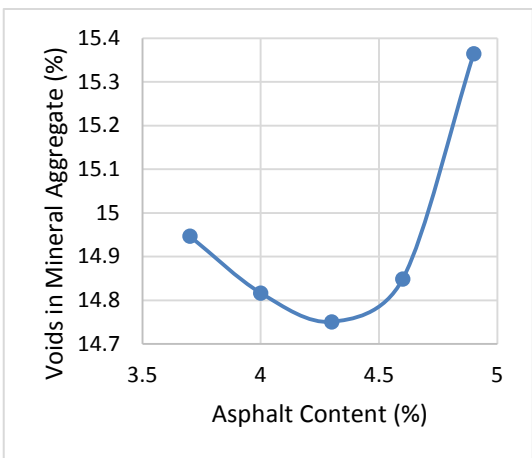
b. Density



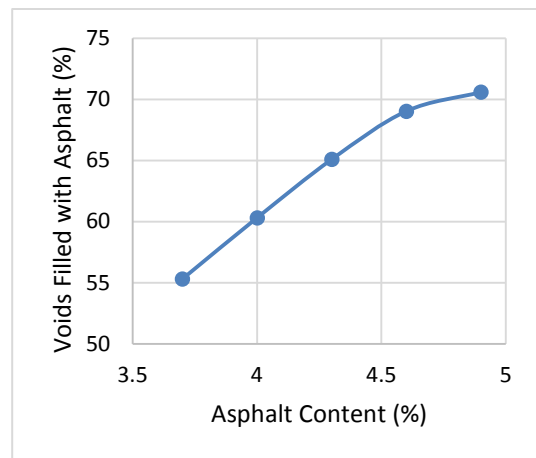
c. Marshall Stability, kN



d. Marshall Flow



e. Voids in Mineral Aggregate (VMA)



f. Voids Filled with Asphalt (VFA)

Figure (A-15) Marshall Mix Design Properties for H3B mixture